

**SUMOylation regulates the function of  
*Drosophila* Jun and helps maintain gut immune  
homeostasis**

**A Thesis  
Submitted in partial fulfillment of the requirements  
of the degree of  
Doctor of Philosophy  
By**

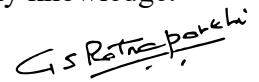
**Amarendranath Soory  
20132001**



**Indian Institute of Science Education and Research Pune  
2021**

## Certificate

I certify that the thesis entitled “*SUMOylation regulates the function of Drosophila Jun and helps maintain gut immune homeostasis*” presented by Mr. Amarendranath Soory represents his original work which was carried out by him at IISER, Pune under my guidance and supervision during the period from August 2015 to June 2021. The work presented here or any part of it has not been included in any other thesis submitted previously for the award of any degree or diploma from any other University or institutions. I further certify that the above statements made by him in regard to his thesis are correct to the best of my knowledge.



Girish Ratnaparkhi

11.06.2021

## Declaration

I declare that the work reported in this thesis is the original work done by me under the guidance of Dr. Girish Ratnaparkhi. This written submission represents my idea in my own words and where others' ideas have been included; I have adequately cited and referenced the original sources. I also declare that I have adhered to all principles of academic honesty and integrity and have not misrepresented or fabricated or falsified any idea/data/fact/source in my submission. I understand that violation of the above will be cause for disciplinary action by the Institute and can also evoke penal action from the sources which have thus not been properly cited or from whom proper permission has not been taken when needed.



Amarendranath Soory

11.06.2021

## Acknowledgements

I would like to thank my Ph.D supervisor and mentor, Dr. Girish Ratnaparkhi for giving me all the freedom to explore a research topic of my interest. I consider myself extremely fortunate to work with a person who likes to explore and integrate new technologies into research. I am thankful to him for convincing me to try out CRISPR/Cas9 mediated genome editing which has enhanced and made this work impactful. I owe it to Girish for being very benevolent, kind and supporting me during all the tough times. His positive approach towards students is a quality that is highly desirable in any research environment.

I thank my research advisory committee members, Dr. Deepa Subramanyam, Dr. Jomon Joseph and Dr. Nagaraj Balasubramanian for their timely suggestions and inputs during yearly seminars and for making sure that I complete my lab notebook. I am grateful to Dr. Deepti Trivedi Vyas, NCBS, Bengaluru for her immense help and inputs in designing the CRISPR strategy for Jra. I thank Dr. Sveta Chakrabarti for helping me with several gut-specific reagents and protocols. I thank Dr. Sanjeev Galande for allowing me to use reagents and instruments for the RNA sequencing. I thank Dr. Krishnapal Karmodia for his inputs in designing the sequencing experiments. I thank Dr. Richa Ricky, Dr. Anuradha Ratnaparkhi and Dr. Girish Deshpande for their inputs and suggestions about my work besides all the fun discussions.

I am happy to have worked with wonderful colleagues in the GR lab. I thank all the past and present members of the lab for an intellectually stimulating environment in the lab. I thank Mithila Handu, Senthil Deivasigamani, Vallari Shukla, Bhagyashree Kaduskar, Kriti Chaplot, Prajna Nayak, Shweta Tendulkar, Sushmitha Hegde, Aparna Thulasidharan, Subhradip Das, Lovleen Garg, Kundan Kumar, Namrita Kulkarni and Sanhita Sarkar for a friendly lab environment. Sushmitha and Aparna deserve a special mention for always giving me an honest/genuine feedback and have been a big support to me throughout. Both of them are my go-to people in the lab whenever there was a problem. I will dearly miss them and all the gossip they brought to me. I thank Kriti Chaplot for being supportive during the tough times and shall cherish the many arguments/fights I had with her. I acknowledge Senthilkumar Deivasigamani for teaching me the basics of *Drosophila* genetics. I thank all the trainees who have worked with me and bearing with all the tantrums I threw. I thank Saurabh Pradhan and Ankita Sharma for their great help with the library prep and troubleshooting during the RNA seq experiments. I thank Sushmitha and Girish for taking care of my flies during the lockdown.

I thank Snehal, Yashwanth and Ashwini for feeding the flies and maintaining the fly stocks. I thank Vijay Vittal and Santosh Poddar for the help in the microscopy facility. I thank Mrinalini Virkar, Mahesh Rote, Shabnam Patil, Piyush Gadekar, Kalpesh Thakare among many others for their constant support during my time at IISER. I thank the leadership in the Bio department and IISER for making the institute a name to reckon with. I thank IISER, CSIR-SRF direct and all the funding agencies for providing me with adequate monetary resources to survive.

I thank Akhila, Kashyap, Divya and Aditi for all those memorable hangouts we had all these years. I thank Mukul, Swati, Bharat, Shivani, Sandip, Jay, Neeladri, Ron, Tomin, Dhriti, Mehak, Anish, Adarsh, Deepak, Aditi. D, Harpreet, Charu and Anshul for the adventures we had together and for staying strong as a group. I thank Suresh, Rakesh, Raghuveer, Pavan, Ravi, Chanakya and Kalyan, my friends from engineering for always being there whenever need and throwing sarcasm at me for pursuing a PhD whenever possible. I will cherish the memories with them for years to come.

I am indebted to my parents, Dr. Ravindranath Soory and Padmaja Rani Soory for their unconditional love and support throughout my life. Thank you both for the strength, freedom and inspiration to chase my dreams. I am extremely lucky to have parents who have supported me through every stage of my life and respected every decision of mine. It was my father who has encouraged me to ask questions and introduced me to the fascinating world of science at a very young age. His passion and zeal towards learning new things in life is awe-inspiring. My mother who is the best cook in the world always surprises me with the excitement she shows for every small success of mine. Their sacrifices and hardships have always motivated me to be better at every aspect of life and I dedicate this thesis to them. I thank my in-laws, Dr. Raghavendra Prasad and Dr. Padmavathi for all the support, interest and excitement in my work. I finally thank my wife Akhila Gungi, for standing strong with me in many up and downs for the past 13 years. She has been the main pillar of my success and had a major role in making me a better person. I adore her passion and dedication at work and envy her coding skills. She has been my biggest strength; emotional support and I couldn't have done this without her.

It was a fun ride at the end!

Sincerely,  
Amar.

## Abstract

To invoke a robust immune response, the host must recognise the invading pathogen and produce a battery of nullifying agents to neutralize the infection. One key feature for a successful host-defence is to find the right balance between positive and negative regulation of several immune effector pathways. There is ample evidence to suggest that post-translational modifications (PTMs) play a crucial role in the regulation of immune regulatory pathways during infection. Small Ubiquitin-like Modifier (SUMO) is one such post-translational modifier that has been implicated as an important regulator of the immune response, in recent years. To understand the role of SUMOylation in the regulation of innate immunity in *Drosophila*, as a first step, we identified, using quantitative mass spectrometry, a set of 700 proteins that display significantly altered SUMOylation status upon infection in S2 cells. These SUMO targets include several important transcriptional regulators, not the least of which are the Fos/Jun heterodimer, also known as the AP1 complex.

Here, we validate the SUMO conjugation of the *Drosophila* AP1 complex and attempt to uncover its role in host defence. Both Jun (Jra; Jun related antigen) and Fos (Kay; Kayak) are SUMO conjugated as tested using in-vitro and in-vivo SUMO conjugation assays. SUMO conjugation resistant (SCR) variants of both Fos and Jun were generated by uncovering SUMO acceptor lysine residues and replacing these with arginine residues. Further, we have used CRISPR/Cas9 technology to edit the *Drosophila* genome and have generated a Jra<sup>SCR</sup> mutant fly line. Using specific knockdowns, I established Jra as a negative regulator of the gut immune response in *Drosophila*, a role that is previously known. Flies expressing Jra<sup>SCR</sup> are sensitive to gut infection by gram-negative bacteria, *P. entomophila*, and succumb early. 3'mRNA sequencing analysis of the guts of Jra<sup>SCR</sup> flies revealed that a subset of defence genes are insufficiently activated post-infection. The genes affected include transcriptional targets of Jra like *Chinmo*, *Fkh*, *Ets21C*, and also the NFkB factors *Relish* and *Dorsal*. Our data suggests that Jra is a negative regulator of the gut immune response and SUMO conjugation of Jra attenuates the negative regulation by Jra to evoke a strong immune response. We propose that the SUMOylation of Jra is a key regulatory step that fine-tunes the activation of innate immune pathways during infection and maintains gut immune homeostasis.

## Synopsis

Post-translational modifications (PTMs) of proteins play a crucial role in regulating the function of substrate proteins by modulating their activity, stability, sub-cellular localization and interaction with other proteins. Small Ubiquitin-like Modifier (SUMO) is one such post-translational modifier, which covalently and reversibly conjugates to the side chain of a lysine residue of a substrate/target protein. SUMOylation of proteins plays a crucial role in many cellular processes, including the regulation of signalling pathways in eukaryotic cells. One important process regulated by SUMO is immune signalling, with proteins that are part of immune signalling cascades, being substrates for SUMO conjugation. However, mechanistic roles for individual SUMO conjugation of these target proteins are unclear. We are using *Drosophila* as a model to understand the roles of SUMO conjugation of proteins in immune signalling cascades. Our methodology includes the use of using quantitative mass spectrometry to identify proteins that show altered SUMOylation in response to infection, followed by generation of SUMO conjugation resistant (SCR) variants for a subset of these proteins using the *Drosophila* genetic toolbox. A comparison of the ability of the SCR mutant to wild type could uncover a role for SUMO conjugation of that substrate during the immune response. For my thesis, I have worked to understand the role of SUMOylation of the heterodimeric AP-1 complex, which consists of the transcriptional regulators Jra and Kay in regulating the gut immune response in *Drosophila*.

In the first chapter of this thesis, I performed a thorough literature search and reviewed our current understanding of the innate immune response in *Drosophila*. The *Drosophila* immune system has the cellular and humoral arm(s) that are functionally analogous to the innate immune components seen in vertebrates. Blood cells are the primary constituent of the cellular arm and predominantly function to entrap, encapsulate and engulf the invading pathogens. The humoral arm comprises secreted defence factors, such as anti-microbial peptides (AMPs) that are produced by a variety of organs and tissues like the gut, fat body, blood cells and brain, amongst others, that neutralize the pathogen. In the chapter, I have detailed the molecular mechanisms that lead to the activation of key signalling pathways that govern innate immunity in *Drosophila*, with an emphasis on PTMs. I have also summarised a

few known examples of the effect of phosphorylation, ubiquitination and SUMOylation of proteins during infection.

In the second chapter, I introduce a proteomic screen that we performed, which identified a list of 700 proteins with altered SUMOylation status upon an immune challenge. From this list, I chose to work on the AP-1 dimer proteins, Jun related antigen (Jra) and Kayak (Kay). Jra and Kayak act downstream of the Jun N-terminal kinase (JNK) signal transduction cascade. In addition to roles in immune signalling, Jra and Kay play crucial roles in regulating cell-shape change, neuronal plasticity and apoptosis. I cloned both the proteins in expression vectors and co-expressed them individually with the components of *Drosophila* SUMO conjugation machinery. Upon affinity pulldown and western blotting, I could confirm that these two proteins are post-translationally modified by SUMO. To identify the lysine residues that are targets for SUMO conjugation, I performed a site-directed mutagenesis screen replacing lysine residues with arginine residues. Arginine side chains cannot be modified by SUMO leading to the generation of an SCR variant. Jra is found to be conjugated by SUMO on two lysine residues, residues 29 and 190. Similarly, I identified that Kay was SUMOylated on a single lysine residue at residue 357. I used this information and reproduced the data in *Drosophila* S2 cells which is an *in-vivo* system and confirmed the identity of SUMO acceptor lysine residues in Jra and Kay.

The third Chapter relates to the development of reagents generated to study Jra and Kay. I generated UAS transgenic fly lines that overexpress different SCR variants of Jra and Kay. I tested their expression and performed genetic null lethality rescue crosses. Importantly, I used CRISPR/Cas9 technology to modify the genomic locus of Jra and generate an SCR variant of Jra that is resistant to SUMO conjugation of lysine 29 and 190. These Jra<sup>SCR</sup> flies are homozygous viable and show interesting phenotypes.

In the fourth chapter, I described the role of Jra in regulating the gut immune response. Here, I performed gut-specific knockdown of Jra followed by infection with a gram-negative pathogen *Pseudomonas entomophila*. I followed the survival of the flies post-infection and observed that flies with reduced function of Jra live longer with reduced bacterial loads. This established Jra as a negative regulator of the gut immune response, a previously unknown role. Since I aim to study the effect of SUMOylation on the function of Jra, I also looked at the role of components of SUMO conjugation machinery in regulating the gut immune response. It was interesting to find that all the components work concurrently to suppress the gut-specific



immune response. Using the Jra<sup>SCR</sup> line, I have discovered that Jra<sup>SCR</sup> is a hypermorph of Jra as flies respond poorly to infection and succumb early. Using 3' mRNA sequencing of the RNA extracted from the gut tissue, I have identified that Jra<sup>SCR</sup> flies show inadequate activation of several key defence genes including AMPs necessary to neutralize the pathogen. I further used a Jra specific ChIP-seq dataset that was published to map Jra binding on the promoter of the significantly differentially genes from the RNA seq dataset. Since Jra<sup>RNAi</sup> and Jra<sup>SCR</sup> function as hypomorph and hypermorph respectively, I focused the analysis on genes that showed opposite expression patterns. The genes that had an enriched peak of Jra on the promoters and showed opposite expression patterns were considered to be confident transcriptional targets of Jra. These include *Relish*, *Dorsal*, *Fkh*, *Chinmo* and *Ets21C* that have known roles to regulate the gut immune response in *Drosophila*. This indicates that Jra regulates the transcription of several genes defence genes and modulates the immune response. Further, SUMO conjugation of Jra is necessary to evoke a proper immune response against an invading pathogen. We propose that SUMOylation of Jra fine-tunes the function of Jra and regulates gut immune homeostasis in *Drosophila*.

#### **Publications/ Manuscripts in Preparation**

1. Handu M, Kaduskar B, Ravindranathan R, **Soory A**, Giri R, Elango VB, Gowda H, Ratnaparkhi GS (2015). SUMO-Enriched Proteome for *Drosophila* Innate Immune Response. *G3 (Bethesda)*. Aug 18;5(10):2137-54. doi: 10.1534/g3.115.020958
2. Hegde S, **Soory A**, Kaduskar B, Ratnaparkhi GS. SUMO conjugation regulates immune signalling. *Fly (Austin)*. 2020 Mar-Dec;14(1-4):62-79. doi: 10.1080/19336934.2020.1808402
3. **Soory A**, Ratnaparkhi GS SUMOylation of Jun fine-tunes the *Drosophila* gut immune response. 10.1101/2021.08.12.456072;
4. Kumar P, **Soory A**, Mustfa S, Sarmah D, Chatterjee S, Bossis G, Ratnaparkhi GS, Srikanth CV Bidirectional regulation of AP-1 and SUMO genes modulates inflammation condition during *Salmonella Typhimurium* infection. *Manuscript in Preparation*

## Table of Contents

|   |           |
|---|-----------|
| <b>Chapter 1 : Introduction to Immune signalling in <i>Drosophila</i> .....</b>   | <b>1</b>  |
| 1.1 Innate immunity in <i>Drosophila</i> .....  | 1         |
| 1.1.1 Cellular immunity .....   | 1         |
| 1.1.1 Humoral immunity.....   | 3         |
| 1.2 Immune signalling in <i>Drosophila</i> .....  | 4         |
| 1.2.1 Imd Signalling pathway .....  | 4         |
| 1.2.2 JNK signalling pathway.....   | 7         |
| 1.2.3 Toll signalling pathway.....  | 9         |
| 1.2.4 JAK/STAT signalling pathway.....  | 13        |
| 1.3 Role of post-translational modifiers in the regulation of immune signalling .....   | 15        |
| 1.3.1 Phosphorylation .....   | 15        |
| 1.3.2 Ubiquitination .....  | 16        |
| 1.3.3 SUMOylation.....  | 18        |
| Aim of the study.....   | 20        |
| 1.4 References.....   | 21        |
| <b>Chapter 2 The <i>Drosophila</i> AP-1 dimer proteins Jun related antigen (Jra) and Kayak (Kay) are post-translationally modified by SUMO.....</b> | <b>36</b> |
| 2.1 Abstract.....   | 36        |
| 2.2 Introduction.....   | 37        |

|  |           |
|--|-----------|
| 2.2.1 Proteomic screen to identify targets with differential SUMOylation status .....                              | 37        |
| 2.2.2 Diverse roles of the JNK signalling pathway in Drosophila.....   | 39        |
| 2.3 Results and Discussion .....   | 44        |
| 2.3.1 Demonstration of SUMOylation of Jra and Kay .....  | 44        |
| 2.3.2 Identification of lysine acceptor sites in Jra and Kay .....   | 45        |
| 2.3.3 In-vivo demonstration of SUMOylation of Jra and Kay in S2 cell .....   | 48        |
| 2.4 Discussion.....  | 50        |
| 2.5 Materials and Methods.....   | 52        |
| 2.5.1 Cloning and generation of constructs .....   | 52        |
| 2.5.2 Bacterial SUMOylation assay.....   | 53        |
| 2.5.3 S2 cell culture and transfections .....  | 53        |
| 2.5.4 Pulldown, Immunoprecipitation and Western blotting.....  | 54        |
| 2.6 References.....  | 56        |
| <b>Chapter 3 : Generation of SUMO Conjugation resistant mutants of Jra and Kay.....</b>                            | <b>60</b> |
| 3.1 Abstract.....  | 60        |
| 3.2 Introduction.....  | 61        |
| 3.2.1 The UAS-GAL4 system serves as a tool to overexpress transgenes of interest in a spatio-temporal manner ..... | 61        |
| 3.2.2 CRISPR/Cas9 as a tool to edit the genome and generate transgenics in Drosophila .....                        | 61        |
| 3.3 Results and Discussion .....   | 67        |

|   |           |
|---|-----------|
| 3.3.1 Rescue of embryonic lethality of jra and kay null flies using UAS transgenics.....                            | 67        |
| 3.3.2 Editing the genomic locus of jra and kay using CRISPR/Cas9 .....  | 69        |
| 3.4 Summary .....   | 78        |
| 3.5 Materials and Methods.....  | 80        |
| 3.5.1 Fly husbandry and lines used .....  | 80        |
| 3.5.2 Cloning.....  | 81        |
| 3.5.3 Western blotting.....   | 82        |
| 3.5.4 Genomic DNA isolation .....   | 83        |
| 3.6 References.....   | 84        |
| <b>Chapter 4 : SUMOylation of Jra regulates gut immune response and helps maintain gut immune homeostasis .....</b> | <b>87</b> |
| 4.1 Abstract.....   | 87        |
| 4.2 Introduction.....   | 88        |
| 4.2.1 Drosophila midgut as a tool to study the immune response .....  | 88        |
| 4.2.2 Pseudomonas entomophila: A robust gram-negative pathogen.....   | 92        |
| 4.3 Results and Discussion .....  | 94        |
| 4.3.1 Jra is a negative regulator of the gut immune response .....  | 94        |
| 4.3.2 Components of SUMO conjugation machinery negatively regulate gut immunity in Drosophila.....                  | 100       |
| 4.3.3 SUMO conjugation of Jra attenuates the suppression of immune response by Jra .....                            | 102       |

|   |            |
|---|------------|
| 4.3.4 Jra is a suppressor of defence genes in the gut .....                         | 109        |
| 4.3.5 Jra <sup>SCR</sup> is a stronger suppressor of defence genes in the gut ..... | 114        |
| 4.4 Summary .....   | 123        |
| 4.5 Materials and methods .....   | 128        |
| 4.5.1 Fly husbandry and lines .....   | 128        |
| 4.5.2 Bacterial culture, gut infection and fly survival assays: .....               | 129        |
| 4.5.3 Bacterial clearance assay .....   | 130        |
| 4.5.4 Gut dissections, immunostaining and microscopy.....                           | 130        |
| 4.5.5 qRT-PCR.....  | 131        |
| 4.5.6 RNA isolation, cDNA library preparation and sequencing .....                  | 131        |
| 4.5.7 Read mapping, counts generation and differential expression analysis .....    | 131        |
| 4.5.8 ChIP-seq data analysis .....  | 132        |
| 4.6 References.....   | 133        |
| <b>Appendix I : 3'mRNA seq and ChIP seq analysis .....</b>                          | <b>139</b> |
| I.a 3'mRNA seq analysis .....   | 139        |
| I.b Codes used for 3'mRNA seq analysis .....  | 140        |
| I.c ChIP-seq analysis.....  | 141        |
| I.d Codes used for plotting Jra occupancy on ChIP-seq files .....                   | 142        |
| <b>Appendix II : Generation of Jra antibody .....</b>                               | <b>166</b> |

## List of Figures

|  |    |
|--|----|
| Figure 1.1: Innate immunity in <i>Drosophila</i> .....   | 3  |
| Figure 1.2: Imd and JNK signalling pathways.....   | 8  |
| Figure 1.3: Toll signalling pathway .....  | 12 |
| Figure 1.4: JAK-STAT signalling pathway .....  | 14 |
| Figure 1.5: Targets of SUMO conjugation in immune signalling .....   | 19 |
| Figure 2.1: The SUMO cycle.....  | 37 |
| Figure 2.2: Jra and Kay show altered SUMOylation status upon an immune challenge in <i>Drosophila</i> S2 cells.....        | 39 |
| Figure 2.3: Schematic representing the canonical JNK signalling pathway in <i>Drosophila</i> . ...                         | 40 |
| Figure 2.4: Multiple sequence alignment (MSA) of homologs .....  | 43 |
| Figure 2.5: Jra and Kay are SUMOylated in in-vitro.....  | 44 |
| Figure 2.6: Identification of putative SUMO acceptor lysine residues by JASSA.....   | 45 |
| Figure 2.7: Site-directed mutagenesis screen to identify SUMO acceptor lysine residues in Jra and Kay. ....                | 47 |
| Figure 2.8: Demonstration of complete loss of SUMOylation in Jra and Kay.....  | 48 |
| Figure 2.9: Demonstration of SUMOylation of Jra and Kay in S2 cells and confirmation of SUMO acceptor lysine residues..... | 49 |
| Figure 2.10: Summary of SUMO acceptor lysine residues. ....  | 51 |
| Figure 3.1: Schematic of working of UAS-GAL4 system.....   | 61 |
| Figure 3.2: CRISPR/Cas9 mediated strategy to generate genomic edits.....   | 65 |
| Figure 3.3: Demonstration of expression of UAS transgenic flies .....  | 67 |
| Figure 3.4: Schematic of rescue crosses. ....  | 68 |

|  |     |
|--|-----|
| Figure 3.5: Schematic of the approach used for the generation of Jra <sup>SCR</sup> and Kay <sup>SCR</sup> using CRISPR/Cas9 technology..... | 70  |
| Figure 3.6: Schematic of integration of pHD-scarless-Jra <sup>SCR</sup> into the genomic locus of Jra ..                                     | 72  |
| Figure 3.7: Schematic of genetic crosses to generate Jra <sup>SCR</sup> flies.....   | 74  |
| Figure 3.8: Snapshot of sequencing showing three independent lines. ....   | 75  |
| Figure 3.9: Snapshot describing the ssODN used to incorporate the desired mutation in Kay .....  | 76  |
| Figure 3.10: Schematic of genetic crosses to generate Kay <sup>SCR</sup> flies.....  | 77  |
| Figure 4.1: Anatomical features of the gut in <i>Drosophila</i> .....  | 91  |
| Figure 4.2: Jra <sup>RNAi</sup> and Jra <sup>DN</sup> enhance the survival of flies post-infection .....                                     | 95  |
| Figure 4.3: Jra hypomorphs enhance the survival of flies post-infection .....  | 95  |
| Figure 4.4: Overexpression of Bsk <sup>DN</sup> enhances survival upon gut infection.....  | 96  |
| Figure 4.5: Overexpression of Kay <sup>DN</sup> does not alter the survival upon gut infection.....  | 97  |
| Figure 4.6: jra <sup>IA109/+</sup> clears bacteria significantly faster than the wild type .....   | 98  |
| Figure 4.7: Jra hypomorphs do not show any significant change in pH3 positive cells as compared to wildtype flies.....                       | 99  |
| Figure 4.8: Knockdown of SUMO machinery components enhances the survival in <i>Drosophila</i> . .....  | 101 |
| Figure 4.9: Jra <sup>SCR</sup> flies show reduced survival upon infection .....  | 102 |
| Figure 4.10: Jra <sup>SCR</sup> behaves like a hypermorph in the heterozygous combination of the null allele.....                            | 104 |
| Figure 4.11: Bacterial clearance and number of pH3 positive cells in Jra <sup>SCR</sup> and Jra <sup>WT</sup> .....                          | 105 |
| Figure 4.12: Puckered has no effect on the lifespan during a gut infection.....  | 106 |
| Figure 4.13: Overexpression of Jra <sup>WT</sup> in the gut, shows partial rescue of Jra <sup>SCR</sup> phenotype.                           | 107 |

|  |     |
|--|-----|
| Figure 4.14: Overexpression of Jra <sup>WT</sup> in the jra expressing domain, shows complete rescue of Jra <sup>SCR</sup> phenotype. ....         | 108 |
| Figure 4.15: Quantitation showing the kinetics of activation of Jra transcripts in >w <sup>1118</sup> and >Jra <sup>RNAi</sup> .....               | 110 |
| Figure 4.16: Representation of the data obtained from >w <sup>1118</sup> and >Jra <sup>RNAi</sup> 3' mRNA sequencing experiment.....               | 112 |
| Figure 4.17: Quantitation showing the kinetics of activation of Jra transcripts in Jra <sup>SCR</sup> and Jra <sup>WT</sup> during infection. .... | 115 |
| Figure 4.18: Representation of the data obtained from Jra <sup>WT</sup> and Jra <sup>SCR</sup> 3' mRNA sequencing experiment.....                  | 117 |
| Figure 4.19: Occupancy of Jra on the gene body of significantly differentially expressed genes .....   | 121 |
| Figure 4.20: Regulation of gut specific immune response by SUMOylation of Jra.....   | 125 |
| Figure II.1: Purification of Jra .....   | 166 |
| Figure II.2: Purified Jra after size exclusion chromatography.....   | 167 |
| Figure II.3: Binding of anti-Jra sera to Jra in an indirect ELISA experiment .....   | 168 |
| Figure II.4: Binding of purified anti-Jra antibody to Jra in an indirect ELISA experiment ..   | 168 |



## List of tables

|   |     |
|---|-----|
| Table 2.1: List of primers.....   | 52  |
| Table 3.1: Outcome of null lethality rescue crosses. A) Jra. B) Kay.....  | 69  |
| Table 3.2: List of flylines used .....  | 80  |
| Table 3.3: List of primers used .....   | 81  |
| Table 4.1: Representative list of genes in >Jra <sup>RNAi</sup> as compared to w <sup>1118</sup> at UC condition... | 110 |
| Table 4.2: Representative list of immune-related genes in >w <sup>1118</sup> and >Jra <sup>RNAi</sup> datasets..... | 114 |
| Table 4.3: Representative list of immune-related genes in Jra <sup>WT</sup> and Jra <sup>SCR</sup> datasets.....    | 119 |
| Table 4.4: List of bonafide Jra targets that show opposite expression patterns.....                                 | 122 |
| Table 4.5: Fly lines used .....   | 128 |
| Table I.1: List of genes with enriched Jra peak on their promoters.....   | 143 |

## **Chapter 1 : Introduction to Immune signalling in *Drosophila***

### **1.1 Innate immunity in *Drosophila***

*Drosophila* is one of the most successfully used model organism to study basic concepts of immunity. This remarkable success comes from the similarity of the histopathological and physiological features to that of higher mammals. *Drosophila* like all metazoans has a robust innate immunity that is functionally analogous to mammalian innate immunity. The innate immunity in *Drosophila* is broadly classified into cellular immunity and humoral immunity. Cellular immunity is driven by the different types of cells present in the hemolymph and humoral immunity is driven by the fat body, the gut, the brain and the malphigian tubules which produce several effector molecules like anti-microbial peptides (AMPs), reactive oxygen species (ROS) and, neutralizing enzyme. In the following sections of this chapter, I discuss several keys components and pathways the regulate the innate immunity in the fruit fly

#### **1.1.1 Cellular immunity**

*Drosophila* like all other arthropods has an open circulatory system. This means that all the body organs are bathed in the hemolymph and the transfer of nutrients takes place directly from the hemolymph. The hemolymph is analogous to the blood of higher organisms and predominantly has three types of cells; the plasmatocytes, the lamellocytes and the crystal cells (Figure 1.1). These collectively are referred to as hemocytes and constitute the robust cellular immunity in *Drosophila*. Plasmatocytes are the largest in number and contribute to around 95% of the hemocytes. There are the predominant phagocytotic cells in *Drosophila* and perform a series of functions like the removal of apoptotic cells, synthesis and secretion of the extracellular matrix in addition to attacking and neutralizing the invading pathogen. During

development, plasmatocytes are crucial in eliminating apoptotic cells. Plasmatocytes recognize the apoptotic cell bodies by several classes of receptors present on the cell surface. These include scavenger receptors like Croquemort, Eater, Draper and members of the nimrod family (Franc et al., 1999; Kocks et al., 2005; Kuraishi et al., 2009; Kurucz et al., 2007; Somogyi et al., 2008; Tung et al., 2013). Interestingly, the same class of receptors play an important role in recognising foreign particles as observed from several loss of function mutants which have defects in recognising and phagocytosing invading pathogens (Hashimoto et al., 2009; Philips et al., 2005; Ramet et al., 2002). A recent study suggests synergistic crosstalk among the receptors is required for bacterial phagocytosis (Melcarne et al., 2019). Crystal cells that account for 5% of the hemocytes constitute the second cell type. They play a crucial role in regulating melanization reaction upon injury which is analogous to a blood clot. These cells express key enzymes required for the melanization process called prophenoloxidases (PPO). Activation of PPOs by a cascade of serine proteases is a critical step during the melanization process (Ayres and Schneider, 2008; Castillejo-Lopez and Hacker, 2005; Tang et al., 2008). PPOs further oxidizes phenols to quinones that in turn polymerises into melanin. The third cell type, the lamellocytes constitute less than 1% of all the hemocytes. The best-documented function of the lamellocytes is their ability to encapsulate the eggs of wasp *Leptopilina boulardi* (Lanot et al., 2001; Rizki and Rizki, 1992). The differentiation of hemocytes to lamellocytes play a crucial role during a response to wasp infestation (Markus et al., 2009) and JAK/STAT signalling plays a major role. When the hemocytes encounter a wasp egg, they secrete Upd ligands which activate the JAK/STAT signalling in the muscle tissue. This signal is necessary for hemocytes to differentiate into lamellocytes and encapsulate the wasp eggs (Yang et al., 2015). Other pathways like the Toll and the JNK signalling pathways are also necessary to drive differentiation of hemocytes to lamellocytes (Schmid et al., 2014; Williams et al., 2006; Zettervall et al., 2004). Since hemocytes constantly circulate in the hemolymph, there are the

first cells to arrive at the site of injury or the site of entry of a pathogen. Although the contribution of AMP production by hemocytes is low (Charroux and Royet, 2009; Defaye et al., 2009; Nehme et al., 2011), they regulate other immune organs like the fat body and the gut to activate the AMP production (Agaisse et al., 2003; Brennan et al., 2007; Shia et al., 2009). Recent evidence suggests the ROS from hemocytes primes the immune system through the activation of Toll and JAK/STAT pathways (Chakrabarti and Visweswariah, 2020).

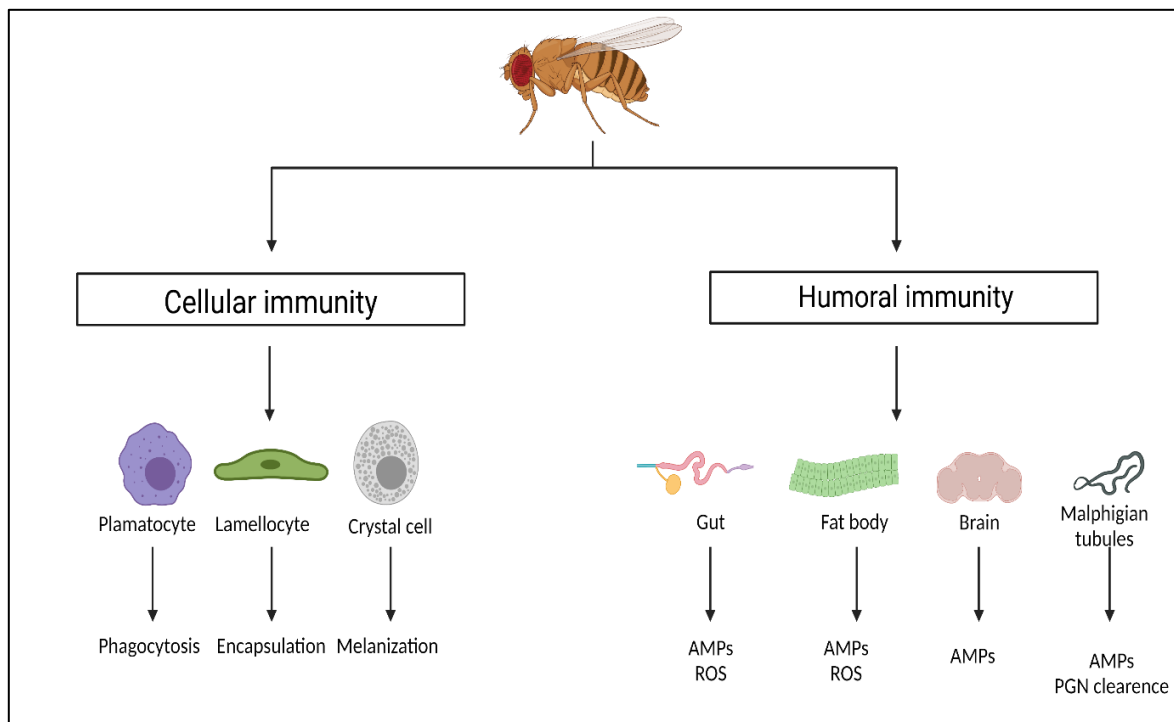


**Figure 1.1: Innate immunity in *Drosophila***

Schematic showing the components of the innate immunity in *Drosophila*. Innate immunity is divided into the cellular arm and the humoral arm. The cellular arm is governed by the cells of the hemolymph that perform the function of phagocytosis, encapsulation and melanization. The humoral is predominantly governed by the fat body and organs like the gut, brain and malphigian tubules providing supporting roles Adapted from (Buchon et al., 2014; Gold and Bruckner, 2015; Vlisidou and Wood, 2015).

### 1.1.1 Humoral immunity

Humoral immunity in *Drosophila* comprises all the nullifying agents that target the invading pathogen. The AMPs constitute the major arm of humoral immunity. AMPs are short peptides that are usually 100-150 amino acids in length. More than 20 AMPs have been discovered in

the fly genome and are grouped into 7 classes (Lemaitre and Hoffmann, 2007). AMPs are generally not found when there is no infection but the activation increases several-fold when there is an active infection. The fat body is one of the primary source of AMPs during an infection (Hanson and Lemaitre, 2020). However, recent evidence suggests the other organs like the gut (Buchon et al., 2013; Lemaitre and Miguel-Aliaga, 2013), brain (Kounatidis et al., 2017) and malphigian tubules (Li et al., 2020; Troha et al., 2019) also play an important role in secreting AMPs (Figure 1.1). Apart from fighting the infections, AMPs also modulate other physiological aspects like neurodegeneration and ageing (Hanson and Lemaitre, 2020). Key immune signalling pathways that generate AMPs are described in the next section. Another important aspect of humoral immunity is the production of ROS against the pathogen. Two NADPH enzymes, Duox and Nox predominantly govern the generation of ROS in the fly. Flies lacking both these enzymes are susceptible to enteric infection and succumb early (Bae et al., 2010; Ha et al., 2005; Jones et al., 2013).

## **1.2 Immune signalling in *Drosophila***

For any organism to evoke a robust immune response against an invading pathogen, a precise activation of several signalling pathways is very important. The signalling pathways that govern the innate immunity in *Drosophila* are conserved. The primary immune effector pathways in *Drosophila* are the Toll and the Imd pathways. Apart from these two pathways, the activation of other pathways like JNK and JAK-STAT is crucial and plays a supporting role in the battle against the pathogen. The following section summarises key signalling events that lead to the activation of these pathways

### **1.2.1 Imd Signalling pathway**

The Imd pathway came into existence by the discovery of a mutation in a gene that showed reduced levels of AMPs and survival of flies upon an immune challenge. This gene was

characterised and named *immune-deficient* (Imd) (Lemaitre et al., 1995a). The activation of the Imd pathway starts with the recognition of the bacterial cell wall components. Peptidoglycan (PGN) is one of the abundant molecules in the cell walls of bacteria and is recognised by the Peptidoglycan recognition proteins (PGRPs) (Figure 1.2). The activation of the Imd pathway is specific to the DAP-type peptidoglycan predominantly seen in gram-negative bacteria and few species of gram-positive bacteria like *Bacillus* and *Listeria* (Kaneko et al., 2006). *Drosophila* has 13 genes that encode for PGRPs which include cell-surface receptors, intracellular proteins and secreted extracellular proteins which are divided into two groups based on the presence or absence of amidase activity (Werner et al., 2003; Werner et al., 2000; Zaidman-Remy et al., 2006). PGRP-LC is the principal receptor that activates the Imd signalling pathway once bound to DAP-type peptidoglycan (Choe et al., 2002; Gottar et al., 2002; Ramet et al., 2002). PGRP-LC has 2 characterised splice variants: PGRP-LCx that recognises the polymeric PGN; PGRP-LCa that acts as a coreceptor to PGRP-LCx to recognize monomeric PGN (Chang et al., 2006; Lim et al., 2006). In addition to PGRP-LC, another PGRP protein, PGRP-LE also activates the Imd pathway independently of PGRP-LC (Kaneko et al., 2006; Neyen et al., 2012; Takehana et al., 2002). PGRP-LE lacks the typical transmembrane domain that is observed in PGRP-LC, is present in the cytoplasm and is known to recognise intracellular pathogens (Yano et al., 2008). Both PGRP-LC and PGRP-LE interact with Imd (Aggarwal and Silverman, 2008). Imd is a death-domain containing protein that is orthologous to mammalian RIP1. Interestingly, PGRP-LC, PGRP-LE, Imd and other members of the pathway contain a domain that is similar to RIP homotypic interaction motifs (RHIMs). In mammals RIPK1 and RIPK2 that also contain the RHIM domain form amyloid complexes and induce necroptosis (Li et al., 2012). Recent studies have identified that PGRP-LC, PGRP-LE and Imd form amyloid fibrils and important for the signal transduction which suggests an evolutionarily conserved mechanism to activate NFκB pathway (Kleino et al., 2017). Upon

activation, Imd forms a complex with an adaptor protein, Fadd and a caspase, Dredd (Choe et al., 2005; Leulier et al., 2002). Dredd is activated by Iap2, an E3 ubiquitin ligase. Activated Dredd cleaves Imd at the N-terminus and this exposes a binding site for Iap2. Iap2 further activates Imd by ubiquitination (Meinander et al., 2012; Paquette et al., 2010). Activated and cleaved Imd recruits the Tak1/Tab2 kinase complex and this complex is necessary to further activate the IKK complex members Ird5 (IKK $\beta$ ) and Kenny (IKK $\gamma$ ) (Kleino et al., 2005; Lu et al., 2001; Rutschmann et al., 2000b). The most downstream effector of the Imd pathway is the NF $\kappa$ B transcription factor Relish (Rel). The members of the NF $\kappa$ B family are sequestered in the cytoplasm in an inactive form by the I $\kappa$ Bs. Rel is a peculiar member of the NF $\kappa$ B family in *Drosophila* that has the I $\kappa$ B domain present in the C-terminus of the protein. For Rel to be active, the C-terminal I $\kappa$ B domain has to be cleaved exposing the nuclear localization signal and allowing it to homodimerize. The activation of Rel is a two-step process. The first one involves phosphorylation by the IKK complex (Silverman et al., 2000) and the second involves the cleavage of the C-terminus by the caspase, Dredd (Stoven et al., 2000; Stoven et al., 2003). Once Rel is activated by phosphorylation and cleaved by caspase action, the N-terminus polypeptide (Rel<sup>68</sup>) translocates into the nucleus and activates the transcription of several antimicrobial peptides (AMPs) (Badinloo et al., 2018; Stoven et al., 2000). These AMPs show remarkable specificity to the type of the pathogen (Hanson et al., 2019). Recent studies show that Rel also binds to a cofactor called Akirin and regulates the transcription of a specific subset of targets (Bonney et al., 2014). In addition to activating the transcription of AMPs, Rel also activates the transcription of a gene called *pirk*. The expression of *pirk* is necessary to turn off the Imd pathway. Pirk interferes with the interaction of PGRP-LC and Imd and inhibits the signalling cascade (Kleino et al., 2008)(Aggarwal et al., 2008). Caspar another negative

regulator blocks the Imd pathway by inhibiting the Dredd dependant cleavage and activation of Relish (Kim et al., 2006).

### ***1.2.2 JNK signalling pathway***

The JNK pathway is highly conserved and one of the 3 MAPK pathways that respond to stress. Members of the JNK pathway in *Drosophila* have been well studied during the dorsal closure stage of early embryonic development (Rios-Barrera and Riesgo-Escovar, 2013). The JNK pathway can be directly activated by the TNF/TNFR duo Eiger and Wengen, to regulate apoptosis (Igaki et al., 2011; Kanda et al., 2002; Kauppila et al., 2003). However, most often, the JNK signalling pathway relays signals from other pathways. One classic example of this is the activation of the JNK pathway by the Imd pathway (Figure 1.2). As mentioned in the previous section, Imd activates Tak1 and post this step, the pathway bifurcates into two (Kleino et al., 2005; Lu et al., 2001; Rutschmann et al., 2000b). Tak1 is a bonafide JNKKK and required to activate the downstream JNKK, Hemipterous (Hep) which further relays the signal to Basket (Bsk). Bsk then activates the transcription factors Jra and Kay (Boutros et al., 2002; Delaney et al., 2006; Silverman et al., 2003).



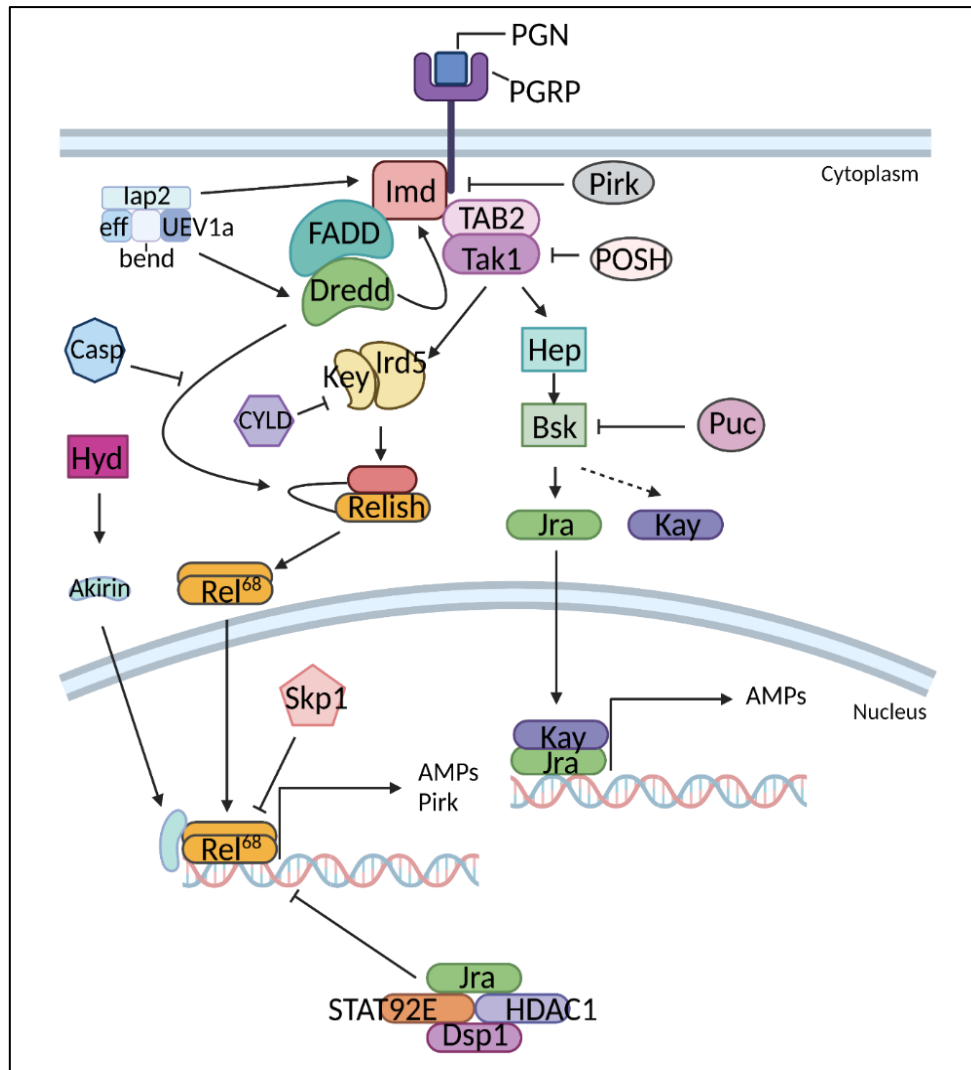


**Figure 1.2: Imd and JNK signalling pathways**

Schematic describing the activation of Imd and JNK signalling pathways in *Drosophila* during an immune challenge. The DAP-type peptidoglycan is recognised by the PGRP-LC receptor on the cell surface. The adapter molecule Imd is activated and through a series of complex steps involving several post-translational modifiers, the signal is relayed to Tak1. The pathway bifurcates at this stage and Tak1 acts as a kinase for the IKK complex and JNKK, Hep. The signal from IKK transduces to Rel and this leads to the nuclear localization of Rel and activation of AMPs. In parallel, Hep activates JNK and JNK in turn activates Jra and Kay forming a heterodimer. The heterodimer translocates into the nucleus and activates the transcription of AMPs apart from blocking Rel dependent transcription. Adapted from (Myllymaki et al., 2014).

Though it is known that the JNK pathway is activated upon an immune stimulus (Sluss et al., 1996), the outcome of the activation of this pathway has been subjected to much debate and discussion. Initial reports identified that the JNK pathway is not required for the activation of AMPs. Rather, it is required for the activation of genes necessary for injury and tissue repair

during a septic prick (Boutros et al., 2002). The JNK pathway is also necessary for the activation of genes involved in cellular immune response (Silverman et al., 2003). Interestingly, another study reported that the JNK pathway is necessary for the activation of AMPs (Delaney et al., 2006). The same study suggests that the activation of Imd and JNK is independent of each other. A much more comprehensive study to understand the role of JNK signalling in regulating the immune response was performed by Kim and colleagues. They report that the loss of components of the JNK pathway increases the transcription of several AMPs upon an immune challenge. Further, the JNK transcription factor Jra interacts with HDAC1, STAT92E and Dsp1 to form a repressosome complex and represses the transcription of Rel dependent genes and thereby negatively regulates the Imd mediated immune response (Kim et al., 2007; Kim et al., 2005). Not many proteins are known that regulate the JNK pathway. The ubiquitin ligase POSH regulates the levels of Tak1 (Tsuda et al., 2005) and in turn, could regulate the activation of the JNK pathway. There is evidence that Rel regulates proteasomal degradation of Tak1 and thus shuts the JNK signalling (Park et al., 2004). However, the Rel dependent genes that regulate proteasomal degradation of Tak1 are yet to be identified. Another interesting regulation of the JNK pathway is by a feedback loop. Active Jra positively regulates the transcription of a phosphatase called *puckered* (Puc). Puc targets Bsk and dephosphorylates it attenuating the signalling cascade (Martin-Blanco et al., 1998).

### ***1.2.3 Toll signalling pathway***

The components of the Toll signalling pathway were discovered in the Heidelberg screen that showed defects in the dorsoventral patterning in the early embryo (Nusslein-Volhard et al., 1980; Nusslein-Volhard et al., 1984). A decade later, the Toll signalling pathway was linked to the increased expression of *CecA1*, an AMP by overexpressing the active form of Toll, i.e. Toll<sup>10B</sup> (Rosetto et al., 1995). This has led to a series of remarkable papers published in the following years that have revealed several molecular players in the pathway and their role in

regulating the immune response in *Drosophila*. Initial work indicated that the Toll pathway was specific to immunity against fungi and not bacteria. There are 9 Toll receptor paralogs in *Drosophila* and few have been implicated in regulating the immune response (Imler and Hoffmann, 2001; Imler et al., 2000; Ooi et al., 2002; Tauszig et al., 2000). The activation of the canonical Toll pathway does not happen by direct binding of the bacterial component to the receptor. Rather, the Toll signalling pathway is activated by binding of a ligand called Spätzle (Spz) (Morisato and Anderson, 1994; Schneider et al., 1994) (Figure 1.3). Spz is secreted as an inactive precursor and is cleaved and activated by SPE upon an immune challenge (Jang et al., 2006). Three independent pathways were discovered to activate SPE. The Lys-type peptidoglycan present in the cell wall of the gram-positive bacteria is recognised by the PGRP-SA and GNBPI extracellular receptor complex (Buchon et al., 2009b). Alternatively, Lys-type peptidoglycan can also be recognised by PGRP-SD (Bischoff et al., 2004).  $\beta$ -glucan present in Fungi is recognised by GNBPI3 (Gottar et al., 2006). Both these pathways independently converge at modular serine protease (ModSP). ModSP activates another serine protease Grass. Grass along with 4 other pseudoproteases Spirit, Spheroid, Sphinx1 and Sphinx2 forms a complex and finally activate SPE (Buchon et al., 2009b; El Chamy et al., 2008; Kambris et al., 2006). The third pathway involves activation of SPE by Persephone (Psh). Psh is cleaved and activated by direct binding of virulence factors from Fungi and gram-positive bacteria (El Chamy et al., 2008; Gottar et al., 2006). Interestingly, a recent study has demonstrated that Psh acts as a receptor and senses a wide range of bacterial pathogens through virulence factors (Issa et al., 2018). The pathway at the surface of the cell is activated when Spz binds to Toll and causes a conformational change in the receptor (Gangloff et al., 2008; Weber et al., 2005). This conformational change aids in the recruitment of the adaptor protein MyD88 via the TIR domain (Horng and Medzhitov, 2001; Tauszig-Delamasure et al., 2002). This interaction recruits a dimer of an adaptor protein, Tube and a

kinase, Pelle via the DD domain of Tube to MyD88 (Moncrieffe et al., 2008; Sun et al., 2002; Xiao et al., 1999). The downstream NFkB transcription factors Dorsal and Dif are sequestered in the cytoplasm by the Ikb ortholog, Cactus. Cactus must be degraded for the signal to transduce and Dorsal or Dif to translocate into the nucleus (Wu and Anderson, 1998). The kinase activity of Pelle is required for the degradation of Cactus and it is believed that Cactus phosphorylation is necessary for its degradation (Huang et al., 2010; Towb et al., 2001). It is still unclear whether Dorsal or Dif or both together activate the transcription of AMPs. There is evidence that Dorsal and Dif form heterodimers *in-vitro* (Gross et al., 1996). The transcripts of Dorsal increase in the fat body upon an immune challenge and the translocation of Dorsal into the nucleus is necessary for the activation of *diptericin* and *cecropin* (Edwards et al., 1997; Gross et al., 1996; Yang and Steward, 1997). Dif seems to be important for the immune response in larvae (Ip et al., 1993). Yet, Dorsal and Dif seem to be redundant in their function in the activation of *Drosomycin* (Manfruelli et al., 1999; Rutschmann et al., 2000a). In addition to activation of AMP response against the invading pathogen, the Toll pathways also play several crucial roles. The activation of the Toll pathway is necessary for fighting off the parasitoid wasp infection (Hultmark, 2003; Zettervall et al., 2004). Activation of Toll pathways leads to an increase in the number of haemocytes and further differentiation into lamellocytes that encapsulate and kill the wasp (Lemaitre et al., 1995b; Qiu et al., 1998; Sorrentino et al., 2004).

The Toll and Imd pathways show a remarkable specificity in recognising the type of pathogen and the type of AMPs secreted to negate the pathogens. However, there is ample evidence that suggests that both these pathways cross-talk to each other. Also, it is observed that the NFkB transcription factors interact with each other to direct a specific outcome (Tanji et al., 2007; Tanji et al., 2010). The physiological role of these major pathways has been poorly understood

and needs to be studied in greater details to gain better insights into the regulation of the immune response.

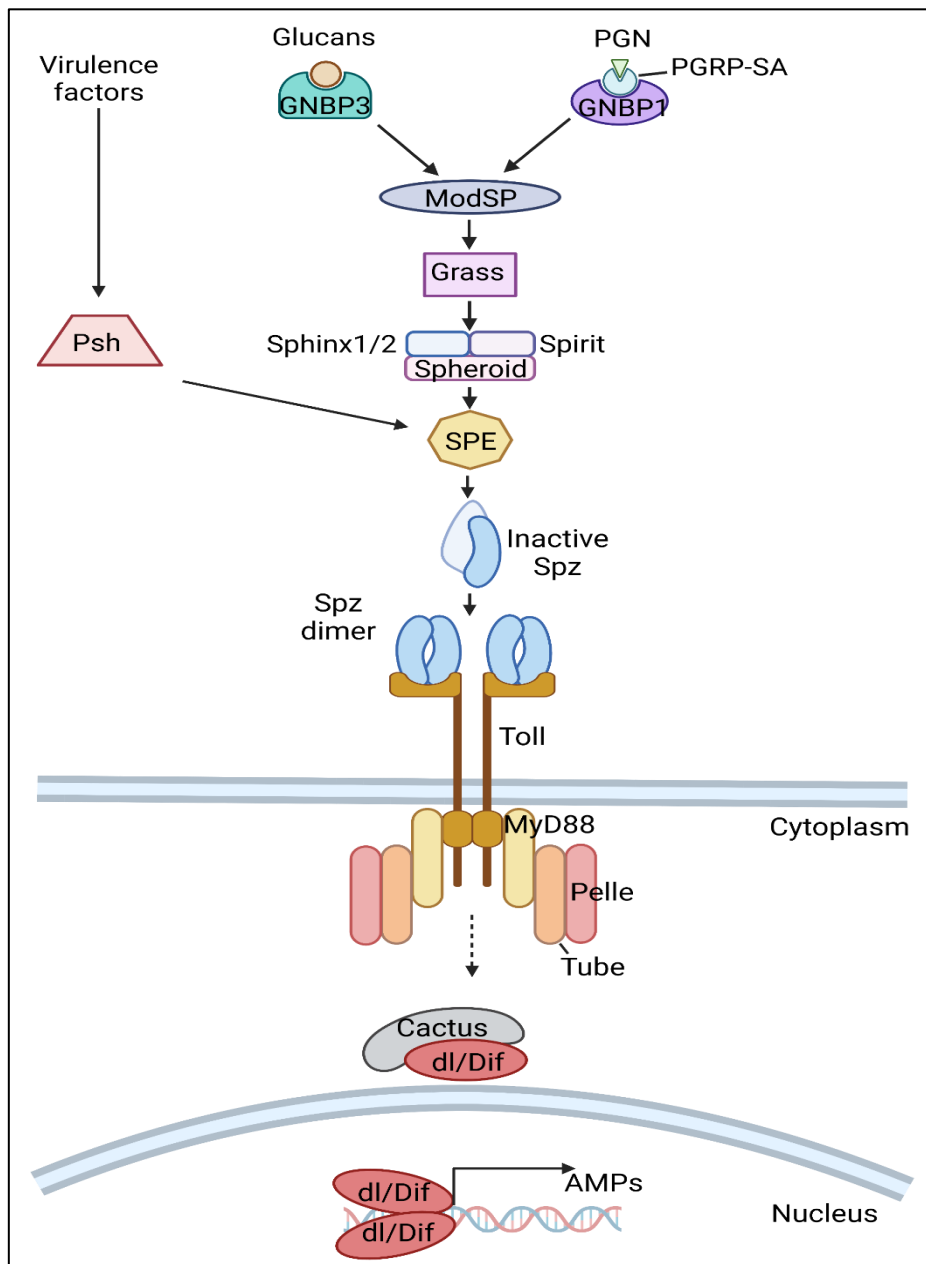


**Figure 1.3: Toll signalling pathway**

The Toll signalling pathway is activated when the extra-cellular ligand spatzle that is matured by SPE binds to the Toll receptor. The binding of lys-type PGN to PGRP-SA and GNBP1 complex and the binding of  $\beta$ -Glucans (present in cell wall of fungi) to GNBP3 activates SPE through a series of steps involving several serine proteases. The intracellular cascade involves the activation of MyD88, Tube and Pelle which ultimately leads to degradation of the I $\kappa$ B cactus and nuclear localization of NF $\kappa$ B factor, dl and Dif to transcribe AMPs. Adapted from (Valanne et al., 2011).

#### ***1.2.4 JAK/STAT signalling pathway***

JAK/STAT pathway is one of the well-studied pathways in the context of immunity in mammals. Mutations affecting the members of the pathway have serious implications in regulating inflammation, pathogen recognition and, auto-immunity (Casanova et al., 2012; O'Shea and Plenge, 2012). Moreover, this pathway can be triggered by a plethora of cytokines and numerous players involved in the pathway makes it a complex pathway to study and understand. *Drosophila* as a model system offers less redundancy in terms of the number of players that are involved core JAK/STAT pathway. There is a single JAK and a single STAT gene in the fly genome. The activation of the JAK/STAT pathway starts with the binding of the extracellular ligands to the receptor Dome (Figure 1.4). The Unpaired (Upd) ligands are the most well-studied ligands that activate the JAK/STAT pathway in *Drosophila* (Agaisse et al., 2003; Gilbert et al., 2005; Harrison et al., 1998; Hombria et al., 2005; Wright et al., 2011). Much of the current understanding of the activation of the *Drosophila* JAK/STAT signalling pathway comes from the work done in mammalian model systems. Binding of the Upds to Dome causes Dome to dimerise. This recruits the only know JAK, hopscotch (Hop) (Perrimon and Mahowald, 1986). Hop is a kinase and phosphorylates Dome (Binari and Perrimon, 1994). This causes a conformational change in the cytoplasm tail of Dome and the transcription factor STAT92E (Hou et al., 1996; Yan et al., 1996) is recruited to the cytoplasmic tail of Dome via its SH2 domain. Hop then phosphorylates STAT92E and this is required for dimerization and nuclear localization of STAT92E (Kiu and Nicholson, 2012). The activation of the JAK/STAT pathway is dampened by one of its targets, the Suppressor of cytokine signalling (SOCS). Socs36E is thought to interact with Dome and inhibit its phosphorylation by Hop (Stec et al., 2013). By an independent mechanism, Socs36E forms a ubiquitin E3 ligase complex with elongin and culin to regulate the levels of Dome on the cell surface (Vidal et al., 2010). Protein inhibitor of activated STAT (PIAS), a SUMO E3 ligase regulates the activity of PIAS by

SUMOylation in mammals. In *Drosophila*, PIAS inhibits the activity of STAT92E (Betz et al., 2001). However, if this inhibition is SUMOylation dependent remains to be unclear. The role of the JAK/STAT pathway in regulating the immune response is well studied in the gut. Several pathogenic bacteria seem to activate the pathway when orally fed (Buchon et al., 2009a; Cronin et al., 2009).

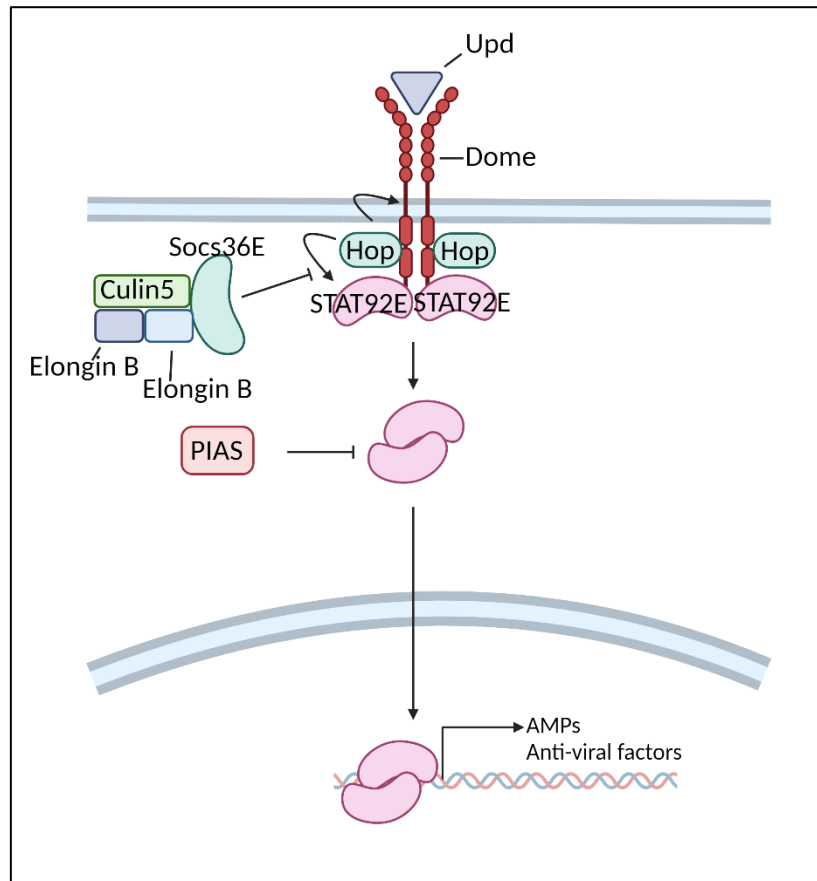


**Figure 1.4: JAK-STAT signalling pathway**

The JAK-STAT pathway in *Drosophila* is activated by the binding of the Upd ligands to the receptor, Dome. This binding causes a conformational change in the receptor and the ortholog of JAK, Hop is recruited to the intracellular domain of the receptor. Hop phosphorylates Dome and this leads to the recruitment of STAT92E to Dome. Hop further phosphorylates STAT92E and this causes STAT92E to dimerise and translocate into the nucleus activating AMPs and other factors. Socs36E, a member of the ubiquitin E3 ligase complex ubiquitinates Hop and drives its degradation. Another protein, the SUMO E3 ligase PIAS negatively regulates STAT92E.

Activation of JAK/STAT is necessary for transcriptional activation of gut-specific AMPs like Drs13. The JAK/STAT pathway in *Drosophila* is also implicated in the regulation of immune

response against viruses (Dostert et al., 2005). Components of the JAK/STAT pathway are strongly induced upon viral infection like *Drosophila* X virus and Flock House virus (Kemp et al., 2013). *Drosophila* C virus also activates the JAK/STAT pathway. Deficiency in the activation of the JAK/STAT pathway increases the viral load in the fly. Also, several genes that are activated upon DCV infection contain STAT binding sites on their promoters (Dostert et al., 2005).

### **1.3 Role of post-translational modifiers in the regulation of immune signalling**

Covalent and reversible conjugation of a functional group or a small protein to a target protein adds another dimension to the function of the target protein. Such additions of functional groups and other small protein molecules are referred to as post-translational modifications (PTMs). PTMs of proteins range from the addition of small functional groups like phospho, methyl and, acetyl to the addition of larger molecules like proteins or lipids. In recent times, there is an increase in the number of studies to identify different PTMs in proteins to understand the complexity involved in signalling pathways. There is ample evidence that the mammalian immune-related pathways are regulated by several PTMs (Liu et al., 2016). However, the regulation of *Drosophila* immune specific signalling pathways by PTMs is not well understood. The following section is to summarize few known examples of such regulation by phosphorylation, ubiquitination and SUMOylation during immune response in *Drosophila*.

#### **1.3.1 Phosphorylation**

Protein phosphorylation is one of the well characterised post-translational modifications. Many kinases act in immune signalling pathways and hence phosphorylation plays a crucial role in the regulation of the function of several proteins. One of the early phosphorylation events in the Imd pathway is the phosphorylation of the IKK complex by the Tak1/Tab2 kinase complex. Genetic evidence suggests that the Tak1/Tab2 complex is necessary to activate the IKK



complex comprising Ird5 and Kenny (Kleino et al., 2005; Lu et al., 2001; Rutschmann et al., 2000b). The IKK complex phosphorylates Rel on multiple residues on the N-terminus and assumed to prime it for Dredd dependant proteolytic cleavage (Silverman et al., 2000). In addition to this, IKK $\beta$ , Ird5 also phosphorylates Rel on S528 and S529. These phosphorylation events are unrelated to the activation of Rel but are required for the recruitment of the RNA polymerase to Rel during transcriptional activation of AMPs (Erturk-Hasdemir et al., 2009). The key phosphorylation events in the Toll signalling pathway occur at the level of degradation of the I $\kappa$ B, Cactus and activation of the NF $\kappa$ B, Dorsal. Ample evidence from understanding the early embryonic dorso-ventral patterning suggests that phosphorylation of these two players is of utmost importance for the signal to transduce further (Belvin et al., 1995; Drier et al., 1999; Gillespie and Wasserman, 1994; Govind, 1999; Reach et al., 1996). However, the phosphorylation events during Dorsal/Dif activation in the immune context is not well studied. The Janus kinase or Hopscotch of the JAK/STAT pathway is a bonafide kinase that regulates several branches of the pathway. Genetic evidence suggests that Hop is necessary to activate the downstream events in the pathway but the evidence of phosphorylation remains at large (Chen et al., 2002). The phosphorylation of Stat92E by Hop is well documented. An increase in phosphorylation of the Tyr-704 has been observed when the two proteins are co-expressed in S2 cells. Also, this increases the transcriptional activity of STAT *in-vitro* (Yan et al., 1996). The JNK pathway is a core kinase pathway where every step is regulated by phosphorylation and each step is characterised and well studied during early embryonic development. Different phosphorylation events are categorically listed in every member of the pathway (Botella et al., 2001; Ciapponi et al., 2001; Clavier et al., 2016; Kockel et al., 2001; Riesgo-Escovar and Hafen, 1997; Stronach and Perrimon, 2002). However, the role of phosphorylation of the JNK family members during an immune response has not been studied.

### ***1.3.2 Ubiquitination***

Ubiquitination is protein type post-translational modification. Ubiquitin is a small protein with a characteristic globular  $\beta$ -grasp fold that covalently conjugates to a lysine of a target protein. Ubiquitination plays an important role in regulating the Imd pathway. Regulation of the Imd pathway by ubiquitination is bidirectional and aids in both activation and repression of the pathway. Ubiquitin E3 ligases play a crucial role in the regulation of the Imd pathway. Iap2 aids in the ubiquitination and activation of the caspase Dredd (Meinander et al., 2012). Iap2 forms a complex with Bendless and Effete, the ubiquitin-conjugating enzymes that drive this crucial step (Zhou et al., 2005). Iap2 has another interesting role. It is required for the K63-dependant polyubiquitination of Imd. This step is crucial for the recruitment of the Tak1/Tab2 kinase complex to Imd (Paquette et al., 2010). In contrast to this, the ubiquitin-specific protease, Scny prevents the K63-dependant polyubiquitination of Imd and instead promotes K48-dependant polyubiquitination and subsequent degradation of Imd attenuating the signal transduction (Thevenon et al., 2009). In addition to this, Fat facets (Faf) also ubiquitinates Imd and negatively regulates the activation of AMPs (Yagi et al., 2013). Tak1 is another documented example of regulation by ubiquitin dependant degradation. The RING-finger domain-containing ubiquitin ligase POSH ubiquitinates Tak1 and inhibits activation of downstream events (Tsuda et al., 2005). CYLD is a ubiquitin-specific protease and interacts with the IKK $\gamma$  subunit Kenny and regulates the AMP response (Tsichritzis et al., 2007). The SCF family members of ubiquitin ligases also play a role in the regulation of the Imd pathway. Particularly, Skp1 ubiquitinates activated Rel in the nucleus and drives it for ubiquitin dependant proteasomal degradation (Khush et al., 2002). The co-factor Akirin is also ubiquitinated by the E3 ligase Hyd. This is essential for the proper interaction of Akirin with Rel and the further production of AMPs (Cammarata-Mouchtouris et al., 2020). SOCS proteins interact with other proteins to form the ubiquitin E3 ligase complex. Socs36E in *Drosophila* interacts with Culin-5, Elongin B and Elongin C to form a complex. This complex formation

drives the Dome internalization and subsequent lysosomal degradation (Stec et al., 2013). However, it is unclear if this is a ubiquitin dependant mechanism.

### ***1.3.3 SUMOylation***

SUMOylation is another PTM that belongs to the Ubiquitin-like (Ubl) protein modifiers. Like Ubiquitin, SUMO covalently conjugates to a lysine of a target protein and modulates its function, localization and, interaction with other proteins. The effect of SUMOylation in regulating the immune response in *Drosophila* is not well studied and few studies exist that describe the role of SUMOylation in regulating the function of immune specific proteins. . For example, Ird5 the IKK $\gamma$  homolog in *Drosophila* is SUMOylated upon infection on K152. SUMOylation of Ird5 is essential to activate the transcription of AMPs (Fukuyama et al., 2013). It is reported that the negative regulator of the Imd pathway, Caspar is SUMOylated on K551 (Handu et al., 2015). SUMO conjugation resistant mutants of Caspar generated by editing the genomic locus of Caspar using CRISPR/Cas9 show reduced lifespan of *Drosophila* (Kaduskar et al., 2020). However, the role of SUMOylation of Caspar in the regulation of Dredd dependant cleavage of Relish and activation of the Imd pathway remains to be unknown. The NF $\kappa$ B transcription factor Dorsal is SUMOylated on K382. Loss of SUMO conjugation increases the activity of Dorsal and suggests that SUMO conjugation is required to attenuate the transcriptional activity of Dorsal (Bhaskar et al., 2000). SUMOylation and subsequent ubiquitination of the mammalian I $\kappa$ B is well-studied (Aillet et al., 2012; Desterro et al., 1998). However, there is no physical evidence that the fly ortholog Cactus, is SUMO conjugated. Interestingly, strong genetic evidence suggests that the SUMO pathway and the Toll pathway in *Drosophila* interact with each other. Loss of function mutants of Ubc9 show phenotypes similar to that of the hyperactive Toll pathway (Chiu et al., 2005). The JAK/STAT pathway transcription factor STAT92E is SUMOylated on K152. SUMO conjugation of STAT92E is necessary to attenuate the transcriptional activity (Gronholm et al., 2010).

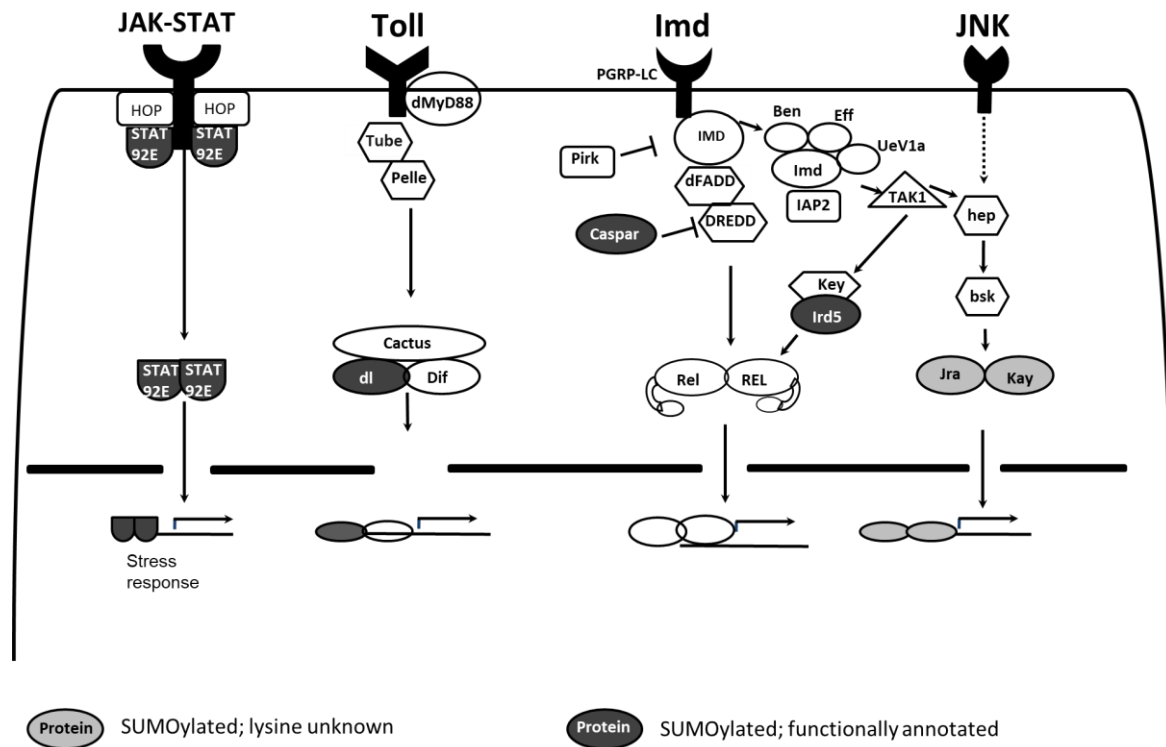


**Figure 1.5: Targets of SUMO conjugation in immune signalling**

Representation of the key immune signalling pathways namely Imd, JNK, Toll and Jak-STAT in *Drosophila*. Proteins that are SUMOylated are represented in shades of grey. Darker shade represents the identification of the target lysine residue and functional annotation of loss of SUMO conjugation. The lighter shade of grey represents proteins identified to be SUMOylated with functional annotation of the target lysine residue.

The context-specific role of PTMs in the regulation of protein function serves as an important parameter to understand complex events involved during a signalling cascade. Also, PTMs add another layer of regulation to fine tune the activity of a protein which is critical if the steps that precede like transcription or post transcriptional regulation fail. Also, PTMs are rapid and can bring about changes in activity of proteins in shorter time scales. Capturing these PTMs *in-vivo* poses a challenge as they are highly dynamic events and change rapidly. Work done in mammalian systems using high-throughput mass-spectrometric techniques sheds light on a few of these PTMs under different physiological contexts (Hendriks et al., 2017; Hendriks and Vertegaal, 2016; Kim et al., 2011; Ochoa et al., 2020; Park et al., 2015). In *Drosophila*, only a few studies exist which list out the different PTMs of proteins in a specific context (Nie et al.,

2009; Pirone et al., 2017; Ramirez et al., 2015). Using immune-precipitation followed by quantitative mass-spectrometry, we have identified a list of ~700 proteins to show altered SUMOylation status upon an immune challenge (Handu et al., 2015). The list includes known SUMO targets like STAT92E and Ird5 (Figure 1.5) besides a large number of proteins that were unidentified as targets for SUMO conjugation like Jra, Kay, AGO2 and, Pvr

It was exciting to pick the AP-1 dimer proteins Jun related antigen (Jra) and Kayak (Kay) as confident targets in the screen. Both these proteins show increased SUMOylation upon an immune challenge in S2 cells and the role of these proteins in regulating the immune response in *Drosophila* is unclear. This allows us to explore their function and the physiological relevance of SUMOylation of Jra and Kay during an immune response.

### **Aim of the study**

To understand the role of SUMOylation in regulating the function of Jra and Kay during the immune response in *Drosophila*.

### **Specific Aims**

- To demonstrate SUMOylation of Jra and Kay.
- To identify the SUMO acceptor lysine residues in Jra and Kay and generate a variant that is resistant to SUMO conjugation.
- To generate SUMO conjugation resistant transgenic fly lines of Jra and Kay. To perform null rescue using the transgenic line.
- To edit the genomic locus of Jra and Kay using CRISPR/Cas9 and generate SUMO conjugation resistant flies of Jra and Kay.
- To understand the role of SUMOylation of Jra and Kay in regulating the gut immune response in *Drosophila*.

## 1.4 References

1. Agaisse, H., Petersen, U.M., Boutros, M., Mathey-Prevot, B., and Perrimon, N. (2003). Signalling role of hemocytes in *Drosophila* JAK/STAT-dependent response to septic injury. *Dev Cell* 5, 441-450.
2. Aggarwal, K., Rus, F., Vriesema-Magnuson, C., Erturk-Hasdemir, D., Paquette, N., and Silverman, N. (2008). Rudra interrupts receptor signalling complexes to negatively regulate the IMD pathway. *PLoS Pathog* 4, e1000120.
3. Aggarwal, K., and Silverman, N. (2008). Positive and negative regulation of the *Drosophila* immune response. *BMB Rep* 41, 267-277.
4. Aillet, F., Lopitz-Otsoa, F., Egana, I., Hjerpe, R., Fraser, P., Hay, R.T., Rodriguez, M.S., and Lang, V. (2012). Heterologous SUMO-2/3-ubiquitin chains optimize I $\kappa$ B degradation and NF- $\kappa$ B activity. *PLoS One* 7, e51672.
5. Ayres, J.S., and Schneider, D.S. (2008). A signalling protease required for melanization in *Drosophila* affects resistance and tolerance of infections. *PLoS Biol* 6, 2764-2773.
6. Badinloo, M., Nguyen, E., Suh, W., Alzahrani, F., Castellanos, J., Klichko, V.I., Orr, W.C., and Radyuk, S.N. (2018). Overexpression of antimicrobial peptides contributes to aging through cytotoxic effects in *Drosophila* tissues. *Arch Insect Biochem Physiol* 98, e21464.
7. Bae, Y.S., Choi, M.K., and Lee, W.J. (2010). Dual oxidase in mucosal immunity and host-microbe homeostasis. *Trends Immunol* 31, 278-287.
8. Belvin, M.P., Jin, Y., and Anderson, K.V. (1995). Cactus protein degradation mediates *Drosophila* dorsal-ventral signalling. *Genes Dev* 9, 783-793.
9. Betz, A., Lampen, N., Martinek, S., Young, M.W., and Darnell, J.E., Jr. (2001). A *Drosophila* PIAS homologue negatively regulates stat92E. *Proc Natl Acad Sci U S A* 98, 9563-9568.
10. Bhaskar, V., Valentine, S.A., and Courey, A.J. (2000). A functional interaction between dorsal and components of the Smt3 conjugation machinery. *J Biol Chem* 275, 4033-4040.
11. Binari, R., and Perrimon, N. (1994). Stripe-specific regulation of pair-rule genes by hopscotch, a putative Jak family tyrosine kinase in *Drosophila*. *Genes Dev* 8, 300-312.
12. Bischoff, V., Vignal, C., Boneca, I.G., Michel, T., Hoffmann, J.A., and Royet, J. (2004). Function of the *Drosophila* pattern-recognition receptor PGRP-SD in the detection of Gram-positive bacteria. *Nat Immunol* 5, 1175-1180.

13. Bonnay, F., Nguyen, X.H., Cohen-Berros, E., Troxler, L., Batsche, E., Camonis, J., Takeuchi, O., Reichhart, J.M., and Matt, N. (2014). Akirin specifies NF-kappaB selectivity of *Drosophila* innate immune response via chromatin remodeling. *EMBO J* 33, 2349-2362.
14. Botella, J.A., Baines, I.A., Williams, D.D., Goberdhan, D.C., Proud, C.G., and Wilson, C. (2001). The *Drosophila* cell shape regulator c-Jun N-terminal kinase also functions as a stress-activated protein kinase. *Insect Biochem Mol Biol* 31, 839-847.
15. Boutros, M., Agaisse, H., and Perrimon, N. (2002). Sequential activation of signalling pathways during innate immune responses in *Drosophila*. *Dev Cell* 3, 711-722.
16. Brennan, C.A., Delaney, J.R., Schneider, D.S., and Anderson, K.V. (2007). Psidin is required in *Drosophila* blood cells for both phagocytic degradation and immune activation of the fat body. *Curr Biol* 17, 67-72.
17. Buchon, N., Broderick, N.A., and Lemaitre, B. (2013). Gut homeostasis in a microbial world: insights from *Drosophila melanogaster*. *Nat Rev Microbiol* 11, 615-626.
18. Buchon, N., Broderick, N.A., Poidevin, M., Pradervand, S., and Lemaitre, B. (2009a). *Drosophila* intestinal response to bacterial infection: activation of host defence and stem cell proliferation. *Cell Host Microbe* 5, 200-211.
19. Buchon, N., Poidevin, M., Kwon, H.M., Guillou, A., Sottas, V., Lee, B.L., and Lemaitre, B. (2009b). A single modular serine protease integrates signals from pattern-recognition receptors upstream of the *Drosophila* Toll pathway. *Proc Natl Acad Sci U S A* 106, 12442-12447.
20. Buchon, N., Silverman, N., and Cherry, S. (2014). Immunity in *Drosophila melanogaster*--from microbial recognition to whole-organism physiology. *Nat Rev Immunol* 14, 796-810.
21. Cammarata-Mouchtouris, A., Nguyen, X.H., Acker, A., Bonnay, F., Goto, A., Orian, A., Fauvarque, M.O., Boutros, M., Reichhart, J.M., and Matt, N. (2020). Hyd ubiquitinates the NF-kappaB co-factor Akirin to operate an effective immune response in *Drosophila*. *PLoS Pathog* 16, e1008458.
22. Casanova, J.L., Holland, S.M., and Notarangelo, L.D. (2012). Inborn errors of human JAKs and STATs. *Immunity* 36, 515-528.
23. Castillejo-Lopez, C., and Hacker, U. (2005). The serine protease Sp7 is expressed in blood cells and regulates the melanization reaction in *Drosophila*. *Biochem Biophys Res Commun* 338, 1075-1082.

24. Chakrabarti, S., and Visweswariah, S.S. (2020). Intramacrophage ROS Primes the Innate Immune System via JAK/STAT and Toll Activation. *Cell Rep* 33, 108368.
25. Chang, C.I., Chelliah, Y., Borek, D., Mengin-Lecreulx, D., and Deisenhofer, J. (2006). Structure of tracheal cytotoxin in complex with a heterodimeric pattern-recognition receptor. *Science* 311, 1761-1764.
26. Charroux, B., and Royet, J. (2009). Elimination of plasmatocytes by targeted apoptosis reveals their role in multiple aspects of the *Drosophila* immune response. *Proc Natl Acad Sci U S A* 106, 9797-9802.
27. Chen, H.W., Chen, X., Oh, S.W., Marinissen, M.J., Gutkind, J.S., and Hou, S.X. (2002). mom identifies a receptor for the *Drosophila* JAK/STAT signal transduction pathway and encodes a protein distantly related to the mammalian cytokine receptor family. *Genes Dev* 16, 388-398.
28. Chiu, H., Ring, B.C., Sorrentino, R.P., Kalamarz, M., Garza, D., and Govind, S. (2005). dUbc9 negatively regulates the Toll-NF-kappa B pathways in larval hematopoiesis and drosomycin activation in *Drosophila*. *Dev Biol* 288, 60-72.
29. Choe, K.M., Lee, H., and Anderson, K.V. (2005). *Drosophila* peptidoglycan recognition protein LC (PGRP-LC) acts as a signal-transducing innate immune receptor. *Proc Natl Acad Sci U S A* 102, 1122-1126.
30. Choe, K.M., Werner, T., Stoven, S., Hultmark, D., and Anderson, K.V. (2002). Requirement for a peptidoglycan recognition protein (PGRP) in Relish activation and antibacterial immune responses in *Drosophila*. *Science* 296, 359-362.
31. Ciapponi, L., Jackson, D.B., Mlodzik, M., and Bohmann, D. (2001). *Drosophila* Fos mediates ERK and JNK signals via distinct phosphorylation sites. *Genes Dev* 15, 1540-1553.
32. Clavier, A., Rincheval-Arnold, A., Baillet, A., Mignotte, B., and Guenal, I. (2016). Two different specific JNK activators are required to trigger apoptosis or compensatory proliferation in response to Rbfl in *Drosophila*. *Cell Cycle* 15, 283-294.
33. Cronin, S.J., Nehme, N.T., Limmer, S., Liegeois, S., Pospisilik, J.A., Schramek, D., Leibbrandt, A., Simoes Rde, M., Gruber, S., Puc, U., *et al.* (2009). Genome-wide RNAi screen identifies genes involved in intestinal pathogenic bacterial infection. *Science* 325, 340-343.
34. Defaye, A., Evans, I., Crozatier, M., Wood, W., Lemaitre, B., and Leulier, F. (2009). Genetic ablation of *Drosophila* phagocytes reveals their contribution to both development and resistance to bacterial infection. *J Innate Immun* 1, 322-334.



35. Delaney, J.R., Stoven, S., Uvell, H., Anderson, K.V., Engstrom, Y., and Mlodzik, M. (2006). Cooperative control of *Drosophila* immune responses by the JNK and NF-kappaB signalling pathways. *EMBO J* 25, 3068-3077.
36. Desterro, J.M., Rodriguez, M.S., and Hay, R.T. (1998). SUMO-1 modification of IkappaBalpha inhibits NF-kappaB activation. *Mol Cell* 2, 233-239.
37. Dostert, C., Jouanguy, E., Irving, P., Troxler, L., Galiana-Arnoux, D., Hetru, C., Hoffmann, J.A., and Imler, J.L. (2005). The Jak-STAT signalling pathway is required but not sufficient for the antiviral response of *Drosophila*. *Nat Immunol* 6, 946-953.
38. Drier, E.A., Huang, L.H., and Steward, R. (1999). Nuclear import of the *Drosophila* Rel protein Dorsal is regulated by phosphorylation. *Genes Dev* 13, 556-568.
39. Edwards, D.N., Towb, P., and Wasserman, S.A. (1997). An activity-dependent network of interactions links the Rel protein Dorsal with its cytoplasmic regulators. *Development* 124, 3855-3864.
40. El Chamy, L., Leclerc, V., Caldelari, I., and Reichhart, J.M. (2008). Sensing of 'danger signals' and pathogen-associated molecular patterns defines binary signalling pathways 'upstream' of Toll. *Nat Immunol* 9, 1165-1170.
41. Erturk-Hasdemir, D., Broemer, M., Leulier, F., Lane, W.S., Paquette, N., Hwang, D., Kim, C.H., Stoven, S., Meier, P., and Silverman, N. (2009). Two roles for the *Drosophila* IKK complex in the activation of Relish and the induction of antimicrobial peptide genes. *Proc Natl Acad Sci U S A* 106, 9779-9784.
42. Franc, N.C., Heitzler, P., Ezekowitz, R.A., and White, K. (1999). Requirement for croquemort in phagocytosis of apoptotic cells in *Drosophila*. *Science* 284, 1991-1994.
43. Fukuyama, H., Verdier, Y., Guan, Y., Makino-Okamura, C., Shilova, V., Liu, X., Maksoud, E., Matsubayashi, J., Haddad, I., Spirohn, K., *et al.* (2013). Landscape of protein-protein interactions in *Drosophila* immune deficiency signalling during bacterial challenge. *Proc Natl Acad Sci U S A* 110, 10717-10722.
44. Gangloff, M., Murali, A., Xiong, J., Arnot, C.J., Weber, A.N., Sandercock, A.M., Robinson, C.V., Sarisky, R., Holzenburg, A., Kao, C., *et al.* (2008). Structural insight into the mechanism of activation of the Toll receptor by the dimeric ligand Spatzle. *J Biol Chem* 283, 14629-14635.
45. Gilbert, M.M., Weaver, B.K., Gergen, J.P., and Reich, N.C. (2005). A novel functional activator of the *Drosophila* JAK/STAT pathway, unpaired2, is revealed by an in vivo reporter of pathway activation. *Mech Dev* 122, 939-948.

46. Gillespie, S.K., and Wasserman, S.A. (1994). Dorsal, a *Drosophila* Rel-like protein, is phosphorylated upon activation of the transmembrane protein Toll. *Mol Cell Biol* *14*, 3559-3568.
47. Gold, K.S., and Bruckner, K. (2015). Macrophages and cellular immunity in *Drosophila melanogaster*. *Semin Immunol* *27*, 357-368.
48. Gottar, M., Gobert, V., Matskevich, A.A., Reichhart, J.M., Wang, C., Butt, T.M., Belvin, M., Hoffmann, J.A., and Ferrandon, D. (2006). Dual detection of fungal infections in *Drosophila* via recognition of glucans and sensing of virulence factors. *Cell* *127*, 1425-1437.
49. Gottar, M., Gobert, V., Michel, T., Belvin, M., Duyk, G., Hoffmann, J.A., Ferrandon, D., and Royet, J. (2002). The *Drosophila* immune response against Gram-negative bacteria is mediated by a peptidoglycan recognition protein. *Nature* *416*, 640-644.
50. Govind, S. (1999). Control of development and immunity by rel transcription factors in *Drosophila*. *Oncogene* *18*, 6875-6887.
51. Gronholm, J., Ungureanu, D., Vanhatupa, S., Ramet, M., and Silvennoinen, O. (2010). Sumoylation of *Drosophila* transcription factor STAT92E. *J Innate Immun* *2*, 618-624.
52. Gross, I., Georgel, P., Kappler, C., Reichhart, J.M., and Hoffmann, J.A. (1996). *Drosophila* immunity: a comparative analysis of the Rel proteins dorsal and Dif in the induction of the genes encoding diptericin and cecropin. *Nucleic Acids Res* *24*, 1238-1245.
53. Ha, E.M., Oh, C.T., Bae, Y.S., and Lee, W.J. (2005). A direct role for dual oxidase in *Drosophila* gut immunity. *Science* *310*, 847-850.
54. Handu, M., Kaduskar, B., Ravindranathan, R., Soory, A., Giri, R., Elango, V.B., Gowda, H., and Ratnaparkhi, G.S. (2015). SUMO-Enriched Proteome for *Drosophila* Innate Immune Response. *G3 (Bethesda)* *5*, 2137-2154.
55. Hanson, M.A., Dostalova, A., Ceroni, C., Poidevin, M., Kondo, S., and Lemaitre, B. (2019). Synergy and remarkable specificity of antimicrobial peptides in vivo using a systematic knockout approach. *Elife* *8*.
56. Hanson, M.A., and Lemaitre, B. (2020). New insights on *Drosophila* antimicrobial peptide function in host defence and beyond. *Current Opinion in Immunology* *62*, 22-30.
57. Harrison, D.A., McCoon, P.E., Binari, R., Gilman, M., and Perrimon, N. (1998). *Drosophila* unpaired encodes a secreted protein that activates the JAK signalling pathway. *Genes Dev* *12*, 3252-3263.
58. Hashimoto, Y., Tabuchi, Y., Sakurai, K., Kutsuna, M., Kurokawa, K., Awasaki, T., Sekimizu, K., Nakanishi, Y., and Shiratsuchi, A. (2009). Identification of lipoteichoic acid as

a ligand for draper in the phagocytosis of *Staphylococcus aureus* by *Drosophila* hemocytes. *J Immunol* *183*, 7451-7460.

59. Hendriks, I.A., Lyon, D., Young, C., Jensen, L.J., Vertegaal, A.C., and Nielsen, M.L. (2017). Site-specific mapping of the human SUMO proteome reveals co-modification with phosphorylation. *Nat Struct Mol Biol* *24*, 325-336.
60. Hendriks, I.A., and Vertegaal, A.C. (2016). A comprehensive compilation of SUMO proteomics. *Nat Rev Mol Cell Biol* *17*, 581-595.
61. Hombria, J.C., Brown, S., Hader, S., and Zeidler, M.P. (2005). Characterisation of Upd2, a *Drosophila* JAK/STAT pathway ligand. *Dev Biol* *288*, 420-433.
62. Horng, T., and Medzhitov, R. (2001). *Drosophila* MyD88 is an adapter in the Toll signalling pathway. *Proc Natl Acad Sci U S A* *98*, 12654-12658.
63. Hou, X.S., Melnick, M.B., and Perrimon, N. (1996). Marelle acts downstream of the *Drosophila* HOP/JAK kinase and encodes a protein similar to the mammalian STATs. *Cell* *84*, 411-419.
64. Huang, H.R., Chen, Z.J., Kunes, S., Chang, G.D., and Maniatis, T. (2010). Endocytic pathway is required for *Drosophila* Toll innate immune signalling. *Proc Natl Acad Sci U S A* *107*, 8322-8327.
65. Hultmark, D. (2003). *Drosophila* immunity: paths and patterns. *Current Opinion in Immunology* *15*, 12-19.
66. Igaki, T., Kanda, H., Okano, H., Xu, T., and Miura, M. (2011). Eiger and wengen: the *Drosophila* orthologs of TNF/TNFR. *Adv Exp Med Biol* *691*, 45-50.
67. Imler, J.L., and Hoffmann, J.A. (2001). Toll receptors in innate immunity. *Trends Cell Biol* *11*, 304-311.
68. Imler, J.L., Tauszig, S., Jouanguy, E., Forestier, C., and Hoffmann, J.A. (2000). LPS-induced immune response in *Drosophila*. *Journal of endotoxin research* *6*, 459-462.
69. Ip, Y.T., Reach, M., Engstrom, Y., Kadalayil, L., Cai, H., González-Crespo, S., Tatei, K., and Levine, M. (1993). Dif, a dorsal-related gene that mediates an immune response in *Drosophila*. *Cell* *75*, 753-763.
70. Issa, N., Guillaumot, N., Lauret, E., Matt, N., Schaeffer-Reiss, C., Van Dorselaer, A., Reichhart, J.M., and Veillard, F. (2018). The Circulating Protease Persephone Is an Immune Sensor for Microbial Proteolytic Activities Upstream of the *Drosophila* Toll Pathway. *Mol Cell* *69*, 539-550 e536.

71. Jang, I.H., Chosa, N., Kim, S.H., Nam, H.J., Lemaitre, B., Ochiai, M., Kambris, Z., Brun, S., Hashimoto, C., Ashida, M., *et al.* (2006). A Spatzle-processing enzyme required for toll signalling activation in *Drosophila* innate immunity. *Dev Cell* *10*, 45-55.
72. Jones, R.M., Luo, L., Ardita, C.S., Richardson, A.N., Kwon, Y.M., Mercante, J.W., Alam, A., Gates, C.L., Wu, H., Swanson, P.A., *et al.* (2013). Symbiotic lactobacilli stimulate gut epithelial proliferation via Nox-mediated generation of reactive oxygen species. *EMBO J* *32*, 3017-3028.
73. Kaduskar, B., Trivedi, D., and Ratnaparkhi, G.S. (2020). Caspar SUMOylation regulates *Drosophila* lifespan. *MicroPubl Biol* *2020*.
74. Kambris, Z., Brun, S., Jang, I.H., Nam, H.J., Romeo, Y., Takahashi, K., Lee, W.J., Ueda, R., and Lemaitre, B. (2006). *Drosophila* immunity: a large-scale in vivo RNAi screen identifies five serine proteases required for Toll activation. *Curr Biol* *16*, 808-813.
75. Kanda, H., Igaki, T., Kanuka, H., Yagi, T., and Miura, M. (2002). Wengen, a member of the *Drosophila* tumor necrosis factor receptor superfamily, is required for Eiger signalling. *J Biol Chem* *277*, 28372-28375.
76. Kaneko, T., Yano, T., Aggarwal, K., Lim, J.H., Ueda, K., Oshima, Y., Peach, C., Erturk-Hasdemir, D., Goldman, W.E., Oh, B.H., *et al.* (2006). PGRP-LC and PGRP-LE have essential yet distinct functions in the *Drosophila* immune response to monomeric DAP-type peptidoglycan. *Nat Immunol* *7*, 715-723.
77. Kauppila, S., Maaty, W.S., Chen, P., Tomar, R.S., Eby, M.T., Chapo, J., Chew, S., Rathore, N., Zachariah, S., Sinha, S.K., *et al.* (2003). Eiger and its receptor, Wengen, comprise a TNF-like system in *Drosophila*. *Oncogene* *22*, 4860-4867.
78. Kemp, C., Mueller, S., Goto, A., Barbier, V., Paro, S., Bonnay, F., Dostert, C., Troxler, L., Hetru, C., Meignin, C., *et al.* (2013). Broad RNA interference-mediated antiviral immunity and virus-specific inducible responses in *Drosophila*. *J Immunol* *190*, 650-658.
79. Khush, R.S., Cornwell, W.D., Uram, J.N., and Lemaitre, B. (2002). A ubiquitin-proteasome pathway represses the *Drosophila* immune deficiency signalling cascade. *Curr Biol* *12*, 1728-1737.
80. Kim, L.K., Choi, U.Y., Cho, H.S., Lee, J.S., Lee, W.-b., Kim, J., Jeong, K., Shim, J., Kim-Ha, J., and Kim, Y.-J. (2007). Down-regulation of NF- $\kappa$ B target genes by the AP-1 and STAT complex during the innate immune response in *Drosophila*. *PLoS Biol* *5*, e238.
81. Kim, M., Lee, J.H., Lee, S.Y., Kim, E., and Chung, J. (2006). Caspar, a suppressor of antibacterial immunity in *Drosophila*. *Proc Natl Acad Sci U S A* *103*, 16358-16363.

82. Kim, T., Yoon, J., Cho, H., Lee, W.B., Kim, J., Song, Y.H., Kim, S.N., Yoon, J.H., Kim-Ha, J., and Kim, Y.J. (2005). Downregulation of lipopolysaccharide response in *Drosophila* by negative crosstalk between the AP1 and NF-kappaB signalling modules. *Nat Immunol* 6, 211-218.
83. Kim, W., Bennett, E.J., Huttlin, E.L., Guo, A., Li, J., Possemato, A., Sowa, M.E., Rad, R., Rush, J., Comb, M.J., *et al.* (2011). Systematic and quantitative assessment of the ubiquitin-modified proteome. *Mol Cell* 44, 325-340.
84. Kiu, H., and Nicholson, S.E. (2012). Biology and significance of the JAK/STAT signalling pathways. *Growth Factors* 30, 88-106.
85. Kleino, A., Myllymaki, H., Kallio, J., Vanha-aho, L.M., Oksanen, K., Ulvila, J., Hultmark, D., Valanne, S., and Ramet, M. (2008). Pirk is a negative regulator of the *Drosophila* Imd pathway. *J Immunol* 180, 5413-5422.
86. Kleino, A., Valanne, S., Ulvila, J., Kallio, J., Myllymaki, H., Enwald, H., Stoven, S., Poidevin, M., Ueda, R., Hultmark, D., *et al.* (2005). Inhibitor of apoptosis 2 and TAK1-binding protein are components of the *Drosophila* Imd pathway. *EMBO J* 24, 3423-3434.
87. Kockel, L., Homsy, J.G., and Bohmann, D. (2001). *Drosophila* AP-1: lessons from an invertebrate. *Oncogene* 20, 2347-2364.
88. Kocks, C., Cho, J.H., Nehme, N., Ulvila, J., Pearson, A.M., Meister, M., Strom, C., Conto, S.L., Hetru, C., Stuart, L.M., *et al.* (2005). Eater, a transmembrane protein mediating phagocytosis of bacterial pathogens in *Drosophila*. *Cell* 123, 335-346.
89. Kounatidis, I., Chtarbanova, S., Cao, Y., Hayne, M., Jayanth, D., Ganetzky, B., and Ligoxygakis, P. (2017). NF-kappaB Immunity in the Brain Determines Fly Lifespan in Healthy Aging and Age-Related Neurodegeneration. *Cell Rep* 19, 836-848.
90. Kuraishi, T., Nakagawa, Y., Nagaosa, K., Hashimoto, Y., Ishimoto, T., Moki, T., Fujita, Y., Nakayama, H., Dohmae, N., Shiratsuchi, A., *et al.* (2009). Pretaporter, a *Drosophila* protein serving as a ligand for Draper in the phagocytosis of apoptotic cells. *EMBO J* 28, 3868-3878.
91. Kurucz, E., Markus, R., Zsamboki, J., Folkl-Medzihradzky, K., Darula, Z., Vilmos, P., Udvardy, A., Krausz, I., Lukacsovich, T., Gateff, E., *et al.* (2007). Nimrod, a putative phagocytosis receptor with EGF repeats in *Drosophila* plasmatocytes. *Curr Biol* 17, 649-654.
92. Lanot, R., Zachary, D., Holder, F., and Meister, M. (2001). Postembryonic hematopoiesis in *Drosophila*. *Dev Biol* 230, 243-257.
93. Lemaitre, B., and Hoffmann, J. (2007). The host defence of *Drosophila melanogaster*. *Annu Rev Immunol* 25, 697-743.

94. Lemaitre, B., Kromer-Metzger, E., Michaut, L., Nicolas, E., Meister, M., Georgel, P., Reichhart, J.M., and Hoffmann, J.A. (1995a). A recessive mutation, immune deficiency (*imd*), defines two distinct control pathways in the *Drosophila* host defence. *Proc Natl Acad Sci U S A* *92*, 9465-9469.
95. Lemaitre, B., Meister, M., Govind, S., Georgel, P., Steward, R., Reichhart, J.M., and Hoffmann, J.A. (1995b). Functional analysis and regulation of nuclear import of dorsal during the immune response in *Drosophila*. *Embo j* *14*, 536-545.
96. Lemaitre, B., and Miguel-Aliaga, I. (2013). The digestive tract of *Drosophila melanogaster*. *Annu Rev Genet* *47*, 377-404.
97. Leulier, F., Vidal, S., Saigo, K., Ueda, R., and Lemaitre, B. (2002). Inducible expression of double-stranded RNA reveals a role for dFADD in the regulation of the antibacterial response in *Drosophila* adults. *Curr Biol* *12*, 996-1000.
98. Li, X., Rommelaere, S., Kondo, S., and Lemaitre, B. (2020). Renal Purge of Hemolymphatic Lipids Prevents the Accumulation of ROS-Induced Inflammatory Oxidized Lipids and Protects *Drosophila* from Tissue Damage. *Immunity* *52*, 374-387 e376.
99. Lim, J.H., Kim, M.S., Kim, H.E., Yano, T., Oshima, Y., Aggarwal, K., Goldman, W.E., Silverman, N., Kurata, S., and Oh, B.H. (2006). Structural basis for preferential recognition of diaminopimelic acid-type peptidoglycan by a subset of peptidoglycan recognition proteins. *J Biol Chem* *281*, 8286-8295.
100. Liu, J., Qian, C., and Cao, X. (2016). Post-Translational Modification Control of Innate Immunity. *Immunity* *45*, 15-30.
101. Lu, Y., Wu, L.P., and Anderson, K.V. (2001). The antibacterial arm of the *Drosophila* innate immune response requires an IkappaB kinase. *Genes Dev* *15*, 104-110.
102. Manfrulli, P., Reichhart, J.M., Steward, R., Hoffmann, J.A., and Lemaitre, B. (1999). A mosaic analysis in *Drosophila* fat body cells of the control of antimicrobial peptide genes by the Rel proteins Dorsal and DIF. *EMBO J* *18*, 3380-3391.
103. Markus, R., Laurinyecz, B., Kurucz, E., Honti, V., Bajusz, I., Sipos, B., Somogyi, K., Kronhamn, J., Hultmark, D., and Ando, I. (2009). Sessile hemocytes as a hematopoietic compartment in *Drosophila melanogaster*. *Proc Natl Acad Sci U S A* *106*, 4805-4809.
104. Martin-Blanco, E., Gampel, A., Ring, J., Virdee, K., Kirov, N., Tolkovsky, A.M., and Martinez-Arias, A. (1998). puckered encodes a phosphatase that mediates a feedback loop regulating JNK activity during dorsal closure in *Drosophila*. *Genes Dev* *12*, 557-570.

105. Meinander, A., Runchel, C., Tenev, T., Chen, L., Kim, C.H., Ribeiro, P.S., Broemer, M., Leulier, F., Zvelebil, M., Silverman, N., *et al.* (2012). Ubiquitylation of the initiator caspase DREDD is required for innate immune signalling. *EMBO J* 31, 2770-2783.
106. Melcarne, C., Ramond, E., Dudzic, J., Bretscher, A.J., Kurucz, E., Ando, I., and Lemaitre, B. (2019). Two Nimrod receptors, NimC1 and Eater, synergistically contribute to bacterial phagocytosis in *Drosophila melanogaster*. *FEBS J* 286, 2670-2691.
107. Moncrieffe, M.C., Grossmann, J.G., and Gay, N.J. (2008). Assembly of oligomeric death domain complexes during Toll receptor signalling. *J Biol Chem* 283, 33447-33454.
108. Morisato, D., and Anderson, K.V. (1994). The spätzle gene encodes a component of the extracellular signalling pathway establishing the dorsal-ventral pattern of the *Drosophila* embryo. *Cell* 76, 677-688.
109. Myllymaki, H., Valanne, S., and Ramet, M. (2014). The *Drosophila* imd signalling pathway. *J Immunol* 192, 3455-3462.
110. Nehme, N.T., Quintin, J., Cho, J.H., Lee, J., Lafarge, M.C., Kocks, C., and Ferrandon, D. (2011). Relative roles of the cellular and humoral responses in the *Drosophila* host defence against three gram-positive bacterial infections. *PLoS One* 6, e14743.
111. Neyen, C., Poidevin, M., Roussel, A., and Lemaitre, B. (2012). Tissue- and ligand-specific sensing of gram-negative infection in *Drosophila* by PGRP-LC isoforms and PGRP-LE. *J Immunol* 189, 1886-1897.
112. Nie, M., Xie, Y., Loo, J.A., and Courey, A.J. (2009). Genetic and proteomic evidence for roles of *Drosophila* SUMO in cell cycle control, Ras signalling, and early pattern formation. *PLoS One* 4, e5905.
113. Nusslein-Volhard, C., Lohs-Schardin, M., Sander, K., and Cremer, C. (1980). A dorso-ventral shift of embryonic primordia in a new maternal-effect mutant of *Drosophila*. *Nature* 283, 474-476.
114. Nusslein-Volhard, C., Wieschaus, E., and Kluding, H. (1984). Mutations affecting the pattern of the larval cuticle in *Drosophila melanogaster* : I. Zygotic loci on the second chromosome. *Wilehm Roux Arch Dev Biol* 193, 267-282.
115. O'Shea, J.J., and Plenge, R. (2012). JAK and STAT signalling molecules in immunoregulation and immune-mediated disease. *Immunity* 36, 542-550.
116. Ochoa, D., Jarnuczak, A.F., Vieitez, C., Gehre, M., Soucheray, M., Mateus, A., Kleefeldt, A.A., Hill, A., Garcia-Alonso, L., Stein, F., *et al.* (2020). The functional landscape of the human phosphoproteome. *Nat Biotechnol* 38, 365-373.

117. Ooi, J.Y., Yagi, Y., Hu, X., and Ip, Y.T. (2002). The *Drosophila* Toll-9 activates a constitutive antimicrobial defence. *EMBO Rep* 3, 82-87.
118. Paquette, N., Broemer, M., Aggarwal, K., Chen, L., Husson, M., Erturk-Hasdemir, D., Reichhart, J.M., Meier, P., and Silverman, N. (2010). Caspase-mediated cleavage, IAP binding, and ubiquitination: linking three mechanisms crucial for *Drosophila* NF-kappaB signalling. *Mol Cell* 37, 172-182.
119. Park, J.M., Brady, H., Ruocco, M.G., Sun, H., Williams, D., Lee, S.J., Kato, T., Jr., Richards, N., Chan, K., Mercurio, F., *et al.* (2004). Targeting of TAK1 by the NF-kappa B protein Relish regulates the JNK-mediated immune response in *Drosophila*. *Genes Dev* 18, 584-594.
120. Park, J.M., Park, J.H., Mun, D.G., Bae, J., Jung, J.H., Back, S., Lee, H., Kim, H., Jung, H.J., Kim, H.K., *et al.* (2015). Integrated analysis of global proteome, phosphoproteome, and glycoproteome enables complementary interpretation of disease-related protein networks. *Sci Rep* 5, 18189.
121. Perrimon, N., and Mahowald, A.P. (1986). l(1)hopscotch, a larval-pupal zygotic lethal with a specific maternal effect on segmentation in *Drosophila*. *Developmental Biology* 118, 28-41.
122. Philips, J.A., Rubin, E.J., and Perrimon, N. (2005). *Drosophila* RNAi screen reveals CD36 family member required for mycobacterial infection. *Science* 309, 1251-1253.
123. Pirone, L., Xolalpa, W., Sigurethsson, J.O., Ramirez, J., Perez, C., Gonzalez, M., de Sabando, A.R., Elortza, F., Rodriguez, M.S., Mayor, U., *et al.* (2017). A comprehensive platform for the analysis of ubiquitin-like protein modifications using in vivo biotinylation. *Sci Rep* 7, 40756.
124. Qiu, P., Pan, P.C., and Govind, S. (1998). A role for the *Drosophila* Toll/Cactus pathway in larval hematopoiesis. *Development* 125, 1909-1920.
125. Ramet, M., Manfrulli, P., Pearson, A., Mathey-Prevot, B., and Ezekowitz, R.A. (2002). Functional genomic analysis of phagocytosis and identification of a *Drosophila* receptor for *E. coli*. *Nature* 416, 644-648.
126. Ramirez, J., Martinez, A., Lectez, B., Lee, S.Y., Franco, M., Barrio, R., Dittmar, G., and Mayor, U. (2015). Proteomic Analysis of the Ubiquitin Landscape in the *Drosophila* Embryonic Nervous System and the Adult Photoreceptor Cells. *PLoS One* 10, e0139083.



127. Reach, M., Galindo, R.L., Towb, P., Allen, J.L., Karin, M., and Wasserman, S.A. (1996). A gradient of cactus protein degradation establishes dorsoventral polarity in the *Drosophila* embryo. *Dev Biol* 180, 353-364.
128. Riesgo-Escovar, J.R., and Hafen, E. (1997). Common and distinct roles of DFos and DJun during *Drosophila* development. *Science* 278, 669-672.
129. Rios-Barrera, L.D., and Riesgo-Escovar, J.R. (2013). Regulating cell morphogenesis: the *Drosophila* Jun N-terminal kinase pathway. *Genesis* 51, 147-162.
130. Rizki, T.M., and Rizki, R.M. (1992). Lamellocyte differentiation in *Drosophila* larvae parasitized by Leptopilina. *Developmental & Comparative Immunology* 16, 103-110.
131. Rosetto, M., Engstrom, Y., Baldari, C.T., Telford, J.L., and Hultmark, D. (1995). Signals from the IL-1 receptor homolog, Toll, can activate an immune response in a *Drosophila* hemocyte cell line. *Biochem Biophys Res Commun* 209, 111-116.
132. Rutschmann, S., Jung, A.C., Hetru, C., Reichhart, J.M., Hoffmann, J.A., and Ferrandon, D. (2000a). The Rel protein DIF mediates the antifungal but not the antibacterial host defence in *Drosophila*. *Immunity* 12, 569-580.
133. Rutschmann, S., Jung, A.C., Zhou, R., Silverman, N., Hoffmann, J.A., and Ferrandon, D. (2000b). Role of *Drosophila* IKK gamma in a toll-independent antibacterial immune response. *Nat Immunol* 1, 342-347.
134. Schmid, M.R., Anderl, I., Vesala, L., Vanha-aho, L.M., Deng, X.J., Ramet, M., and Hultmark, D. (2014). Control of *Drosophila* blood cell activation via Toll signalling in the fat body. *PLoS One* 9, e102568.
135. Schneider, D.S., Jin, Y., Morisato, D., and Anderson, K.V. (1994). A processed form of the Spätzle protein defines dorsal-ventral polarity in the *Drosophila* embryo. *Development* 120, 1243-1250.
136. Shia, A.K., Glittenberg, M., Thompson, G., Weber, A.N., Reichhart, J.M., and Ligoxygakis, P. (2009). Toll-dependent antimicrobial responses in *Drosophila* larval fat body require Spatzle secreted by haemocytes. *J Cell Sci* 122, 4505-4515.
137. Silverman, N., Zhou, R., Erlich, R.L., Hunter, M., Bernstein, E., Schneider, D., and Maniatis, T. (2003). Immune activation of NF-kappaB and JNK requires *Drosophila* TAK1. *J Biol Chem* 278, 48928-48934.
138. Silverman, N., Zhou, R., Stoven, S., Pandey, N., Hultmark, D., and Maniatis, T. (2000). A *Drosophila* IkappaB kinase complex required for Relish cleavage and antibacterial immunity. *Genes Dev* 14, 2461-2471.

139. Sluss, H.K., Han, Z., Barrett, T., Goberdhan, D.C., Wilson, C., Davis, R.J., and Ip, Y.T. (1996). A JNK signal transduction pathway that mediates morphogenesis and an immune response in *Drosophila*. *Genes Dev* *10*, 2745-2758.
140. Somogyi, K., Sipos, B., Penzes, Z., Kurucz, E., Zsamboki, J., Hultmark, D., and Ando, I. (2008). Evolution of genes and repeats in the Nimrod superfamily. *Mol Biol Evol* *25*, 2337-2347.
141. Sorrentino, R.P., Melk, J.P., and Govind, S. (2004). Genetic analysis of contributions of dorsal group and JAK-Stat92E pathway genes to larval hemocyte concentration and the egg encapsulation response in *Drosophila*. *Genetics* *166*, 1343-1356.
142. Stec, W., Vidal, O., and Zeidler, M.P. (2013). *Drosophila* SOCS36E negatively regulates JAK/STAT pathway signalling via two separable mechanisms. *Mol Biol Cell* *24*, 3000-3009.
143. Stoven, S., Ando, I., Kadalayil, L., Engstrom, Y., and Hultmark, D. (2000). Activation of the *Drosophila* NF-kappaB factor Relish by rapid endoproteolytic cleavage. *EMBO Rep* *1*, 347-352.
144. Stoven, S., Silverman, N., Junell, A., Hedengren-Olcott, M., Erturk, D., Engstrom, Y., Maniatis, T., and Hultmark, D. (2003). Caspase-mediated processing of the *Drosophila* NF-kappaB factor Relish. *Proc Natl Acad Sci U S A* *100*, 5991-5996.
145. Stronach, B., and Perrimon, N. (2002). Activation of the JNK pathway during dorsal closure in *Drosophila* requires the mixed lineage kinase, slipper. *Genes Dev* *16*, 377-387.
146. Sun, H., Bristow, B.N., Qu, G., and Wasserman, S.A. (2002). A heterotrimeric death domain complex in Toll signalling. *Proc Natl Acad Sci U S A* *99*, 12871-12876.
147. Takehana, A., Katsuyama, T., Yano, T., Oshima, Y., Takada, H., Aigaki, T., and Kurata, S. (2002). Overexpression of a pattern-recognition receptor, peptidoglycan-recognition protein-LE, activates imd/relish-mediated antibacterial defence and the prophenoloxidase cascade in *Drosophila* larvae. *Proc Natl Acad Sci U S A* *99*, 13705-13710.
148. Tang, H., Kambris, Z., Lemaitre, B., and Hashimoto, C. (2008). A serpin that regulates immune melanization in the respiratory system of *Drosophila*. *Dev Cell* *15*, 617-626.
149. Tauszig-Delamasure, S., Bilak, H., Capovilla, M., Hoffmann, J.A., and Imler, J.L. (2002). *Drosophila* MyD88 is required for the response to fungal and Gram-positive bacterial infections. *Nat Immunol* *3*, 91-97.

150. Tauszig, S., Jouanguy, E., Hoffmann, J.A., and Imler, J.L. (2000). Toll-related receptors and the control of antimicrobial peptide expression in *Drosophila*. *Proc Natl Acad Sci U S A* 97, 10520-10525.
151. Thevenon, D., Engel, E., Avet-Rochex, A., Gottar, M., Bergeret, E., Tricoire, H., Benaud, C., Baudier, J., Taillebourg, E., and Fauvarque, M.O. (2009). The *Drosophila* ubiquitin-specific protease dUSP36/Scny targets IMD to prevent constitutive immune signalling. *Cell Host Microbe* 6, 309-320.
152. Towb, P., Bergmann, A., and Wasserman, S.A. (2001). The protein kinase Pelle mediates feedback regulation in the *Drosophila* Toll signalling pathway. *Development* 128, 4729-4736.
153. Troha, K., Nagy, P., Pivovar, A., Lazzaro, B.P., Hartley, P.S., and Buchon, N. (2019). Nephrocytes Remove Microbiota-Derived Peptidoglycan from Systemic Circulation to Maintain Immune Homeostasis. *Immunity* 51, 625-637 e623.
154. Tschritzis, T., Gaentzsch, P.C., Kosmidis, S., Brown, A.E., Skoulakis, E.M., Ligoxygakis, P., and Mosialos, G. (2007). A *Drosophila* ortholog of the human cylindromatosis tumor suppressor gene regulates triglyceride content and antibacterial defence. *Development* 134, 2605-2614.
155. Tsuda, M., Langmann, C., Harden, N., and Aigaki, T. (2005). The RING-finger scaffold protein Plenty of SH3s targets TAK1 to control immunity signalling in *Drosophila*. *EMBO Rep* 6, 1082-1087.
156. Tung, T.T., Nagaosa, K., Fujita, Y., Kita, A., Mori, H., Okada, R., Nonaka, S., and Nakanishi, Y. (2013). Phosphatidylserine recognition and induction of apoptotic cell clearance by *Drosophila* engulfment receptor Draper. *J Biochem* 153, 483-491.
157. Valanne, S., Wang, J.H., and Ramet, M. (2011). The *Drosophila* Toll signalling pathway. *J Immunol* 186, 649-656.
158. Vidal, O.M., Stec, W., Bausek, N., Smythe, E., and Zeidler, M.P. (2010). Negative regulation of *Drosophila* JAK-STAT signalling by endocytic trafficking. *J Cell Sci* 123, 3457-3466.
159. Vlisidou, I., and Wood, W. (2015). *Drosophila* blood cells and their role in immune responses. *FEBS J* 282, 1368-1382.
160. Weber, A.N., Moncrieffe, M.C., Gangloff, M., Imler, J.L., and Gay, N.J. (2005). Ligand-receptor and receptor-receptor interactions act in concert to activate signalling in the *Drosophila* toll pathway. *J Biol Chem* 280, 22793-22799.

161. Werner, T., Borge-Renberg, K., Mellroth, P., Steiner, H., and Hultmark, D. (2003). Functional diversity of the *Drosophila* PGRP-LC gene cluster in the response to lipopolysaccharide and peptidoglycan. *J Biol Chem* 278, 26319-26322.
162. Werner, T., Liu, G., Kang, D., Ekengren, S., Steiner, H., and Hultmark, D. (2000). A family of peptidoglycan recognition proteins in the fruit fly *Drosophila melanogaster*. *Proc Natl Acad Sci U S A* 97, 13772-13777.
163. Williams, M.J., Wiklund, M.L., Wikman, S., and Hultmark, D. (2006). Rac1 signalling in the *Drosophila* larval cellular immune response. *J Cell Sci* 119, 2015-2024.
164. Wright, V.M., Vogt, K.L., Smythe, E., and Zeidler, M.P. (2011). Differential activities of the *Drosophila* JAK/STAT pathway ligands Upd, Upd2 and Upd3. *Cell Signal* 23, 920-927.
165. Wu, L.P., and Anderson, K.V. (1998). Regulated nuclear import of Rel proteins in the *Drosophila* immune response. *Nature* 392, 93-97.
166. Xiao, T., Towb, P., Wasserman, S.A., and Sprang, S.R. (1999). Three-Dimensional Structure of a Complex between the Death Domains of Pelle and Tube. *Cell* 99, 545-555.
167. Yagi, Y., Lim, Y.M., Tsuda, L., and Nishida, Y. (2013). fat facets induces polyubiquitination of Imd and inhibits the innate immune response in *Drosophila*. *Genes Cells* 18, 934-945.
168. Yan, R., Small, S., Desplan, C., Dearolf, C.R., and Darnell, J.E., Jr. (1996). Identification of a Stat gene that functions in *Drosophila* development. *Cell* 84, 421-430.
169. Yang, H., Kronhamn, J., Ekstrom, J.O., Korkut, G.G., and Hultmark, D. (2015). JAK/STAT signalling in *Drosophila* muscles controls the cellular immune response against parasitoid infection. *EMBO Rep* 16, 1664-1672.
170. Yang, J., and Steward, R. (1997). A multimeric complex and the nuclear targeting of the *Drosophila* Rel protein Dorsal. *Proc Natl Acad Sci U S A* 94, 14524-14529.
171. Yano, T., Mita, S., Ohmori, H., Oshima, Y., Fujimoto, Y., Ueda, R., Takada, H., Goldman, W.E., Fukase, K., Silverman, N., *et al.* (2008). Autophagic control of listeria through intracellular innate immune recognition in *Drosophila*. *Nat Immunol* 9, 908-916.
172. Zettervall, C.J., Anderl, I., Williams, M.J., Palmer, R., Kurucz, E., Ando, I., and Hultmark, D. (2004). A directed screen for genes involved in *Drosophila* blood cell activation. *Proc Natl Acad Sci U S A* 101, 14192-14197.
173. Zhou, R., Silverman, N., Hong, M., Liao, D.S., Chung, Y., Chen, Z.J., and Maniatis, T. (2005). The role of ubiquitination in *Drosophila* innate immunity. *J Biol Chem* 280, 34048-34055.

## **Chapter 2 The *Drosophila* AP-1 dimer proteins Jun related antigen (Jra) and Kayak (Kay) are post-translationally modified by SUMO**

### **2.1 Abstract**

The AP-1 transcription factors Jun related antigen (Jra) and Kayak (Kay) are evolutionarily conserved proteins that act downstream of the JNK signalling pathway. In *Drosophila*, activation of these transcription factors through phosphorylation by the Jun N-terminal Kinase (Basket) plays a vital role in dorsal closure during early development and suggests the importance of post-translational modifiers in regulating the function of these two proteins. SUMOylation is one such post-translational modification (PTM) that regulates several cellular functions like proteolysis, DNA replication, chromatin remodelling and, transcription regulation . We previously identified Jra and Kay to have an altered SUMOylation status upon an immune challenge in *Drosophila* S2 cells. Here we successfully demonstrated that both Jra and Kay are SUMOylated. Using biochemical assays, we identified two SUMO acceptor lysine residues in Jra to be K29 and K190. Similarly, we identified K357 as the exclusive SUMO acceptor lysine residue in Kay. Mutating lysine to arginine at these positions completely removes SUMOylation. Further, we used S2 cells to validate the findings and confirmed that mutants, K29R+K190R of Jra and K357R of Kay are completely resistant to SUMOylation.

#### Keywords

AP-1, SUMO, transcription factors, Jra, Kay

## 2.2 Introduction

### 2.2.1 Proteomic screen to identify targets with differential SUMOylation status

SUMOylation is a reversible post-translational modification (PTM) where a Ubiquitin-like (Ubl) protein family member, Small Ubiquitin like-Modifier (SUMO) covalently conjugates to the lysine of a target protein.

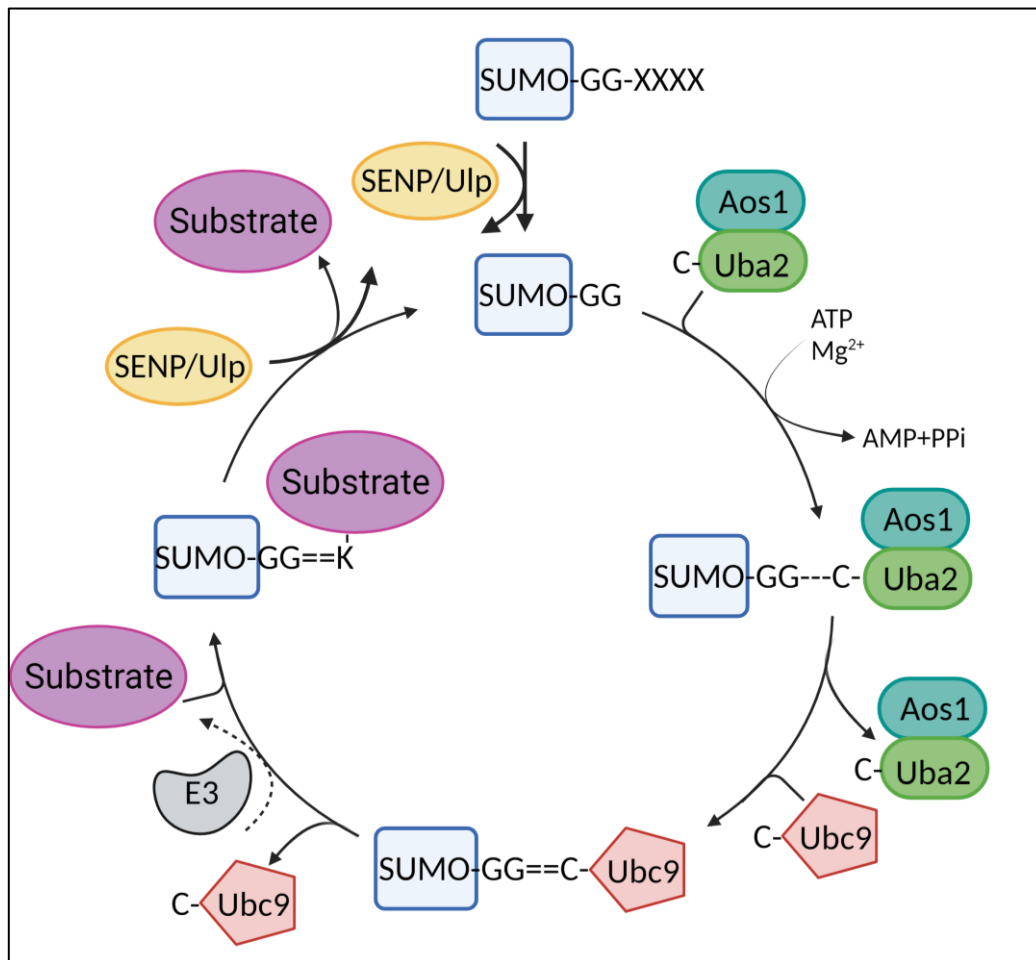


**Figure 2.1: The SUMO cycle**

SUMO is synthesized as an immature precursor. The double glycine (GG) motif on the C-terminus is masked by the presence of other amino acids (XXXX). Sentrin specific proteases (SENPs)/Ubiquitin-like proteases (Ulp) cleave the amino acids on the C-terminus exposing the GG motif of SUMO yielding a mature SUMO. Mature SUMO is freely present throughout the cell and is activated by the SUMO activating enzyme complex comprising of Activator of SUMO 1 (Aos1) and Ubiquitin-like activator 2 (Uba2). This step involves adenylation of the GG motif to a Cysteine (C) present in the active site of Uba2. This is an energy-consuming process and requires ATP. Once activated, the SUMO is transferred to another Cysteine in the Ubiquitin conjugase 9 (Ubc9) protein. Ubc9 is the only known conjugase for the SUMO cycle. SUMO is conjugated to Ubc9 via an iso-peptide bond. Ubc9 is sufficient to transfer the SUMO molecule to the target lysine (K) of a substrate protein. Sometimes, help arrives

via a ligase (also referred to as E3 ligase) that is required for specificity or enhances the transfer process. SUMO is finally liberated from the target protein by the action of SENPs/Ulps and the free SUMO is available for another round of SUMO conjugation.

SUMO conjugation is known to change the fate of the target protein by altering its subcellular localization, half-life and, interaction with other proteins. Also, SUMO is known to play a key role in the regulation of several cellular functions like cell cycle progression, transcription regulation, DNA replication and repair and, chromatin remodelling (Celen and Sahin, 2020; Eifler and Vertegaal, 2015; Flotho and Melchior, 2013; Gareau and Lima, 2010; Hendriks and Vertegaal, 2016; Pichler et al., 2017; Ulrich and Walden, 2010; Zilio et al., 2017). SUMO conjugation/de-conjugation is a cyclic process involving several key proteins described in Figure 2.1. SUMO is thought to prefer a lysine residue present in the consensus motif  $\Psi$ KXD/E (where  $\Psi$  is a hydrophobic amino acid, X is any amino acid and D/E are acidic amino acids). However, recent evidence suggests that SUMO can conjugate to any lysine residue on a protein (Hendriks et al., 2014; Hendriks and Vertegaal, 2016). Genomes of different organisms based on the need and function, often have more than two SUMO paralogs with *Drosophila* having only a single SUMO gene. One of the earliest known pieces of evidence for SUMO conjugation regulating the activity of a *Drosophila* protein comes from the NFkB factor Dorsal (dl). It was observed that mutant dl that is resistant to SUMO conjugation is a more potent transcriptional factor with enhanced activity (Bhaskar et al., 2000). Evidence that SUMO machinery regulates the immune pathway in *Drosophila* comes from studying the Ubc9 protein, Lesswright (*lwr*). Hypomorphic alleles of *lwr* show benign melanotic tumours, characteristic of hyperactivation of the Toll pathway in the *Drosophila* larvae (Chiu et al., 2005). With a limited number of studies, the regulation of immune pathways by SUMO modification is not well characterised. To better understand and elucidate the molecular mechanism of SUMO conjugation in the regulation of the immune response, we used a biochemical approach and immunoprecipitated

SUMO complexes following an LPS challenge in *Drosophila* S2 cells (Figure 2.2A). We identified that around 700 proteins had altered SUMOylation status after an immune challenge. Several key immune regulatory components showed significantly altered SUMOylation status (Figure 2.2B).

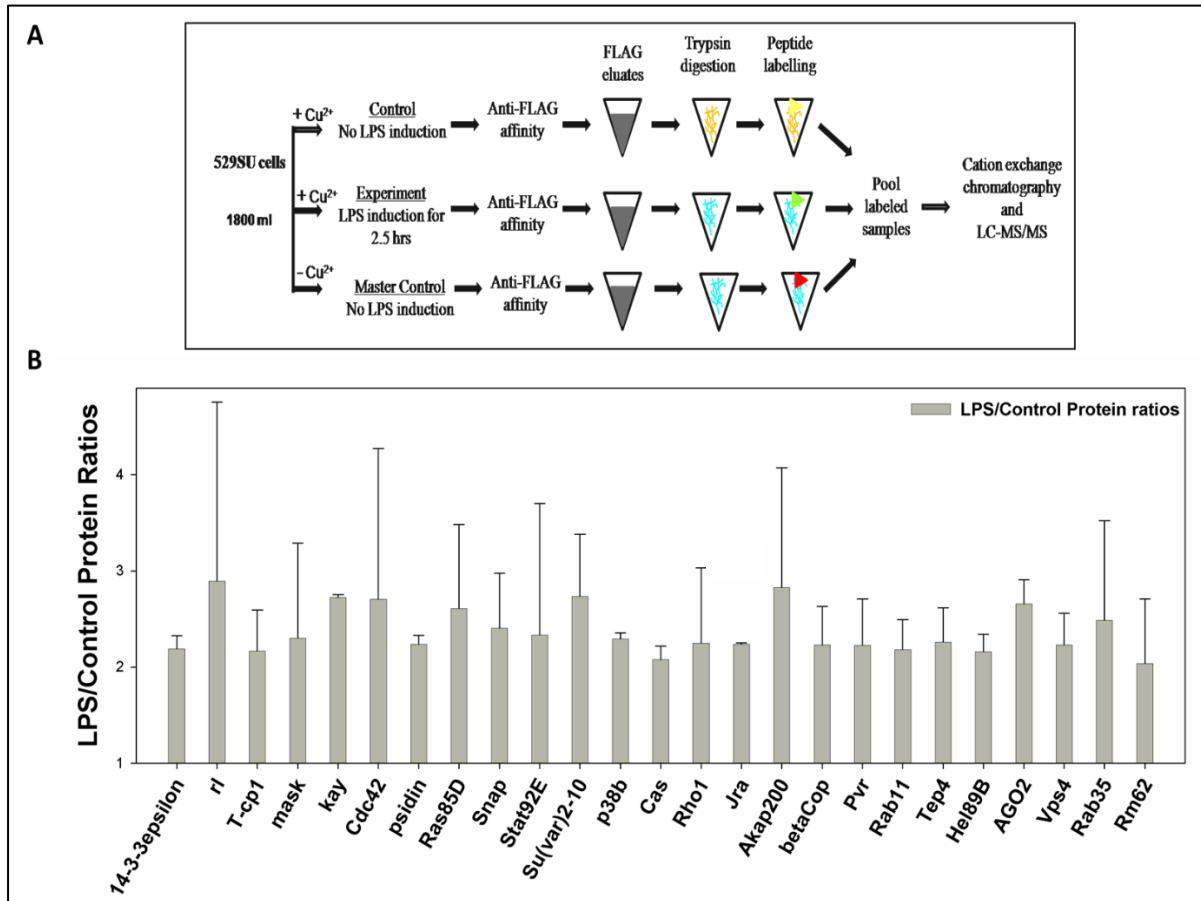


**Figure 2.2: Jra and Kay show altered SUMOylation status upon an immune challenge in *Drosophila* S2 cells.**

**A.** Schematic of Mass spectrometry experiment showing various experimental conditions performed to elucidate the role of SUMOylation in regulating immune function in *Drosophila*.

**B.** Bar plot representation of several key immune effector molecules from Mass spectrometry data. The X-axis represents the ratio of LPS induced cultures vs cultures not induced by LPS. Jra and Kay are represented by asterisks. The graph plotted with data from Handu *et al.* 2015.

### 2.2.2 Diverse roles of the JNK signalling pathway in *Drosophila*

The c-Jun N-terminal kinase (JNK) pathway is one of the highly conserved pathways that has diverse roles in regulating several cellular processes like immunity, tissue morphogenesis,



apoptosis, and cancer progression or suppression (Arthur and Ley, 2013; Dhanasekaran and Reddy, 2008; Eferl and Wagner, 2003; Wagner and Nebreda, 2009; Xia and Karin, 2004). The JNK pathway is a subtype of the Mitogen-activated protein kinase (MAPK) pathway that responds to several stimuli and regulates gene transcription through a series of complex signal transduction steps. In *Drosophila*, there is only one JNK called Basket (Bsk). Bsk is activated canonically by JNK kinases (JNKs) known as Hemipterous (Hep) and MAPK kinase 4 (Mkk4). Upstream of the JNKs, the pathway is branched out and the activation of the JNKs is done by one of the four known JNK kinases (JNKKs) namely Slipper (Slpr), Wallenda (Wnd), TGF $\beta$ -associated kinase 1 (Tak1), and Apoptotic signal-regulating kinase 1 (Ask1). Bsk is the most downstream kinase of the pathway and is known to phosphorylate several transcription factors like the Jun related antigen (Jra) and Kayak (Kay), which are orthologs of c-Jun and c-Fos respectively. These two transcription factors are referred to as the Activator protein (AP-1) complex and these together constitute the canonical JNK signalling pathway in *Drosophila* (Figure 2.3).

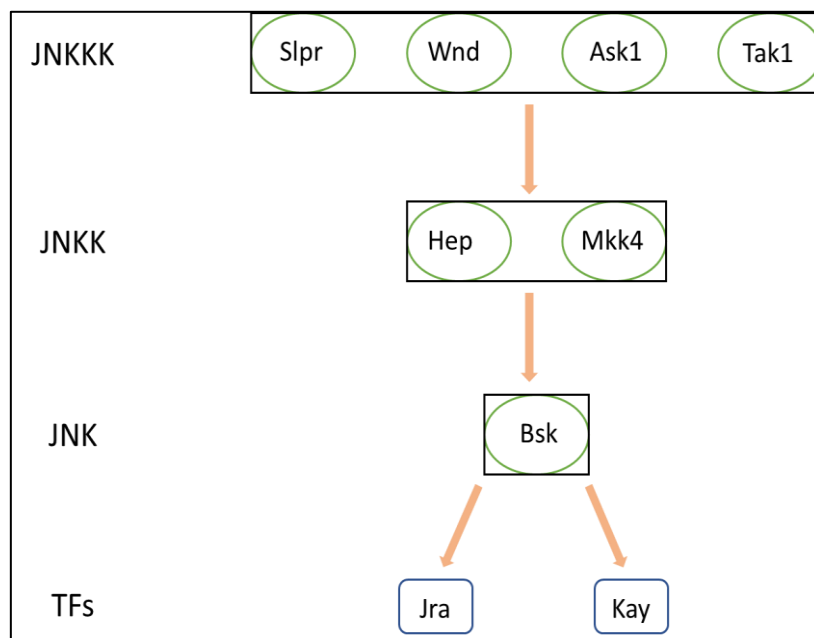


**Figure 2.3:** Schematic representing the canonical JNK signalling pathway in *Drosophila*.

JNK signalling cascade is conserved from yeast to mammals and follows canonical steps in activation of downstream transcriptional factors. The activation of Jra and Kay in *Drosophila* is done in a similar manner. The signal usually is from an extracellular ligand that binds to a cell surface receptor.

The members of the JNK signalling pathway were first identified in the Heidelberg screen as the genes that showed the “dorsal open” phenotype. These embryos had severe defects in a late embryonic stage called the dorsal closure and the phenotype was seen as a hole on the dorsal side of the embryo (Nusslein-Volhard et al., 1984). In the decades that followed, each member of the pathway was thoroughly characterised and the clear role of the JNK signalling pathway in regulating dorsal closure has been elucidated (Glise et al., 1995; Kockel et al., 1997; Riesgo-Escovar et al., 1996; Rios-Barrera and Riesgo-Escovar, 2013; Sluss et al., 1996). Dorsal closure is one of the well-studied stages of embryonic development and is the stage where the last major morphogenetic rearrangement occurs. Null mutants of Jra and Kay do not develop beyond this stage. JNK signalling is strongly active in the dorsal most cells of the embryo during dorsal closure called the leading edge (LE) cells. Bsk is activated by the canonical JNK signalling. However, neither the upstream extracellular ligand nor the cell surface receptor that activates the JNK pathway is still unknown. Once Bsk is active, it phosphorylates Jra in the LE cells and this enhances the association of Jra and Kay to form the AP-1 complex. One of the well characterised transcriptional targets of the AP-1 complex is the mammalian bone morphogen protein (BMP) ortholog, decapentaplegic (Dpp) (Hou et al., 1997; Riesgo-Escovar and Hafen, 1997b). Dpp is actively transcribed in the LE cells and is seen as a gradient that extends into the ventral amnioserosa. Activation of Dpp signalling in the amnioserosa causes cell shape changes and closes the hole on the dorsal side for further development to take place. (Riesgo-Escovar and Hafen, 1997a; Rios-Barrera and Riesgo-Escovar, 2013). JNK signalling also regulates many aspects of neuronal development, plasticity, and function in *Drosophila*. Jra and Kay are required to maintain proper synaptic strength and synaptic plasticity (Etter et al., 2005; Freeman et al., 2010; Kim et al., 2009; Sanyal et al., 2002). JNK signalling in

*Drosophila* also plays crucial roles in regulating apoptosis (Li et al., 2020; Wu et al., 2019; Zhang et al., 2015), apoptosis-induced proliferation and, tumorigenesis (La Marca and Richardson, 2020), cell competition (Baker, 2020). In addition to this, the members of the JNK signalling pathway regulate immune signalling in *Drosophila*, a function very relevant to this study. Loss of function of Jra and Kay increases the activation of several AMPs upon immune challenge (Kim et al., 2005). Further, Jra forms a complex with STAT-92E, HDAC1, and Dsp1 to displace Rel from the promoter of AttA to regulate the immune response (Kim et al., 2007). Interestingly, mammalian c-Jun and c-Fos are SUMOylated and mutants resistant to SUMO conjugation show enhanced transcriptional activity (Bossis et al., 2005; Muller et al., 2000; Tempe et al., 2014). Also, SUMO conjugated c-Fos was observed to be less abundant on the promoters of the target genes (Tempe et al., 2014) suggesting a regulatory role of SUMO conjugation in modulating the function of c-Jun and c-Fos. It was interesting to identify both Jra and Kay with an altered SUMOylation status upon an immune challenge (Handu et al., 2015). Sequence comparison of Jra and Kay to those of orthologs from different model organisms showed us that previously reported and several putative SUMO acceptor lysine residues are highly conserved across different species (Figure 2.4). This observation was worth investigating as SUMO conjugation could be a key regulatory step that modulates the function of Jra and Kay.

In this chapter, we successfully demonstrated the SUMOylation of *Drosophila* AP-1 dimers Jra and Kay in *in-vitro* and *in-vivo*. We used biochemical techniques to screen various SUMO acceptor lysine residues and identified that K29 and K190 are two acceptor residues for Jra and K357, a single acceptor site for Kay. We also demonstrated that Jra<sup>K29R+K190R</sup> and Kay<sup>K357R</sup> are completely resistant to SUMO conjugation in *Drosophila* S2 cells.

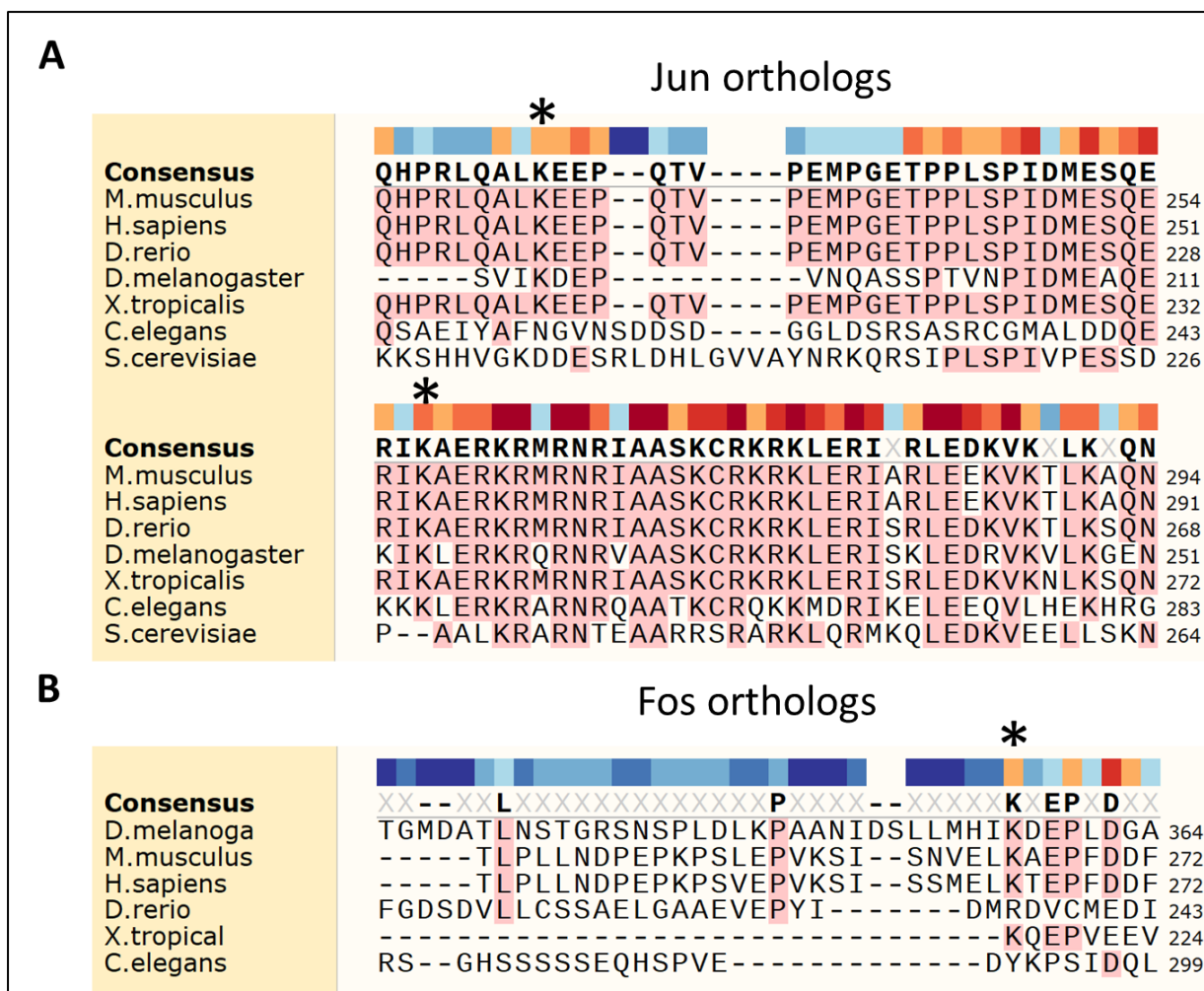


**Figure 2.4: Multiple sequence alignment (MSA) of homologs**

**A.** Snapshot of MSA of Jra orthologs from different model organisms. Previously reported SUMO acceptor lysine residues in mammals; K229 and K254 are shown by an asterisk.

**B.** Snapshot of MSA of Kay orthologs from different model organisms. Previously reported SUMO acceptor lysine residue in mammals; K265 is shown by an asterisk.

Conserved amino acids are highlighted in a shade of red. *D.melanogaster* (fruitfly); *M.musculus* (mouse); *H.sapiens* (human); *X.tropicalis* (frog); *C.elegans* (worm); *S.cerevisiae* (yeast).

## 2.3 Results and Discussion

### 2.3.1 Demonstration of SUMOylation of Jra and Kay

We started by looking for evidence of the SUMO conjugation of Jra and Kay. We used an *in-vitro* approach which was previously described (Nie et al., 2009). The bacterial SUMOylation assay is a modified *in-vitro* assay where four polypeptides that are sufficient to conjugate a mature SUMO (that has the GG motif exposed) to a target protein, are co-expressed with an N-terminal GST fused protein of interest. GST fusion Jra and Kay constructs were independently transformed into cells and co-expressed with 6x His tagged SUMO and other components of the *Drosophila* SUMO machinery. We performed an anti-GST pulldown (PD) followed by western blotting (WB) for both anti-GST and anti-His. We observed that Jra was SUMOylated and the SUMOylated bands were visible as higher molecular weight band on the anti-GST WB. This was confirmed with the presence of three prominent and distinct bands in the anti-His WB (Figure 2.5A). Similarly, we observed that Kay was SUMOylated and the SUMOylated band was seen as a single higher molecular weight band in the anti-His WB (Figure 2.5B).

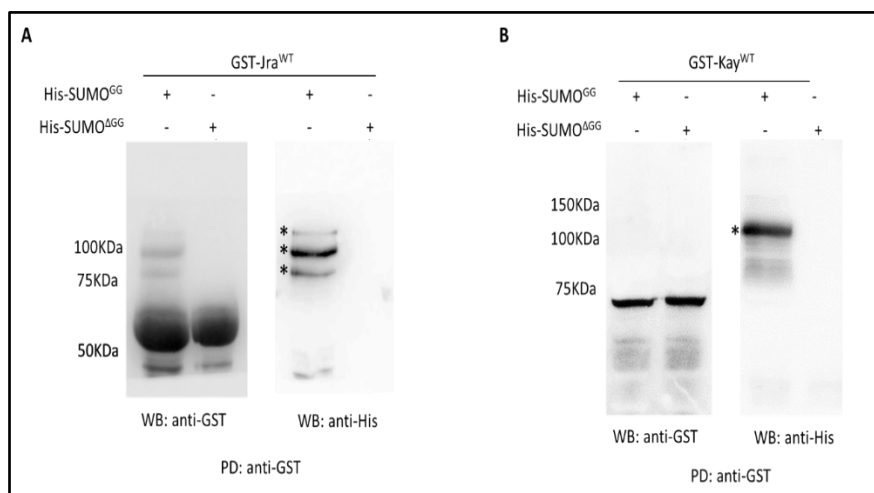


**Figure 2.5: Jra and Kay are SUMOylated in in-vitro.**

**A.** Western blot image of SUMOylated Jra post an anti-GST pulldown. The left image represents the anti-GST western blot and the right image represents the anti-His western blot. Three higher

molecular weight SUMOylated bands were observed in the anti-His WB and are marked with asterisks. His-SUMO<sup>AGG</sup> that lacks the GG motif and cannot conjugate is used as a negative control.

**B.** Western blot image of SUMOylated Kay post an anti-GST pulldown. The left image represents the anti-GST western blot and the right image represents the anti-His western blot. A single higher molecular weight SUMOylated band was observed in the anti-His WB and is marked with an asterisk.

### 2.3.2 Identification of lysine acceptor sites in Jra and Kay

SUMO conjugates to a lysine of a target protein. SUMO is known to prefer lysine residues that are in the consensus SUMO motif ( $\Psi$ KXE/D). To identify the target lysine residues, we used a web-based tool called Joined Advanced SUMOylation Site and Sim Analyser (JASSA) (Beauchair et al., 2015). Prediction by JASSA uses a score, based on the position and frequency of lysine residues from experimentally validated sequences. We used Jra-PB and Kay-PB isoforms as input for the JASSA web interface. We identified a total of ten lysine residues in Jra that were likely to be SUMO acceptor sites (Figure 2.6A). Similarly, we identified six lysine residues as confident hits for Kay (Figure 2.6B).

| A                          |                       |         |                  |      |        |                    |      |        |  |
|----------------------------|-----------------------|---------|------------------|------|--------|--------------------|------|--------|--|
| Putative SUMO sites in Jra |                       |         |                  |      |        |                    |      |        |  |
| Position K                 | Sequence              | Best PS | Consensus direct |      |        | Consensus Inverted |      |        |  |
|                            |                       |         | Type             | PSd  | DB Hit | Type               | PSi  | DB Hit |  |
| K29                        | SGATAIQIIEPTEPVGEEGM  | High    | NDSM             | High | 3      | None               | None |        |  |
| K57                        | NLNTSTPNPNKRPGSLDLNSK | None    | None             | None |        | None               | None | 1      |  |
| K88                        | LVINSPDLSSKTYNTPDLEKI | None    | None             | None |        | None               | None | 1      |  |
| K190                       | TNMTPEFVYIKDEIVNQASSP | High    | SC-SUMO          | High | 5      | None               | None |        |  |
| K214                       | PIDMEAQEKIPLERKRQRNRV | High    | Strong Consensus | High | 10     | None               | None | 2      |  |
| K231                       | RNRVAASKCRKRRLERISKLE | None    | None             | None | 3      | None               | None |        |  |
| K233                       | RVAASKCRKRRLERISKLEDR | None    | None             | None | 1      | None               | None | 2      |  |
| K245                       | ERISKLEDRVKVLKGENVDLA | None    | None             | None |        | None               | None | 1      |  |
| K248                       | SKLEDRVKVLRGENVDLASIV | Low     | Strong Consensus | Low  | 4      | None               | None |        |  |
| K259                       | GENVDLASIVKNLKDHVQQLK | None    | None             | None | 1      | None               | None |        |  |

| B                          |                       |         |                  |      |        |                    |      |        |  |
|----------------------------|-----------------------|---------|------------------|------|--------|--------------------|------|--------|--|
| Putative SUMO sites in Kay |                       |         |                  |      |        |                    |      |        |  |
| Position K                 | Sequence              | Best PS | Consensus direct |      |        | Consensus Inverted |      |        |  |
|                            |                       |         | Type             | PSd  | DB Hit | Type               | PSi  | DB Hit |  |
| K24                        | LFNMPLSPLPKVLGNFETGQS | None    | None             | None |        | None               | None | 2      |  |
| K211                       | STNMTPEEEQKRAVRRERNKQ | None    | None             | None |        | None               | None | 1      |  |
| K228                       | RNKQAAARCRKRVDQTNELT  | None    | None             | None | 1      | None               | None |        |  |
| K344                       | TGRSNSPLDLRKAANIDSLLM | Low     | None             | None |        | Consensus inv      | Low  | 2      |  |
| K357                       | ANIDSLLMHTRDEPLDGATIS | High    | NDSM             | High | 5      | None               | None |        |  |
| K380                       | SLDQDGPPSKRITLPEMSTM  | None    | None             | None | 1      | None               | None |        |  |

**Figure 2.6: Identification of putative SUMO acceptor lysine residues by JASSA**

**A.** Identification of putative SUMO acceptor lysine residues in Jra. A total of 10 lysine residues were identified to be putative targets.

**B.** Identification of putative SUMO acceptor lysine residues in Kay. A total of 6 lysine residues were identified to be putative targets. Column 1: Position of lysine residues in the amino acid sequence; column 2: Protein sequence with 21 amino acid window; column 3: best predictive score (PS); predictive score direct (PSd); predictive score inverted (PSi); negatively charged amino acid-dependent SUMOylation motif (NDSM); synergy control motif-SUMO (SC-SUMO); previously reported SUMOylation sites (DB hit)

To experimentally validate the putative SUMO acceptor lysine residues, we used site-directed mutagenesis to alter the lysine residues to arginine residues using specific primers and check for loss of SUMOylation on a western blot. We modified the target protein such that only one lysine was altered to arginine at a given time. We used all these variants independently and performed the bacterial SUMOylation assay. We targeted seven lysine residues in Jra and performed an anti-GST PD followed by an anti-GST WB and an anti-His WB. We observed a significant change in the pattern of higher molecular weight SUMO bands in the variants Jra<sup>K29R</sup> (Figure 2.7B) and Jra<sup>K190R</sup> (Figure 2.7A). Other variants did not show any change in the band pattern in the anti-His WB. Since mutating single lysine residues at 29<sup>th</sup> and 190<sup>th</sup> positions, only partially removed SUMOylation, we expected that a variant of Jra which harbours lysine to arginine mutation at both the sites concurrently would show complete loss of SUMOylation. As anticipated, the double (K→R) mutant shows complete loss of SUMOylation in an anti-His WB post an anti-GST PD (Figure 2.8A)

We used the same approach for Kay and mutated four lysine residues to arginine residues. Interestingly, a single lysine to arginine mutation on 357<sup>th</sup> position, completely abrogated SUMOylation as seen in the anti-His WB (Figure 2.7C and Figure 2.8B).

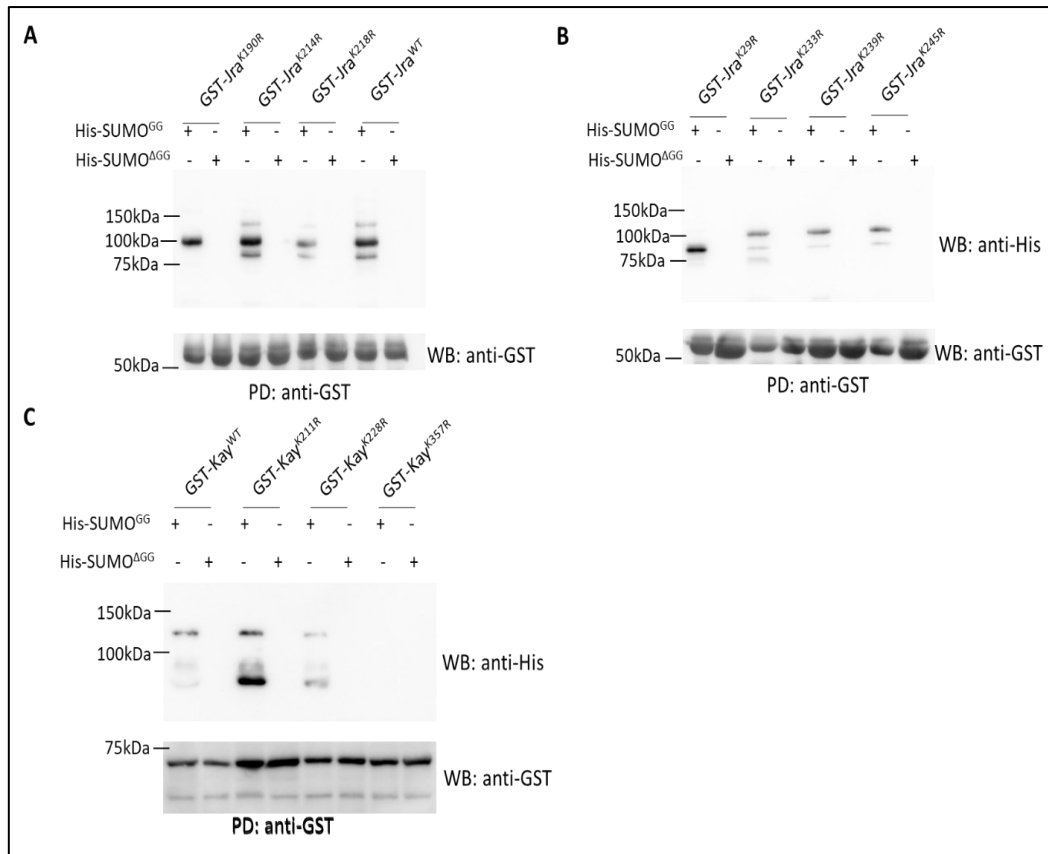


**Figure 2.7: Site-directed mutagenesis screen to identify SUMO acceptor lysine residues in Jra and Kay.**

**A.** Anti-His WB (upper panel) showing the SUMOylated bands of Jra. Lane 1: Jra<sup>K190R</sup> shows partial loss of SUMOylation where the upper and lowermost SUMOylated bands disappear. Lanes 3 and 5 correspond to Jra<sup>K214R</sup> and Jra<sup>K218R</sup> respectively. These variants do not show any loss of bands and behave like the wildtype as seen in lane 7. Anti-GST WB (lower panel) showing equal loading of different variants of GST-Jra.

**B.** Anti-His WB (upper panel) showing the SUMOylated bands of Jra. Lane 1: Jra<sup>K29R</sup> shows partial loss of SUMOylation where the two bands on the top disappear. Lanes 3, 5, and 7 correspond to Jra<sup>K233R</sup>, Jra<sup>K239R</sup>, and Jra<sup>K245R</sup> respectively, and do not show any loss of higher molecular weight SUMO bands. Anti-GST WB (lower panel) showing equal loading of different variants of GST-Jra.

**C.** Anti-His WB (upper panel) showing the SUMOylated bands of Kay. Lane 1: Kay<sup>WT</sup> shows a single higher molecular weight band as described earlier. Lane 3 and lane 5 correspond to Kay<sup>K211R</sup> and Kay<sup>K228R</sup> respectively and do not show and loss of SUMOylation. Lane 7 corresponds to Kay<sup>K357R</sup> and shows complete loss of SUMOylation where the higher molecular weight band is absent. Anti-GST WB (lower panel) showing equal loading of different variants of GST-Kay. Lanes 2, 4, 6, and 8 are used as negative controls where the bacterial cells have been transformed with His-SUMO<sup>ΔGG</sup> that cannot be conjugated to a lysine residue.



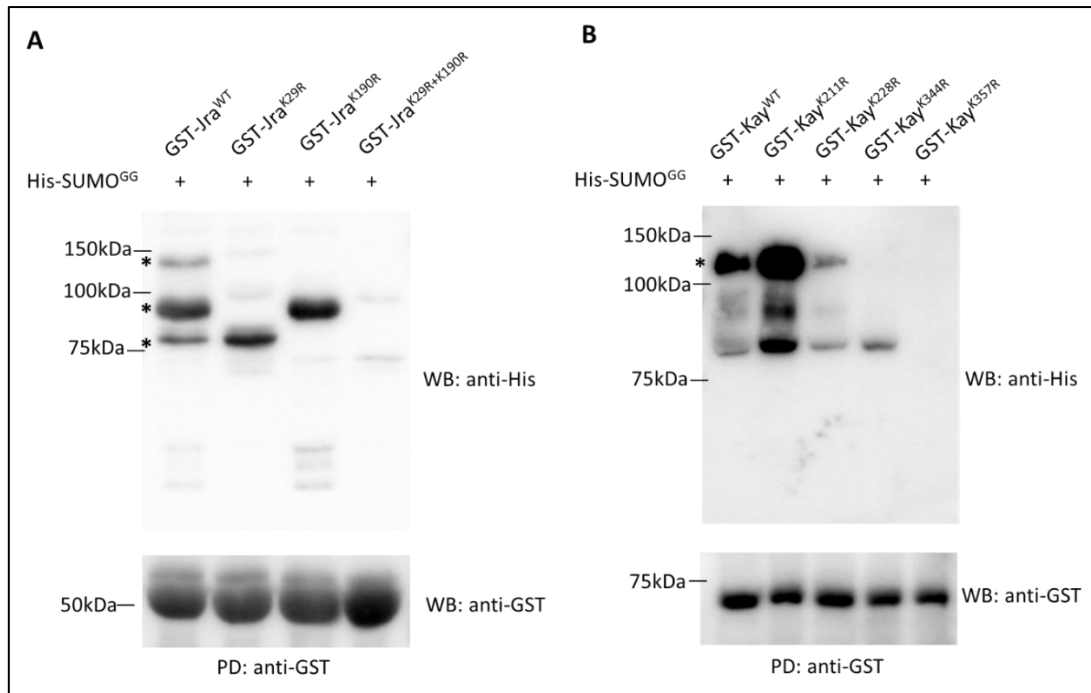


**Figure 2.8: Demonstration of complete loss of SUMOylation in Jra and Kay**

**A.** Anti-His WB (upper panel) showing the three distinct SUMOylated Jra bands in Jra<sup>WT</sup> (lane 1). Partial loss of SUMOylation in Jra<sup>K29R</sup> and Jra<sup>K190R</sup> as seen in lanes 2 and 3 respectively. Complete loss of SUMOylation in Jra<sup>K29R+K190R</sup> that harbours both SUMO resistant mutations as seen in lane 4. Anti-GST WB (lower panel) showing unmodified Jra that serves as input.

**B.** Anti-His WB (upper panel) showing a single SUMOylated Kay band in Kay<sup>WT</sup> (lane 1). No loss of SUMOylation in Kay<sup>K211R</sup> and Kay<sup>K228R</sup> as seen in lanes 2 and 3 respectively. Partial loss of SUMOylation in Kay<sup>K344R</sup> as seen in lane 4. Complete loss of SUMOylation in Kay<sup>K357R</sup> as seen in lane 5. Anti-GST WB (lower panel) showing unmodified Kay that serves as input.

### 2.3.3 *In-vivo* demonstration of SUMOylation of Jra and Kay in S2 cell

As we were successful in demonstrating SUMOylation and identifying SUMO acceptor lysine residues of Jra and Kay in an *in-vitro* assay, we were excited to see if we could reproduce our findings in a system that is native to *Drosophila*. For this, we used the *Drosophila* Schneider 2 (S2) cells that were stably transfected with Flag-SUMO (Bhaskar et al., 2002). These cells were transiently transfected with different variants of 6xHis-tagged Jra and HA-tagged Kay. We performed an anti-His PD followed by an anti-His PD and an anti-Flag WB for Jra. We observed that Jra<sup>WT</sup> shows two SUMOylated bands. Jra<sup>K190R</sup> shows partial loss of SUMOylation. As expected, Jra<sup>K29R+K190R</sup> shows a complete loss of SUMOylation.

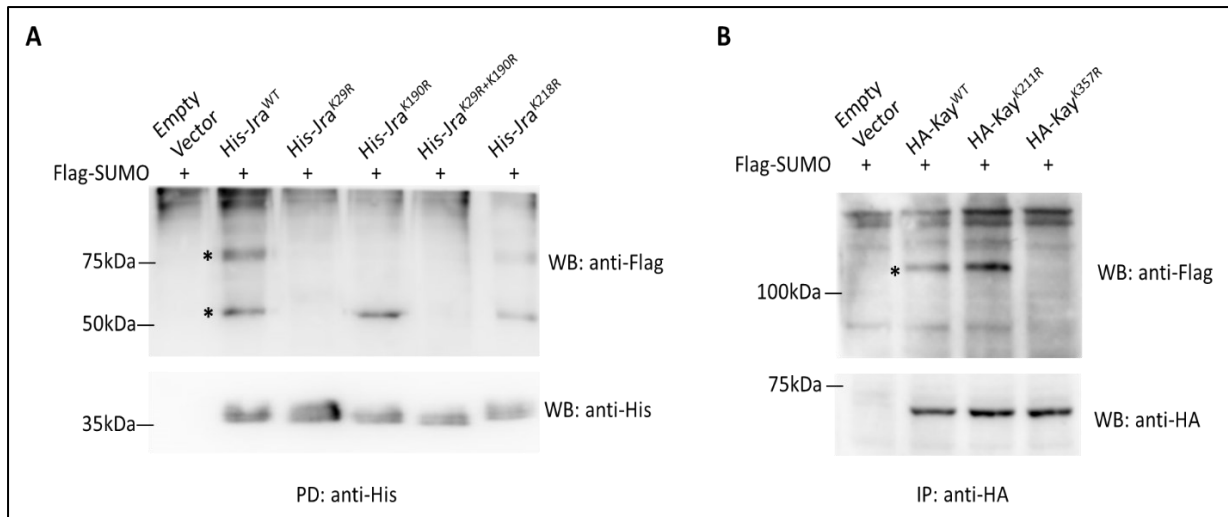


**Figure 2.9: Demonstration of SUMOylation of Jra and Kay in S2 cells and confirmation of SUMO acceptor lysine residues.**

**A.** Anti-Flag WB post an anti-His PD in the upper panel represents the SUMOylated species of Jra. SUMOylated Jra species can be seen as two distinct bands in the 2<sup>nd</sup> lane marked by asterisks (\*). Jra<sup>K190R</sup> in the 4<sup>th</sup> lane shows partial loss of SUMOylation. Jra<sup>K29R</sup> and Jra<sup>K29R+K190R</sup> show complete loss of SUMOylation and can be seen in the 3<sup>rd</sup> and 5<sup>th</sup> lanes without any SUMOylated bands. Jra<sup>K218R</sup> that was previously shown not to alter SUMOylation status in the bacterial assay was used as a control and can be seen in lane 6 with the presence of two SUMOylated bands. The empty vector in lane 1 was used as a negative control. The lower panel (anti-His WB) represents unmodified Jra and serves as input.

**B.** Anti-Flag WB post an anti-HA immunoprecipitation (IP) in the upper panel represents the SUMOylated species of Kay. SUMOylated Kay species can be seen as a single band in the 2<sup>nd</sup> lane marked by an asterisk. Kay<sup>K357R</sup> in the 4<sup>th</sup> lane shows complete loss of SUMOylation as seen in the bacterial SUMOylation assay. Kay<sup>K211R</sup> was shown not to alter SUMOylation status in the bacterial assay was used as a control and can be seen in lane 3 with the presence of the same band pattern as that of Kay<sup>WT</sup>. The empty vector was used as a negative control. The lower panel represents unmodified Kay (anti-HA WB) and serves as input. 529SU cells stably expressed Flag-SUMO under the control of the Metallothionine promoter.

Interestingly, Jra<sup>K29R</sup> shows a complete loss of SUMOylation like Jra<sup>K29R+K190R</sup> (Figure 2.9A). Similarly, we performed an anti-HA IP followed by anti-HA WB and anti-Flag WB for Kay. We observed that Kay<sup>WT</sup> shows a single SUMOylated band. Kay<sup>K357R</sup> shows a complete loss of SUMOylation as expected (Figure 2.9B).

## 2.4 Summary

We have used the bacterial SUMOylation assay system to demonstrate the SUMOylation of Jra and Kay. We have performed anti-GST pulldowns followed by western blotting with anti-GST and anti-His antibodies. We have observed that Jra is heavily SUMOylated and the higher molecular weight SUMOylated species can be seen in the anti-GST WB. The anti-His WB clearly shows three distinct higher molecular weight SUMOylated bands (Figure 2.5A). This points out the possibility that there could be more than one SUMO acceptor lysine residues in Jra and the three bands indicate different SUMOylated species in different combinations. Similarly, we have observed a single higher molecular weight SUMOylated band in the anti-His WB for Kay suggesting a single SUMO acceptor lysine (Figure 2.5B). We have compared orthologous sequences from different model organisms to identify conserved lysine residues and also used a web-based tool, JASSA, to predict the lysine acceptor residues in Jra and Kay. JASSA has identified ten and six putative lysine acceptor sites for Jra and Kay respectively (Figure 2.6). We have used this information to generate seven lysine to arginine mutations for Jra and four lysine to arginine mutations for Kay. We have then performed the bacterial SUMOylation assay on each of these constructs to identify the SUMO acceptor lysine residues in both Jra and Kay. We have identified that Jra<sup>K29R</sup> and Jra<sup>K190R</sup> show partial loss of SUMOylation (Figure 2.7A-B, Figure 2.8A). K190 in Jra is conserved in various animal models and previously been reported to be SUMOylated in mammals. Interestingly, K29 was unique to *Drosophila* and is absent in other species. We further validated our findings from the bacterial SUMOylation assay in *Drosophila* 529SU cells. These cells are S2 cells stably transfected with a mature form of SUMO tagged to Flag on the N-terminus. We have transfected different variants of His-Jra and HA-Kay and performed anti-His PDs and anti-HA IPs. We have observed that Jra<sup>WT</sup> has two SUMOylated bands (Figure 2.9A) as opposed to three that were observed in the in-vitro system (Figure 2.8A). This finding shed light on the

fact that the SUMOylated band patterns in the bacterial SUMOylation assay could be different from that of a system native to *Drosophila* and it's imperative to validate the findings from the bacterial assay in S2 cells. Further, we have observed that Jra<sup>K190R</sup> shows partial loss of SUMOylation as seen in the in-vitro system. Surprisingly, Jra<sup>K29R</sup> shows a complete loss of SUMOylation. We hypothesize that this could be because SUMOylation on K29 is necessary for SUMOylation on K190 to occur and the absence of K29 does not allow K190 to get SUMOylated. Also, the double mutant of K29R+K190R completely loses SUMOylation (Figure 2.9A, Figure 2.10A, Figure 2.10B). Similarly, we have observed that Kay was SUMOylated on a single lysine residue at the 357<sup>th</sup> position (Figure 2.9B and Figure 2.10C).

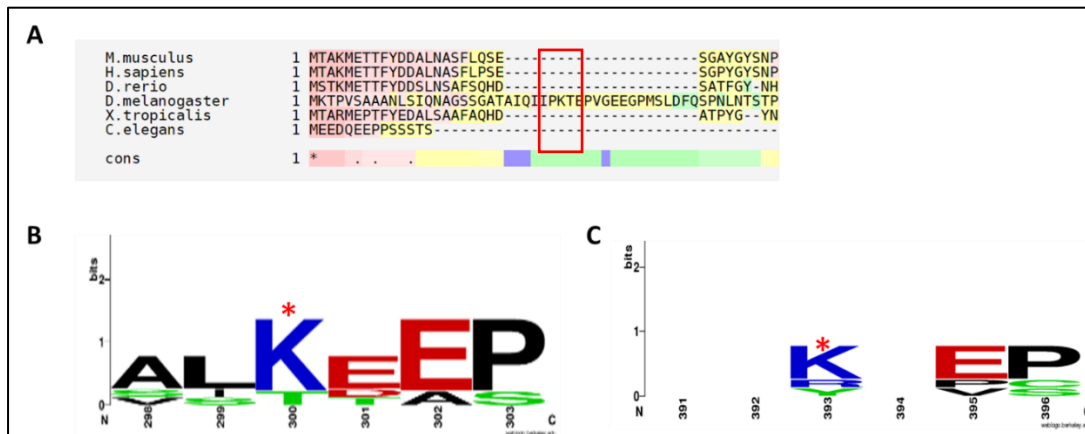


**Figure 2.10: Summary of SUMO acceptor lysine residues.**

**A.** Multiple sequence alignment (MSA) of orthologues of Jra from different model organisms showing 1-50 amino acids in Jra. K29 (highlighted in the red box) is present in a sequence that is unique to *Drosophila* and is absent in other organisms. MSA was performed using the Espresso module of T-coffee (<http://tcoffee.org.cat/apps/tcoffee/index.html>) (Notredame et al., 2000)).

**B-C.** WebLogo (<https://weblogo.berkeley.edu/>) (Crooks et al., 2004)) representation of Jra<sup>K190</sup> (B) and Kay<sup>K357</sup> (C) post MSA, showing the conserved SUMO acceptor lysine residues.

We were successful in demonstrating SUMOylation of *Drosophila* AP-1 dimers Jra and Kay and identified the SUMO acceptor lysine residues. Jra<sup>K29R+K190R</sup> and Kay<sup>K357R</sup> show complete loss of SUMOylation and these SUMO conjugation resistant (SCR) mutants are henceforth referred to as Jra<sup>SCR</sup> and Kay<sup>SCR</sup> respectively.

## 2.5 Materials and Methods

### 2.5.1 Cloning and generation of constructs

Jra ([FBpp0087498](#)) and Kay ([FBpp0084846](#)) cDNA was amplified from the *Drosophila* gold collection library ([https://www.fruitfly.org/EST/gold\\_collection.shtml](https://www.fruitfly.org/EST/gold_collection.shtml)) using specific primers. These amplicons were independently cloned into pGEX-4T1 for bacterial SUMOylation assay and pRM-HA3 vector for transfection into S2 cells using a modified Seamless Ligation Cloning Extract (SLiCE) protocol (Zhang et al., 2012). The site-directed mutagenesis approach with specific primers was used to convert all the lysine residues to arginine residues to abrogate SUMO conjugation. All the clones were confirmed by sequencing and used for downstream experiments. PPY cells used for restriction-free cloning was a kind gift from Dr. Winfried Edelmann.

**Table 2.1: List of primers**

|    | Primer        | Sequence (5'-> 3')                             | Description                                  |
|----|---------------|--|--|
| 1  | pGEX-Jra F    | CTGGTTCCCGTGGATCCCCGGAATTCATGAAAACCCCGTTCC     | Primer pair used to amplify Jra for pGEX-4T1 |
| 2  | pGEX-Jra R    | TCGTCAGTCAGTCACGATGCGGCCGCTTATTGGTCTGTCGAGTTCG |  |
| 3  | Jra-K245R F   | GGAGGATCGCGTGAGGGTACTTAAGGGC                   | Primer pair used to mutate K245R in Jra      |
| 4  | Jra-K245R R   | GCCCTTAAGTACCCTCACGCGATCCTCC                   |  |
| 5  | Jra-K29R F    | TCAGATCATACCTAGGACCGAGCCCGTTGG                 | Primer pair used to mutate K29R in Jra       |
| 6  | Jra-K29R R    | CCAACGGGCTCGGTCTTAGGTATGATCTGA                 |  |
| 7  | Jra-K218R F   | AAGCTGGAGCGCAGGAGGCAGCGTAACC                   | Primer pair used to mutate K218R in Jra      |
| 8  | Jra-K218R R   | GGTTACGCTGCCTCCTGCGCTCCAGCTT                   |  |
| 9  | Jra-K233R F   | TGCCGCAAGCGCAGGTTGGAGCGCATCT                   | Primer pair used to mutate K233R in Jra      |
| 10 | Jra-K233R R   | AGATGCGCTCCAACCTGCGCTTGC GGCA                  |  |
| 11 | Jra-K239R F   | GAGCGCATCTCAAGGCTGGAGGATCGCG                   | Primer pair used to mutate K239R in Jra      |
| 12 | Jra-K239R R   | CGCGATCCTCCAGCCTTGAGATGCGCTC                   |  |
| 13 | Jra-K190R F   | TCGGTGATTAAGGACGAGCCC                          | Primer pair used to mutate K190R in Jra      |
| 14 | Jra-K190R R   | GGGCTCGTCCTTAATCACCGA                          |  |
| 15 | pRM-His-Jra F | ATGCACCACCATCACCATGGAGGCGGAATGAAAACCCCGTTCCGC  | Primer pair used to amplify Jra for pRM-HA3  |
| 16 | pRM-His-Jra R | GCAGGTCGACTCTAGAGGATCCTTATTGGTCTGTCGAGTTCG     |  |

|    |              |   |  |
|----|--------------|---|--|
| 17 | pGEX-Kay F   | CTGGTTCCGCGTGGATCCCCGGAATTCATGACGCTGGACAGCTACAAC  | Primer pair used to amplify Kay for pGEX-4T1 |
| 18 | pGEX-Kay R   | TCGTCAGTCAGTCACGATGCGGCCGCTTATAAGCTGACCAGCTTGGGA  |  |
| 19 | Kay-K211R F  | GAGGAGCAGAGGCGGGCCGTG                             | Primer pair used to mutate K211R in Kay      |
| 20 | Kay-K211R R  | CACGGCCCGCCTCTGCTCCTC                             |  |
| 21 | Kay-K220R F  | GAGCGGAACAGGCAGGCGGGCG                            | Primer pair used to mutate K220R in Kay      |
| 22 | Kay-K220R R  | CGCCGCTGCCTGTTCCGCTC                              |  |
| 23 | Kay-K344R F  | TTGGATCTCAGGCCGGCGGGC                             | Primer pair used to mutate K344R in Kay      |
| 24 | Kay-K344R R  | CGCCGCCGGCCTGAGATCCAA                             |  |
| 25 | Kay-K357R F  | CTGATGCACATCAGGGACGAGCCACTC                       | Primer pair used to mutate K257R in Kay      |
| 26 | Kay-K357R R  | GAGTGGCTCGTCCCTGATGTGCAT                          |  |
| 27 | pRM-HA-Kay F | ACGATGTTCCAGATTACGCTGGAGGCGAAATGACGCTGGACAGCTACAA | Primer pair used to amplify Jra for pRM-HA3  |
| 28 | pRM-HA-Kay R | GCAGGTCGACTCTAGAGGATCCTTATAAGCTGACCAGCTTGG        |  |

### 2.5.2 Bacterial SUMOylation assay

This system is a modified in-vitro SUMOylation assay that was previously described (Nie et al., 2009). The quartet vector comprising of the *Drosophila* SUMO machinery components was co-transformed with GST fused Jra or Kay. The bacterial culture is induced with 1mM of Isopropyl  $\beta$ -D-1-thiogalactopyranoside (IPTG) for 6 hours at 25C. 10ml of the bacterial culture was harvested in 1ml 50mM *tris* aminomethane (TRIS) buffer containing 150mM NaCl, 1mM Dithiothreitol (DTT), 1ug/ml lysozyme, and 1mM phenylmethylsulfonyl fluoride (PMSF). The cells were lysed using a VibraCell™ probe sonicator with 2/3sec ON/OFF cycle for 2 min at 60% amplitude.

### 2.5.3 S2 cell culture and transfections

S2 cells that were stably transfected with Flag-SUMO (referred to as 529SU cells) were a kind gift from Albert Courey. The cells were grown and maintained in Gibco® Schneider's *Drosophila* Medium (Thermo Fischer Scientific, # 21720024) supplemented with 10% heat-inactivated fetal bovine serum (FBS) (Thermo Fischer Scientific, #10082147) at 23C. Cells

were passaged once every 3-4 days and discarded after 20 passages. We used 40-50% confluent cells in 6 well flasks and the volume of the culture was set to 2ml for all our transfections. We transfected 1ug of plasmid using TransIT®-Insect Transfection Reagent (Mirus, #6100) as per the manufacturer's protocol. 6h post-transfection, we induced the cells with 0.5M CuSO<sub>4</sub>. The cells were harvested after 48h of induction, centrifuged at 300g for 10 minutes in a cold centrifuge. The cells were washed once with 1X-Phosphate buffer saline (PBS) and lysed in a buffer that best suited the downstream application.

#### ***2.5.4 Pulldown, Immunoprecipitation and Western blotting***

All the beads used were equilibrated in the appropriate buffer before binding to the lysates. Anti-GST PD for the bacterial SUMOylation assay was done using Pierce™ Glutathione Agarose beads (Thermo Fischer Scientific, #16101). Post lysis, the bacterial lysate was incubated with the equilibrated beads for 12-14h at 4C. The beads were then washed 3 times with the lysis buffer with 0.1% triton-X100. We used Ni-NTA superflow resin (Qiagen, #30430) to pull down His-Jra from 529SU cells and performed the experiment as per the manufacturer's protocol. To maintain stringent denaturing conditions, we used 8M Urea throughout the experiment in all the buffers. For the anti-HA IP, we lysed the 529SU cells in 1x radioimmunoprecipitation assay (RIPA) buffer supplemented with 1X cOmplete™, EDTA-free Protease Inhibitor Cocktail (PIC) (Sigma-Aldrich, # 11873580001) and 20mM N-ethylmaleimide (NEM) (Sigma-Aldrich, #E3876) for 20 min at 4C. The lysate was then incubated with Monoclonal anti-HA agarose beads (Sigma-Aldrich, A2095) at 4C for 12-14h. Post binding, the beads were washed 3x with 1x RIPA buffer and processed for western blotting. We used Pierce™ BCA Protein Assay Kit to estimate the protein concentration from 529SU cell lysates. We used 1mg of total protein for PD and IP experiments and 50ug of total protein for inputs. For all the western blotting experiments, we first separated the proteins using 12% polyacrylamide gel followed by a transfer onto a 0.45µm polyvinylidene fluoride (PVDF)

membrane (Sigma-Aldrich, #P2938). Post transfer, all the blots were blocked with 5% skimmed milk dissolved in 1x TRIS buffer saline (TBS) with 0.1% Tween-20 (Sigma-Aldrich, #P9416) detergent. The following antibodies were used as primary antibodies for the WB. Anti-His (SCBT, #sc-8036; used in 1:2000), anti-GST (SCBT, #459; used in 1:5000), anti-Flag (Sigma-Aldrich, #F7425; used in 1:2000) and anti-HA (Sigma-Aldrich, #04-902; used in 1:1000). The following are the secondary antibodies used. Peroxidase conjugated anti-mouse (Jackson Immunoresearch, #115-035-003; used in 1:10000) and peroxidase-conjugated anti-rabbit (Jackson Immunoresearch, #111-035-003; used in 1:10000). All the blots were developed using Immobilon Western Chemiluminescent HRP Substrate (Sigma-Aldrich, #WBKLS).



## 2.6 References

1. Arthur, J.S., and Ley, S.C. (2013). Mitogen-activated protein kinases in innate immunity. *Nat Rev Immunol* 13, 679-692.
2. Baker, N.E. (2020). Emerging mechanisms of cell competition. *Nat Rev Genet* 21, 683-697.
3. Beauclair, G., Bridier-Nahmias, A., Zagury, J.F., Saib, A., and Zamborlini, A. (2015). JASSA: a comprehensive tool for prediction of SUMOylation sites and SIMs. *Bioinformatics* 31, 3483-3491.
4. Bhaskar, V., Smith, M., and Courey, A.J. (2002). Conjugation of Smt3 to dorsal may potentiate the *Drosophila* immune response. *Mol Cell Biol* 22, 492-504.
5. Bhaskar, V., Valentine, S.A., and Courey, A.J. (2000). A functional interaction between dorsal and components of the Smt3 conjugation machinery. *J Biol Chem* 275, 4033-4040.
6. Bossis, G., Malnou, C.E., Farras, R., Andermarcher, E., Hipskind, R., Rodriguez, M., Schmidt, D., Muller, S., Jariel-Encontre, I., and Piechaczyk, M. (2005). Down-regulation of c-Fos/c-Jun AP-1 dimer activity by sumoylation. *Mol Cell Biol* 25, 6964-6979.
7. Celen, A.B., and Sahin, U. (2020). Sumoylation on its 25th anniversary: mechanisms, pathology, and emerging concepts. *FEBS J*.
8. Chiu, H., Ring, B.C., Sorrentino, R.P., Kalamarz, M., Garza, D., and Govind, S. (2005). dUbc9 negatively regulates the Toll-NF-kappa B pathways in larval hematopoiesis and drosomycin activation in *Drosophila*. *Dev Biol* 288, 60-72.
9. Crooks, G.E., Hon, G., Chandonia, J.M., and Brenner, S.E. (2004). WebLogo: a sequence logo generator. *Genome Res* 14, 1188-1190.
10. Dhanasekaran, D.N., and Reddy, E.P. (2008). JNK signalling in apoptosis. *Oncogene* 27, 6245-6251.
11. Eferl, R., and Wagner, E.F. (2003). AP-1: a double-edged sword in tumorigenesis. *Nat Rev Cancer* 3, 859-868.
12. Eifler, K., and Vertegaal, A.C.O. (2015). SUMOylation-Mediated Regulation of Cell Cycle Progression and Cancer. *Trends Biochem Sci* 40, 779-793.
13. Etter, P.D., Narayanan, R., Navratilova, Z., Patel, C., Bohmann, D., Jasper, H., and Ramaswami, M. (2005). Synaptic and genomic responses to JNK and AP-1 signalling in *Drosophila* neurons. *BMC Neurosci* 6, 39.
14. Flotho, A., and Melchior, F. (2013). Sumoylation: a regulatory protein modification in health and disease. *Annu Rev Biochem* 82, 357-385.

15. Freeman, A., Bowers, M., Mortimer, A.V., Timmerman, C., Roux, S., Ramaswami, M., and Sanyal, S. (2010). A new genetic model of activity-induced Ras signalling dependent pre-synaptic plasticity in *Drosophila*. *Brain Res* 1326, 15-29.
16. Gareau, J.R., and Lima, C.D. (2010). The SUMO pathway: emerging mechanisms that shape specificity, conjugation and recognition. *Nat Rev Mol Cell Biol* 11, 861-871.
17. Glise, B., Bourbon, H., and Noselli, S. (1995). hemipterous encodes a novel *Drosophila* MAP kinase kinase, required for epithelial cell sheet movement. *Cell* 83, 451-461.
18. Handu, M., Kaduskar, B., Ravindranathan, R., Soory, A., Giri, R., Elango, V.B., Gowda, H., and Ratnaparkhi, G.S. (2015). SUMO-Enriched Proteome for *Drosophila* Innate Immune Response. *G3 (Bethesda)* 5, 2137-2154.
19. Hendriks, I.A., D'Souza, R.C., Yang, B., Verlaan-de Vries, M., Mann, M., and Vertegaal, A.C. (2014). Uncovering global SUMOylation signalling networks in a site-specific manner. *Nat Struct Mol Biol* 21, 927-936.
20. Hendriks, I.A., and Vertegaal, A.C. (2016). A comprehensive compilation of SUMO proteomics. *Nat Rev Mol Cell Biol* 17, 581-595.
21. Hou, X.S., Goldstein, E.S., and Perrimon, N. (1997). *Drosophila* Jun relays the Jun amino-terminal kinase signal transduction pathway to the Decapentaplegic signal transduction pathway in regulating epithelial cell sheet movement. *Genes Dev* 11, 1728-1737.
22. Kim, L.K., Choi, U.Y., Cho, H.S., Lee, J.S., Lee, W.-b., Kim, J., Jeong, K., Shim, J., Kim-Ha, J., and Kim, Y.-J. (2007). Down-regulation of NF- $\kappa$ B target genes by the AP-1 and STAT complex during the innate immune response in *Drosophila*. *PLoS Biol* 5, e238.
23. Kim, S.M., Kumar, V., Lin, Y.Q., Karunanithi, S., and Ramaswami, M. (2009). Fos and Jun potentiate individual release sites and mobilize the reserve synaptic vesicle pool at the *Drosophila* larval motor synapse. *Proc Natl Acad Sci U S A* 106, 4000-4005.
24. Kim, T., Yoon, J., Cho, H., Lee, W.B., Kim, J., Song, Y.H., Kim, S.N., Yoon, J.H., Kim-Ha, J., and Kim, Y.J. (2005). Downregulation of lipopolysaccharide response in *Drosophila* by negative crosstalk between the AP1 and NF-kappaB signalling modules. *Nat Immunol* 6, 211-218.
25. Kockel, L., Zeitlinger, J., Staszewski, L.M., Mlodzik, M., and Bohmann, D. (1997). Jun in *Drosophila* development: redundant and nonredundant functions and regulation by two MAPK signal transduction pathways. *Genes Dev* 11, 1748-1758.
26. La Marca, J.E., and Richardson, H.E. (2020). Two-Faced: Roles of JNK Signalling During Tumourigenesis in the *Drosophila* Model. *Front Cell Dev Biol* 8, 42.

27. Li, Z., Wu, C., Ding, X., Li, W., and Xue, L. (2020). Toll signalling promotes JNK-dependent apoptosis in *Drosophila*. *Cell Div* 15, 7.
28. Muller, S., Berger, M., Lehembre, F., Seeler, J.S., Haupt, Y., and Dejean, A. (2000). c-Jun and p53 activity is modulated by SUMO-1 modification. *J Biol Chem* 275, 13321-13329.
29. Nie, M., Xie, Y., Loo, J.A., and Courey, A.J. (2009). Genetic and proteomic evidence for roles of *Drosophila* SUMO in cell cycle control, Ras signalling, and early pattern formation. *PLoS One* 4, e5905.
30. Notredame, C., Higgins, D.G., and Heringa, J. (2000). T-Coffee: A novel method for fast and accurate multiple sequence alignment. *J Mol Biol* 302, 205-217.
31. Nusslein-Volhard, C., Wieschaus, E., and Kluding, H. (1984). Mutations affecting the pattern of the larval cuticle in *Drosophila melanogaster* : I. Zygotic loci on the second chromosome. *Wilehm Roux Arch Dev Biol* 193, 267-282.
32. Pichler, A., Fatouros, C., Lee, H., and Eisenhardt, N. (2017). SUMO conjugation - a mechanistic view. *Biomol Concepts* 8, 13-36.
33. Riesgo-Escovar, J.R., and Hafen, E. (1997a). Common and distinct roles of DFos and DJun during *Drosophila* development. *Science* 278, 669-672.
34. Riesgo-Escovar, J.R., and Hafen, E. (1997b). *Drosophila* Jun kinase regulates expression of decapentaplegic via the ETS-domain protein Aop and the AP-1 transcription factor DJun during dorsal closure. *Genes Dev* 11, 1717-1727.
35. Riesgo-Escovar, J.R., Jenni, M., Fritz, A., and Hafen, E. (1996). The *Drosophila* Jun-N-terminal kinase is required for cell morphogenesis but not for DJun-dependent cell fate specification in the eye. *Genes Dev* 10, 2759-2768.
36. Rios-Barrera, L.D., and Riesgo-Escovar, J.R. (2013). Regulating cell morphogenesis: the *Drosophila* Jun N-terminal kinase pathway. *Genesis* 51, 147-162.
37. Sanyal, S., Sandstrom, D.J., Hoeffler, C.A., and Ramaswami, M. (2002). AP-1 functions upstream of CREB to control synaptic plasticity in *Drosophila*. *Nature* 416, 870-874.
38. Sluss, H.K., Han, Z., Barrett, T., Goberdhan, D.C., Wilson, C., Davis, R.J., and Ip, Y.T. (1996). A JNK signal transduction pathway that mediates morphogenesis and an immune response in *Drosophila*. *Genes Dev* 10, 2745-2758.
39. Tempe, D., Vives, E., Brockly, F., Brooks, H., De Rossi, S., Piechaczyk, M., and Bossis, G. (2014). SUMOylation of the inducible (c-Fos:c-Jun)/AP-1 transcription complex occurs on target promoters to limit transcriptional activation. *Oncogene* 33, 921-927.

40. Ulrich, H.D., and Walden, H. (2010). Ubiquitin signalling in DNA replication and repair. *Nat Rev Mol Cell Biol* *11*, 479-489.
41. Wagner, E.F., and Nebreda, A.R. (2009). Signal integration by JNK and p38 MAPK pathways in cancer development. *Nat Rev Cancer* *9*, 537-549.
42. Wu, C., Li, Z., Ding, X., Guo, X., Sun, Y., Wang, X., Hu, Y., Li, T., La, X., Li, J., *et al.* (2019). Snail modulates JNK-mediated cell death in *Drosophila*. *Cell Death Dis* *10*, 893.
43. Xia, Y., and Karin, M. (2004). The control of cell motility and epithelial morphogenesis by Jun kinases. *Trends Cell Biol* *14*, 94-101.
44. Zhang, S., Chen, C., Wu, C., Yang, Y., Li, W., and Xue, L. (2015). The canonical Wg signalling modulates Bsk-mediated cell death in *Drosophila*. *Cell Death Dis* *6*, e1713.
45. Zhang, Y., Werling, U., and Edelmann, W. (2012). SLiCE: a novel bacterial cell extract-based DNA cloning method. *Nucleic Acids Res* *40*, e55.
46. Zilio, N., Eifler-Olivi, K., and Ulrich, H.D. (2017). Functions of SUMO in the Maintenance of Genome Stability. *Adv Exp Med Biol* *963*, 51-87.

## Chapter 3 : Generation of SUMO Conjugation resistant mutants of Jra and Kay

### 3.1 Abstract

In the previous chapter, we demonstrated that *Drosophila* AP-1 transcription factors Jun related antigen (Jra) and Kayak (Kay) are SUMO conjugated. We also have successfully identified the SUMO acceptor lysine residues and made SUMO conjugation resistant (SCR) variants of both the proteins, referred to as Jra<sup>SCR</sup> and Kay<sup>SCR</sup>. To understand the physiological role of SUMO conjugation of these proteins in *Drosophila*, we generated UAS transgenic fly lines that can be used to over-express wild-type and SCR variants of Jra and Kay in a specific tissue using the appropriate *GAL4*. Additionally, we successfully used the CRISPR/Cas9 technology to edit the genomic locus of *jra* and generated an SCR mutant.

### Keywords

Transgenics, CRISPR/Cas9, Genome editing

## 3.2 Introduction

### 3.2.1 The UAS-GAL4 system serves as a tool to overexpress transgenes of interest in a spatio-temporal manner

The UAS-Gal4 system is a versatile system that is used for targeted gene expression in *Drosophila*. This system has two main components, a transcriptional activator, Gal4 protein and upstream activation sequence (UAS) to which the Gal4 binds to and drives the expression of the transgene downstream (Figure 3.1). Gal4 originally identified in yeast is induced by the presence of galactose in the medium and belongs to a group of genes in an operonic region that is necessary for galactose uptake and metabolism. Gal4 drives the expression of other Gal genes by binding to a region upstream of these genes, that is analogous to the enhancer elements observed in higher eukaryotes, called the upstream activator sequence (UAS) (Duffy, 2002). This principle was explored and adapted to drive gene expression in *Drosophila* in a monumental article by Brand and Perrimon (Brand and Perrimon, 1993).

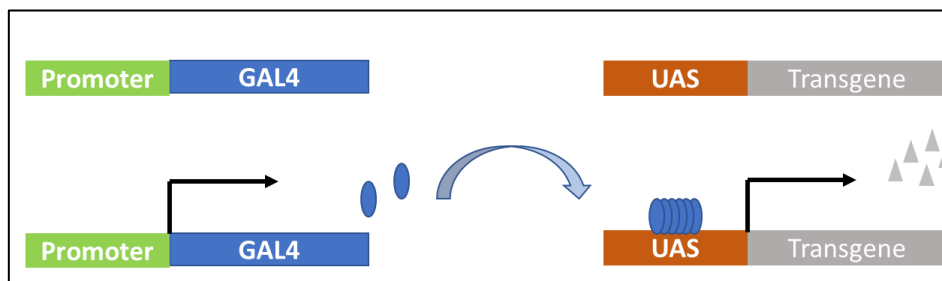


**Figure 3.1: Schematic of working of UAS-GAL4 system.**

The GAL4 activator is cloned downstream of a tissue-specific promoter. The transgene of interest is cloned downstream of the UAS elements. When two flies having both these elements are crossed, the tissue-specific promoter drives the expression of the Gal4 gene. The Gal4 protein in turn binds to the UAS elements and drives the expression of the transgene clones downstream to the UAS elements. This system offers stringent control of the expression of the transgene in a spatio-temporal manner. For further reading, refer to (Duffy, 2002)

### 3.2.2 CRISPR/Cas9 as a tool to edit the genome and generate transgenics in *Drosophila*

The CRISPR/Cas9 system, now an extremely popular and indispensable research tool in biomedical research, was first identified as a set of highly repetitive sequences in *E. coli* (Ishino

et al., 1987). Post this discovery, it took more than 25 years to understand the role of such repetitive sequences. The advent of robust genome sequencing technologies and ease of sequencing the small bacterial genomes proved the existence of such repetitive sequence in several other microbes. This has intensified the curiosity in understanding the role of such repetitive sequences present in many bacterial phyla. By early 2000, Mojica and colleagues identified these repetitive elements to be a characteristic feature of the members of Archae (Mojica et al., 2000) and by 2002, the term CRISPR was coined as clustered regularly interspaced short palindromic repeats (Jansen et al., 2002). The existence of CRISPR in several bacterial organisms led to the hypothesis that it could be an adaptive immune mechanism to fight off invading bacteriophages (Bolotin et al., 2005; Mojica et al., 2005; Pourcel et al., 2005) and the first experimental evidence came from a study by Barrangou and colleagues (Barrangou et al., 2007). Over the following years, several research labs all over the world have substantially contributed to understanding the molecular mechanism on how CRISPR/Cas9 acquires the protospacer sequences from the phages, incorporates them into the CRISPR locus, and generates crRNA to cleave the genetic material of the invading bacteriophage. This has led to a clearer understanding of several components of the CRISPR/Cas9 system and people have started exploring and tweaking the system for varied applications. During this, two landmark papers, one from Moineau and colleagues and the other from Charpentier and colleagues, further explored the possibility of the type-II CRISPR system in genome engineering. It was reported that the Cas9 enzyme is the only nuclease that mediates DNA cleavage (Garneau et al., 2010). Also, the biogenesis of the trans-activating RNA (tracrRNA) that is a key step in recruiting the crRNA and Cas9 to initiate a dsDNA break has been discovered (Deltcheva et al., 2011). In addition to this, the generation of the sgRNA that is formed by fusing the tracrRNA and the crRNA has shown enough evidence to generate dsDNA breaks in *in-vitro* (Jinek et al., 2012). After this, two independent groups successfully used this technology to

edit the genome in mammalian cells (Cong et al., 2013; Mali et al., 2013a; Mali et al., 2013b). This was followed by a series of papers that have used this technology to make dsDNA breaks and generate a plethora of mutations in the genome of several model organisms. Two independent groups have simultaneously reported techniques to edit the genome of *Drosophila* using CRISPR/Cas9 (Gratz et al., 2013; Ren et al., 2013).

CRISPR/Cas9 system is the most popular genome editing technology in current times. This system has three main components; the nuclease Cas9 that makes double-stranded breaks on the genome, the gRNA that guides the Cas9 to a sequence of interest and an essential PAM sequence on the genome adjacent to which the breaks occurs. Most often, there is a fourth component in the form of a donor template that is used to modify a stretch of the genome in the desired fashion. The robust genetic tools in flies paved the way to generate several Cas9 drivers that would allow the generation of germline-specific transgenic flies. One great advantage of expressing Cas9 in the germ cells is that the Cas9 protein gets maternally deposited into the embryo and with the presence of gRNA, the pole cells can be edited and the mutations appear in the next generation. In addition to this, hundreds of tissue-specific Cas9 transgenics have been generated by several research groups and these can be used to drive the expression of the Cas9 gene in a controlled manner and can be used to generate transgenics in somatic cells. (Port and Bullock, 2016; Port et al., 2014; Xue et al., 2014). The second important component of this system is the gRNA that guides the Cas9 to a specific sequence. The gRNA sequence is usually 18-20 nucleotides long and complementary to the target DNA. The gRNA is designed in such a way that the target site is adjacent to the protospacer adjacent motif (PAM) sequence which is also the third important component of the CRISPR system. The PAM sequence is usually 2-6 bases long and is specific to the origin of Cas9 nuclease. It is observed that PAM sequence is necessary and mutations in the PAM sequence leads to inefficient dsDNA break by the Cas9 and the frequency of occurrence of PAM site governs the



ability to modify a genomic locus using CRISPR/Cas9 technology (Mojica et al., 2009; Shah et al., 2013; Sternberg et al., 2014). The fourth component is the donor template that is required to make specific changes in the genomic locus that is being modified. As mentioned previously, there are several Cas9 transgenic fly lines available that can be used to generate mutations in the germline as well as somatic cells in a tissue-specific manner by combining the CRISPR/Cas9 system with the UAS-Gal4 system. The gRNA that is specific to the sequence of the genome being edited, can be either injected at the posterior end of the embryo where the pole cells are present or a gRNA transgenic can be generated by cloning the gRNA sequence in a plasmid and incorporating it into the genome. Both the protocols yield desirable results. Using a single gRNA causes insertions or deletions at the site of the cut by a process called non-homologous end-joining (NHEJ). Introducing in-dels in the genome can have several effects, there could be a truncated protein if a stop codon is inserted, the protein synthesised could be out of the frame and can attain a novel function. Instead of using a single gRNA that would yield undesirable outcomes, people have started using two different gRNA to remove a stretch of DNA from the genomic locus. This is highly favourable to make large genomic deletions and generate null flies for a desirable protein or generate variants of a protein with certain domains deleted. In addition to this, CRISPR/Cas9 system is also used to make point mutations in the desired stretch of genomic DNA. This is done by supplying a donor template that has the desired mutations. The donor template has regions that are homologous to the genomic stretch that is being targeted. The donor template gets incorporated into the genomic locus by a phenomenon called homology dependent repair (HDR) as seen in Figure 3.2. Two types of donor templates are currently in use in *Drosophila*. One of the donor templates is a plasmid that has long homology arms that are complementary to the region being edited. This plasmid usually has a dominant phenotypic marker that scores for a positive insertion. One example is pHD-scarless-dsRed. An advantage of using plasmids as donor templates is it

allows the incorporation of large sequences of exogenous DNA into the genomic locus which is ideal for tagging a protein with a fluorescent molecule like GFP. The second type of donor template is a single-stranded oligodeoxynucleotide (ssODN). ssODN is usually 100-150bp long and is used to target a shorter stretch of the genomic locus. Both these donor templates are extensively used in *Drosophila* to generate several kinds of mutations/modifications (Bier et al., 2018; Hsu et al., 2014; Jiang and Doudna, 2017; Pickar-Oliver and Gersbach, 2019; Wang et al., 2016).

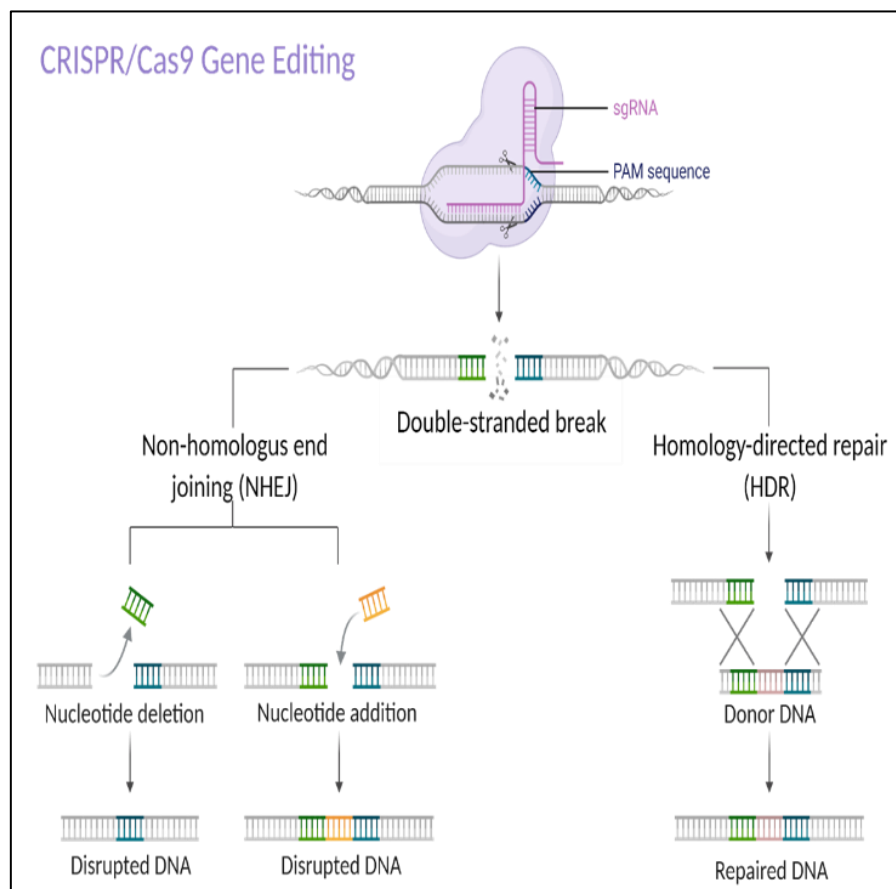


**Figure 3.2: CRISPR/Cas9 mediated strategy to generate genomic edits**

The double-stranded break caused by the CRISPR/Cas9 complex takes 2 different routes depending on the availability of a donor template. If the donor template is absent, the DNA ends are randomly ligated by NHEJ. This leads to either deletion of a few nucleotides or addition of few nucleotides. Both these changes cause disruptions in the protein sequence. If the donor template is present and has homologous sequences present, the sequences along with the homologous sequence get incorporated into the locus by HDR.

In this chapter, I discuss the successful generation of several UAS-Gal4 based SCR variant fly lines of Jra and Kay. In addition to this, we used the CRISPR/Cas9 technology to edit the genome of Jra and generated a JraSCR fly line.

### 3.3 Results and Discussion

#### 3.3.1 Rescue of embryonic lethality of *jra* and *kay* null flies using UAS transgenics.

We started by checking the expression of Jra and Kay in the transgenic flies we generated. We crossed our UAS transgenic fly lines to another fly line that had *daughterless-Gal4* which has ubiquitous expression. 6-8 day old adult flies were used to extract total protein and perform WB. We observed a band at the desired molecular weight for all the UAS transgenics of Jra (Figure 3.3A) and UAS-Kay<sup>WT</sup> of Kay (Figure 3.3B). This suggests that the UAS transgenic lines were expressing the desired transgene.

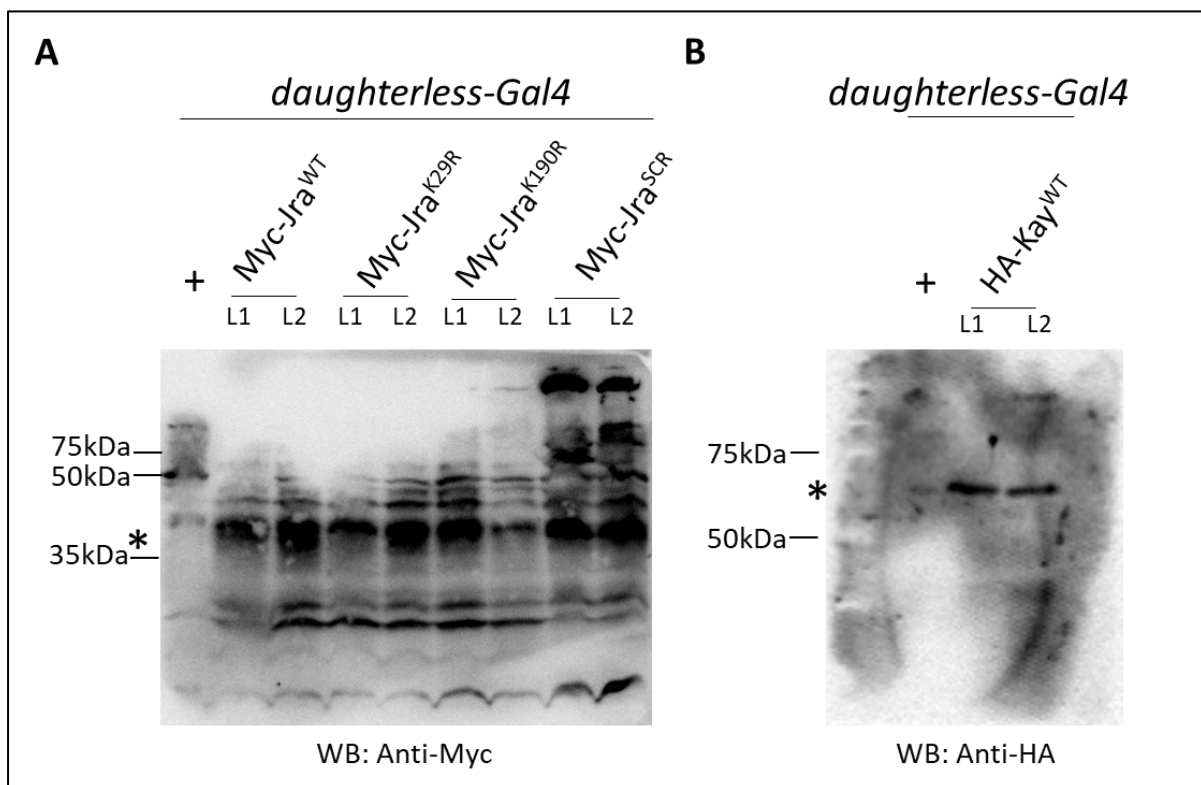


**Figure 3.3: Demonstration of expression of UAS transgenic flies**

**A.** Anti-Myc Western blot image of Myc-tagged variants of Jra showing expression of the transgenes generated. Lane 2-3: Jra<sup>WT</sup>, lane 4-5: Jra<sup>K29R</sup>, lane 6-7: Jra<sup>K190R</sup> and lane 8-9: Jra<sup>SCR</sup>. Overexpressed Myc-tagged Jra (in lanes 2-9) can be seen as a band at ~40kDa that is marked by an asterisk and the same band is absent in lane 1 that serves as control where the *daughterless-Gal4* fly was crossed to a w<sup>11118</sup> wildtype fly. L1 and L2 represent 2 independent lines.

**B.** Anti-HA WB image of HA-tagged WT variants of Kay showing expression of transgenes generated. Lanes 3-4: Kay<sup>WT</sup>. Overexpressed HA-Kay can be seen at ~60kDa that is marked by an asterisk and the same is absent in lane 2 that serves as a control. L1 and L2 represent 2 independent lines

We could in principle use these transgenics to overexpress different transgenes in a spatio-temporal manner to look for phenotypes. However, the presence of an endogenous WT gene of Jra and Kay posed a challenge wherein the effect of the overexpressed SCR mutant would always be diluted by the WT gene. We then hypothesised that it would be ideal to perform all the experiments where there is only one allele of either Jra or Kay present. As mentioned in the previous chapter, Jra and Kay play a key role in regulating cell shape changes during dorsal closure, an early embryonic developmental event. Genetic analysis reveals that the null mutants are lethal as the development halts at the dorsal closure stage. We used the UAS transgenics that were generated to rescue the lethality of Jra and Kay null flies. Figure 3.3 summarises the schematic of Jra (Figure 3.4A) and Kay (Figure 3.4B) null rescue.

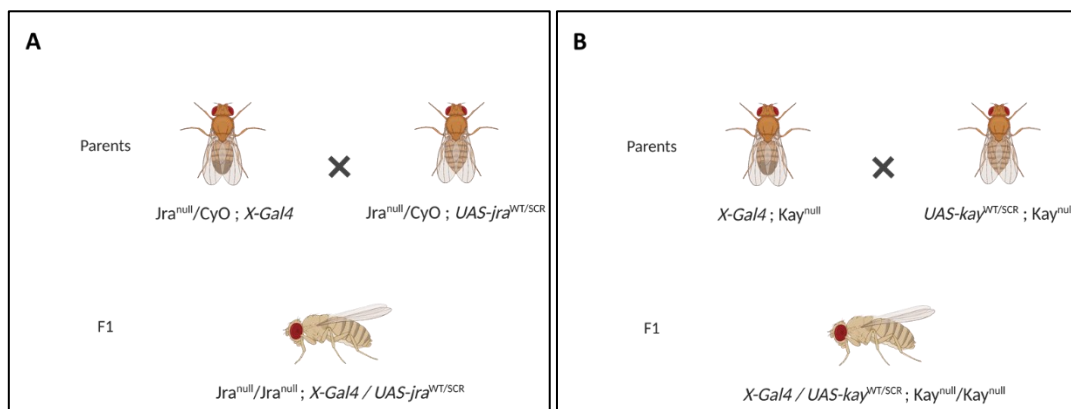


**Figure 3.4: Schematic of rescue crosses.**

**A.** Jra is present on the 2<sup>nd</sup> chromosome. We generated our UAS lines targeting the 3<sup>rd</sup> chromosome to reduce the burden of recombination during the genetic rescue. We first balanced the  $Jra^{null}$  flies with a 3<sup>rd</sup> chromosome Gal4 line. Similarly, we balanced another fly with  $Jra^{null}$  and UAS- $Jra^{WT/SCR}$ . We crossed the above-mentioned lines to get a fly that was homozygous to  $Jra^{null}$  on the 2<sup>nd</sup> chromosome and had one copy of each Gal4 and UAS- $Jra^{WT/SCR}$  on the 3<sup>rd</sup> chromosome.

**B.** Kay is present on the 3<sup>rd</sup> chromosome. We generated our UAS lines targeting the 2<sup>nd</sup> chromosome. We first balanced the  $Kay^{null}$  flies with a 2<sup>nd</sup> chromosome Gal4 line. Similarly, we balanced another fly with  $Kay^{null}$  and UAS- $Kay^{WT/SCR}$ . We crossed the above-mentioned lines to get a fly that was homozygous to  $Kay^{null}$  on the 3<sup>rd</sup> chromosome and had one copy of each Gal4 and UAS- $Jra^{WT/SCR}$  on the 2<sup>nd</sup> chromosome.

We used several ubiquitous drivers to rescue the null lethality of Jra and Kay. We performed the null lethality rescue experiments at 25°C and 29°C. We did not observe any homozygous

flies for the null allele at both 25°C and 29°C suggesting that the null lethality could not be rescued with the Gal4 lines used. The Gal4 lines used and the outcomes of each rescue are summarised in table 3.1.

**Table 3.1: Outcome of null lethality rescue crosses. A) Jra. B) Kay**

The genetic rescue of Jra and Kay null lethality was attempted at 2 different temperatures. 25°C is the standard temperature to grow the flies and the expression of the UAS constructs is generally adequate at this temperature. Since the UAS-Gal4 system is sensitive to temperature, the genetic rescue of null lethality was also attempted at 29°C. At both temperatures, there were no flies that were homozygous to *Jra*<sup>null</sup> and *Kay*<sup>null</sup>. Column1 – Gal4 used; column2 – the tissue-specific expression of the Gal4; column 3&4 – outcomes of the crosses at 25°C and 29°C.

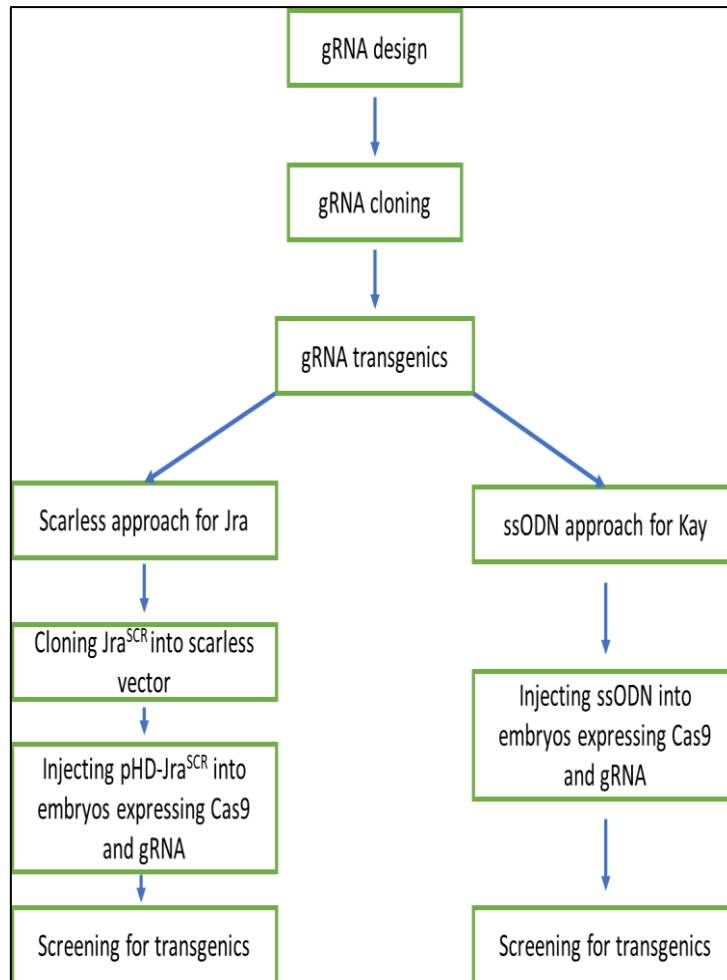
|                     |            | Rescue of Jra null lethality |        |
|---------------------|------------|------------------------------|--------|
|                     |            | @25C                         | @29C   |
| Gal4                | Expression |                              |        |
| <i>daughterless</i> | Ubiquitous | Failed                       | Failed |
| <i>armadillo</i>    | Ubiquitous | Failed                       | Failed |
| <i>tubulin</i>      | Ubiquitous | Failed                       | Failed |

|                     |              | Rescue of Kay null lethality |        |
|---------------------|--------------|------------------------------|--------|
|                     |              | @25C                         | @29C   |
| Gal4                | Expression   |                              |        |
| <i>daughterless</i> | Ubiquitous   | Failed                       | Failed |
| <i>actin</i>        | Ubiquitous   | Failed                       | Failed |
| <i>kayak</i>        | Kay specific | Failed                       | Failed |

### 3.3.2 Editing the genomic locus of *jra* and *kay* using CRISPR/Cas9

CRISPR/Cas9 technology has emerged as a powerful tool to edit the genome and generate single amino acid mutations in recent times. The advantage of using CRISPR/Cas9 is that the expression of the mutant generated is under the control of its native promoter. This was our best choice as we were interested in only mutating two amino acids in *Jra* and single amino acid in *Kay*. The strategy to generate SCR mutants for *Jra* and *Kay* using CRISPR/Cas9 technology is shown below (Figure 3.5).



**Figure 3.5: Schematic of the approach used for the generation of Jra<sup>SCR</sup> and Kay<sup>SCR</sup> using CRISPR/Cas9 technology**

The execution of CRISPR/Cas9 mediated genome editing started with designing a gRNA targeting a specific site in both Jra and Kay. Once an appropriate gRNA was selected, the sequence was cloned into a vector for expression on embryos. This was followed by the generation of the gRNA transgenic lines for a higher success rate. Post this, different approaches were used for Jra and Kay. Scarless approach was used for Jra as there were 2 mutations to be incorporated and the sites were far apart from one other. ssODN approach was used for Kay since there was only one site to be mutated.

*gRNA design:* gRNAs for both Jra and Kay were designed using the CRISPR optimal target finder (<http://targetfinder.flycrispr.neuro.brown.edu/>). We selected those gRNA that had zero off-target effects and those which were close to the site to be mutated. The gRNA sequences for Jra and Kay are 5' CCCC GTTCCGCTGCTGCG 3' and 5' CTCAGGATCCAGCCTGGACC 3' respectively.

*gRNA cloning:* The gRNA selected from the previous step were cloned into the pBFv-U6.2B vector. The vector has a ubiquitin promoter that expresses the gRNA ubiquitously. pBFv-U6.2B vector also has attB sites for targeted insertion into the genome.

*gRNA transgenics:* We generated stable gRNA transgenic flies to increase the efficiency of CRISPR/Cas9 mediated mutagenesis. Since the pBFv-U6.2B vector had attB sites, we used the attP-attB mediated site-specific insertion and targeted the attP40 site on the second chromosome of *Drosophila* for both Jra and Kay.

*Scarless editing strategy for Jra:* There are predominantly two ways to incorporate mutations in a genomic locus based on the type of donor template used. The most commonly used is the single-stranded oligodeoxynucleotide (ssODN) where a short single-stranded DNA of about 80-12-nucleotides is supplied as a donor template. This strategy is used to generate small modifications. This strategy was not suitable for Jra as the two K→R modifications were far apart. Hence, we used the scarless approach for Jra. Scarless editing uses PBac transposons that target TTAA sites for insertion into the genome. We designed the gRNA such that it targets a site close to a TTAA site. We used the pHD-scarless-dsRed vector that has a dsRed marker, specifically expressed in the eye and can be used as a proxy for a positive HDR and subsequent insertion of the cassette into the genome. The dsRed cassette is flanked by PBac transposon inverted repeats (IR) that target a TTAA site and the IRs, in turn, are flanked by the homology regions (HR) specific to the genomic region of interest (Figure 3.6). We incorporated the desired K→R mutations in the 3'HR region and assembled two fragments of Jra and two fragments of the vector using Gibson assembly and sequenced the 5'HR and 3'HR regions of the vector post assembly. The detailed schematic is described. The sequenced vector was injected into embryos expressing Cas9 and gRNA. The F1 males and females were crossed to the 2<sup>nd</sup> chromosome balancer line. We scored for positive insertions of the cassette by the presence of red fluorescence in the eye of the fly.



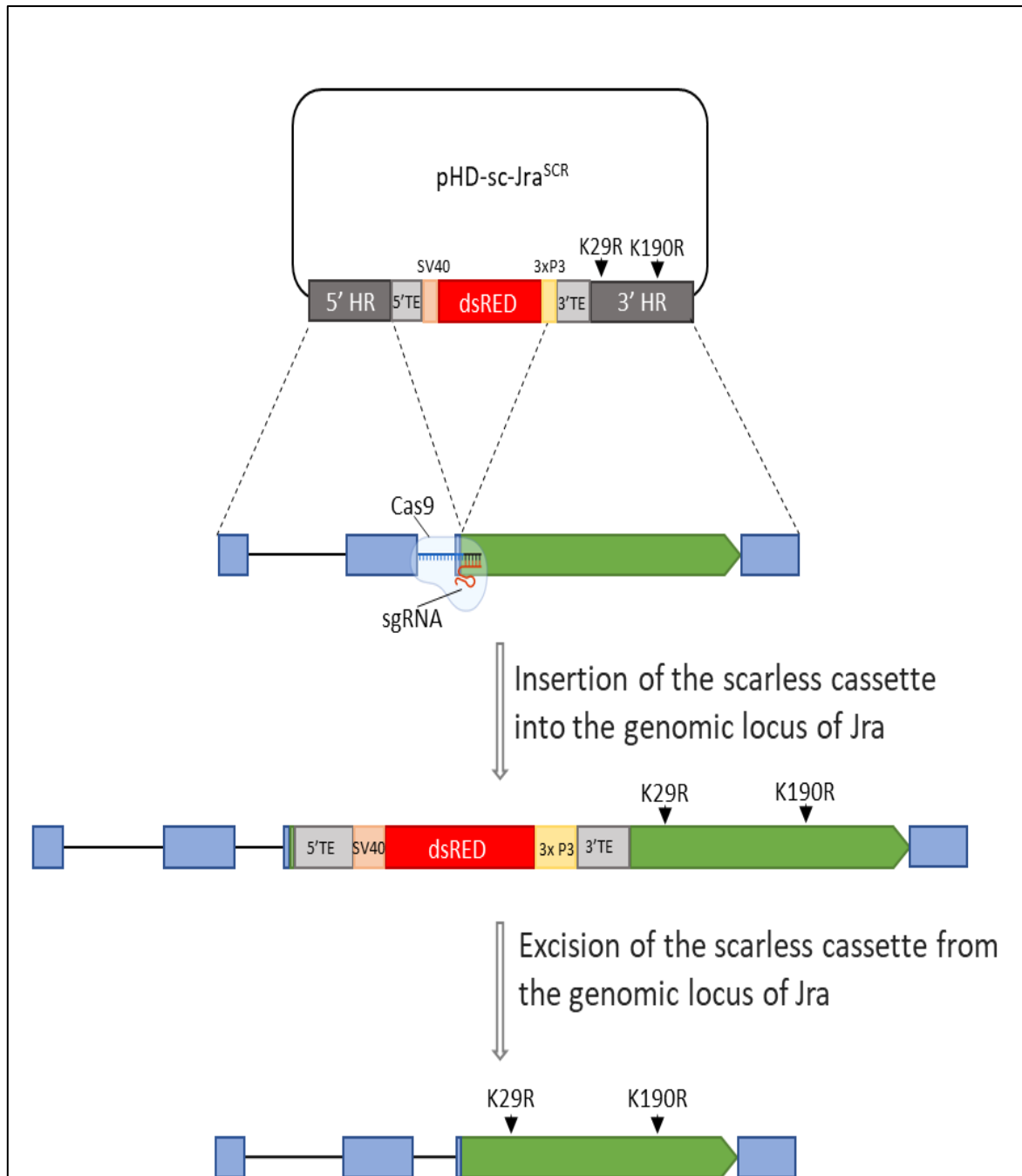


**Figure 3.6: Schematic of integration of pHD-scarless-Jra<sup>SCR</sup> into the genomic locus of Jra**

Different components of the scarless vector depicted. 5'HR targeted 1<sup>st</sup>, 2<sup>nd</sup> and a small part of the 3<sup>rd</sup> exon shown in blue. The majority of CDS that was a part of the remaining 3<sup>rd</sup> exon was part of the 3'HR region. piggyBac transposon elements (TE) are required for scarless excision of the cassette. Positive insertions can be screened by the presence of dsRed driven by P3 promoter specific to the eye. SV40 serves as a translational end point.

The flies that were balanced and had red fluorescence in the eye were crossed to flies ubiquitously expressing PBac transposase. The transposase would act on the PBac transposons present in the scarless cassette and excise it out. The TTAA site that is duplicated upon insertion of the cassette is restored into a single genomic TTAA site and this leaves no mark on the cassette making the entire process scarless. A very small fraction of flies would lose the fluorescent marker and these flies were further balanced, stabilised and sequenced. We used the genomic DNA extracted from *w<sup>1118</sup>* fly as a template and amplified the entire genomic locus of Jra as 2 different fragments referred to as 5'HR and 3'HR. The 3'HR fragment had the CDS and while amplifying the fragments, we incorporated the desired lysine to arginine mutations of 29<sup>th</sup> and 190<sup>th</sup> position. We then linearised the pHD-scarless-dsRed vector into 2 different fragments. We purified all 4 fragments and ligated them. We screened 112 bacterial colonies for the presence of all 4 fragments. Two of those 112 colonies had all 4 fragments. The 2 plasmids were purified, sequenced and clone 62 was injected. We were successfully able to hop out the dsRed cassette from six lines and all the six lines were sequenced. Surprisingly, only two out of the six lines had the K→R mutations at both positions (29<sup>th</sup> and 190<sup>th</sup>). We also observed that three of the six lines harboured the K→R mutation only on the 29<sup>th</sup> position and not the 190<sup>th</sup> position and finally one of the six lines did not harbour any K→R mutations and this line was used as a CRISPR control for all the further experiments.

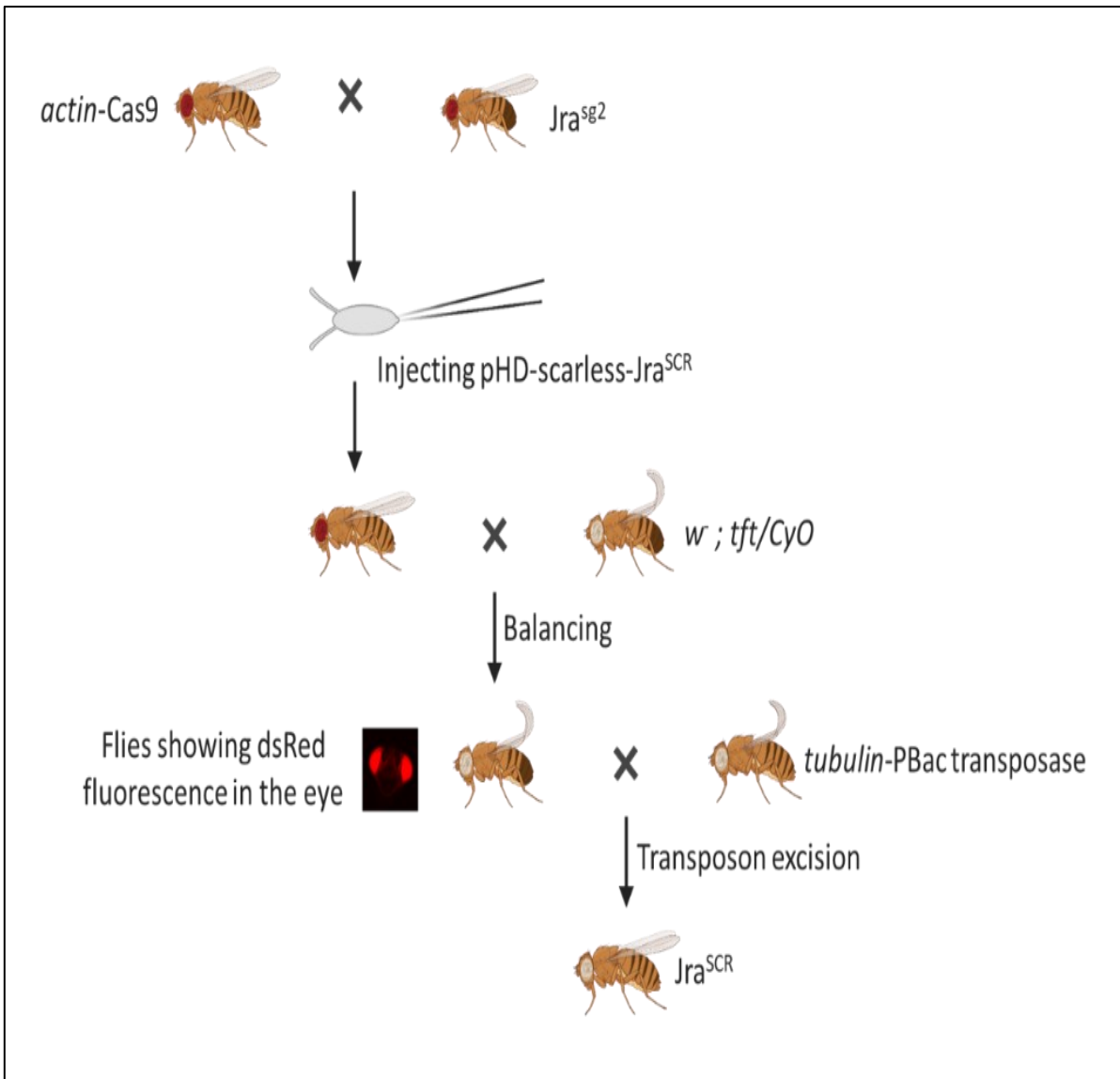


**Figure 3.7: Schematic of genetic crosses to generate *Jra<sup>SCR</sup>* flies**

To start with, *actin-Cas9* flies were crossed with the stable *Jra* gRNA transgenic fly, *Jra<sup>sg2</sup>*. The embryos from the cross were injected with *pHD-scarless-Jra<sup>SCR</sup>*. Out of the total 600 embryos injected, 530 emerged into adults. Out of these 530 flies, 490 were females and 40 were males. We balanced and stabilised all the 530 lines and observed that 82 of them had red fluorescence in their eyes and the rest that didn't have red fluorescence, were discarded. We have used 20 fly lines out of the 82 positives and crossed them to flies expressing PBac transposase. We were successful in hopping out the transposon cassette from 6 lines and all of them were sequenced. Only 2 of the 6 lines harboured both the desired lysine to arginine mutations.

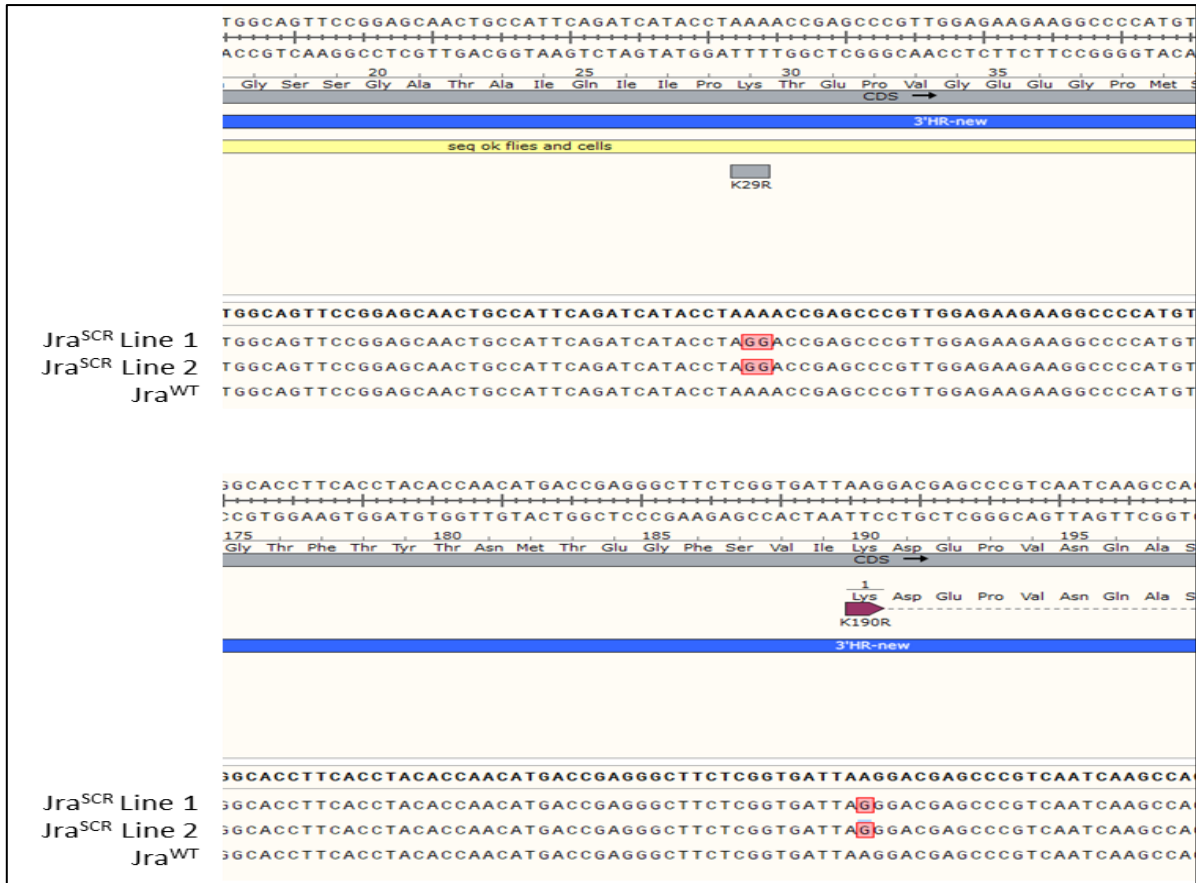


**Figure 3.8: Snapshot of sequencing showing three independent lines.**

The fly line that did not harbour any K->R mutations on 29<sup>th</sup> and 190<sup>th</sup> position was used as control and are referred to as Jra<sup>WT</sup>. The two independent lines that harboured K->R mutations on 29<sup>th</sup> and 190<sup>th</sup> position are referred to as Jra<sup>SCR</sup> line 1 and Jra<sup>SCR</sup> line 2. Line 1 was most used for further experiments in the next chapter.

*ssODN strategy for Kay:* We used the ssODN strategy for incorporating a single K357R mutation into Kay. After the Cas9 and gRNA complex cut the genome, the desired manipulation can be done by supplying a donor template in the form of a single-stranded oligodeoxynucleotide (ssODN). The advantage ssODNs have over dsDNA is that they completely lack the need for cloning, are easy to synthesize, and are cost-effective. We targeted the exon-8 of Kay as seen in Figure 3.9. We designed the ssODN in such a way that when the K->R conversion is made, it incorporates a restriction site for enzyme BstUI. This restriction site was later used to screen for positive insertions. We injected approximately 600 embryos expressing Cas9 and gRNA with the ssODN. 375 of them eclosed and around 300 flies emerged into adults and were fertile. We balanced these flies with a 3<sup>rd</sup> chromosome balance and

stabilised them. At this stage, if the ssODN got integrated into the genomic locus, only one sister chromatid would have the integration. We used 3 males from each of the stabilised lines and crossed them to balancers again. This made sure that we increased the probability of scoring for a positive insertion. We generated around 900 independent lines and stabilised them by self-crossing them. Once the flies were stable and homozygous, we used specific primers to amplify the sequence of Kay and restriction digested them using BstUI. We performed the PCRs and subsequent restriction digestion in 96 well plates with both positive and negative controls. Unfortunately, after screening all the 900 lines, we could not get any positive hit for restriction digestion. We randomly picked 20 lines and sequenced them post PCR and have not seen the mutation incorporated in any of them. Together, we couldn't generate a CRISPR/Cas9 modified Kay<sup>SCR</sup> line.

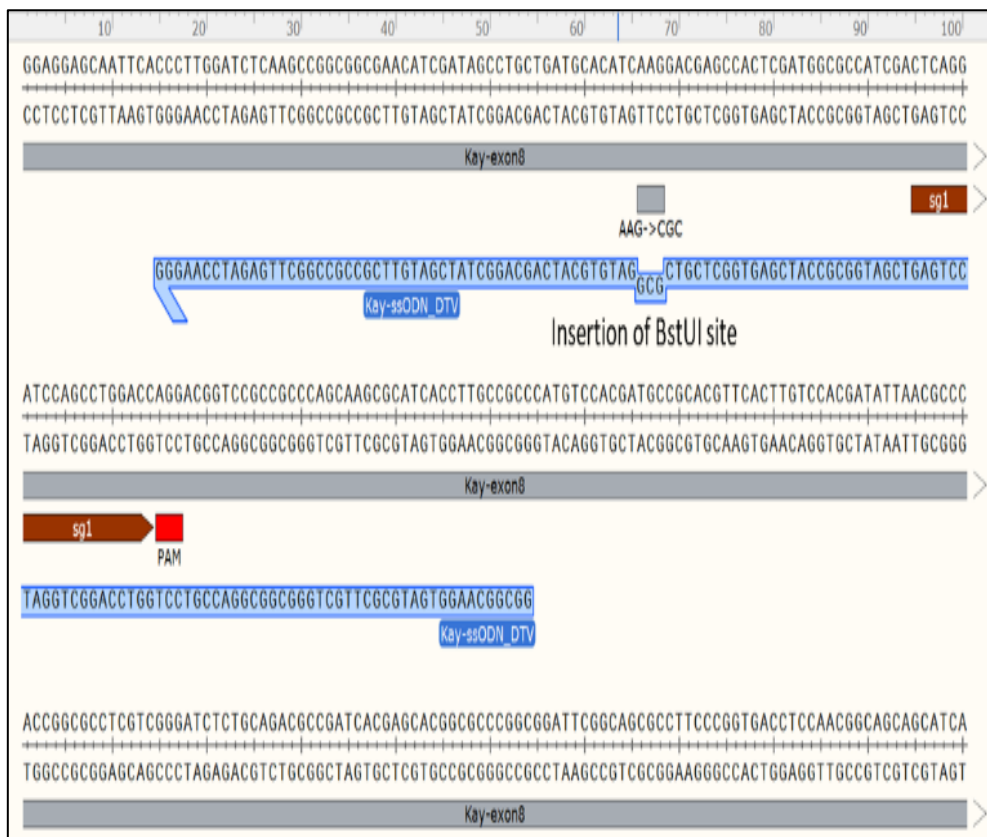


**Figure 3.9: Snapshot describing the ssODN used to incorporate the desired mutation in Kay**  
 The ssOND was designed to target the – strand. Mutating AAG to CGC changed K357 to R357 and incorporated a restriction site for BstUI (CG’CG).

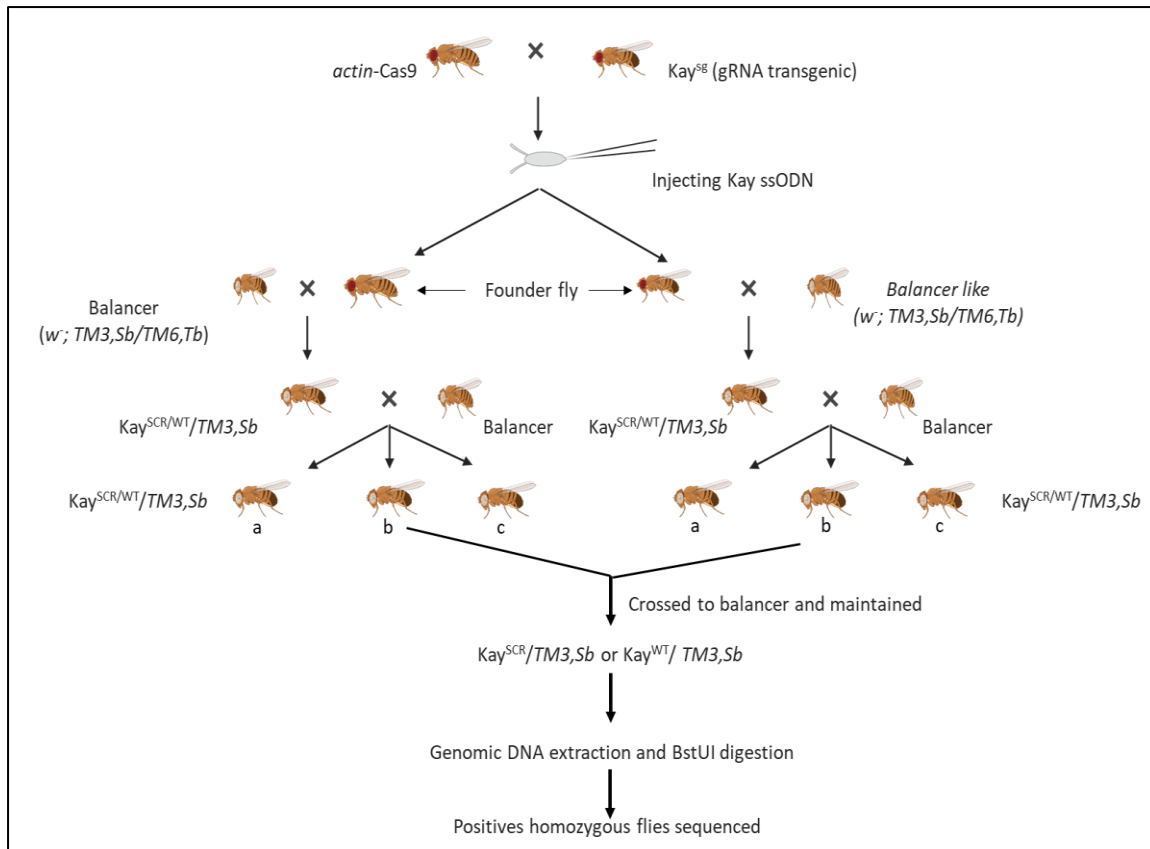


**Figure 3.10: Schematic of genetic crosses to generate *Kay<sup>SCR</sup>* flies**

The Cas9 and gRNA transgenic flies were crossed as a first step and the ssODN was injected into the embryos of the cross. We injected around 600 embryos and of which only 300 emerged as fertile adults. We balanced all the 300 lines with *w; TM3, Sb/TM6, Tb* and stabilised them. We then took 3 males from each of those 300 balanced lines and crossed them again with a balancer line. This way, we balanced and stabilised 900 independent lines that could harbour the desired mutation. We self crossed the 900 lines and separated the homozygous flies. We extracted genomic DNA from a single fly from each independent cross, performed PCR to amplify a part of exon-8 of *Kay* and finally performed restriction digestion using the *BstUI* enzyme.

### 3.4 Summary

We have used the pUASP-attB vector and generated different SCR mutant transgenic fly lines for overexpression. We have designed the insertions of the vector such that all the SCR mutants of Jra were incorporated into the attP2 site on the 3<sup>rd</sup> chromosome and all the SCR mutants of Kay were incorporated into the attP40 site on the 2<sup>nd</sup> chromosome. This design gave us a free hand for genetic manipulations as Jra and Kay are present on the 2<sup>nd</sup> and 3<sup>rd</sup> chromosome respectively. We have tested for the expression of these fly lines and have attempted to rescue the genetic lethality caused by the null mutants of Jra and Kay by overexpressing Jra<sup>WT</sup> and Kay<sup>WT</sup> along with other SCR mutants. Unfortunately, despite using ubiquitous and specific Gal4 drivers, we were unable to rescue the null lethality. One reason for this could be the precise timing and strength of the Gal4 driver. However, we have used *kay-Gal4* to rescue Kay null lethality and were unsuccessful. We believe that *kay-Gal4* used, incorporates sequence 2kb upstream of the TSS (Hartwig et al., 2008), this might not be sufficient to replicate the exact expression pattern of Kay. We have then used the CRISPR/Cas9 technology to generate mutants of Jra and Kay that had the appropriate K→R mutations in the native genomic locus under the native promoter. During this, we have made gRNA transgenic lines for both Jra and Kay. For Jra, we have used the scarless editing approach where a dsDNA plasmid was used as a donor template (Gratz et al., 2014). Through a series of genetic crosses and a thorough screening process, we were able to hop the transposon, stabilize and sequence 6 out of 53 positive insertions. Only 2 of those 6 lines had the K→R mutations on both the sites. To sum up, by the end of the entire CRISPR/Cas9 exercise, we ended up with 2 positive hits of the 600 lines injected with pHD-scarlessdsRed-Jra<sup>SCR</sup>. Thus, the efficiency of this particular experiment is at 1 in 300. We have observed that 3 of the 6 lines sequenced harboured only one K→R mutation and did not have the other. Incidentally, in all the 3 lines, only K29R was found. This could be because of the presence of K29 close to the gRNA target site. It is often observed

that during HDR, regions farther away from the cut site do not efficiently transfer onto the genomic locus. The 2 lines sequenced are homozygous viable and show interesting phenotypes that are described in the later chapters. We have used the ssODN approach for Kay where a single-stranded DNA with the desired K357R mutation is supplied as a donor template. Post an elaborate screening procedure, we could not obtain any lines that were positive for the desired mutation. Few plausible reasons for this could be that the gRNA is not very efficient in guiding the Cas9 to make a proper double-stranded break or the genomic locus of Kay could not be accessible to the Cas9/gRNA hybrid to make a proper cut. We are exploring different approaches like the Co-CRISPR strategy (Levi et al., 2020) and scarless editing strategy to make a CRISPR/Cas9 mutated Kay<sup>SCR</sup>.



### 3.5 Materials and Methods

#### 3.5.1 Fly husbandry and lines used

Flies were grown on standard cornmeal agar at 25C in a 12h light-dark cycle. The following lines were used in this study.

**Table 3.2: List of flylines used**

|    | Line (Genotype)  | Source     | Description   |
|----|--|------------|---|
| 1  | <i>UAS-Jra<sup>WT</sup>+B2:B13+B2:B14</i>  | This study | pUASp-attB-Jra <sup>WT</sup> inserted into atp40 site         |
| 2  | <i>UAS-Jra<sup>K29R</sup></i>  | This study | pUASp-attB-Jra <sup>K29R</sup> inserted into atp40 site       |
| 3  | <i>UAS-Jra<sup>K190R</sup></i>   | This study | pUASp-attB-Jra <sup>K190R</sup> inserted into atp40 site      |
| 4  | <i>UAS-Jra<sup>K29R+K190R</sup></i>  | This study | pUASp-attB-Jra <sup>K29R+K190R</sup> inserted into atp40 site |
| 5  | <i>UAS-Kay<sup>WT</sup></i>  | This study | pUASp-attB-Kay <sup>WT</sup> inserted into atp2 site          |
| 6  | <i>UAS-Jra<sup>K211R</sup></i>   | This study | pUASp-attB-Kay <sup>K211R</sup> inserted into atp2 site       |
| 7  | <i>UAS-Jra<sup>K357R</sup></i>   | This study | pUASp-attB-Kay <sup>K357R</sup> inserted into atp2 site       |
| 8  | <i>w[*]; P{w[+mW.hs]=GAL4-da.G32}2; MKRS/TM6B, Tb[1]</i>                               | BDSC:55851 | <i>daughterless-Gal4</i> used to rescue Kay null lethality    |
| 9  | <i>cn[1] Jra[IA109] bw[1] speck[1]/CyO</i>   | BDSC:3273  | Jra null  |
| 10 | <i>P{ry[+t7.2]=neoFRT}82B kay[2] ca[1]/TM6B, Tb[1] ca[1]</i>                           | BDSC:42217 | Kay null  |
| 11 | <i>w[*]; Kr[If-1]/CyO; P{w[+mW.hs]=GAL4-da.G32}UH1</i>                                 | BDSC:55850 | <i>daughterless-Gal4</i> used to rescue Jra null lethality    |
| 12 | <i>w[*]; P{w[+mW.hs]=GAL4-arm.S}4a<br/>P{w[+mW.hs]=GAL4-arm.S}4b/TM3, Sb[1] Ser[1]</i> | BDSC:1561  | <i>armadillo-Gal4</i> used to rescue Jra null lethality       |
| 13 | <i>Tubulin-Gal4/MKRS</i>   | NCBS       | <i>tubulin-Gal4</i> used to rescue Jra null lethality         |
| 14 | <i>Actin-Gal4</i>  | NCBS       | <i>actin-Gal4</i> used to rescue Kay null lethality           |
| 15 | <i>w1118; In(2LR)Gla, wgGla-1/CyO; Herm{3xP3-ECFP, I±tub-piggyBacK10}M10</i>           | BDSC:32073 | <i>Tubulin</i> pBac transposase                               |
| 16 | <i>y[1] M{Act5C-Cas9.P.RFP-}ZH-2A w[1118] DNAlig4[169]</i>                             | BDSC:58492 | <i>Actin5c</i> Cas9   |

|    |                            |            |                                      |
|----|----------------------------|------------|--------------------------------------|
| 17 | <i>Jra</i> <sup>sg2</sup>  | This study | gRNA targetting exon 3 of <i>Jra</i> |
| 18 | <i>Kay</i> <sup>gRNA</sup> | This study | gRNA targetting exon 8 of <i>Kay</i> |

### 3.5.2 Cloning

pUASp-AttB was procured from the *Drosophila* Genomics Resource Centre (DGRC, #1358) and was used for targeted insertions into the genome. Different variants of *Jra* and *Kay* were amplified from pGEX clones described in Ch-2 using specific primers and N-terminal c-Myc and HA tags were incorporated into *Jra* and *Kay* respectively. Purified plasmids of *Jra* and *Kay* were injected into embryos that had AttP2 and AttP40 sites respectively so that all the *Jra* transgenics are present on the 3<sup>rd</sup> chromosome and *Kay* transgenics on the 2<sup>nd</sup> chromosome. pBFv-U6.2B vector used for cloning *Jra* and *Kay* specific gRNA and pHD-scarless vector into which *Jra*<sup>SCR</sup> was cloned was a generous gift from Dr. Deepti Trivedi Vyas (NCBS, Bengaluru). *Jra*<sup>SCR</sup> fragments previously described were ligated along with vector fragments using Gibson assembly (NEB, #E5510S) and sequenced. BstUI used for screen *Kay*<sup>SCR</sup> positives is from New England Biolabs (NEB, R0518).

**Table 3.3: List of primers used**

|   | Primer                      | Sequence (5'→3')   | Description                                   |
|---|-----------------------------|--|---|
| 1 | pUASp-attB- <i>Jra</i> F    | GATCAGATCCGCGGCCGCATGGAACAAAACTTATT<br>TCTGAAGAAGATCTGGGAGGCGGAATGAAAACCCCGT<br>TTCCG  | Primer pair to amplify <i>Jra</i> for pRM-HA3 |
| 2 | pUASp-attB- <i>Jra</i> R    | CGTTCGAGGTCGACTCTAGAG'GATCCTTATTGGTCTGTC<br>GAGTTCGG                                   |   |
| 3 | pUASp-attB-HR- <i>Jra</i> F | CGTTAGGTCCTGTTTCATTGGTACCCGCCCGGGATCAGA<br>TCCGCGGCCGC                                 | Primer pair to amplify pRM-HA3 for <i>Jra</i> |
| 4 | pUASp-attB-HR- <i>Jra</i> R | TCCTCGAGTTAACGTTACGTTAACGTTAACGTTTCGAGGT<br>CGACTCTAGAG                                |   |
| 5 | pUASp-attB- <i>Kay</i> F    | GATCAGATCCGCGGCCGCATGTACCCATACGATGTTT<br>CAGATTACGCTGGAGGCGGAATGACGCTGGACAGCTAC<br>AAC | Primer pair to amplify <i>Kay</i> for pRM-HA3 |
| 6 | pUASp-attB- <i>Kay</i> R    | TCTAGAGGATCCAGATCCACTAGTTTATAAGCTGACCAG<br>CTTGAC                                      |   |
| 7 | pUASp-attB-HR- <i>Kay</i> F | CGTTAGGTCCTGTTTCATTGGTACCCGCCCGGGATCAGA<br>TCCGCGGCCGC                                 | Primer pair to amplify pRM-HA3 for <i>Kay</i> |
| 8 | pUASp-attB-HR- <i>Kay</i> R | CGTTAACGTTAACGTTTCGAGGTCGACTCTAGAGGATCCA<br>GATCCACTAGT                                |   |

|    |                  |  |  |
|----|------------------|--|--|
| 9  | 5'-pHD-sc F      | GGAAGAGCCGTCGCTCTTCCCG   | Primer pair to amplify 5' fragment of pHD-sc     |
| 10 | 5'-pHD-sc R      | GATCGCAGGTGCTGCCACCTG  |  |
| 11 | 3'-pHD-sc F      | TTAACCTAGAAAGATAATCATATTG                                      | Primer pair to amplify 3' fragment of pHD-sc     |
| 12 | 3'-pHD-sc R      | TTAACCTAGAAAGATAGTCTGCG  |  |
| 13 | 5'-HR-Jra F      | CGGGGAAGAGCGACGGCTCTCCGAGCATCAGTGTTTTCTGGAG                    | Primer pair to amplify 5' HR of Jra              |
| 14 | 5'-HR-Jra R      | CGCAGACTATCTTTCTAGGGTTAAGTTCGCGGCAGCCGA AACC GGCGTTTTTCATGTTGC |  |
| 15 | 3'-HR-Jra F      | CAATATGATTATCTTTCTAGGGTTAAGTATTCAGAATGCT GGC                   | Primer pair to amplify 3' HR of Jra              |
| 16 | 3'-HR-Jra R      | CAGGTGGCAGCACCTGCGATCCCAGGAGTTCGCTGTTAG TTAGG                  |  |
| 17 | pHD-Jra-3'-seq R | TCAGCGTCTGGGTTCCCATCGG   | Primer to sequence 3' HR of Jra post cloning     |
| 18 | pHD-Jra-5'-seq R | ACAGCGACGGATTTCGCGCTATTTAGAAAAG                                | Primer to sequence 5' HR of Jra post cloning     |
| 19 | gJra F           | TCATATTTTGTTCCCTTTTCAATTGTAA                                   | Primer pair to amplify the genomic region of Jra |
| 20 | gJra R           | ATATATCAAGTGCAGAAAATATACGTATATTTTAAAA                          |  |

### 3.5.3 Western blotting

10-15 flies were lysed in 1x radioimmunoprecipitation assay (RIPA) buffer supplemented with 1X cOmplete™, EDTA-free Protease Inhibitor Cocktail (PIC) (Sigma-Aldrich, # 11873580001) for 20 min at 4C. Post lysis, the total protein was quantitated using Pierce™ BCA Protein Assay Kit (ThermoFischer scientific, #23225) and 100ug of total protein from each sample was loaded. For all the western blotting experiments, we have first separated the proteins using 12% polyacrylamide gel followed by a transfer onto a 0.45µm polyvinylidene fluoride (PVDF) membrane (Sigma-Aldrich, #P2938). Post transfer, all the blots were blocked with 5% skimmed milk dissolved in 1x TRIS buffer saline (TBS) with 0.1% Tween-20 (Sigma-Aldrich, #P9416) detergent. The following antibodies were used as primary antibodies for the WB. Anti-Myc (Sigma-Aldrich, #C3956; used in 1:2000) and anti-HA (Sigma-Aldrich, #04-902; used in 1:1000). The following are the secondary antibodies

used. Peroxidase conjugated anti-mouse (Jackson ImmunoResearch, #115-035-003; used in 1:10000) and peroxidase-conjugated anti-rabbit (Jackson ImmunoResearch, #111-035-003; used in 1:10000). All the blots were developed using Immobilon Western Chemiluminescent HRP Substrate (Sigma-Aldrich, #WBKLS).

#### ***3.5.4 Genomic DNA isolation***

Single flies were homogenised in 50ul of a buffer containing 10mM TRIS, 1mM EDTA and 20uM Proteinase K. The homogenate is incubated at 37C for 30 min followed by 85C for 5 min. Finally, the homogenate is given a hard spin and 2ul of the supernatant was used for a 50ul PCR reaction.

### 3.6 References

1. Barrangou, R., Fremaux, C., Deveau, H., Richards, M., Boyaval, P., Moineau, S., Romero, D.A., and Horvath, P. (2007). CRISPR provides acquired resistance against viruses in prokaryotes. *Science* 315, 1709-1712.
2. Bier, E., Harrison, M.M., O'Connor-Giles, K.M., and Wildonger, J. (2018). Advances in Engineering the Fly Genome with the CRISPR-Cas System. *Genetics* 208, 1-18.
3. Bolotin, A., Quinquis, B., Sorokin, A., and Ehrlich, S.D. (2005). Clustered regularly interspaced short palindrome repeats (CRISPRs) have spacers of extrachromosomal origin. *Microbiology (Reading)* 151, 2551-2561.
4. Brand, A.H., and Perrimon, N. (1993). Targeted gene expression as a means of altering cell fates and generating dominant phenotypes. *Development* 118, 401-415.
5. Cong, L., Ran, F.A., Cox, D., Lin, S., Barretto, R., Habib, N., Hsu, P.D., Wu, X., Jiang, W., Marraffini, L.A., *et al.* (2013). Multiplex genome engineering using CRISPR/Cas systems. *Science* 339, 819-823.
6. Deltcheva, E., Chylinski, K., Sharma, C.M., Gonzales, K., Chao, Y., Pirzada, Z.A., Eckert, M.R., Vogel, J., and Charpentier, E. (2011). CRISPR RNA maturation by trans-encoded small RNA and host factor RNase III. *Nature* 471, 602-607.
7. Duffy, J.B. (2002). GAL4 system in *Drosophila*: a fly geneticist's Swiss army knife. *Genesis* 34, 1-15.
8. Garneau, J.E., Dupuis, M.E., Villion, M., Romero, D.A., Barrangou, R., Boyaval, P., Fremaux, C., Horvath, P., Magadan, A.H., and Moineau, S. (2010). The CRISPR/Cas bacterial immune system cleaves bacteriophage and plasmid DNA. *Nature* 468, 67-71.
9. Gratz, S.J., Cummings, A.M., Nguyen, J.N., Hamm, D.C., Donohue, L.K., Harrison, M.M., Wildonger, J., and O'Connor-Giles, K.M. (2013). Genome engineering of *Drosophila* with the CRISPR RNA-guided Cas9 nuclease. *Genetics* 194, 1029-1035.
10. Gratz, S.J., Ukken, F.P., Rubinstein, C.D., Thiede, G., Donohue, L.K., Cummings, A.M., and O'Connor-Giles, K.M. (2014). Highly specific and efficient CRISPR/Cas9-catalyzed homology-directed repair in *Drosophila*. *Genetics* 196, 961-971.

11. Hartwig, C.L., Worrell, J., Levine, R.B., Ramaswami, M., and Sanyal, S. (2008). Normal dendrite growth in *Drosophila* motor neurons requires the AP-1 transcription factor. *Dev Neurobiol* 68, 1225-1242.
12. Hsu, P.D., Lander, E.S., and Zhang, F. (2014). Development and applications of CRISPR-Cas9 for genome engineering. *Cell* 157, 1262-1278.
13. Ishino, Y., Shinagawa, H., Makino, K., Amemura, M., and Nakata, A. (1987). Nucleotide sequence of the *iap* gene, responsible for alkaline phosphatase isozyme conversion in *Escherichia coli*, and identification of the gene product. *J Bacteriol* 169, 5429-5433.
14. Jansen, R., Embden, J.D., Gaastra, W., and Schouls, L.M. (2002). Identification of genes that are associated with DNA repeats in prokaryotes. *Mol Microbiol* 43, 1565-1575.
15. Jiang, F., and Doudna, J.A. (2017). CRISPR-Cas9 Structures and Mechanisms. *Annu Rev Biophys* 46, 505-529.
16. Jinek, M., Chylinski, K., Fonfara, I., Hauer, M., Doudna, J.A., and Charpentier, E. (2012). A programmable dual-RNA-guided DNA endonuclease in adaptive bacterial immunity. *Science* 337, 816-821.
17. Levi, T., Sloutskin, A., Kalifa, R., Juven-Gershon, T., and Gerlitz, O. (2020). Efficient In Vivo Introduction of Point Mutations Using ssODN and a Co-CRISPR Approach. *Biol Proced Online* 22, 14.
18. Mali, P., Aach, J., Stranges, P.B., Esvelt, K.M., Moosburner, M., Kosuri, S., Yang, L., and Church, G.M. (2013a). CAS9 transcriptional activators for target specificity screening and paired nickases for cooperative genome engineering. *Nat Biotechnol* 31, 833-838.
19. Mali, P., Yang, L., Esvelt, K.M., Aach, J., Guell, M., DiCarlo, J.E., Norville, J.E., and Church, G.M. (2013b). RNA-guided human genome engineering via Cas9. *Science* 339, 823-826.
20. Mojica, F.J., Diez-Villasenor, C., Garcia-Martinez, J., and Soria, E. (2005). Intervening sequences of regularly spaced prokaryotic repeats derive from foreign genetic elements. *J Mol Evol* 60, 174-182.
21. Mojica, F.J., Diez-Villasenor, C., Soria, E., and Juez, G. (2000). Biological significance of a family of regularly spaced repeats in the genomes of Archaea, Bacteria and mitochondria. *Mol Microbiol* 36, 244-246.

22. Mojica, F.J.M., Diez-Villasenor, C., Garcia-Martinez, J., and Almendros, C. (2009). Short motif sequences determine the targets of the prokaryotic CRISPR defence system. *Microbiology (Reading)* 155, 733-740.
23. Pickar-Oliver, A., and Gersbach, C.A. (2019). The next generation of CRISPR-Cas technologies and applications. *Nat Rev Mol Cell Biol* 20, 490-507.
24. Port, F., and Bullock, S.L. (2016). Creating Heritable Mutations in *Drosophila* with CRISPR-Cas9. *Methods Mol Biol* 1478, 145-160.
25. Port, F., Chen, H.M., Lee, T., and Bullock, S.L. (2014). Optimized CRISPR/Cas tools for efficient germline and somatic genome engineering in *Drosophila*. *Proc Natl Acad Sci U S A* 111, E2967-2976.
26. Pourcel, C., Salvignol, G., and Vergnaud, G. (2005). CRISPR elements in *Yersinia pestis* acquire new repeats by preferential uptake of bacteriophage DNA, and provide additional tools for evolutionary studies. *Microbiology (Reading)* 151, 653-663.
27. Ren, X., Sun, J., Housden, B.E., Hu, Y., Roesel, C., Lin, S., Liu, L.P., Yang, Z., Mao, D., Sun, L., *et al.* (2013). Optimized gene editing technology for *Drosophila melanogaster* using germ line-specific Cas9. *Proc Natl Acad Sci U S A* 110, 19012-19017.
28. Shah, S.A., Erdmann, S., Mojica, F.J., and Garrett, R.A. (2013). Protospacer recognition motifs: mixed identities and functional diversity. *RNA Biol* 10, 891-899.
29. Sternberg, S.H., Redding, S., Jinek, M., Greene, E.C., and Doudna, J.A. (2014). DNA interrogation by the CRISPR RNA-guided endonuclease Cas9. *Nature* 507, 62-67.
30. Wang, H., La Russa, M., and Qi, L.S. (2016). CRISPR/Cas9 in Genome Editing and Beyond. *Annu Rev Biochem* 85, 227-264.
31. Xue, Z., Ren, M., Wu, M., Dai, J., Rong, Y.S., and Gao, G. (2014). Efficient gene knock-out and knock-in with transgenic Cas9 in *Drosophila*. *G3 (Bethesda)* 4, 925-929.

## Chapter 4 : SUMOylation of Jra regulates gut immune response and helps maintain gut immune homeostasis

### 4.1 Abstract

We previously demonstrated that Jra is post-translationally modified by SUMO. We identified the SUMO acceptor lysine residues to be K29 and K190. We generated a SUMO conjugation resistant fly line of Jra using CRISPR/Cas9 technology. In this chapter, we extensively used the Jra<sup>SCR</sup> line to uncover the role of SUMO conjugation in modulating the function of Jra. We first established Jra as a negative regulator of the gut immune response as we observed loss of Jra in the gut helps the flies fight *P.entomophila* infection better. Using different genetic combinations and experiments, we have established that Jra<sup>SCR</sup> is a hypermorph of Jra and report that Jra<sup>SCR</sup> flies succumb early with increased bacterial loads. Using 3' mRNA sequencing of the guts, we identified that the activation of several immune effectors is suppressed in Jra<sup>SCR</sup> flies post-infection. Our data suggests that Jra is a suppressor of the gut immune response and transcriptionally regulates key genes like *Rel*, *dl*, *Fkh*, *Chinmo*, and *Ets21C* during infection. We propose that SUMO conjugation of Jra is necessary and an important regulatory step to attenuate the suppression of the immune response by Jra.

### Keywords

AMPs, transcriptional regulation, immune response, defence genes



## 4.2 Introduction

### 4.2.1 *Drosophila* midgut as a tool to study the immune response

The gut of *Drosophila* is one of the key organs that performs digestion and nutrient absorption. It also serves as an important first line of defence against any invading pathogens as flies feed on decaying food material in the wild. The *Drosophila* gut is compartmentalised into three main parts: the foregut that comprises of the mouthparts, oesophagus, crop and proventriculus; the middle midgut that is analogous to the mammalian intestine and is the main hub for the absorption of nutrients; the terminal hindgut that plays a role in excretion (Lemaitre and Miguel-Aliaga, 2013) (Figure 4.1 A,B). The midgut of *Drosophila* is a highly organised, plastic, and dynamic structure that is of endodermal origin. The midgut primarily has four cell types (Figure 4.1C). The first cell type is the multipotent intestinal stem cells (ISCs) that have tremendous regenerative properties and give rise to all other cell types in the gut (Micchelli and Perrimon, 2006). These stem cells divide asymmetrically to give rise to a daughter ISC and another cell called the enteroblast (EB) that is capable of entering into mitosis and differentiating into other cell types. The maintenance and proliferation of ISCs is very crucial to attain proper homeostasis in the gut and this is governed by several key signalling pathways like Notch, EGFR, Jak/STAT and JNK. (Biteau et al., 2008; Biteau and Jasper, 2011; Deng et al., 2015; Jiang and Edgar, 2009; Jiang et al., 2011; Jiang et al., 2009; Li et al., 2013; Ohlstein and Spradling, 2007; Takashima et al., 2013). The EB cells formed as a result of asymmetric cell division are larger compared to ISCs and constitute the second cell type in the adult midgut. The ISCs and EBs are positive for the expression of the proliferative marker Escargot (*esg*). ISCs in addition to *esg* are positive for the notch ligand, Delta (*Dl*). Depending on the signals received, EBs differentiate into either endo-enterocytes/entero-endocrine (EEs) or enterocytes (ECs). The EE cells are the primary secretory and endocrine cells of the midgut and are marked by the presence of Prospero (*Pros*). ECs are the largest cell population in the adult midgut.

They are large polyploid cells that absorb nutrients as their prime function and are the most immune active cells in the entire midgut. Most of the ECs are positive of the expression of Myo81F and Nubbin (Nub). All the cells in the midgut rest on the basement membrane (BM) which in turn is covered by a layer of muscle tissue and the apical side of the cells that face the lumen of the gut is covered by a thick layer of chitinous mucous called the peritrophic matrix (PM) (Miguel-Aliaga et al., 2018). In addition to this, the midgut is divided into different anatomical regions. Buchon and colleagues categorically divided the midgut into five regions and have meticulously worked out the gene expression patterns in the midgut (Buchon et al., 2013)(<https://flygut.epfl.ch/>).

When a pathogen enters the gut via the oral route, the midgut of *Drosophila* initiates a robust immune response to fight off the invading pathogen. The activation of the expression of AMPs constitutes the major response against gut pathogens. The Toll and the Imd pathways are predominant signalling pathways that activate the transcription of AMPs. These immune signalling pathways in the adult midgut seem to be compartmentalised. The Toll pathway is active in the foregut and the hindgut, and the Imd pathway governs immune response in the midgut. The components of the canonical Imd pathway are highly expressed in the midgut of *Drosophila*. Two receptors that recognize the DAP-type peptidoglycan (PGN) are expressed in the gut. PGRP-LC is membrane-bound and recognises PGN present in the lumen and PGRP-LE (Bosco-Drayon et al., 2012; Neyen et al., 2012) is an intracellular receptor and recognises PGN ingested by the cell. Interestingly, the expression of both these receptors is distinct and present at the opposite end of the midgut with PGRP-LC being only expressed in the anterior midgut and PGRP-LE only expressed in the posterior midgut (Buchon et al., 2013). However, it is not well understood why such a spatially distinct expression pattern of these receptors exists. The gut of *Drosophila* is home to several species of commensal bacteria that express PGN on their cell walls. The recognition of PGN from commensal bacteria by PGRPs could

lead to heightened activation of the Imd pathway and could in turn lead to inflammation in the gut and could be detrimental to the fly. To avoid this, several negative regulators act on the Imd pathway and keep the activation of the AMPs under check. Negative regulation of the Imd pathway in the gut comes from two PGRP molecules like PGRP-SC members and PGRP-LB. Both these extracellular molecules, clear free-floating PGN in the lumen of the gut and dampen the immune activation by Imd (Bischoff et al., 2006; Paredes et al., 2011; Zaidman-Remy et al., 2006). In addition to these, Pirk regulates systemic immunity by displacing PGRP-LC from the membrane and performs the same function in the gut and regulates Imd activation (Bosco-Drayon et al., 2012; Kleino et al., 2008). Another interesting example is the regulation of AMP production in the hindgut by the homeobox-containing transcription factor caudal (Cad). Cad represses AMPs independent of the Imd pathway (Ryu et al., 2008). In addition to these, other negative regulators of the systemic immune response like Caspar (Casp) (Kim et al., 2006) and the JNK pathway components, Basket (Bsk), Jun-related antigen (Jra) and Kayak (Kay) (Kim et al., 2007; Kim et al., 2005) have not been studied in the context of the gut immunity. Another important mechanism active in the gut to eliminate pathogens is the production of reactive oxygen species (ROS). ROS causes severe damage to the invading pathogen by oxidising DNA, RNA, membrane lipids, and thus protecting the fly. The gut of *Drosophila* generates a strong ROS attack in response to several pathogenic bacterial species and the generation of ROS is predominantly controlled by two NADPH enzymes, dual oxidase (Duox) and NADPH oxidase (Nox), and mutations in these two enzymes make the flies susceptible to gut infection (Bae et al., 2010; Ha et al., 2005; Jones et al., 2013). A key finding describes that uracil derived from pathogenic bacteria in the lumen of the gut activates Duox in the gut which in turn eliminates the bacteria by producing ROS and induces intestinal cell repair. Interestingly, uracil is not released by the gut commensals making them immune to clearance by ROS secreted by Duox (Lee et al., 2013).

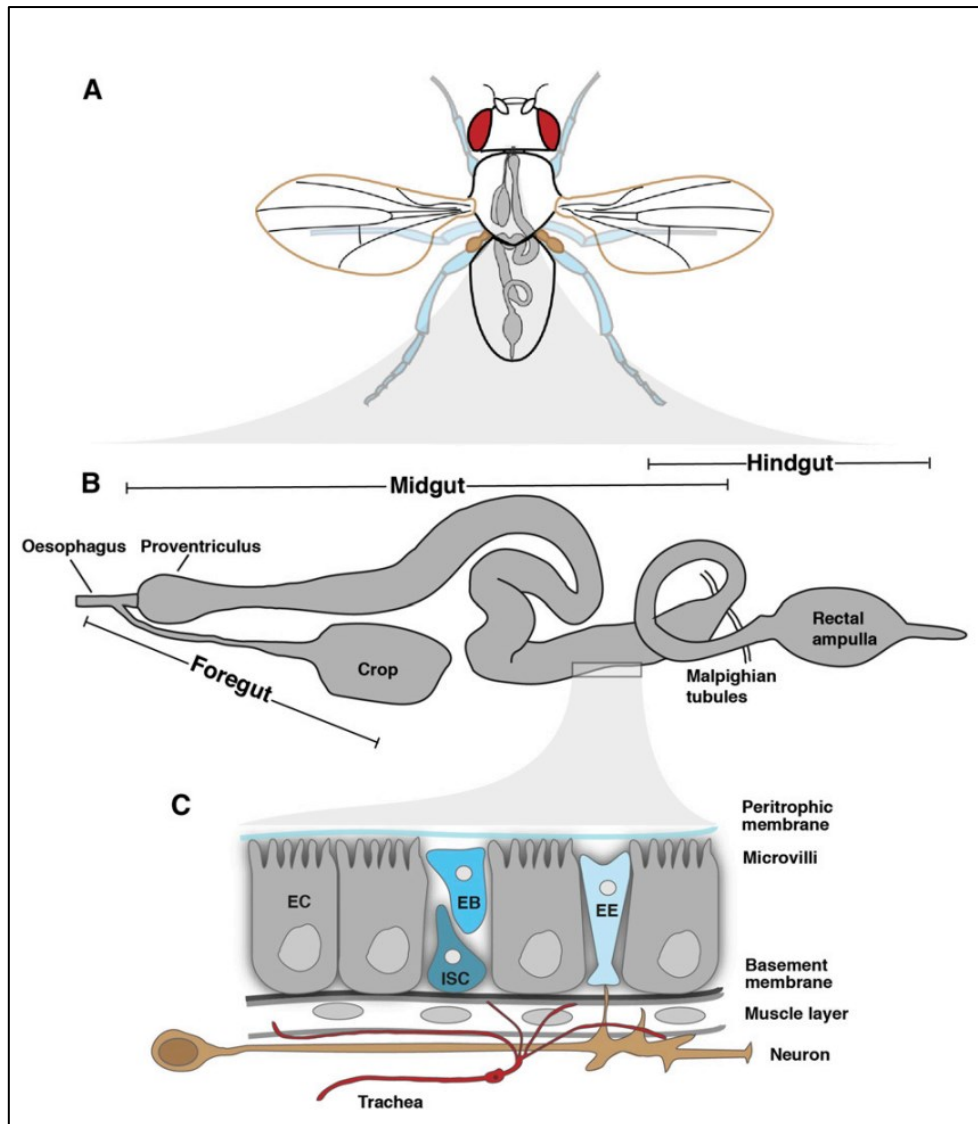


**Figure 4.1: Anatomical features of the gut in *Drosophila***

**A.** Organisation of the gut in the body of the adult fly

**B.** Compartmentalization of the gut into foregut, midgut and hindgut

**C.** Different types of cells seen in the adult midgut. The ISCs are pluripotent and divide into all other cell types. The EBs differentiate into ECs and EEs. ECs perform the majority of the absorption and are the most immune active cells. EEs are endocrine cell and secrete several hormones. All the cell type are cemented on a basement membrane which in turn rests on a muscle layer. The cells, BM and muscle layer are innervated by neurons and trachea. On the apical side that faces the lumen, a thick mucus peritrophic membrane is present. Reproduced from Miguel-Aliaga et al., 2018

When there is an active infection in the gut, there is apoptosis and cell death of the cells of the tissue (Buchon et al., 2009). In addition to this, the enterocytes that are infected and damaged, delaminate from the gut tissue to prevent further damage of the gut tissue, and this is

synergistically regulated by the action of the Imd and JNK signalling pathways (Zhai et al., 2018). Due to increased cell death upon infection, the number of enterocytes in the gut is reduced and has to be actively replenished to maintain homeostasis. The ISCs play a major role in maintaining the cells in the gut tissue during gut infection. ISC proliferation during an infection is governed by a large network of interconnected signalling pathways. Pathways like Notch, EGFR, JNK, Hippo, Tor, Wg and, Jak/STAT , are active during an infection in the gut. Work done from several labs indicated that Myc could be a convergence point of several pathways to regulate ISC proliferation during an infection (Amcheslavsky et al., 2011; Ren et al., 2013; Ren et al., 2010). In addition to this, the Jak/STAT pathway in parallel to the EGFR pathway also regulates the proliferation of ISCs during an immune challenge to maintain gut homeostasis (Buchon et al., 2010; Jiang and Edgar, 2009; Jiang et al., 2011; Jiang et al., 2009)(Bonfini et al., 2016; Buchon et al., 2014; Capo et al., 2019; Miguel-Aliaga et al., 2018; Troha and Buchon, 2019).

#### ***4.2.2 Pseudomonas entomophila: A robust gram-negative pathogen***

*Pseudomonas entomophila* (Pe) is one of the very few *Pseudomonas* species that infects and kills insects. It was originally isolated from the gut of *Drosophila* caught in the wild. A close relative to *Pseudomonas putida*, *Pseudomonas entomophila* has more than 5000 genes (Vodovar et al., 2006) and is an obligate aerobe. Since its identification, *P.entomophila* has been one of the most used pathogens to study gut immunity in *Drosophila*. *P.entomophila* is a gram-negative pathogen that activates the systemic immune response in the fly when fed orally at high doses. *P.entomophila* invokes a strong AMP response via the Imd signalling pathway (Chakrabarti et al., 2012) due to the presence of DAP type peptidoglycan that is recognised by PGRP-LC receptor on the cell surface. The success of *P.entomophila* comes from its ability to survive the harsh acidic environment in the midgut during the early stages of the infection. It however breaches the intestinal barrier and colonizes in the haemolymph of the fly during the

later stages of infection. In addition to this, *P. entomophila* exhibits a strong proteolytic activity when grown on blood agar or skimmed milk agar. This is attributed to the presence of a plethora of proteolytic enzymes and pore-forming toxins that act as robust virulence factors. One important proteolytic enzyme that contributes to the virulence of *P. entomophila* is the zinc metalloprotease AprA which is one of the most abundant proteins in the culture supernatant of *P. entomophila*. It is shown that AprA mutant *P. entomophila* fail to infect the fly and are cleared faster upon infection. Another factor GacA strongly corresponds to the virulence of *P. entomophila*. GacA is a part of a two-component regulatory system that regulates the secretion of AprA. Like AprA mutants, GacA mutants too do not invoke a proper immune response in the fly. In addition to these, PrtR also plays an important role in the virulence of the microbe (Liehl et al., 2006). A key aspect of *P. entomophila*'s success comes from the ability to perturb the physiology of the host. An interesting piece of work from Chakrabarti and colleagues provides evidence that *P. entomophila* inhibits protein synthesis in the host. The protein synthesis blockage by the bug is via perturbation in two prominent stress-responsive pathways. The first is by GCN2 pathway where GCN2 mediated phosphorylation of eIF2a blocks translation. The second is by AMPK mediated downregulation of the TOR pathway which results in the dephosphorylation of 4EBP and subsequent blockage of translation (Chakrabarti et al., 2012). It is reported that *P. entomophila* affects the feeding of the host. Once it enters the fly body via the gut, it has been observed that the crop increases in size due to the presence of food material that gets stalled without being passed into the midgut. However, the possibility that this physiological change could be a host driven response to oral infection cannot be ignored. Histological sections and electron micrograph images of the midgut reveal severe damage to microvilli and enhanced apoptosis in the gut tissue, which may help breach the gut epithelial barrier and increase the possibility of the pathogen colonising other organs in the fly (Vodovar et al., 2005).

## 4.3 Results and Discussion

### 4.3.1 *Jra* is a negative regulator of the gut immune response

As mentioned in the previous chapters, the role of the JNK signalling pathway and the downstream transcription factors in regulating immune response is ambiguous in *Drosophila* (Delaney et al., 2006; Kim et al., 2007; Kim et al., 2005; Silverman et al., 2003). Also, the role of AP-1 in regulating the gut immunity of *Drosophila* has not been well studied. We started by looking at the role of *Jra* in regulating the gut immunity of *Drosophila*. As a first step, we knocked down *Jra* specifically in the enterocytes of the gut using *Myo81F-Gal4<sup>ts</sup>* (*NP1-Gal4<sup>ts</sup>*). We then orally fed these flies with a gram-negative pathogen, *Pseudomonas entomophila* (*Pe*), scored for dead flies each day, and plotted this as a function of survival. We crossed the *NP1-Gal4* line to *w<sup>1118</sup>* and used the flies as a control. We observed that the control flies succumbed to infection under 5 days. Interestingly, *Jra<sup>RNAi</sup>* flies show an enhanced survival upon infection and succumb late. This finding was reproduced by overexpressing a dominant-negative allele of *Jra* (*Jra<sup>DN</sup>*) in the gut which also shows an enhanced survival upon oral infection (Figure 4.2). The unchallenged (UC) flies however not shown any differences in lifespan. In addition to RNAi, we used the two most well characterised null mutants, *jra<sup>IA109</sup>* and *jra<sup>76-19</sup>* and orally infected them with *Pe*. We crossed both the lines to the *w<sup>1118</sup>* line and used the progeny with one copy of the null and one copy of the wildtype allele. This ensured that the flies were hypomorphic for the function of *Jra*. We observed that UC flies do not show any significant change in lifespan. However, we report that the control *w<sup>1118</sup>* flies succumb early to gut infection wherein more than 50% of flies die within 2 days post-infection. Concurrent to the overexpression of *Jra<sup>RNAi</sup>* and *Jra<sup>DN</sup>*, both the hypomorphs show enhanced survival upon oral infection with *Pe* (Figure 4.3).

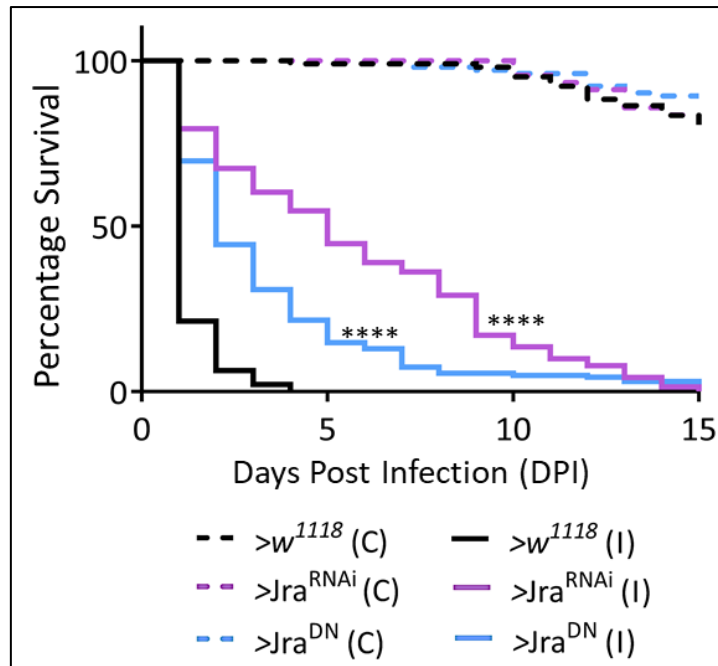


**Figure 4.2:  $Jra^{RNAi}$  and  $Jra^{DN}$  enhance the survival of flies post-infection**

Survival curves of unchallenged (UC, dashed lines) or *Pe* infected (I, closed), 6-8d/o female flies after over-expression of  $Jra^{RNAi}$  (magenta) and  $Jra^{DN}$  (blue) using enterocyte specific NP1-Gal4<sup>ts</sup>. The Gal4 control is represented in black. Data pooled from three independent experiments. Log rank test for trend comparing  $>Jra^{RNAi}$  (I) and  $>Jra^{DN}$  (I) to  $>w^{1118}$  (I); \*\*\*\* $p < 0.0001$ . number of flies used in the experiment;  $>w^{1118}$  (C) – 103;  $>w^{1118}$  (I) – 141;  $>Jra^{RNAi}$  (C) – 91;  $>Jra^{RNAi}$  (I) – 141;  $>Jra^{DN}$  (C) – 103;  $>Jra^{DN}$  (I) – 159.

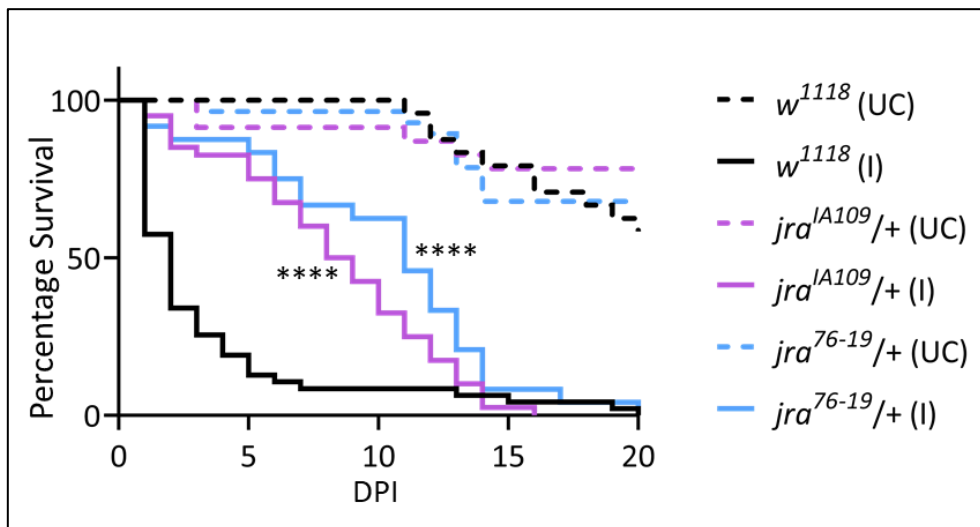


**Figure 4.3:  $Jra$  hypomorphs enhance the survival of flies post-infection**

Survival curves of unchallenged (UC, dashed lines) or *Pe* infected (I, closed), 6-8d/o female flies:  $w^{1118}$  (black),  $jra^{IA109/+}$  (magenta) and  $jra^{76-19/+}$  (blue). Data from a single experiments. Log rank test for trend comparing  $jra^{IA109/+}$  (I) and  $jra^{76-19/+}$  (I) to  $w^{1118}$  (I); \*\*\*\* $p < 0.0001$ . number of flies used in the experiment;  $w^{1118}$  (C) – 24;  $w^{1118}$  (I) – 47;  $>jra^{IA109/+}$  (C) – 23;  $>jra^{IA109/+}$  (I) – 40;  $jra^{76-19/+}$  (C) – 28;  $jra^{76-19/+}$  (I) – 24.



We further explored the role of other members of the JNK signalling pathway in regulating gut immunity in *Drosophila*. For this, we first tested the only known JNK, Basket (Bsk). We overexpressed the dominant-negative form of Bsk (Bsk<sup>DN</sup>) and looked at the lifespan post oral infection with *Pe*. We observed that overexpression of Bsk<sup>DN</sup> in the enterocytes of the gut enhances lifespan as compared to control. Interestingly, Bsk<sup>DN</sup> (UC) flies also showed enhanced survival as compared to control suggesting a possible role of regulating lifespan via signalling from the gut (Figure 4.4).

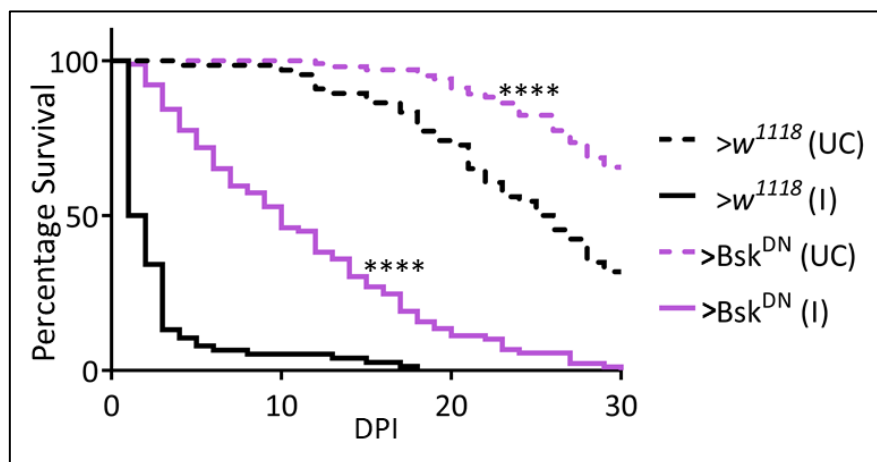


**Figure 4.4: Overexpression of Bsk<sup>DN</sup> enhances survival upon gut infection**

Survival curves of unchallenged (UC, dashed lines) or *Pe* infected (I, closed), 6-8d/o female flies after over-expression of Bsk<sup>DN</sup> (magenta) using enterocyte specific NP1-Gal4<sup>ts</sup>. The Gal4 control is represented in black. Data pooled from three independent experiments. Log-rank test for trend comparing >Bsk<sup>DN</sup> (I) to >w<sup>1118</sup> (I) and >Bsk<sup>DN</sup> (C) to >w<sup>1118</sup> (C); \*\*\*\*p<0.0001. number of flies used in the experiment; >w<sup>1118</sup> (C) – 64; >w<sup>1118</sup> (I) – 76; >Bsk<sup>DN</sup> (C) – 102; >Bsk<sup>DN</sup> (I) – 89.

We also looked at the role of Kayak (Kay, which heterodimerizes with Jra and forms the AP-1 complex) in regulating gut immunity. For this, we overexpressed a dominant-negative allele of Kay in the enterocytes using *NP1-Gal4<sup>ts</sup>* and looked at the lifespan post oral infection. We observed that unlike perturbation of Jra and Bsk, perturbation of Kay doesn't significantly alter the lifespan post an immune challenge (Figure 4.5).

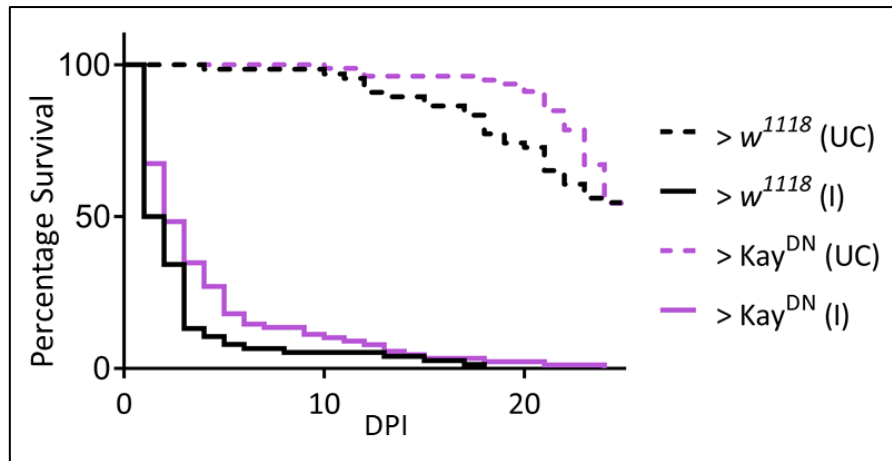


**Figure 4.5: Overexpression of Kay<sup>DN</sup> does not alter the survival upon gut infection**

Survival curves of unchallenged (UC, dashed lines) or *Pe* infected (I, closed), 6-8d/o female flies after over-expression of Kay<sup>DN</sup> (magenta) using enterocyte specific NP1-Gal4<sup>ts</sup>. The Gal4 control is represented in black. Data pooled from two independent experiments. Log-rank test for trend comparing >Kay<sup>DN</sup> (I) to >w<sup>1118</sup> (I) and >Kay<sup>DN</sup> (C) to >w<sup>1118</sup> (C). number of flies used in the experiment; >w<sup>1118</sup> (C) – 64; >w<sup>1118</sup> (I) – 76; >Bsk<sup>DN</sup> (C) – 102; >Bsk<sup>DN</sup> (I) – 89.

Our data from the lifespan experiments suggested that loss of *Jra* enhances the survival upon gut infection. We hypothesised that one way by which this could be happening is by alleviated clearance of bacteria upon knockdown of *Jra*. To test this hypothesis, we monitored the bacterial load in *w<sup>1118</sup>* and *jra<sup>IA109/+</sup>* flies during gut infection. We fed the flies of both the genotypes with a concentrated culture of *Pe* for 2 hours. We crushed each fly separately in sterile PBS and plated appropriate dilutions of the lysate (to count individual colonies) at 2, 8 and 24 hpi. As hypothesised, we observed that as time progressed, with infection, *jra<sup>IA109/+</sup>* flies were able to clear the bacteria faster than the wild type. This can be noted as increased bacterial clearance (Figure 4.6) as *jra<sup>IA109/+</sup>* flies have significantly reduced bacterial load at 4 and 24 hpi as compared to *w<sup>1118</sup>*. Interestingly, we did not observe any change in bacterial load per fly at 2 hpi when the flies were continuously feeding for 2 hours. This suggests that probably the feeding rate in both the genotypes is similar and serves as a control

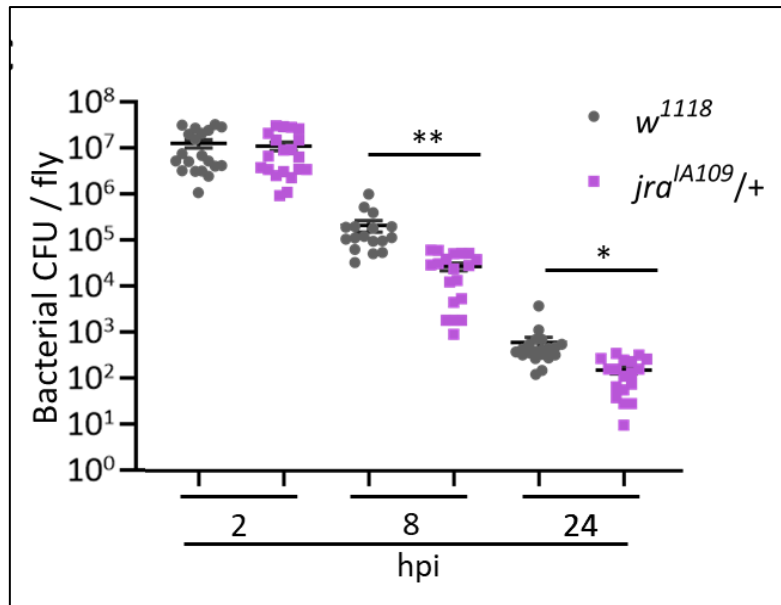


**Figure 4.6: *jra<sup>IA109/+</sup>* clears bacteria significantly faster than the wild type**

Scatter dot plot representing bacterial load as colony forming units (CFUs) post gut infection with *Pe*. The decrease in bacterial CFUs can be seen in *jra<sup>IA109/+</sup>* (purple) at 8 and 24 hpi. Student's t-test was performed comparing *w<sup>1118</sup>* and *jra<sup>IA109/+</sup>* at respective timepoint post infection. \*\* $p=0.0025$ ; \* $p=0.0194$ . Number of flies used in the experiment; *w<sup>1118</sup>* (2 hpi) – 20; *jra<sup>IA109/+</sup>* (2 hpi) – 20; *w<sup>1118</sup>* (8 hpi) – 17; *jra<sup>IA109/+</sup>* (8 hpi) – 19; *w<sup>1118</sup>* (24 hpi) – 20 ; *jra<sup>IA109/+</sup>* (24 hpi) – 19. Means and SEMs represented.

Enteric infection by *Pseudomonas entomophila* causes severe disruption to the gut epithelium in the later stages of infection as mentioned in the previous sections of this chapter. In addition to the AMPs and other defence responsive molecules that the cells of the gut secrete, the gut must restore the damaged cells in the gut. The gut has a pool of ISCs that do the job of regenerating the gut epithelium whenever there is damage to the tissue. *Pe* causes severe damage to the gut tissue and this triggers the division of the ISCs into EBs and further differentiation of the EBs to ECs. This increase in cell division can be monitored by immunostaining the gut tissue for phospho-Histone 3 (pH3). As described previously, there is ample evidence to suggest the JNK signalling regulates ISCs proliferation. However, the role of JNK signalling in regulating ISC proliferation upon an immune challenge has not been well studied and the role of the downstream transcription factors remain completely unknown. To check if Jra has a role in regulating ISC proliferation and tissue renewal upon infection, we fed

$w^{1118}$  and  $jra^{IA109/+}$  flies for 8 hours with a concentrated culture of *Pe*, dissected out the gut tissue and immunostained the gut tissue with anti-pH3 antibody and imaged them. We then quantitated the pH3 positive cells in the entire midgut and as expected, there was a strong induction of mitoses in the midgut post-infection as compared to UC. The increase in mitosis events was significantly observed in both  $w^{1118}$  and  $jra^{IA109/+}$  flies upon infection. However, there was no significant change between  $w^{1118}$  (I) and  $jra^{IA109/+}$  (I) suggesting that Jra might not play a role in regulating the intestinal stem cell proliferation upon an immune challenge.

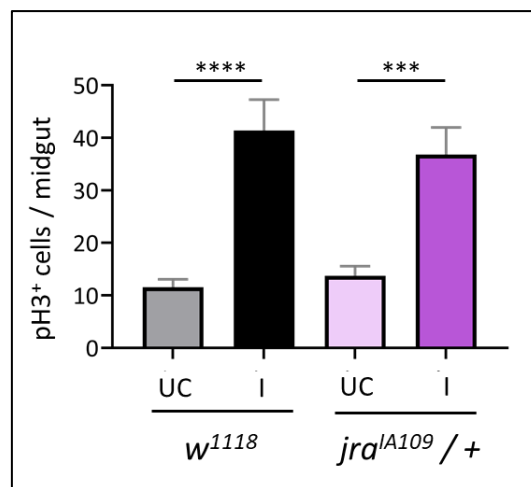


**Figure 4.7: Jra hypomorphs do not show any significant change in pH3 positive cells as compared to wildtype flies**

Quantitation of the number of pH3<sup>+</sup> cells per midgut of UC flies and flies orally fed with *Pe* \*\*\*\*:p<0.0001; \*\*\*p=0.0011 as determined by 2-way ANOVA with Tukey's post-hoc test. Number of gut used;  $w^{1118}$  (UC) – 16;  $w^{1118}$  (I) – 17;  $jra^{IA109/+}$  (UC) – 14;  $w^{1118}$  (I) – 17. Means and SEMs represented.

Our data suggest that Jra is a negative regulator of gut immune response in *Drosophila*. We have shown that knockdown of Jra in the gut is sufficient to enhance the survival of the flies post-infection. We have also shown that Bsk that is upstream of Jra also acts as a negative regulator of the gut immune response. and we hypothesize that the JNK signalling pathway is a negative regulator of gut immunity and is acting predominantly via Jra.

### ***4.3.2 Components of SUMO conjugation machinery negatively regulate gut immunity in Drosophila***

Once we established the role for Jra as a negative regulator of the gut immune response, a previously unknown role, we were curious about the role of SUMO conjugation of Jra in the gut immune context. As described in the previous chapter, we generated a SUMO conjugation resistant Jra fly (where the SUMO target lysine residues 29 and 190 were mutated to arginine residues in the genomic locus) using CRISPR/Cas9 technology. Before looking at the role of SUMO conjugation in regulating Jra function, it was important to establish a role for SUMO protein in the gut post an immune challenge. The role of SUMO in regulating immunity in *Drosophila* seems to be highly context-dependent and tissue-specific. Hypomorphic mutants of *Ubc9* (the only known SUMO conjugating enzyme) show increased inflammation by overproduction of the AMP Drosomycin without an immune challenge (Chiu et al., 2005) and with an immune challenge (Paddibhatla et al., 2010) by regulating key components of the Toll signalling pathway. In a systemic infection to the fly with *E.coli*, hypomorphs of *Ubc9* seem to respond rather poorly and succumb early. Also, they are unable to clear the bacteria from their system and have suppressed activation of AMPs (Fukuyama et al., 2013). Similar observations were made in S2 cells of *Drosophila*, where knockdown of SUMO tends to lower the mRNA levels of *metchnikowin* (Mtk), another AMP, upon an immune challenge. Interestingly, knockdown of SUMO also reduced the mRNA levels of the NF- $\kappa$ B transcription factor *Relish* (Rel) (Handu et al., 2015). To understand the contribution of SUMO protein in regulating gut immunity, Using RNAi, we knocked down the only known SUMO gene (*Smt3*) in *Drosophila* using *NPI-Gal4<sup>ts</sup>*. We then orally fed the flies with *Pe* and tracked the lifespan of the flies post-infection.

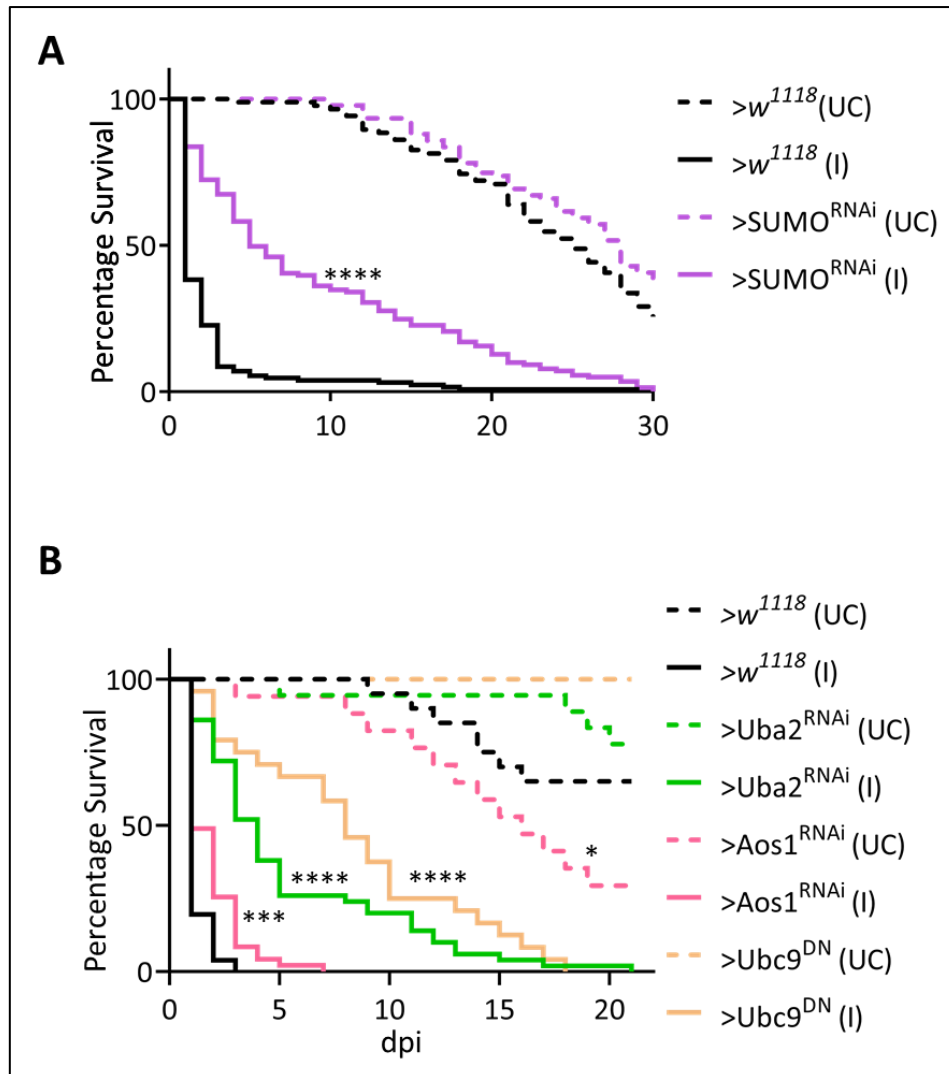


**Figure 4.8: Knockdown of SUMO machinery components enhances the survival in *Drosophila*.**

**A.** Survival curves of unchallenged (UC, dotted) and orally infected with *Pe* (I, closed), flies:  $w^{1118}$  (black) and  $>SUMO^{RNAi}$  (purple). Data pooled from a three experiments. Log rank test for trend comparing  $>SUMO^{RNAi}$  (I) to  $w^{1118}$  (I); \*\*\*\* $p < 0.0001$ . Number of flies used in the experiment;  $>w^{1118}$  (C) – 86;  $>w^{1118}$  (I) – 128;  $>SUMO^{RNAi}$  (C) – 91;  $>SUMO^{RNAi}$  (I) – 141.

**B.** Survival curves of unchallenged (UC, dotted) and orally infected with *Pe* (I, closed) after perturbing different components of the SUMO cycle machinery. Data pooled from one independent experiments. Log rank test for trend comparing  $>Uba2^{RNAi}$  (I),  $>Aos1^{RNAi}$  (I) and  $>Ubc9^{DN}$  to  $w^{1118}$  (I). \*:  $p = 0,03$ ; \*\*\*:  $p = 0.0008$  \*\*\*\* $p < 0.0001$ . number of flies used in the experiment;  $>w^{1118}$  (C) – 20;  $>w^{1118}$  (I) – 51;  $>Uba2^{RNAi}$  (C) – 18;  $>Uba2^{RNAi}$  (I) – 50;  $>Aos1^{RNAi}$  (C) – 17;  $>Aos1^{RNAi}$  (I) – 47;  $>Ubc9^{DN}$  (C) – 17;  $>Ubc9^{DN}$  (I) – 24.

We report that loss of SUMO in the gut has enhanced the survival of flies post-infection as compared to infected controls (Figure 4.8A) suggesting that SUMO works by suppressing the gut immunity of *Drosophila*. Also, the other components of the SUMO machinery, the SUMO activating enzyme complex (Aos2/Uba2) and the SUMO conjugating enzyme (Ubc9) show a

similar trend and enhance the survival of the flies post an immune challenge with *Pe* (Figure 4.8B). This suggests that all the components of SUMO conjugation machinery do play a crucial role in suppressing the gut immunity of *Drosophila* during an infection. Interestingly, the loss of *Aos1* in the gut in unchallenged conditions decreased the lifespan of the fly as compared to unchallenged control flies. This result implicates that *Aos1* function in the gut is necessary for the fly to survive and needs detailed investigation.

#### 4.3.3 SUMO conjugation of *Jra* attenuates the suppression of immune response by *Jra*

After observing that SUMO regulates gut immunity in *Drosophila*, we looked at the role of SUMO conjugation of *Jra* in regulating gut immunity. For this, we used the CRISPR/Cas9 modified *Jra*<sup>SCR</sup> flies and the CRISPR control fly line, (that did not harbour any mutations and was wildtype for the protein sequence) hereby referred to as *Jra*<sup>WT</sup> flies, for our experiments. We fed these flies with a concentrated culture of *Pe* and scored for the number of deaths per day in a life span experiment post-infection.

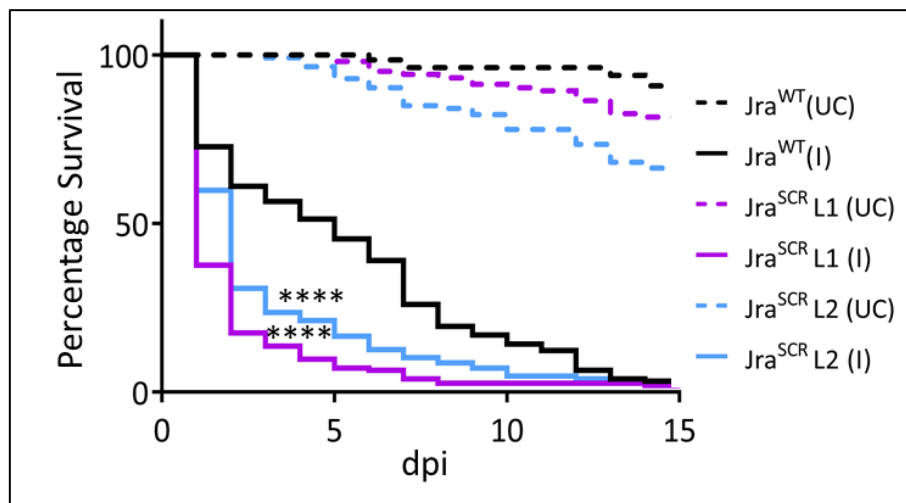


**Figure 4.9: *Jra*<sup>SCR</sup> flies show reduced survival upon infection**

Survival curves of unchallenged (UC, dashed lines) or *Pe* orally infected (I, closed lines), CRISPR/Cas9 modified *Jra*<sup>WT</sup> (black) and *Jra*<sup>SCR</sup> flies. L1 (red) and L2 (blue) indicate two independent lines used in the experiment. Data pooled from three experiments. Log-rank test for trend comparing *Jra*<sup>SCR</sup> L1 (I) and *Jra*<sup>SCR</sup> L2 (I) *Jra*<sup>WT</sup> (I); \*\*\*\*p<0.0001. Number of flies used in the experiment; *Jra*<sup>WT</sup> (UC) – 142; *Jra*<sup>WT</sup> (I) – 154; *Jra*<sup>SCR</sup> L1 (UC) – 103; *Jra*<sup>SCR</sup> L1 (I) – 154; *Jra*<sup>SCR</sup> L2 (UC) – 111; *Jra*<sup>SCR</sup> L2 (I) – 127.

We observed that  $Jra^{SCR}$  flies responded poorly to infection and succumbed early. This result was concurrent with two independent lines (line 1 and line 2) we generated. According to our data, the  $Jra^{SCR}$  flies show a phenotype opposite to that of a hypomorph (Figure 4.2 and Figure 4.3). We report that  $Jra^{SCR}$  is a hypermorphic allele of  $Jra$  and we show with a SUMO conjugation resistant mutant of  $Jra$  that SUMO conjugation of  $Jra$  attenuates the suppression of the immune response. To gain more confidence in the nature of the SCR allele of  $Jra$ , we looked at the lifespan of flies in the heterozygous combination with the null allele post-infection. We independently crossed the  $jra^{IA109}$  flies to  $Jra^{WT}$  and  $Jra^{SCR}$  flies and have performed lifespan experiments post-feeding with *Pe*. We have observed that  $jra^{IA109}/Jra^{WT}$  flies lived longer than homozygous  $Jra^{WT}$  flies upon infection. This result was previously seen in  $jra^{IA109}/+$  and suggested that reducing the function of  $Jra$  was sufficient to enhance the ability of the fly to fight off infection. A similar phenotype was observed in  $jra^{IA109}/Jra^{SCR}$  as they survived longer than homozygous  $Jra^{SCR}$  flies. Interestingly, when we compared the lifespan of  $jra^{IA109}/Jra^{WT}$  to that of  $jra^{IA109}/Jra^{SCR}$ , we observed that  $jra^{IA109}/Jra^{SCR}$  significantly succumbed early than  $jra^{IA109}/Jra^{WT}$  strengthening our hypothesis that  $Jra^{SCR}$  is a hypermorphic allele of  $Jra$ . We then looked at the bacterial clearance in  $Jra^{SCR}$  and  $Jra^{WT}$  flies post-infection. We observed that  $Jra^{SCR}$  flies do not clear the bacteria as well as  $Jra^{WT}$  flies (Figure 4.11A). This could be one of the reasons for the enhanced deaths observed in  $Jra^{SCR}$  flies. We also looked to see if there were changes in the number of mitosis events in  $Jra^{SCR}$  and  $Jra^{WT}$  postinfection. We observed that both fly lines show a significantly increased number of pH3 positive cells upon infection (as compared to UC) but we did not observe any significant change in the number of pH3 cells between  $Jra^{WT}$  and  $Jra^{SCR}$  suggesting that  $Jra$  does not control stem cell proliferation and tissue renewal during gut infection.



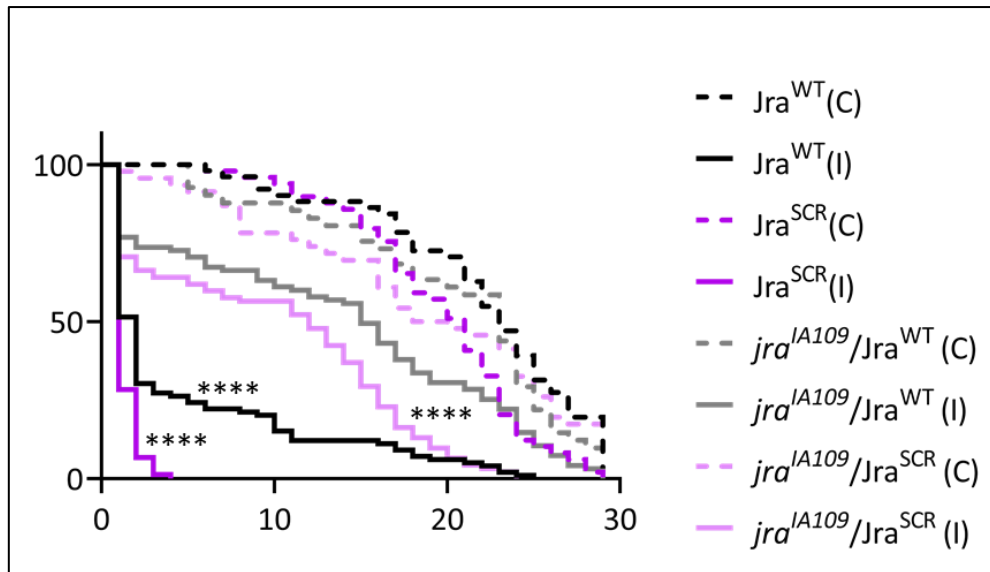


**Figure 4.10:  $Jra^{SCR}$  behaves like a hypermorph in the heterozygous combination of the null allele**

Survival curves of unchallenged (UC, dotted) and orally infected with *Pe* (I, closed), flies:  $Jra^{WT}$  (black),  $Jra^{SCR}$  (purple),  $jra^{IA109}/Jra^{WT}$  (grey) and  $jra^{IA109}/Jra^{SCR}$  (lavender). Data pooled from two experiments. Log rank test for trend comparing  $jra^{IA109}/Jra^{WT}(I)$  to  $Jra^{WT}(I)$  and  $jra^{IA109}/Jra^{SCR}(I)$  to  $Jra^{SCR}(I)$   $jra^{IA109}/Jra^{SCR}(I)$  to  $jra^{IA109}/Jra^{WT}(I)$ . \*\*\*\* $p < 0.0001$ . Number of flies used in the experiment;  $Jra^{WT}(UC)$  – 51;  $Jra^{WT}(I)$  – 99;  $Jra^{SCR}(UC)$  – 49;  $Jra^{SCR}(I)$  – 74;  $jra^{IA109}/Jra^{WT}(UC)$  – 41;  $jra^{IA109}/Jra^{WT}(I)$  – 95;  $jra^{IA109}/Jra^{SCR}(UC)$  – 46;  $jra^{IA109}/Jra^{SCR}(I)$  – 92.

Till now, we have done experiments and shown data by depleting the JNK signalling using hypomorphic alleles of the components of the pathway that Bsk acts via Jra and negatively regulates the gut immune response in *Drosophila*. We were curious to check how would hyperactivating the pathways regulate the immune response. To increase the activity of the JNK signalling pathway, we have used a hypomorph of the Bsk specific phosphatase called puckered (Puc). Puc is required to dephosphorylate Bsk and attenuate the signalling cascade. Using a hypomorphic allele of Puc that cannot dephosphorylate Bsk completely, keeps the pathway activated. Having a hypomorphic allele of puc ( $puc^{E69}$ ) did not show any significant change in the survival of the flies in neither  $Jra^{WT}$  nor  $Jra^{SCR}$ . This could probably implicate that Puc has no role in regulating this particular aspect of JNK signalling during gut infection.

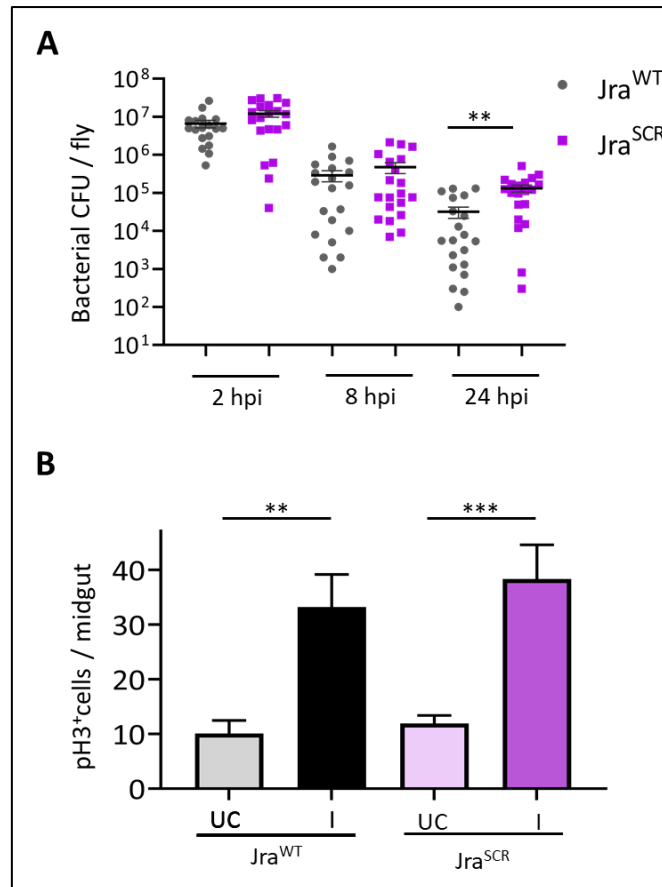


**Figure 4.11: Bacterial clearance and number of pH3<sup>+</sup> cells in Jra<sup>SCR</sup> and Jra<sup>WT</sup>**

**A.** Scatter dot plot representing bacterial load as colony forming units (CFUs) post oral feeding with *Pe* Student's t-test was performed comparing Jra<sup>WT</sup> and Jra<sup>SCR</sup> at respective timepoint post infection. \*\*p=0.0015; Number of flies used in the experiment; Jra<sup>WT</sup> (2 hpi) – 18; Jra<sup>SCR</sup> (2 hpi) – 20; Jra<sup>WT</sup> (8 hpi) – 20; Jra<sup>SCR</sup> (8 hpi) – 20; Jra<sup>WT</sup> (24 hpi) – 20 ; Jra<sup>SCR</sup> (24 hpi) – 20. Means and SEMs represented.

**B.** Quantitation of the number of pH3<sup>+</sup> cells per midgut of UC flies and flies orally fed with *Pe* \*\*:p=0.0071; \*\*\*p=0.0005 as determined by 2-way ANOVA with Tukey's post-hoc test. Number of gut used; Jra<sup>WT</sup> (UC) – 20; Jra<sup>WT</sup> (I) – 23; Jra<sup>SCR</sup> (UC) – 24; Jra<sup>SCR</sup> (I) – 24. Means and SEMs represented.

This also sheds light on the probability of Bsk having another phosphatase in regulating its activity. In a different approach, we tried to increase the activity of the JNK pathway by over expressing a constitutively active form of the JNKK called hemipterous (Hep) that activates Bsk by phosphorylation. Our attempts to overexpress a constitutively active form of Hep (Hep<sup>CA</sup>) using *NP-Gal4<sup>ts</sup>* has not been successful as very few adult flies emerged from the cross and these were not sufficient to do any further experiments. However, we have not characterised this particular phenotype further and it would be worth studying in the future.

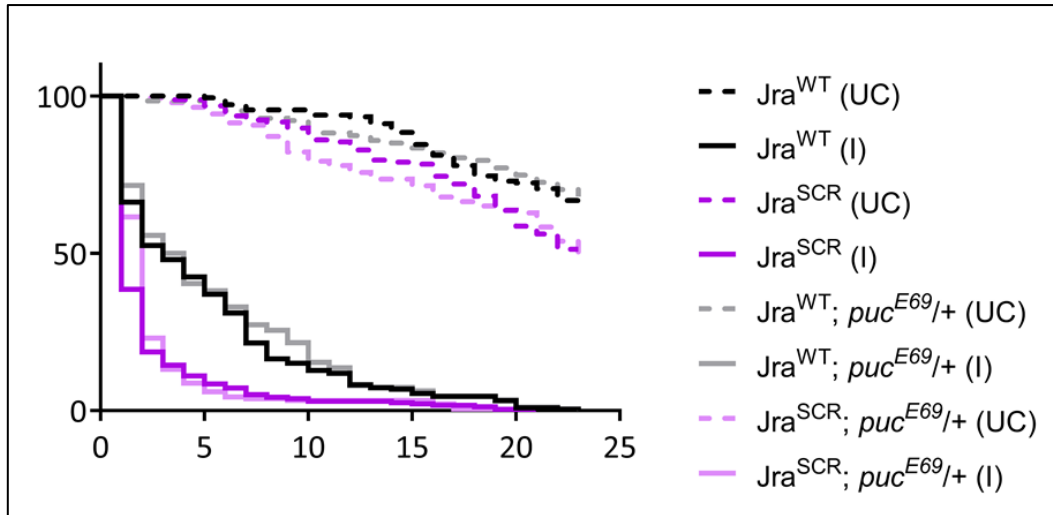


**Figure 4.12: Puckered has no effect on the lifespan during a gut infection**

Survival curves of unchallenged (UC, dotted) and orally infected with *Pe* (I, closed), flies:  $Jra^{WT}$  (black),  $Jra^{SCR}$  (purple),  $Jra^{WT}; puc^{E69/+}$  (grey) and  $Jra^{SCR}; puc^{E69/+}$  (lavender). Data pooled from three experiments. Log rank test for trend comparing  $Jra^{WT}; puc^{E69/+}$  (I) to  $Jra^{WT}$  (I) and  $Jra^{SCR}; puc^{E69/+}$  (I) to  $Jra^{SCR}$  (I); Number of flies used in the experiment;  $Jra^{WT}$  (UC) – 181;  $Jra^{WT}$  (I) – 219;  $Jra^{SCR}$  (UC) – 157;  $Jra^{SCR}$  (I) – 236;  $Jra^{WT}; puc^{E69/+}$  (UC) – 127;  $Jra^{WT}; puc^{E69/+}$  (I) – 176;  $Jra^{SCR}; puc^{E69/+}$  (UC) – 140;  $Jra^{SCR}; puc^{E69/+}$  (I) – 182.

We further were curious about the genetic interaction of the WT allele with the SCR allele of *Jra*. For this, we tried to rescue the early lethality caused by  $Jra^{SCR}$  upon infection by overexpressing a WT allele in different tissues. As we see a considerable increase in lifespan of flies post knockdown of *Jra* in the gut, we overexpressed WT allele in the gut. To perform this experiment, we first recombined  $Jra^{SCR}$  with the *NPI-Gal4<sup>ts</sup>*. After confirming

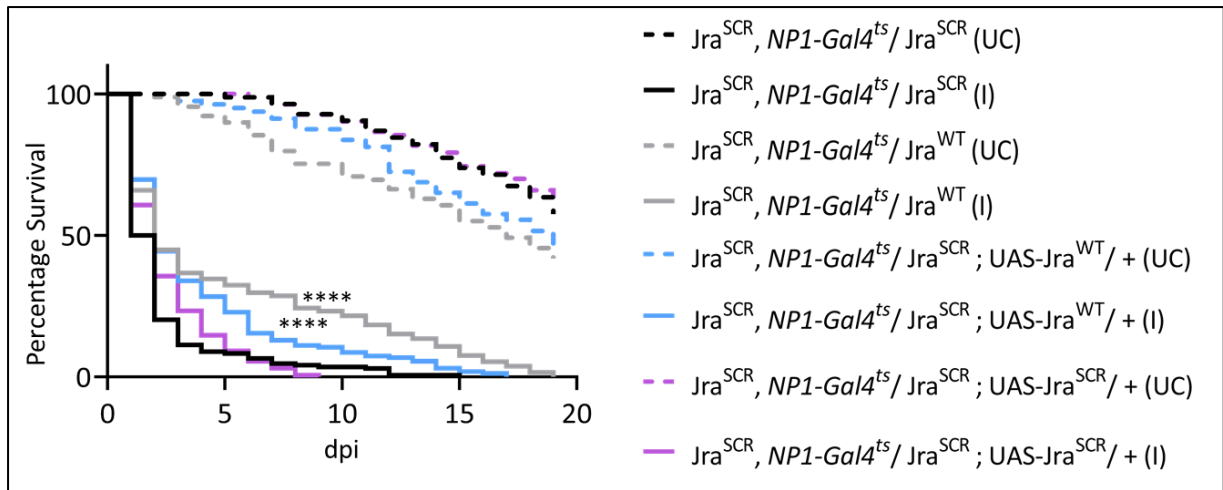


**Figure 4.13: Overexpression of  $Jra^{WT}$  in the gut, shows partial rescue of  $Jra^{SCR}$  phenotype.**

Survival curves of unchallenged (UC, dotted) and orally infected with *Pe* (I, closed), flies:  $Jra^{SCR}, NP1-Gal4^{ts}/Jra^{SCR}$  (black),  $Jra^{SCR}, NP1-Gal4^{ts}/Jra^{WT}$  (grey),  $Jra^{SCR}, NP1-Gal4^{ts}/Jra^{SCR}; UAS-Jra^{WT}/+$  (blue) and  $Jra^{SCR}, NP1-Gal4^{ts}/Jra^{SCR}; UAS-Jra^{SCR}/+$  (purple). Data pooled from three experiments. Log rank test for trend comparing  $Jra^{SCR}, NP1-Gal4^{ts}/Jra^{WT}$  (I),  $Jra^{SCR}, NP1-Gal4^{ts}/Jra^{SCR}; UAS-Jra^{WT}/+$  (I) and  $Jra^{SCR}, NP1-Gal4^{ts}/Jra^{SCR}; UAS-Jra^{SCR}/+$  to  $Jra^{SCR}, NP1-Gal4^{ts}/Jra^{SCR}$  (I); \*\*\*\* $p < 0.0001$ . Number of flies used in the experiment;  $Jra^{SCR}, NP1-Gal4^{ts}/Jra^{SCR}$  (UC) – 84;  $Jra^{SCR}, NP1-Gal4^{ts}/Jra^{SCR}$  (I) – 168;  $Jra^{SCR}, NP1-Gal4^{ts}/Jra^{WT}$  (UC) – 89;  $Jra^{SCR}, NP1-Gal4^{ts}/Jra^{WT}$  (I) – 185;  $Jra^{SCR}, NP1-Gal4^{ts}/Jra^{SCR}; UAS-Jra^{WT}/+$  (UC) – 80;  $Jra^{SCR}, NP1-Gal4^{ts}/Jra^{SCR}; UAS-Jra^{WT}/+$  (I) – 162;  $Jra^{SCR}, NP1-Gal4^{ts}/Jra^{SCR}; UAS-Jra^{SCR}/+$  (UC) – 82;  $Jra^{SCR}, NP1-Gal4^{ts}/Jra^{SCR}; UAS-Jra^{SCR}/+$  (I) – 163.

that both the alleles are properly stabilised on a single chromosome, we crossed the line with appropriate lines to get desired genotypes. We observed that having a single copy of the  $Jra^{WT}$  allele in a heterozygous combination with  $Jra^{SCR}$  is sufficient to rescue the lethality that is seen in homozygous  $Jra^{SCR}$  flies (closed grey line compared to the closed black line, Figure 4.13). A similar trend is observed when we overexpressed  $Jra^{WT}$  in the enterocytes of the midgut in flies homozygous for  $Jra^{SCR}$  (closed blue line compared to the closed black line, Figure 4.13). Though the trend was similar, there was a significant difference in the lifespan of  $Jra^{SCR}, NP1-Gal4^{ts}/Jra^{WT}$  and  $Jra^{SCR}, NP1-Gal4^{ts}/Jra^{SCR}; UAS-Jra^{WT}/+$  (closed blue line compared to the closed grey line, Figure 4.13). We report that overexpression of  $Jra^{WT}$  in the midgut only partially rescues the lethality seen in  $Jra^{SCR}, NP1-Gal4^{ts}/Jra^{SCR}$ . This suggests that the contribution of *Jra* to regulate gut immunity is not entirely from the gut and there could be other organs in the body where *Jra* is active and signalling to regulate the gut immune response. This

should be looked into as there are few studies that demonstrate a cross-talk between organs during an immune challenge. Overexpression of  $Jra^{SCR}$  in homozygous  $Jra^{SCR}$  flies did not show any reduction of survival as one would expect. We think this may be because the system is already saturated by  $Jra^{SCR}$  and adding more  $Jra^{SCR}$  does not have any further effect.

Since rescuing the lethality by overexpressing  $Jra^{WT}$  in the gut has been only partially successful, we hypothesised that overexpressing  $Jra^{WT}$  in a  $Jra$  specific domain should rescue the lethality completely. For this, we used *jra-Gal4*, which has the core promoter of  $Jra$  along with enhancer elements that span ~3kb upstream of the promoter (Pfeiffer et al., 2008) and performed a survival assay. There was a significant increase in the lifespan of flies that had

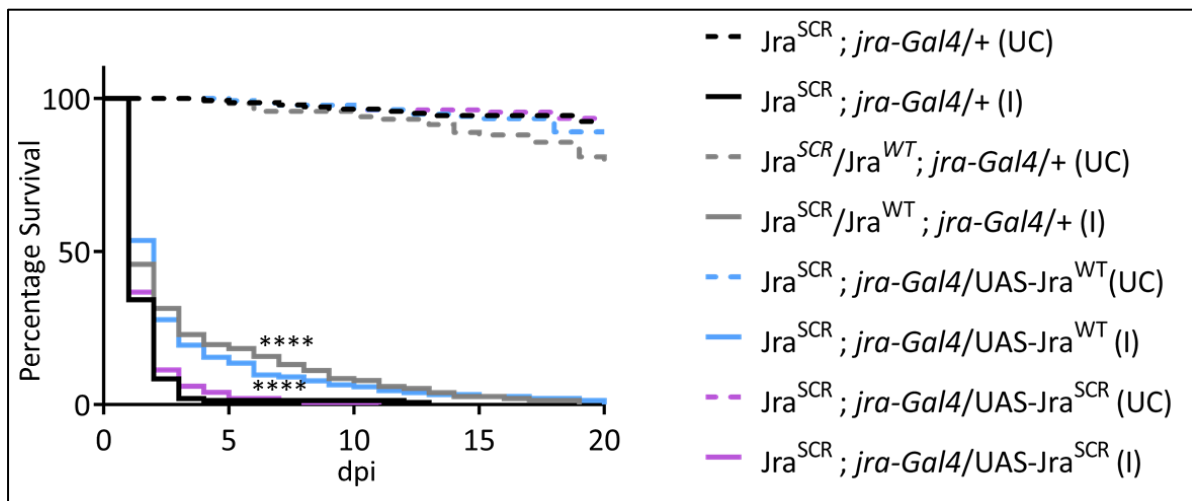


**Figure 4.14: Overexpression of  $Jra^{WT}$  in the  $jra$  expressing domain, shows complete rescue of  $Jra^{SCR}$  phenotype.**

Survival curves of unchallenged (UC, dotted) and orally infected with *Pe* (I, closed), flies:  $Jra^{SCR}; jra-Gal4/+$  (black),  $Jra^{SCR}/Jra^{WT}; jra-Gal4/+$  (grey),  $Jra^{SCR}; jra-Gal4/UAS-Jra^{WT}$  (blue) and  $Jra^{SCR}; jra-Gal4/UAS-Jra^{SCR}$  (purple). Data pooled from three experiments. Log rank test for trend comparing  $Jra^{SCR}/Jra^{WT}; jra-Gal4/+$  (I),  $Jra^{SCR}; jra-Gal4/UAS-Jra^{WT}$  (I) and  $Jra^{SCR}; jra-Gal4/UAS-Jra^{SCR}$  to  $Jra^{SCR}; jra-Gal4/+$  (I); \*\*\*\* $p < 0.0001$ . Number of flies used in the experiment;  $Jra^{SCR}; jra-Gal4/+$  (UC) – 142;  $Jra^{SCR}; jra-Gal4/+$  (I) – 155;  $Jra^{SCR}/Jra^{WT}; jra-Gal4/+$  (UC) – 117;  $Jra^{SCR}/Jra^{WT}; jra-Gal4/+$  (I) – 153;  $Jra^{SCR}; jra-Gal4/UAS-Jra^{WT}$  (UC) – 136;  $Jra^{SCR}; jra-Gal4/UAS-Jra^{WT}$  (I) – 155;  $Jra^{SCR}; jra-Gal4/UAS-Jra^{SCR}$  (UC) – 132;  $Jra^{SCR}; jra-Gal4/UAS-Jra^{SCR}$  (I) – 150.

a single copy of  $Jra^{WT}$  allele in heterozygous combination with  $Jra^{SCR}$  as compared to homozygous  $Jra^{SCR}$  flies (closed grey line compared to the closed black line, Figure 4.14).

Excitingly, and as expected, overexpression of  $Jra^{WT}$  using *jra-Gal4* successfully and

completely rescued the lifespan of  $Jra^{SCR}$  homozygous flies (closed blue line compared to the closed black line, Figure 4.14). This rescue was as good as the rescue observed in  $Jra^{SCR}$  and  $Jra^{WT}$  heterozygous flies (closed blue line compared to the closed grey line, Figure 4.14). This suggests that the expression of *Jra* is tightly regulated and that the contribution of *Jra* in regulating the gut immune response could be coming from other organs besides the gut.

#### ***4.3.4 Jra is a suppressor of defence genes in the gut***

Our data so far suggested that *Jra* is a negative regulator of the gut immune response and a SUMO conjugation resistant mutant of *Jra* is unable to fight off the invading pathogen. SUMOylation of *Jra* could be a crucial and necessary step to attenuate the inhibitory activity of *Jra* on the immune response and fight off infection. To gain better insights into the molecular mechanism by which *Jra* regulates gut immunity, we characterised the transcriptome of the midguts. For this experiment, we knocked down *Jra* specifically in the enterocytes of the midgut using *NPI-Gal4<sup>ts</sup>* and compared the transcriptomes of the midguts with that of the control flies at 4, 12 and 24 hours post-infection (hpi). Before we performed the 3' mRNA sequencing experiment, we first looked at relative levels of *Jra* mRNA using quantitative real-time PCR (qRT-PCR) and mapped the kinetics of activation of *Jra* during the infection. We observed that mRNA levels of *Jra* increase upon infection and peak at 12 hpi in our experimental setup and infection conditions. We identified that in the UC state, the midguts of  $>Jra^{RNAi}$  flies had around 30% of *Jra* mRNA as compared to that of  $>w^{1118}$  flies indicating a considerable knockdown of *Jra*. This was true as the infection progressed and the levels of *Jra* mRNA at 12 and 24 hpi is significantly lower in  $>Jra^{RNAi}$  flies as compared to  $>w^{1118}$  flies (Figure 4.15).

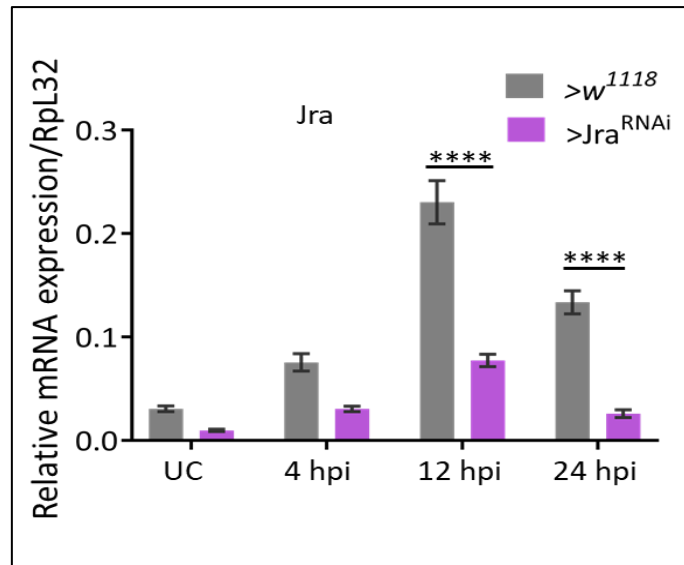


**Figure 4.15: Quantitation showing the kinetics of activation of Jra transcripts in >w<sup>1118</sup> and >Jra<sup>RNAi</sup>**

The bar graph represents relative mRNA levels of Jra as normalised to RpL32 without and with gut infection. >Jra<sup>RNAi</sup> shows a significant reduction of levels of Jra at 12 and 24 hpi. \*\*\*\*: p<0.0001 as determined by 2-way ANOVA with Tukey post-hoc test for multiple comparisons. Data from three independent experiments. Means and SEMs represented.

We then compared the transcriptome of >w<sup>1118</sup> and >Jra<sup>RNAi</sup> at UC condition. We report that 292 genes were significantly differentially expressed. Of these, 168 genes were upregulated and 124 genes were downregulated in >Jra<sup>RNAi</sup> as compared to >w<sup>1118</sup> (Figure 4.16B) and these could be direct transcriptional targets of Jra. We observed several defence genes to be both upregulated and downregulated in >Jra<sup>RNAi</sup>. Interestingly, we identified the gut-specific AMPs like *Drsoymysin-like 2* (*Drsl2*) and *Drsl3* and peptidoglycan recognition proteins *PGRP-SC1a* and *PGRP-SC1b* to be significantly upregulated (FDR<0.1) in >Jra<sup>RNAi</sup> (Table 4.1).

**Table 4.1: Representative list of genes in >Jra<sup>RNAi</sup> as compared to w<sup>1118</sup> at UC condition.**

The left panel in shades of red represents genes that were downregulated and the right panel in green represents genes that were upregulated. Genes previously know to function in regulating immunity are highlighted with an asterisk (\*).

| Downregulated |         | Upregulated |         |
|---------------|---------|-------------|---------|
| Gene Symbol   | log2 FC | Gene Symbol | log2 FC |
| alpha-Est10   | -2.30   | blot        | 1.58    |
| Arpc1         | -2.10   | Drsl2       | 1.36    |
| Bace          | -1.17   | Drsl3       | 2.00    |
| CalpB         | -1.26   | GstD5       | 2.15    |
| cher          | -1.25   | GstD8       | 2.36    |
| daw           | -1.95   | GstD9       | 1.47    |
| Eaat1         | -1.52   | GstE1       | 1.42    |
| lpk2          | -1.08   | hh          | 1.71    |
| Jon25Bii      | -1.56   | LysB        | 2.83    |
| Jra           | -1.22   | LysC        | 1.69    |
| MtnB          | -1.17   | LysD        | 3.58    |
| mwh           | -1.43   | LysE        | 2.96    |
| ninaD         | -1.67   | LysS        | 3.27    |
| Npc2f         | -1.52   | PGRP-SC1a   | 1.67    |
| Rilpl         | -1.22   | PGRP-SC1b   | 1.16    |
| santa-maria   | -1.31   | Ser6        | 1.97    |
| slo           | -1.24   | sordd2      | 1.84    |
| Src42A        | -1.30   | tei         | 3.26    |
| Zip42C.2      | -1.32   | TotC        | 3.00    |

We performed the principal component analysis (PCA) to estimate the robustness of the entire dataset at each time point. We plotted the first two principal components and observed that the data sets were distinct as the infection progressed and were seen as separate clusters (Figure 4.14A). We then looked at differences in the transcriptome in  $>w^{1118}$  and  $>Jra^{RNAi}$  during the infection. We first normalised data from each infection time point to UC of that genotype and have separated the total genes that were significantly differentially expressed (FDR<0.1). We identified a total of 3505 genes to be differentially expressed in all the timepoints together and plotted the total number of upregulated and downregulated genes at each time point of the respective genotype (Figure 4.14C). Further, we compared the log2 fold change (FC) values of significantly differentially expressed genes that were common in both genotypes at a particular time point, (Figure 4.14D) and concentrated our downstream analysis on those genes that were common in both the genotypes. We then performed a gene ontology (GO) analysis on all the 3505 genes that were significantly differentially expressed across the entire dataset and noticed that several key GO terms like metabolic process, response to stress, Toll and Imd signalling pathway were significantly enriched (Figure 4.14E).



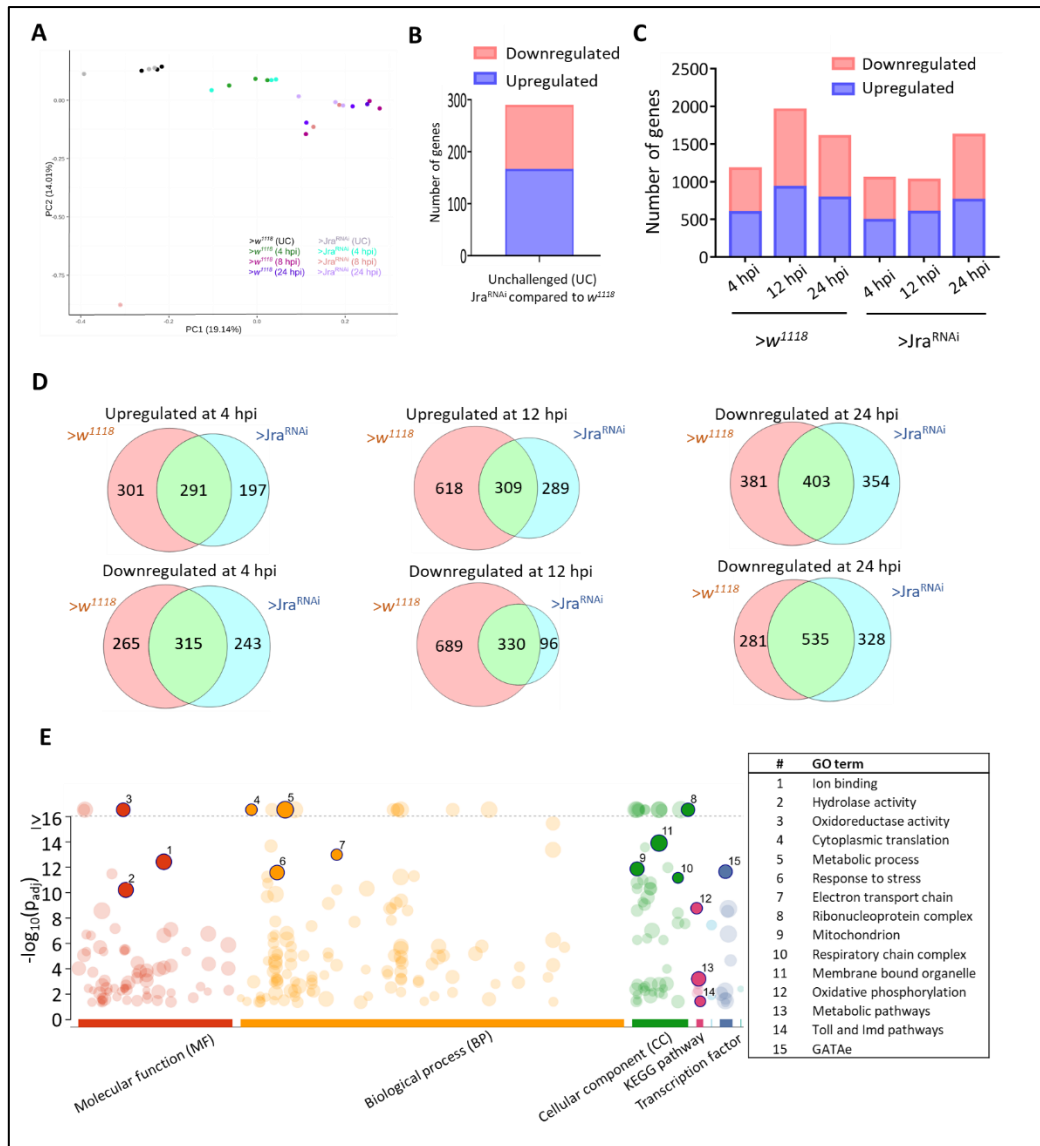


**Figure 4.16: Representation of the data obtained from  $>w^{1118}$  and  $>Jra^{RNAi}$  3' mRNA sequencing experiment**

**A.** Principal component analysis (PCA) plot showing the first two principal components of the entire data set.

**B.** Bar plot representation of the total number of significantly differentially expressed genes (FDR<0.1) obtained by comparing  $>w^{1118}$  and  $>Jra^{RNAi}$  under UC conditions post a 3' mRNA sequencing experiment.

**C.** Bar plot representation of the total number of significantly differentially expressed genes (FDR<0.1) obtained at different hpi after comparing to UC in  $>w^{1118}$  and  $>Jra^{RNAi}$ .

**D.** Venn diagram of significantly differentially expressed genes (FDR<0.1) upregulated and downregulated in  $>w^{1118}$  and  $>Jra^{RNAi}$ . The intersection shown in a shade of green represents genes that are common in  $>w^{1118}$  and  $>Jra^{RNAi}$  and all the analysis was done on those genes.

**E.** Gene ontology (GO) enrichment analysis of all the significantly differentially expressed genes from the entire data set. Some key GO terms are highlighted and described.

Another interesting observation was that several transcription factors were significantly differentially expressed in our data. However, we did not see any particular process or pathway being affected due to the knockdown of Jra in the gut. To establish a better understanding of the underlying molecular mechanism, we investigated the genes with previously known immune-related function. We compared the log<sub>2</sub> FC values between >w<sup>1118</sup> and >Jra<sup>RNAi</sup> across different time points post normalization with UC. We observed that log<sub>2</sub> FC values of several AMPs were higher in >Jra<sup>RNAi</sup> compared to >w<sup>1118</sup> at 4 hpi. Also, we observed several key factors that regulate the classical Imd, Toll, and Jak-STAT pathways to be higher in the guts of >Jra<sup>RNAi</sup> as opposed to >w<sup>1118</sup>. However, we did not observe a significant difference in the transcripts of the Imd pathway transcription factor Relish. Interestingly, the log<sub>2</sub> FC values of several other transcription factors like *Fkh*, *ETS21C*, and *Chinmo*, which have a role in regulating immune response, were higher in >Jra<sup>RNAi</sup> than >w<sup>1118</sup> (

Table 4.2). Together, our data from the transcriptome analysis suggests that loss of Jra in the gut enhances the production of AMPs without an immune challenge. Upon an immune challenge, the kinetics of activation of the AMPs in >Jra<sup>RNAi</sup> is faster than >w<sup>1118</sup> and this could lead to early clearance of bacteria before it could cause damage. Finally, our data suggests that Jra negatively regulates the transcriptional activation of several key immune regulatory genes in the gut post an immune challenge.

**Table 4.2: Representative list of immune-related genes in >w<sup>1118</sup> and >Jra<sup>RNAi</sup> datasets**

Log<sub>2</sub> FC values at different time points post-infection of genes with previously reported immune-related function. Log<sub>2</sub> FC values that are less than -0.58 are shown in shades of green and log<sub>2</sub> FC values that are greater than 0.58 are shown in shades of brown.

| Flybase ID                         | Flybase symbol | Function                       | LFC at 4HPI compared to UC |                      | LFC at 12HPI compared to UC |                      | LFC at 24HPI compared to UC |                      |
|------------------------------------|----------------|--------------------------------|----------------------------|----------------------|-----------------------------|----------------------|-----------------------------|----------------------|
|                                    |                |                                | >w <sup>1118</sup>         | >Jra <sup>RNAi</sup> | >w <sup>1118</sup>          | >Jra <sup>RNAi</sup> | >w <sup>1118</sup>          | >Jra <sup>RNAi</sup> |
| <b>Antimicrobial peptides</b>      |                |                                |                            |                      |                             |                      |                             |                      |
| FBgn0012042                        | AttA           | Antimicrobial peptide          | 0.99                       | 3.03                 | 1.94                        | 0.28                 | 1.91                        | -0.45                |
| FBgn0041581                        | AttB           | Antimicrobial peptide          | 0.78                       | 2.36                 | 1.38                        | -1.07                | 1.09                        | 0.07                 |
| FBgn0041579                        | AttC           | Antimicrobial peptide          | 1.27                       | 2.21                 | 1.81                        | -0.08                | 1.65                        | -1.06                |
| FBgn0038530                        | AttD           | Antimicrobial peptide          | 1.77                       | 0.8                  | 1.55                        | 0                    | 1.11                        | -0.77                |
| FBgn0004240                        | DptA           | Antimicrobial peptide          | 1.68                       | 2.88                 | 2.94                        | 1.83                 | 2.5                         | 1.56                 |
| FBgn0034407                        | DptB           | Antimicrobial peptide          | 1.67                       | 2.59                 | 1.85                        | 0.35                 | 1.61                        | 1.12                 |
| FBgn0000276                        | CecA1          | Antimicrobial peptide          | 1.12                       | 3.61                 | 2.35                        | 1.57                 | 1.68                        | -0.16                |
| FBgn0000277                        | CecA2          | Antimicrobial peptide          | 0.72                       | 2.78                 | 1.38                        | 0.25                 | 1.17                        | -0.4                 |
| FBgn0010388                        | Dro            | Antimicrobial peptide          | 1.06                       | 3.4                  | 3.45                        | 2.65                 | 3.46                        | 1.07                 |
| FBgn0014865                        | Mtk            | Antimicrobial peptide          | 1.53                       | 2.69                 | 2.03                        | 2.06                 | 1.94                        | -0.04                |
| FBgn0283461                        | Drs            | Antimicrobial peptide          | 0.75                       | 0.39                 | 1.33                        | 0.45                 | 2.1                         | -0.08                |
| FBgn0052279                        | DrsI2          | Antimicrobial peptide          | 1.06                       | 0.02                 | 4.17                        | 1.73                 | 3.09                        | 2.07                 |
| FBgn0052283                        | DrsI3          | Antimicrobial peptide          | 1.41                       | 0.31                 | 4.09                        | 2.47                 | 3.51                        | 1.25                 |
| FBgn0052282                        | DrsI4          | Antimicrobial peptide          | 1.18                       | 3.88                 | 5.73                        | 6.82                 | 5.32                        | 4.45                 |
| FBgn0010385                        | Def            | Antimicrobial peptide          | 1.33                       | 1.43                 | 1.68                        | 1.73                 | 2.72                        | 1.55                 |
| <b>Immune regulators</b>           |                |                                |                            |                      |                             |                      |                             |                      |
| FBgn0034068                        |                |                                |                            |                      |                             |                      |                             |                      |
| FBgn0014018                        | Rel            | NF-κB transcription factor     | 1.18                       | 1.08                 | 1.05                        | 1.07                 | 0.3                         | -0.11                |
| FBgn0260632                        | dl             | NF-κB transcription factor     | 0.48                       | 0.57                 | 0.98                        | 1.19                 | 0.8                         | 0.38                 |
| FBgn0041184                        | Socs36E        | Negative regulator of Jak-STAT | 1.26                       | 1.88                 | 2.82                        | 2.86                 | 0.98                        | 0.7                  |
| FBgn0034068                        | Casp           | Inhibitor of Rel activation    | -0.37                      | -0.18                | -0.23                       | -0.5                 | 0.14                        | 0.09                 |
| FBgn0037906                        | PGRP-LB        | Repressor of PGN recognition   | 1.92                       | 1.38                 | -0.47                       | 0.37                 | -0.47                       | 0.37                 |
| FBgn0034647                        | pirk           | Negative regulator of Imd      | 0.97                       | 0.47                 | -2.27                       | -2.6                 | -3.12                       | -2.35                |
| FBgn0000251                        | Cad            | Negative regulator of Imd      | 0.47                       | 0.75                 | 0.8                         | 0.43                 | -0.35                       | 0.09                 |
| <b>JNK pathway components</b>      |                |                                |                            |                      |                             |                      |                             |                      |
| FBgn0001291                        | Jra            | Jun transcription factor       | 0.1                        | -0.12                | 0.96                        | -0.47                | 0.67                        | -0.24                |
| FBgn0243512                        | Puc            | Phosphatase                    | 0.41                       | 0.4                  | 0.94                        | 1.38                 | 0.59                        | 0.44                 |
| FBgn0001297                        | Kay            | Fos transcription factor       | 0.64                       | 0.86                 | 1.52                        | 0.7                  | 0.68                        | 0.38                 |
| FBgn0267339                        | p38c           | MAP kinase                     | 0.85                       | 0.79                 | 1.6                         | 0.19                 | 1.37                        | 1.03                 |
| FBgn0000229                        | bsk            | Jun kinase                     | 0.13                       | -0.02                | 0.36                        | -0.71                | 0.11                        | -0.39                |
| FBgn0035049                        | Mmp1           | Matrix metalloproteinase       | -0.41                      | -0.41                | 0.4                         | 0.89                 | 0.4                         | 0.27                 |
| FBgn0033438                        | Mmp2           | Matrix metalloproteinase       | 0.18                       | -0.03                | 1.1                         | 1.65                 | 0.3                         | 0.23                 |
| <b>Jat-STAT pathway components</b> |                |                                |                            |                      |                             |                      |                             |                      |
| FBgn0016917                        | Stat92E        | STAT transcription factor      | -0.26                      | 0.05                 | 0.2                         | 0.69                 | -0.43                       | -0.16                |
| FBgn0030904                        | upd2           | Ligand                         | 1.68                       | 3.25                 | 3.41                        | 5.48                 | 2.48                        | 3.93                 |
| FBgn0053542                        | upd3           | Ligand                         | 1.57                       | 2.24                 | 3.86                        | 2.84                 | 3.36                        | 2.93                 |
| FBgn0043903                        | dome           | Receptor                       | 0.59                       | 0.57                 | 1.31                        | 1.86                 | 0.39                        | -0.19                |
| FBgn0085358                        | Diedel3        | Ligand                         | -1.21                      | -1.18                | -3.99                       | -2.42                | -3                          | -1.56                |
| <b>Transcriptional regulation</b>  |                |                                |                            |                      |                             |                      |                             |                      |
| FBgn0000659                        | fkh            | Fork head transcription factor | 0.47                       | 0.79                 | 0.83                        | 1.85                 | 0.29                        | 0.14                 |
| FBgn0005660                        | Ets21C         | ETS like transcription factor  | 1.73                       | 2.13                 | 3.2                         | 3.58                 | 2.26                        | 2.11                 |
| FBgn0010762                        | Simj           | Corepressor                    | 0.89                       | 1.72                 | 1.64                        | 2.73                 | 1.82                        | 2.59                 |
| FBgn0030400                        | Pits           | Corepressor                    | 0.85                       | 1.09                 | 1.39                        | 3.09                 | 1.05                        | 1.39                 |
| FBgn0001168                        | h              | Transcriptional repressor      | 2.39                       | 2.5                  | 1.84                        | 2.76                 | 1.12                        | 0.78                 |
| FBgn0024491                        | Bin1           | Corepressor                    | 0                          | 1.61                 | 1.3                         | 3.85                 | 2.4                         | 3.98                 |
| FBgn0003415                        | Skuld          | Transcriptional coregulator    | 0.42                       | 0.5                  | 1.01                        | 2.32                 | 0.68                        | 0.8                  |
| FBgn0086758                        | Chinmo         | transcription factor           | 1.82                       | 2.25                 | 3.26                        | 4.29                 | 3.24                        | 3.61                 |

#### 4.3.5 *Jra<sup>SCR</sup>* is a stronger suppressor of defence genes in the gut

We demonstrated that *Jra* transcriptionally suppresses a subset of key immune effector genes in the gut of *Drosophila* during infection. Reducing the function of *Jra* using gut-specific

knockdown removes the suppression and enhances the transcription of several immune effectors either directly or indirectly and helps the animal fight off infection better. We hypothesised that  $Jra^{SCR}$  being a hypermorph of  $Jra$ , would suppress the expression of immune effectors further and attenuate the immune response. We addressed this by performing another 3' mRNA sequencing on the guts isolated from  $Jra^{WT}$  and  $Jra^{SCR}$  post an immune challenge with *Pe*. We first looked at the levels of  $Jra$  in both the genotypes without infection and as infection progressed. We did not find any difference in the levels of  $Jra$  transcripts in  $Jra^{SCR}$  when compared to  $Jra^{WT}$  (

Figure 4.17). We then compared the transcriptome of  $Jra^{WT}$  and  $Jra^{SCR}$  without any immune challenge. We report that there were only 96 genes that were significantly differentially expressed ( $FDR < 0.1$ ) in  $Jra^{SCR}$  as compared to  $Jra^{WT}$  (Figure 4.18B) suggesting that the gut transcriptome of  $Jra^{SCR}$  is similar to  $Jra^{WT}$  when there is no external stress. We then looked at the changes in the expression of genes post an infection. We isolated guts at 4 hpi and 12 hpi and compared the differentially expressed genes in  $Jra^{WT}$  and  $Jra^{SCR}$  post normalization with UC. We could not isolate guts at 24 hpi as there were at least 30-40% deaths in  $Jra^{SCR}$ .

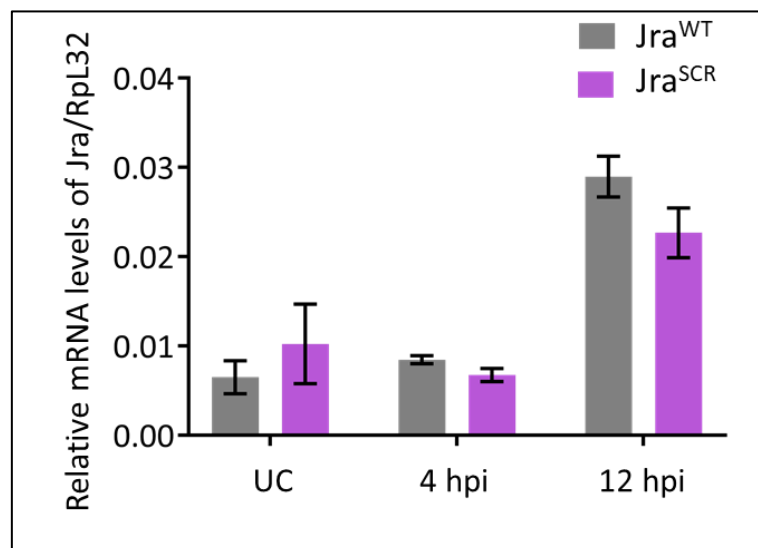


**Figure 4.17: Quantitation showing the kinetics of activation of  $Jra$  transcripts in  $Jra^{SCR}$  and  $Jra^{WT}$  during infection.**

The bar graph represents relative mRNA levels of Jra as normalised to RpL32 without and with gut infection. Jra<sup>SCR</sup> shows no significant difference in levels of Jra at 4 and 12 hpi. 2-way ANOVA with Tukey post-hoc test for multiple comparisons. Data from three independent experiments. Means and SEMs represented.

We performed PCA and plotted PC1 and PC2. We observed that the data set from Jra<sup>SCR</sup> and Jra<sup>WT</sup> very similar without infection and separated as distinct clusters as infection progressed (Figure 4.18A). We then looked at differences in the transcriptome in Jra<sup>WT</sup> and

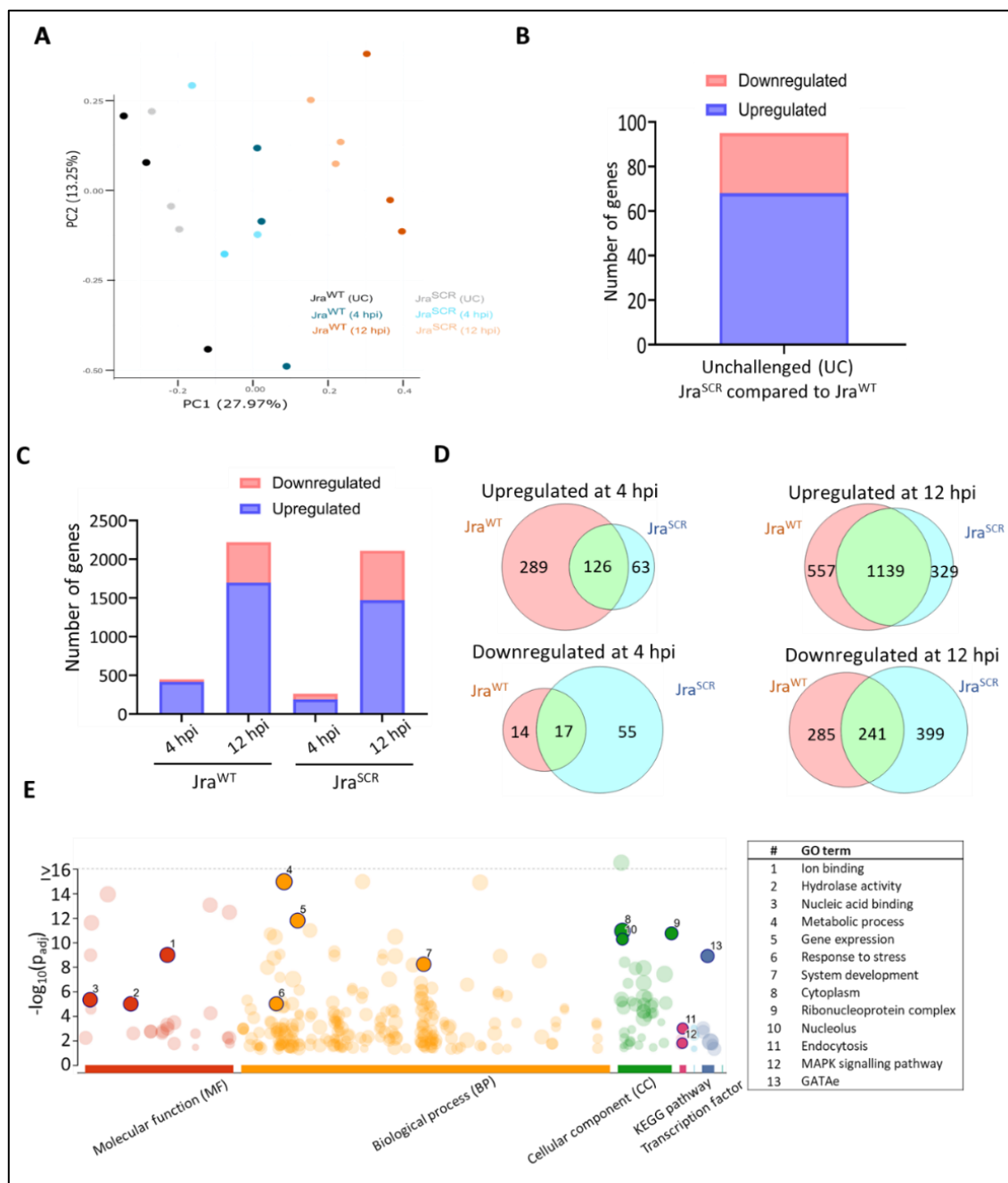


**Figure 4.18: Representation of the data obtained from Jra<sup>WT</sup> and Jra<sup>SCR</sup> 3' mRNA sequencing experiment**

- A.** Principal component analysis (PCA) plot showing the first two principal components of the entire data set.
- B.** Bar plot representation of the total number of significantly differentially expressed genes (FDR<0.1) obtained by comparing Jra<sup>WT</sup> and Jra<sup>SCR</sup> under UC conditions post a 3' mRNA sequencing experiment.
- C.** Bar plot representation of the total number of significantly differentially expressed genes (FDR<0.1) obtained at different hpi after comparing to UC in Jra<sup>WT</sup> and Jra<sup>SCR</sup>.
- D.** Venn diagram of significantly differentially expressed genes (FDR<0.1) upregulated and downregulated in Jra<sup>WT</sup> and Jra<sup>SCR</sup>. The union shown in a shade of green represent genes that are common in Jra<sup>WT</sup> and Jra<sup>SCR</sup>.
- E.** Gene ontology (GO) enrichment analysis of all the significantly differentially expressed genes from the entire data set. Some key GO terms are highlighted and described.

Jra<sup>SCR</sup> during the infection. For this, we used a similar strategy that was used in the previous 3' mRNA sequencing experiment. We identified a total of 3134 genes to be differentially expressed in all the timepoints put together and plotted the total number of upregulated and downregulated genes at each time point of the respective genotype (Figure 4.18 and Figure 4.14C). Further, we compared the log<sub>2</sub> FC values of significantly differentially expressed genes that were common in both genotypes at a particular time point (Figure 4.18D) and concentrated our downstream analysis on those genes that were common in both the genotypes. We then performed a gene ontology (GO) analysis on all the 3134 genes that were significantly differentially expressed across the entire dataset and noticed that several key GO terms metabolic process, gene expression, response to stress and, MAPK signalling pathway were significantly enriched. We then looked at the same set of genes (Table 4.2) that had a known immune-related function in *Drosophila*. In a specific subset of genes, we observed a trend that was opposite to that of the trend observed in the >Jra<sup>RNAi</sup> dataset. The log<sub>2</sub> FC values of a few AMPs (AttB, AttD, Drsl2, and Drsl3) were lower in Jra<sup>SCR</sup> as compared to that of Jra<sup>WT</sup>. The lower levels of AMPs could be one of the reasons for Jra<sup>SCR</sup> to succumb early upon infection. Also, we observed that several key factors that regulate the classical Imd, Toll, and Jak-STAT

pathways to be lower in the guts of Jra<sup>SCR</sup> as opposed to Jra<sup>WT</sup>. Surprisingly, we observed a significant decrease in the transcripts of the NFkB factor relish in Jra<sup>SCR</sup> as compared to Jra<sup>WT</sup>. This could be a possible mechanism by which Jra regulates the levels of AMPs. Also, the log2 FC values of several other transcription factors like Fkh, ETS21C, and Chinmo which have a role in regulating immune response were lower in Jra<sup>SCR</sup> than Jra<sup>WT</sup> (Table 4.3). Together, our data from the transcriptome analysis suggests that Jra<sup>SCR</sup> suppresses the production of AMPs during infection and this could lead to the persistence of bacteria in the gut and cause severe damage to the gut wall and colonize other tissues. Our data so far from both the datasets revealed that Jra<sup>RNAi</sup> and Jra<sup>SCR</sup> show opposite expression trends in a subset of immune effectors. We observed that modulating the activity of Jra affects the activation of several key immune effectors and in particular AMPs. Two possible mechanisms explain this phenomenon: Jra could regulate the transcription of AMPs by directly binding to their promoters or Jra could regulate transcription of one or more transcription factors that in turn regulate the activation of AMPs. This can be validated by performing Jra specific Chromatin immunoprecipitation (ChIP) assay followed by sequencing the chromatin. We identified a consortium called model organism Encyclopedia of Regulatory Networks (modERN) that catalogued the regulatory site of 217 transcription factors in *Drosophila* (Kudron et al., 2018). We found Jra as one of the transcription factors for which a ChIP-seq dataset was available from the whole wandering 3<sup>rd</sup> instar larvae of *Drosophila*. We downloaded Jra specific ChIP-seq files from the modern web interface (<https://epic.gs.washington.edu/modERN/>) and used the input normalised files to generate a heatmap showing the occupancy of Jra on the promoters of all the significantly differentially expressed genes from both the 3' mRNA sequencing data sets. We have only chosen data from 4 and 12 hpi for the analysis and the total number of genes were 4376. The occupancy of Jra was visualised on the CDS along with 2kb upstream the TSS and 2kb downstream the TES (Figure 4.19). We identified two distinct clusters; one with highly

enriched occupancy of Jra on the promoters (Cluster\_1), and the other with moderately enriched occupancy of Jra on the promoters (Cluster\_2).

**Table 4.3: Representative list of immune-related genes in Jra<sup>WT</sup> and Jra<sup>SCR</sup> datasets**

Log2 FC values at different time points post-infection of genes with previously reported immune-related function. Log2 FC values that are less than -0.58 are shown in shades of green and log2 FC values that are greater than 0.58 are shown in shades of brown.

| Flybase ID                         | Flybase symbol | Function                       | LFC at 4HPI compared to UC |                    | LFC at 12HPI compared to UC |                    |
|------------------------------------|----------------|--------------------------------|----------------------------|--------------------|-----------------------------|--------------------|
|                                    |                |                                | Jra <sup>WT</sup>          | Jra <sup>SCR</sup> | Jra <sup>WT</sup>           | Jra <sup>SCR</sup> |
| <b>Antimicrobial peptides</b>      |                |                                |                            |                    |                             |                    |
| FBgn0012042                        | AttA           | Antimicrobial peptide          | 0.43                       | 0.31               | 0.53                        | 0.21               |
| FBgn0041581                        | AttB           | Antimicrobial peptide          | 0.54                       | 0.36               | 0.7                         | 0.19               |
| FBgn0041579                        | AttC           | Antimicrobial peptide          | -0.25                      | 0.49               | -0.21                       | 0.72               |
| FBgn0038530                        | AttD           | Antimicrobial peptide          | 1.1                        | 0.28               | 3.7                         | 0.7                |
| FBgn0004240                        | DptA           | Antimicrobial peptide          | -0.02                      | -0.07              | 0.61                        | -0.07              |
| FBgn0034407                        | DptB           | Antimicrobial peptide          | 0.07                       | -0.09              | 0.42                        | 0.04               |
| FBgn0000276                        | CecA1          | Antimicrobial peptide          | 0.15                       | 0.04               | -0.05                       | -0.29              |
| FBgn0000277                        | CecA2          | Antimicrobial peptide          | 0.71                       | -0.01              | 0.81                        | -0.11              |
| FBgn0010388                        | Dro            | Antimicrobial peptide          | -0.19                      | 0.03               | 0.34                        | 0.29               |
| FBgn0014865                        | Mtk            | Antimicrobial peptide          | 0.09                       | 0.05               | 0.68                        | 0.37               |
| FBgn0283461                        | Drs            | Antimicrobial peptide          | 0.16                       | 0                  | 0.02                        | 0                  |
| FBgn0052279                        | Drsl2          | Antimicrobial peptide          | 0.35                       | 0.13               | 3.33                        | 0.31               |
| FBgn0052283                        | Drsl3          | Antimicrobial peptide          | 1.13                       | 0.15               | 6.7                         | 3.18               |
| FBgn0052282                        | Drsl4          | Antimicrobial peptide          | -0.29                      | -0.03              | -0.13                       | -0.08              |
| FBgn0010385                        | Def            | Antimicrobial peptide          | 0.13                       | 0.2                | 1.2                         | 0.13               |
| <b>Immune regulators</b>           |                |                                |                            |                    |                             |                    |
| FBgn0014018                        | Rel            | NF-κB transcription factor     | 2.05                       | 0.71               | 2.21                        | 1.01               |
| FBgn0260632                        | dl             | NF-κB transcription factor     | 0.83                       | 0.45               | 2.38                        | 1.68               |
| FBgn0041184                        | Socs36E        | Negative regulator of Jak-STAT | 2.05                       | 1.11               | 4.11                        | 3.14               |
| FBgn0034068                        | Casp           | Inhibitor of Rel activation    | -0.16                      | -0.17              | -0.18                       | 0                  |
| FBgn0037906                        | PGRP-LB        | Repressor of PGN recognition   | 2.24                       | 1.24               | 1.04                        | 0.58               |
| FBgn0034647                        | pirk           | Negative regulator of Imd      | 2.68                       | 2.72               | -0.21                       | 0.6                |
| FBgn0000251                        | Cad            | Negative regulator of Imd      | 0.1                        | -0.03              | 0.57                        | 0.11               |
| <b>JNK pathway components</b>      |                |                                |                            |                    |                             |                    |
| FBgn0001291                        | Jra            | Jun transcription factor       | 0.67                       | 0.06               | 2.02                        | 1.19               |
| FBgn0243512                        | Puc            | Phosphatase                    | 0.58                       | 0.49               | 1.09                        | 1.01               |
| FBgn0001297                        | Kay            | Fos transcription factor       | 0.73                       | 0.28               | 1.88                        | 1.06               |
| FBgn0267339                        | p38c           | MAP kinase                     | 1.27                       | 0.23               | 2.37                        | 1.2                |
| FBgn0000229                        | bsk            | Jun kinase                     | 0.29                       | -0.07              | 0.33                        | 0.01               |
| FBgn0035049                        | Mmp1           | Matrix metalloproteinase       | 0.7                        | 0.36               | 1.48                        | 0.9                |
| FBgn0033438                        | Mmp2           | Matrix metalloproteinase       | 0.67                       | 0.06               | 1.56                        | 0.75               |
| <b>Jat-STAT pathway components</b> |                |                                |                            |                    |                             |                    |
| FBgn0016917                        | Stat92E        | STAT transcription factor      | 0.17                       | 0                  | 0.7                         | 0.17               |
| FBgn0030904                        | upd2           | Ligand                         | 0.56                       | 0                  | 1.85                        | 5.16               |
| FBgn0053542                        | upd3           | Ligand                         | 2.18                       | 0                  | 5.07                        | 3.72               |
| FBgn0043903                        | dome           | Receptor                       | 0.85                       | 0.31               | 2.21                        | 1.37               |
| FBgn0085358                        | Diedel3        | Ligand                         | -0.44                      | -0.4               | -1.8                        | -0.71              |
| <b>Transcriptional regulation</b>  |                |                                |                            |                    |                             |                    |
| FBgn0000659                        | fkh            | Fork head transcription factor | 0.45                       | 0.16               | 1.44                        | 0.9                |
| FBgn0005660                        | Ets21C         | ETS like transcription factor  | 2.95                       | 1.8                | 5.33                        | 4                  |
| FBgn0010762                        | Simj           | Corepressor                    | 0.52                       | 0.09               | 1.07                        | 0.6                |
| FBgn0030400                        | Pits           | Corepressor                    | 0.4                        | 0.3                | 1.08                        | 0.74               |
| FBgn0001168                        | h              | Transcriptional repressor      | 2.19                       | 1.17               | 2.28                        | 1.62               |
| FBgn0024491                        | Bin1           | Corepressor                    | 0.72                       | 0.2                | 4.07                        | 3.3                |
| FBgn0003415                        | Skuld          | Transcriptional coregulator    | 0.34                       | 0.31               | 1.2                         | 0.63               |
| FBgn0086758                        | Chinmo         | transcription factor           | 0.42                       | 0.08               | 1.79                        | 0.91               |

Peak occupancy of Jra on the gene bodies of the significantly differentially expressed genes from both the 3' mRNA sequencing experiments in this study. Cluster\_1 represents the



significantly enriched ( $p,0.05$ ) occupancy of Jra on the promoters of a set of genes. Cluster\_2 represents all the other genes not found in cluster\_1 and do not show significant occupancy of Jra on the promoters. Heatmap plotted by using Deeptools V3.5.0. 2 kb upstream of transcription start site (TSS) and 2kb downstream of transcription end site (TES) represented. We identified that there were a total of 1042 genes with enriched occupancy of Jra on their promoters in cluster\_1. Surprisingly, we did not identify any AMPs to be present in the Cluster\_1 indicating that Jra might be indirectly regulating the transcription of the APMs by transcriptionally regulating one or more immune effectors. We further looked at the log2 FC values in all the datasets at 12 hpi. We identified 111 genes to have significant log2 FC values with an FDR < 0.1 at 12 hpi. We then explored these 111 genes and looked specifically at those genes that had differences in expression patterns in both the datasets at 12 hpi. For this, we compared the log2 FC ratio of  $>Jra^{RNAi}$  and  $>w^{1118}$  to  $Jra^{SCR}$  and  $Jra^{WT}$  and identified that 60 genes showed opposite expression trends. These 60 genes are bonafide transcriptional targets of Jra and show opposite expression patterns in  $Jra^{SCR}$  and  $Jra^{RNAi}$ . We observed that most of these genes are negatively regulated by Jra, since loss of Jra increased the activation of these genes. Also, we report that a large proportion of these genes were either transcription factors or genes involved in transcriptional regulation. Interestingly, we identified the NFkB transcription factors *relish (Rel)* and *dorsal (dl)* in our list of 60 genes. The immunity response in *Drosophila* is majorly driven by the Imd-Rel and Toll-dl pathway. In addition to this, we identified the factors, *forkhead (fkh)*, *hairy (h)*, *daughterless (da)*, and *Ets21C*, which have a known role in maintaining gut homeostasis to be negatively regulated by Jra (Table 4.4). We are currently performing experiments to see the effect of gut-specific knockdown of a few genes from our list to identify their role in regulating the gut immune response. Our data suggest that Jra transcriptionally regulates key immune effectors in the gut during infection. Finally, we propose that Jra could be a global negative regulator of gut

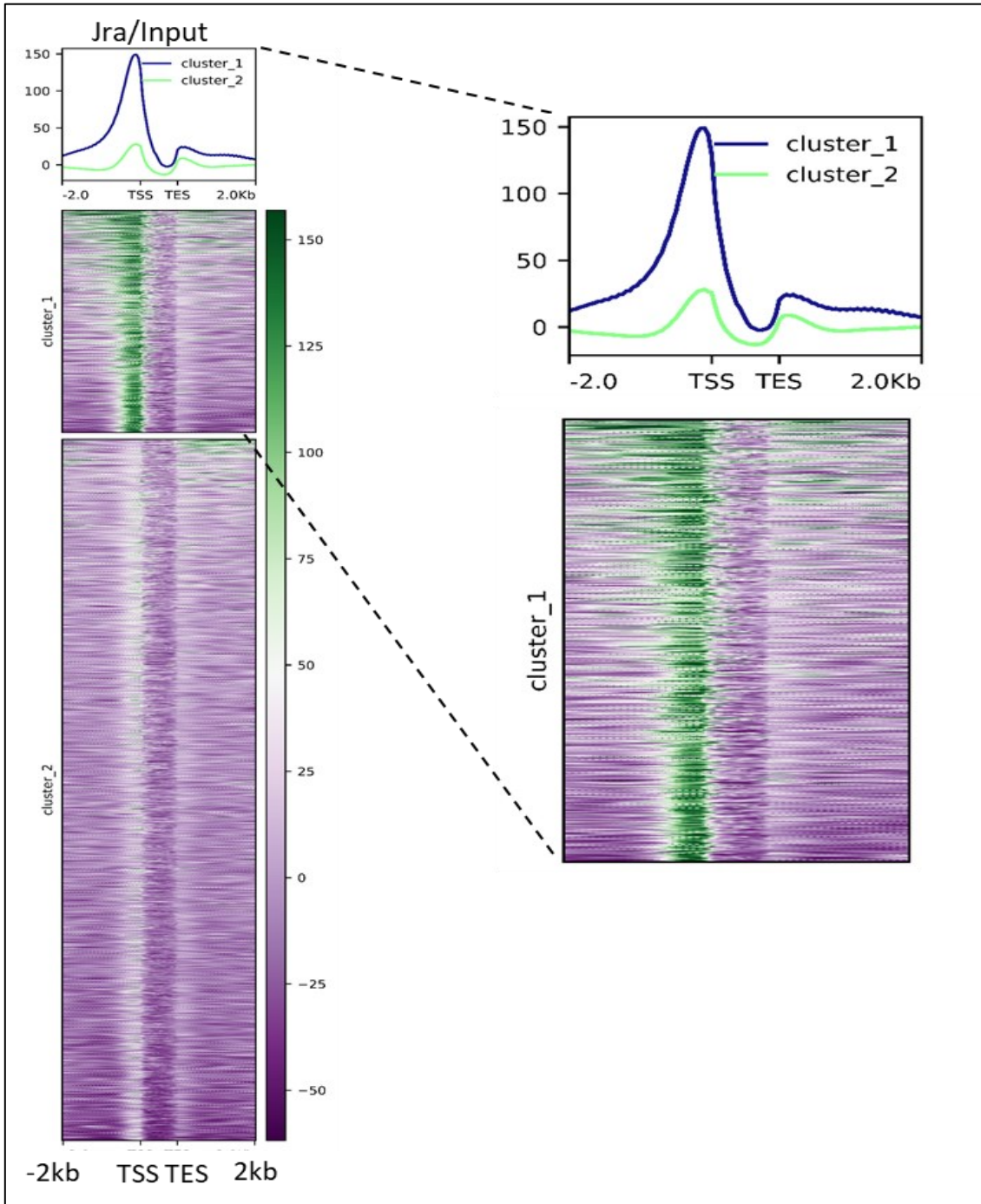


**Figure 4.19: Occupancy of Jra on the gene body of significantly differentially expressed genes**

Peak occupancy of Jra on the gene bodies of the significantly differentially expressed genes from both the 3' mRNA sequencing experiments in this study. Cluster\_1 represents the significantly enriched ( $p,0.05$ ) occupancy of Jra on the promoters of a set of genes. Cluster\_2 represents all the other genes not found in cluster\_1 and do not show significant occupancy of Jra on the promoters. Heatmap plotted by using DeepTools V3.5.0. 2 kb upstream of transcription start site (TSS) and 2kb downstream of transcription end site (TES) represented.

immunity and SUMO conjugation of Jra is a necessary step to attenuate the negative regulation of Jra during an immune challenge and evoke a robust defence response to fight off the infection.

**Table 4.4: List of bonafide Jra targets that show opposite expression patterns**

Log2 FC values of the significantly differentially expressed genes that are bonafide transcriptional targets of Jra and show opposite expression patterns at 12 hpi. Opposite expression patterns formulated by comparing the log2 FC ratios of >Jra<sup>RNAi</sup> and >w<sup>1118</sup> to Jra<sup>SCR</sup> and Jra<sup>WT</sup>.

| Flybase ID  | Flybase symbol | log2 FC at 12 hpi compared to UC |                      |                   |                    | log2 FC ratio                             |  |
|-------------|----------------|----------------------------------|----------------------|-------------------|--------------------|---|--|
|             |                | >w <sup>1118</sup>               | >Jra <sup>RNAi</sup> | Jra <sup>WT</sup> | Jra <sup>SCR</sup> | >Jra <sup>RNAi</sup> / >w <sup>1118</sup> | Jra <sup>SCR</sup> / Jra <sup>WT</sup> |
| FBgn0030400 | Pits           | 1.39                             | 3.09                 | 1.08              | 0.73               | 1.70                                      | -0.35                                  |
| FBgn0050055 | lncRNA:CR30055 | 1.92                             | 3.53                 | 1.89              | 1.14               | 1.61                                      | -0.75                                  |
| FBgn0052636 | lncRNA:CR32636 | 2.08                             | 3.45                 | 1.66              | 0.93               | 1.37                                      | -0.73                                  |
| FBgn0003415 | skd            | 1.02                             | 2.33                 | 1.21              | 0.61               | 1.31                                      | -0.60                                  |
| FBgn0001104 | Galphai        | 1.01                             | 2.10                 | 1.92              | 1.21               | 1.10                                      | -0.70                                  |
| FBgn0010762 | simj           | 1.65                             | 2.74                 | 1.07              | 0.50               | 1.09                                      | -0.57                                  |
| FBgn0030847 | CG12991        | 1.25                             | 2.30                 | 1.55              | 1.03               | 1.05                                      | -0.52                                  |
| FBgn0086758 | chinmo         | 3.26                             | 4.30                 | 1.80              | 1.03               | 1.04                                      | -0.77                                  |
| FBgn0000659 | fkf            | 0.83                             | 1.85                 | 1.45              | 0.93               | 1.02                                      | -0.51                                  |
| FBgn0004656 | fs(1)h         | 0.47                             | 1.48                 | 0.78              | 0.47               | 1.01                                      | -0.31                                  |
| FBgn0032587 | CG5953         | 0.76                             | 1.74                 | 1.85              | 1.21               | 0.98                                      | -0.64                                  |
| FBgn0013343 | Syx1A          | 0.80                             | 1.73                 | 1.03              | 0.76               | 0.94                                      | -0.27                                  |
| FBgn0001168 | h              | 1.84                             | 2.76                 | 2.29              | 1.69               | 0.92                                      | -0.59                                  |
| FBgn0038829 | CG17271        | -2.32                            | -1.41                | -0.55             | -0.57              | 0.91                                      | -0.02                                  |
| FBgn0028953 | CG14478        | 0.69                             | 1.58                 | 0.96              | 0.65               | 0.89                                      | -0.31                                  |
| FBgn0033188 | Drat           | 1.00                             | 1.89                 | 2.32              | 1.11               | 0.89                                      | -1.21                                  |
| FBgn0261556 | CG42674        | 0.75                             | 1.62                 | 1.33              | 1.16               | 0.87                                      | -0.17                                  |
| FBgn0052758 | Snx27          | 1.56                             | 2.41                 | 1.74              | 1.34               | 0.85                                      | -0.40                                  |
| FBgn0267821 | da             | 0.81                             | 1.66                 | 1.23              | 0.67               | 0.85                                      | -0.56                                  |
| FBgn0043364 | cbt            | 2.20                             | 2.94                 | 1.84              | 1.00               | 0.74                                      | -0.84                                  |
| FBgn0031474 | CG2991         | 1.56                             | 2.28                 | 2.42              | 1.61               | 0.71                                      | -0.81                                  |
| FBgn0052296 | Mrtf           | 1.04                             | 1.71                 | 1.54              | 1.02               | 0.67                                      | -0.52                                  |
| FBgn0035997 | phol           | 1.26                             | 1.93                 | 1.22              | 0.55               | 0.67                                      | -0.67                                  |
| FBgn0005771 | noc            | 1.53                             | 2.19                 | 0.91              | 0.74               | 0.67                                      | -0.18                                  |
| FBgn0261988 | Gprk2          | 1.06                             | 1.71                 | 1.36              | 0.71               | 0.65                                      | -0.64                                  |
| FBgn0039644 | rdog           | 1.85                             | 2.47                 | 2.23              | 1.19               | 0.62                                      | -1.04                                  |
| FBgn0003676 | CCT1           | 1.03                             | 1.61                 | 1.10              | 0.66               | 0.58                                      | -0.44                                  |
| FBgn0033356 | CG8229         | 1.19                             | 1.76                 | 0.98              | 0.46               | 0.57                                      | -0.52                                  |
| FBgn0023167 | SmD3           | 0.85                             | 1.41                 | 1.00              | 0.66               | 0.55                                      | -0.33                                  |
| FBgn0033438 | Mmp2           | 1.11                             | 1.66                 | 1.57              | 0.68               | 0.55                                      | -0.89                                  |
| FBgn0042185 | MCU            | 2.68                             | 3.22                 | 2.10              | 1.55               | 0.54                                      | -0.55                                  |
| FBgn0031090 | Rab35          | 1.15                             | 1.69                 | 1.10              | 0.71               | 0.54                                      | -0.39                                  |
| FBgn0031661 | Gmd            | 0.96                             | 1.50                 | 1.72              | 1.14               | 0.54                                      | -0.58                                  |
| FBgn0260962 | pic            | 1.03                             | 1.55                 | 1.33              | 1.10               | 0.52                                      | -0.23                                  |
| FBgn0263993 | CG43736        | 1.05                             | 1.56                 | 1.80              | 1.21               | 0.51                                      | -0.59                                  |
| FBgn0015019 | CCT3           | 0.84                             | 1.34                 | 0.98              | 0.48               | 0.50                                      | -0.50                                  |
| FBgn0035266 | Gk2            | 1.51                             | 2.01                 | 1.06              | 0.62               | 0.49                                      | -0.44                                  |
| FBgn0267923 | lncRNA:CR46204 | 5.60                             | 6.04                 | 6.60              | 4.62               | 0.44                                      | -1.98                                  |
| FBgn0243512 | puc            | 0.95                             | 1.38                 | 1.10              | 1.09               | 0.44                                      | -0.01                                  |
| FBgn0250869 | CG42240        | 4.34                             | 4.76                 | 3.60              | 2.18               | 0.42                                      | -1.42                                  |
| FBgn0036732 | Oatp74D        | 1.71                             | 2.13                 | 2.11              | 1.48               | 0.42                                      | -0.63                                  |
| FBgn0262524 | ver            | 2.18                             | 2.57                 | 2.67              | 1.68               | 0.40                                      | -0.99                                  |
| FBgn0040212 | Dhap-at        | 1.15                             | 1.55                 | 1.64              | 1.34               | 0.39                                      | -0.30                                  |
| FBgn0261862 | whd            | -1.95                            | -1.57                | -0.72             | -1.06              | 0.38                                      | -0.34                                  |
| FBgn0005660 | Ets21C         | 3.20                             | 3.58                 | 5.33              | 4.28               | 0.38                                      | -1.06                                  |
| FBgn0044324 | Chro           | 1.54                             | 1.89                 | 0.90              | 0.57               | 0.35                                      | -0.33                                  |
| FBgn0265623 | Su(z)2         | 1.98                             | 2.32                 | 1.22              | 0.98               | 0.34                                      | -0.24                                  |
| FBgn0031114 | cactin         | 1.34                             | 1.66                 | 1.63              | 0.85               | 0.32                                      | -0.79                                  |
| FBgn0036844 | Mkp3           | 1.23                             | 1.50                 | 1.48              | 1.02               | 0.28                                      | -0.46                                  |
| FBgn0039831 | CG12054        | 1.08                             | 1.32                 | 1.02              | 0.73               | 0.24                                      | -0.29                                  |
| FBgn0260632 | dl             | 0.99                             | 1.20                 | 2.39              | 1.77               | 0.21                                      | -0.61                                  |
| FBgn0014018 | Rel            | 1.05                             | 1.08                 | 2.21              | 1.12               | 0.03                                      | -1.09                                  |
| FBgn0036213 | RpL10Ab        | -1.47                            | -1.48                | -0.73             | -0.49              | -0.01                                     | 0.24                                   |
| FBgn0260462 | CtsF           | -1.95                            | -2.01                | -0.89             | -0.58              | -0.06                                     | 0.31                                   |
| FBgn0010412 | RpS19a         | -1.36                            | -1.42                | -0.66             | -0.43              | -0.06                                     | 0.22                                   |
| FBgn0261592 | RpS6           | -1.52                            | -1.60                | -0.68             | -0.43              | -0.08                                     | 0.25                                   |
| FBgn0010265 | RpS13          | -1.40                            | -1.48                | -0.63             | -0.45              | -0.08                                     | 0.18                                   |
| FBgn0003942 | RpS27A         | -1.31                            | -1.46                | -0.58             | -0.42              | -0.14                                     | 0.16                                   |
| FBgn0013981 | His4r          | -1.43                            | -1.79                | -0.75             | -0.57              | -0.37                                     | 0.18                                   |
| FBgn0260972 | alc            | -1.58                            | -2.16                | -0.74             | -0.46              | -0.58                                     | 0.28                                   |
| FBgn0062412 | CtrlB          | -1.97                            | -2.71                | -1.06             | -0.79              | -0.75                                     | 0.27                                   |

#### 4.4 Summary

Previous work (Kim et al., 2007; Kim et al., 2005) shows that components of the JNK signalling pathway negatively regulate the systemic immune response in *Drosophila* but the role of the JNK signalling pathway during an immune response in the gut has not been well understood. Here we have used specific knockdowns followed by infection with a gram-negative pathogen *Pseudomonas entomophila* and identified that the transcription factor Jun-related antigen (Jra) acts as a suppressor of the gut immune response. This was observed as an increase in the lifespan of the flies with reduced levels of Jra in the gut post-infection (Figure 4.2). We have observed a similar phenotype with an enhanced lifespan in flies that are hypomorphic to Jra post-infection (Figure 4.3). This data has led us to establish Jra as a negative regulator of gut immunity in *Drosophila*, a previously unknown role. We have observed that knocking down basket (Bsk), in the gut also yields a phenotype that was similar to the knockdown of Jra in the gut (Figure 4.4). Interestingly, we did not observe a significant increase in lifespan when we have abrogated the function of the Kayak (Kay) (Figure 4.5). This helped us understand that Jra was acting downstream of the JNK signalling pathway and was predominantly responsible for negatively regulating the gut immune response. The role of post-translational modifications like SUMOylation in regulating the immune response during a bacterial or viral infection is evident from the increasing number of studies in higher organisms in recent years (Everett et al., 2013; Hannoun et al., 2016; Srikanth and Verma, 2017; Verma et al., 2018; Wilson, 2017; Wimmer et al., 2012). However, there is no evidence on how SUMOylation regulates gut immunity in *Drosophila*. To shed light on this, we have knocked down all the SUMO machinery components in the gut and orally infected the flies. We have observed that all the components showed a similar trend of enhanced survival of the flies upon knockdown (Figure 4.8). This indicated that all the members of SUMO conjugation machinery were acting to suppress the immune response in *Drosophila*. This is an exciting finding and should be

explored further to uncover the molecular mechanism of global SUMOylation in regulating the immune response. Once we understood that all the member of SUMO cycle had a role in the regulation of gut immunity, we focused on how the SUMO conjugation of Jra regulates the outcome post an infection. For this, we have used the CRSIPR/Cas9 edited genomic mutant of Jra that was resistant to SUMO conjugation (Jra<sup>SCR</sup>). We have observed that Jra<sup>SCR</sup> flies respond poorly to infection and succumb early (Figure 4.9). Our data indicates that this could be because of the persistence of bacteria in the Jra<sup>SCR</sup> flies (Figure 4.11). This allele of Jra that was resistant to SUMO conjugation showed a phenotype that was opposite to the loss of function or the hypomorph of Jra. Hence, we postulated that this could be a hypermorphic allele of Jra that had increased activity and suppressed the immune response. It was previously reported that Jra negatively regulates the transcription of AMPs, specifically AttA by replacing Rel from the promoter of AttA. However, the mechanism by which the SUMO conjugation of Jra contributes to this was completely unknown. To address this, we have performed two separate 3' mRNA sequencing experiments to unravel the changes in the gut transcriptome of Jra<sup>RNAi</sup> (Figure 4.16) and Jra<sup>SCR</sup> (Figure 4.18) flies with appropriate controls. We have observed that the guts of Jra<sup>RNAi</sup> flies had a higher expression of few AMPs particularly during the early stages of infection (Table 4.2). We have observed opposite expression patterns of the AMPs in Jra<sup>SCR</sup> (Table 4.3) and we propose that the enhanced death in Jra<sup>SCR</sup> flies may be attributed to the low levels of AMPs in the gut which are needed to clear the invading pathogen. Interestingly, we have observed that several key immune effectors were differentially expressed in the guts of Jra<sup>SCR</sup> and Jra<sup>RNAi</sup> flies. We hypothesised that the regulation of immune response by Jra could be beyond just the transcriptional regulation of AMPs. To answer this, we have used a previously published and publicly available Jra ChIP-seq dataset to map the occupancy of Jra on the promoters of all the significantly differently expressed gene from our study.

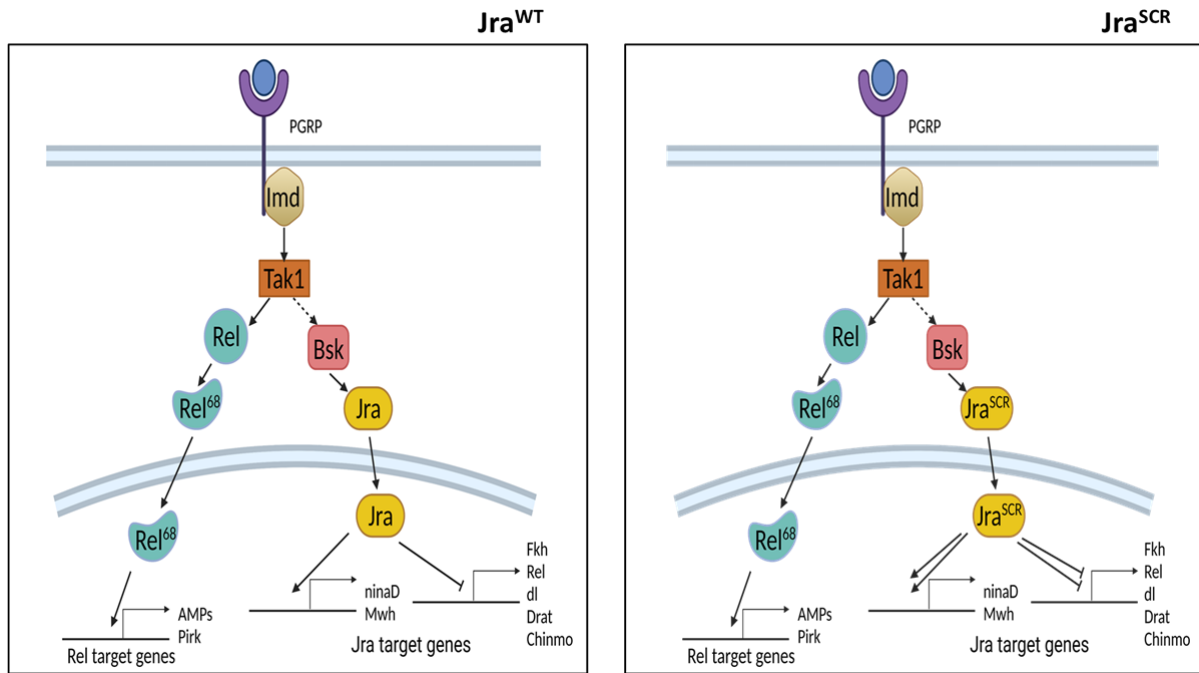


**Figure 4.20: Regulation of gut specific immune response by SUMOylation of Jra**

Following the binding of PGN to PGRP, the Imd pathway and the JNK pathway are activated. The activation of Imd leads to translocation of cleaved Rel into the nucleus and further activation of AMPs and other defence genes. Simultaneously, the activation of JNK leads to translocation of Jra into the nucleus and activation and suppression of the of several defence genes. This is necessary to suppress the immune response and maintain homeostasis (left panel). The SCR mutant of Jra is a hypermorph and the activation and suppression of the defence genes is stronger. This leads to overall suppression of the immune response (right panel). Hence SUMOylation of Jra is necessary to attenuate the suppression of the immune response by Jra.

Since  $Jra^{RNAi}$  and  $Jra^{SCR}$  exhibited exactly opposite phenotypes vis-à-vis gut immunity, we looked at those genes that had opposite expression patterns and also had a significant occupancy of Jra on the promoters (Table 4.4). Strikingly, we see the NFkB factors *relish* (*Rel*) and *dorsal* (*dl*) being present in the set of genes that satisfy the above criteria, indicating that Jra negatively regulates the transcription of *Rel* and *dl* by directly binding to their promoters during infection. In addition to this, we have identified other interesting factors like forkhead (*fkh*) (Bolukbasi et al., 2017; Varma et al., 2014), *Chinmo* (Grmai et al., 2018), *daughterless* (*da*) (Bardin et al., 2010), and *Ets21C* (Mundorf et al., 2019), that play a crucial role in regulating gut homeostasis as direct targets of Jra and are negatively regulated by Jra. Insufficient activation of these essential factors in  $Jra^{SCR}$  could lead to a failure in fighting the

infection, increased bacterial load, and subsequent death, all of which are observed in Jra<sup>SCR</sup> flies. We propose that Jra is a suppressor of immune response in the gut of *Drosophila*. SUMO conjugation of Jra is a crucial and necessary step to attenuate the suppression of the immune response by Jra to fight off infection and attain homeostasis (Figure 4.20).

#### **4.5 Limitations of the study**

In this thesis, we established Jra as a negative regulator of the gut immune response a role that was previously unknown. In addition to this, we demonstrated that Jra is covalently modified by SUMO on K29 and K190. Using CRISPR/Cas9 mediated genome editing, we generated a fly line that was resistant to SUMO conjugation. The Jra<sup>SCR</sup> line responded poorly to infection and succumbed early suggesting that Jra<sup>SCR</sup> is an active allele of Jra. Using transcriptomics, we attribute this phenotype to insufficient activation of a key set of immune modulators required to evoke a robust immune response. Though our data is robust and compelling, we discuss certain caveats in the study.

1. Our understanding that Jra regulates the transcription of Fkh, Rel, Ets21C and Chinmo comes from our RNA seq data. This is further strengthened by the occupancy of Jra on the promoters of the mentioned genes as reported by Jra specific ChIP-seq from the Modern consortium. However, this data is performed in the 3<sup>rd</sup> instar larvae under non-infective conditions. Under immune stress and in the gut, the promoter occupancy of Jra may completely change and the assumption that Jra directly regulates the transcription of genes can be untrue. One effective way to test this out is to perform Jra specific ChIP in the gut with and without infection and compare it to the RNA seq data. This has not been attempted in this thesis as the number of guts required to perform such an experiment would be large. Importantly, we have not tested the Jra specific antibody we generated for this purpose.

2. Our data from the SUMO knockdown in the gut suggests that loss of global SUMOylation is beneficial to the host while loss of SUMOylation on Jra is beneficial to the pathogen. This particular data is rather puzzling and needs detailed analysis. However, perturbing global SUMOylation brings a plethora of changes in the system by reducing SUMOylation on other immune modulators and this could result in the phenotype observed.

3. Our phenotypic data from flies strongly indicates that Jra<sup>SCR</sup> is a hypermorphic allele of Jra. Based on the genetic evidence, we propose that Jra<sup>SCR</sup> has higher activity than Jra<sup>WT</sup> and this higher activity in turn translated to the changes seen in RNA seq dataset. However, we were unable to provide evidence to suggest the difference between Jra<sup>WT</sup> and Jra<sup>SCR</sup> at a molecular level. We hypothesize that this increased activity could possibly be due to two reasons. The first one is that SUMOylation kicks Jra off the promoters of the target genes and therefore restricts its activity. The second is that SUMOylation of Jra changes the interactome of Jra in a highly context specific way and this in turn would show altered activity. Ideally, both these assumptions can be validated by performing ChIP-seq and/or mass-spec after specifically immunoprecipitating Jra. We have not attempted ChIP but have performed IP mass-spec to look at interactors of Jra in whole Jra<sup>WT</sup> and Jra<sup>SCR</sup> flies with and without infection (data not shown). Unfortunately, the data was inconclusive as the efficiency of IP was so low that we could only pick 2 peptides of Jra at the best. Another important problem is that the SUMOylated Jra at any given point is very low and most of Jra in Jra<sup>WT</sup> is unconjugated and behaves like Jra<sup>SCR</sup>. Also, it is extremely challenging to perform such experiments in vivo due to limited sample. However both ChIP and IP mass-spec experiments are possible in tissue culture. One could transfect Jra<sup>WT</sup> and Jra<sup>SCR</sup> and look for changes in promoter occupancy and interactors. One major issue with performing these experiments in tissue culture is the presence of endogenous Jra that would dilute the effect of Jra<sup>SCR</sup>.



4. Another interesting aspect arising from our data is how the SUMOylation of Jra is regulated. Is there a specific E3 ligase responsible for rapidly SUMOylating Jra during infection and attenuating its function? Also, does SUMOylation regulate other PTMs like phosphorylation and ubiquitination of Jra? These exciting questions need thorough investigation to uncover novel mechanisms that regulate the activity of Jra during an immune response.

## 4.5 Materials and methods

### 4.5.1 Fly husbandry and lines

Flies were grown in standard cornmeal agar in a 12-hour light-dark cycle. Only females were used in all the experiments in this study. All *NPI-Gal4<sup>ts</sup>* crosses were grown at 21°C to keep the Gal4 inactivated. 3 days post eclosion, the flies were shifted to 29°C for 3 days (to activate the Gal4 and subsequently the downstream transgene) till the commencement of bacterial feeding.

Table 4.5: Fly lines used

|   | Line/Genotype   | Source            | Description  |
|---|---|-------------------|--|
| 1 | <i>Jra<sup>WT</sup></i>   | This study        | Jra locus modified using CRISPR/Cas9 mutations not incorporated into the genome  |
| 2 | <i>Jra<sup>SCR</sup> L1</i>   | This study        | Jra locus modified using CRISPR/Cas9. K29R+K190R mutations incorporated into the genome. L1 = line 1. Extensively used in this study |
| 3 | <i>Jra<sup>SCR</sup> L2</i>   | This study        | Jra locus modified using CRISPR/Cas9. K29R+K190R mutations incorporated into the genome. L2 = line 2.                                |
| 4 | <i>Myo81F-Gal4, UAS-GFP, tub-gal80<sup>ts</sup> (NPI-Gal4<sup>ts</sup>)</i> | Sveta Chakrabarti | Enterocyte specific Gal4 line. tub-gal80 <sup>ts</sup> for temporal control of Gal4 expression                                       |

|    |   |                  |   |
|----|---|------------------|---|
| 5  | <i>y[1] v[1]; P{y[+t7.7] v[+t1.8]=TRiP.JF01184}attP2</i>                | BDSC:3159<br>5   | UAS-Jra <sup>RNAi</sup>                     |
| 6  | <i>y[1] w[1118]; P{w[+mC]=Jbz}10</i>                                    | BDSC:7218        | UAS-Jra <sup>DN</sup>                       |
| 7  | <i>w[1118] P{w[+mC]=UAS-bsk.DN}2</i>                                    | BDSC:6409        | UAS-Bsk <sup>DN</sup>                       |
| 8  | <i>w[1118]; P{w[+mC]=UAS-Fra.Fbz}5</i>                                  | BDSC:7214        | UAS-Kay <sup>DN</sup>                       |
| 9  | <i>cn[1] Jra[IA109] bw[1] speck[1]/CyO</i>                              | BDSC:3273        | Jra null                                    |
| 10 | <i>Adh[fn23] pr[1] cn[1] Jra[76-19]/CyO</i>                             | BDSC:9880        | Jra null                                    |
| 11 | <i>y[1] v[1]; P{y[+t7.7] v[+t1.8]=TRiP.HM05055}attP2/T M3, Sb[1]</i>    | BDSC:2856<br>9   | UAS-Uba2 <sup>RNAi</sup>                    |
| 12 | <i>y[1] v[1]; P{y[+t7.7] v[+t1.8]=TRiP.HM05183}attP2/T M3, Sb[1]</i>    | BDSC:2897<br>2   | UAS-Aos1 <sup>RNAi</sup>                    |
| 13 | <i>y[1] sc[*] v[1] sev[21]; P{y[+t7.7] v[+t1.8]=TRiP.HMS01540}attP2</i> | BDSC:3612<br>5   | UAS-SUMO <sup>RNAi</sup>                    |
| 14 | <i>UAS-lwr<sup>DN</sup></i>   | Shubha<br>Govind | UAS-Ubc9 <sup>DN</sup>                      |
| 15 | <i>w[*]; cno[3] P{A92}puc[E69] / TM6B,abdA-LacZ</i>                     | DGRC:1090<br>29  | Puc null                                    |
| 16 | <i>w1118; P{GMR61B05-GAL4}attP2</i>                                     | BDSC:4645<br>9   | Jra-Gal4                                    |
| 17 | <i>Jra<sup>SCR</sup>;jra-Gal4</i>                                       | This study       | Jra <sup>SCR</sup> balanced with jra-Gal4   |
| 18 | <i>Jra<sup>SCR</sup>,NP1-Gal4<sup>ts</sup>/CyO</i>                      | This study       | Jra <sup>SCR</sup> recombined with NP1-Gal4 |

#### 4.5.2 Bacterial culture, gut infection and fly survival assays:

*Pseudomonas entomophila* (Pe) used in this study is a kind gift from Sveta Chakrabarti at the Indian Institute of Science. The pathogen was always selected for rifampicin (100ug/ml) resistance and hydrolysis of casein on a milk agar plate. The bacterial pellet obtained for an overnight grown broth was dissolved in 5% sucrose solution so the final OD<sub>600</sub> was 200. For all the survival assays, 6-8 day old female flies were first starved for 2 hours without food and water. Post starvation, the flies were transferred onto a filter disk that was dipped in the concentrated bacterial solution and the flies were allowed to feed for a certain amount of time specific to the experiment. For survival assays, the flies were transferred to a vial containing

standard fly food post-feeding at 20-30 flies/vial and the dead flies were counted every 24 hours. The feeding time wherever the *NPI-Gal4<sup>ts</sup>* was used in any genetic combination was 24 hours. For all the other genotypes, the feeding time was 6 hours.

#### **4.5.3 Bacterial clearance assay**

For assessing the bacterial load, flies were fed on *P.e* for 2 hours. Post feeding, the flies were rinsed in 70% ethanol for 30 seconds and left to dry. Whole flies were crushed in sterile PBS and the lysate was plated on a bacterial agar plate containing rifampicin. The same was repeated at 8 and 24 hpi

#### **4.5.4 Gut dissections, immunostaining and microscopy**

For all the immunofluorescence experiments, the gut were cleared by growing the flies on 5% sugar agar overnight. The next day, flies were fed with *P.e* for 8 hours after 2 hours of starvation. Post feeding, the guts were dissected in ice-cold 1X PBS. The guts were fixed in a solution containing 1X PBS, 0.1% TritonX100 and 4% paraformaldehyde for 20 minutes. Post fixation, the guts were rinsed with 1X PBS, 0.1% TritonX100 to remove excess paraformaldehyde and incubated at room temperature for an hour in a blocking solution that constituted 1X PBS, 0.5% bovine serum albumin, 0.3% TritonX100 and 3% normal goat serum. This is followed by incubation with 1:200 of anti-phosphoHistone3 (pH3) (Cell Signalling Technology, #9701L) antibody diluted in blocking solution. Anti-rabbit alexa568 (Thermo Fisher Scientific) was used as a secondary antibody in 1:1000 dilution. DAPI was added to the antepenultimate wash after secondary antibody staining and the samples were mounted in Slowfade gold antifade mountant (Thermo Fisher Scientific, #36940). The mounted samples were imaged using a 20X oil immersion objective on a Leica SP8 confocal microscope. pH3 positive cells per individual gut were counted using ImageJ post a threshold cutoff.

#### **4.5.5 qRT-PCR**

Total RNA was extracted from the 50-60 midguts using RNeasy Plus Universal Kits (Qiagen, #73404) according to the manufacturer's protocol. 1ug of extracted RNA was used to generate cDNA using a high-capacity cDNA reverse transcriptase kit (Thermo Fisher Scientific, #4374966) using the manufacturer's protocol. The cDNA was diluted in a 1:5 ratio for all the experiments. Custom made Applied biosystem's Taqman low-density arrays were used to quantitate specific transcripts of Jra, Rel, DptA and AttD.

#### **4.5.6 RNA isolation, cDNA library preparation and sequencing**

Total RNA was extracted from 50-60 midguts of adult flies using RNeasy Plus Universal Kits (Qiagen, #73404) according to the manufacturer's protocol. 3' mRNA specific libraries were amplified using QuantSeq 3' mRNA-Seq Library Prep Kit FWD (Lexogen, #015.96) using the manufacturer's instructions. The concentrations of the libraries were estimated using Qubit™ dsDNA HS Assay Kit (Thermo Fisher Scientific, #Q32851). Quality assessment and library size estimation of the individual libraries was done using an HS DNA kit (Agilent, 5067-4626) in a Bioanalyzer 2100. The libraries were pooled in equimolar ratio and single-end 75bp reads were sequenced on the Illumina NextSeq 550 platform.

#### **4.5.7 Read mapping, counts generation and differential expression analysis**

On average, 4-5 million reads were uniquely mapped per sample. Sequencing quality was assessed using FastQC v0.11.5. Post quality control, the reads were mapped to the *Drosophila* genome (dm6) using STAR aligner v.2.5.2a (Dobin et al., 2013). Gene expression levels were measured using the counts generated by HTSeq-count v 0.6.0 (Anders et al., 2015). The gene expression counts were normalized for all samples together and the biological conditions were compared pairwise using DESeq2 (Love et al., 2014). The PCA was performed using a custom

R script to . GO enrichment analysis of the significantly differentially expressed gene set was performed using gProfiler (<https://biit.cs.ut.ee/gprofiler/gost>) (Reimand et al., 2011).

#### ***4.5.8 ChIP-seq data analysis***

Jra specific ChIP-seq dataset (ENCSR471GSA) was obtained from the model organism Encyclopedia of Regulatory Networks (modERN) consortium (<https://epic.gs.washington.edu/modERN/>) (Kudron et al., 2018). Input normalised Bigwig file were obtained and the occupancy of Jra was plotted on the gene body (+/- 2kb of the mRNA) of all the significantly differentially expressed genes from the 2 RNA sequencing datasets using deeptools 3.5.0 (Kudron et al., 2018).

## 4.6 References

1. Amcheslavsky, A., Ito, N., Jiang, J., and Ip, Y.T. (2011). Tuberous sclerosis complex and Myc coordinate the growth and division of *Drosophila* intestinal stem cells. *J Cell Biol* *193*, 695-710.
2. Anders, S., Pyl, P.T., and Huber, W. (2015). HTSeq--a Python framework to work with high-throughput sequencing data. *Bioinformatics* *31*, 166-169.
3. Bae, Y.S., Choi, M.K., and Lee, W.J. (2010). Dual oxidase in mucosal immunity and host-microbe homeostasis. *Trends Immunol* *31*, 278-287.
4. Bardin, A.J., Perdigoto, C.N., Southall, T.D., Brand, A.H., and Schweisguth, F. (2010). Transcriptional control of stem cell maintenance in the *Drosophila* intestine. *Development* *137*, 705-714.
5. Bischoff, V., Vignal, C., Duvic, B., Boneca, I.G., Hoffmann, J.A., and Royet, J. (2006). Downregulation of the *Drosophila* immune response by peptidoglycan-recognition proteins SC1 and SC2. *PLoS Pathog* *2*, e14.
6. Biteau, B., Hochmuth, C.E., and Jasper, H. (2008). JNK activity in somatic stem cells causes loss of tissue homeostasis in the aging *Drosophila* gut. *Cell Stem Cell* *3*, 442-455.
7. Biteau, B., and Jasper, H. (2011). EGF signalling regulates the proliferation of intestinal stem cells in *Drosophila*. *Development* *138*, 1045-1055.
8. Bolukbasi, E., Khericha, M., Regan, J.C., Ivanov, D.K., Adcott, J., Dyson, M.C., Nespital, T., Thornton, J.M., Alic, N., and Partridge, L. (2017). Intestinal Fork Head Regulates Nutrient Absorption and Promotes Longevity. *Cell Rep* *21*, 641-653.
9. Bonfini, A., Liu, X., and Buchon, N. (2016). From pathogens to microbiota: How *Drosophila* intestinal stem cells react to gut microbes. *Dev Comp Immunol* *64*, 22-38.
10. Bosco-Drayon, V., Poidevin, M., Boneca, I.G., Narbonne-Reveau, K., Royet, J., and Charroux, B. (2012). Peptidoglycan sensing by the receptor PGRP-LE in the *Drosophila* gut induces immune responses to infectious bacteria and tolerance to microbiota. *Cell Host Microbe* *12*, 153-165.
11. Buchon, N., Broderick, N.A., Kuraishi, T., and Lemaitre, B. (2010). *Drosophila* EGFR pathway coordinates stem cell proliferation and gut remodeling following infection. *BMC Biol* *8*, 152.

12. Buchon, N., Broderick, N.A., Poidevin, M., Pradervand, S., and Lemaitre, B. (2009). *Drosophila* intestinal response to bacterial infection: activation of host defence and stem cell proliferation. *Cell Host Microbe* 5, 200-211.
13. Buchon, N., Osman, D., David, F.P., Fang, H.Y., Boquete, J.P., Deplancke, B., and Lemaitre, B. (2013). Morphological and molecular characterization of adult midgut compartmentalization in *Drosophila*. *Cell Rep* 3, 1725-1738.
14. Buchon, N., Silverman, N., and Cherry, S. (2014). Immunity in *Drosophila melanogaster*--from microbial recognition to whole-organism physiology. *Nat Rev Immunol* 14, 796-810.
15. Capo, F., Wilson, A., and Di Cara, F. (2019). The Intestine of *Drosophila melanogaster*: An Emerging Versatile Model System to Study Intestinal Epithelial Homeostasis and Host-Microbial Interactions in Humans. *Microorganisms* 7.
16. Chakrabarti, S., Liehl, P., Buchon, N., and Lemaitre, B. (2012). Infection-induced host translational blockage inhibits immune responses and epithelial renewal in the *Drosophila* gut. *Cell Host Microbe* 12, 60-70.
17. Chiu, H., Ring, B.C., Sorrentino, R.P., Kalamarz, M., Garza, D., and Govind, S. (2005). dUbc9 negatively regulates the Toll-NF-kappa B pathways in larval hematopoiesis and drosomycin activation in *Drosophila*. *Dev Biol* 288, 60-72.
18. Delaney, J.R., Stoven, S., Uvell, H., Anderson, K.V., Engstrom, Y., and Mlodzik, M. (2006). Cooperative control of *Drosophila* immune responses by the JNK and NF-kappaB signalling pathways. *EMBO J* 25, 3068-3077.
19. Deng, H., Gerencser, A.A., and Jasper, H. (2015). Signal integration by Ca(2+) regulates intestinal stem-cell activity. *Nature* 528, 212-217.
20. Dobin, A., Davis, C.A., Schlesinger, F., Drenkow, J., Zaleski, C., Jha, S., Batut, P., Chaisson, M., and Gingeras, T.R. (2013). STAR: ultrafast universal RNA-seq aligner. *Bioinformatics* 29, 15-21.
21. Everett, R.D., Boutell, C., and Hale, B.G. (2013). Interplay between viruses and host sumoylation pathways. *Nat Rev Microbiol* 11, 400-411.
22. Fukuyama, H., Verdier, Y., Guan, Y., Makino-Okamura, C., Shilova, V., Liu, X., Maksoud, E., Matsubayashi, J., Haddad, I., Spirohn, K., *et al.* (2013). Landscape of protein-

protein interactions in *Drosophila* immune deficiency signalling during bacterial challenge. *Proc Natl Acad Sci U S A* *110*, 10717-10722.

23. Grmai, L., Hudry, B., Miguel-Aliaga, I., and Bach, E.A. (2018). Chinmo prevents transformer alternative splicing to maintain male sex identity. *PLoS Genet* *14*, e1007203.

24. Ha, E.M., Oh, C.T., Bae, Y.S., and Lee, W.J. (2005). A direct role for dual oxidase in *Drosophila* gut immunity. *Science* *310*, 847-850.

25. Handu, M., Kaduskar, B., Ravindranathan, R., Soory, A., Giri, R., Elango, V.B., Gowda, H., and Ratnaparkhi, G.S. (2015). SUMO-Enriched Proteome for *Drosophila* Innate Immune Response. *G3 (Bethesda)* *5*, 2137-2154.

26. Hannoun, Z., Maarifi, G., and Chelbi-Alix, M.K. (2016). The implication of SUMO in intrinsic and innate immunity. *Cytokine Growth Factor Rev* *29*, 3-16.

27. Jiang, H., and Edgar, B.A. (2009). EGFR signalling regulates the proliferation of *Drosophila* adult midgut progenitors. *Development* *136*, 483-493.

28. Jiang, H., Grenley, M.O., Bravo, M.J., Blumhagen, R.Z., and Edgar, B.A. (2011). EGFR/Ras/MAPK signalling mediates adult midgut epithelial homeostasis and regeneration in *Drosophila*. *Cell Stem Cell* *8*, 84-95.

29. Jiang, H., Patel, P.H., Kohlmaier, A., Grenley, M.O., McEwen, D.G., and Edgar, B.A. (2009). Cytokine/Jak/Stat signalling mediates regeneration and homeostasis in the *Drosophila* midgut. *Cell* *137*, 1343-1355.

30. Jones, R.M., Luo, L., Ardita, C.S., Richardson, A.N., Kwon, Y.M., Mercante, J.W., Alam, A., Gates, C.L., Wu, H., Swanson, P.A., *et al.* (2013). Symbiotic lactobacilli stimulate gut epithelial proliferation via Nox-mediated generation of reactive oxygen species. *EMBO J* *32*, 3017-3028.

31. Kim, L.K., Choi, U.Y., Cho, H.S., Lee, J.S., Lee, W.-b., Kim, J., Jeong, K., Shim, J., Kim-Ha, J., and Kim, Y.-J. (2007). Down-regulation of NF- $\kappa$ B target genes by the AP-1 and STAT complex during the innate immune response in *Drosophila*. *PLoS Biol* *5*, e238.

32. Kim, M., Lee, J.H., Lee, S.Y., Kim, E., and Chung, J. (2006). Caspar, a suppressor of antibacterial immunity in *Drosophila*. *Proc Natl Acad Sci U S A* *103*, 16358-16363.

33. Kim, T., Yoon, J., Cho, H., Lee, W.B., Kim, J., Song, Y.H., Kim, S.N., Yoon, J.H., Kim-Ha, J., and Kim, Y.J. (2005). Downregulation of lipopolysaccharide response in



*Drosophila* by negative crosstalk between the AP1 and NF-kappaB signalling modules. *Nat Immunol* 6, 211-218.

34. Kleino, A., Myllymaki, H., Kallio, J., Vanha-aho, L.M., Oksanen, K., Ulvila, J., Hultmark, D., Valanne, S., and Ramet, M. (2008). Pirk is a negative regulator of the *Drosophila* Imd pathway. *J Immunol* 180, 5413-5422.

35. Kudron, M.M., Victorsen, A., Gevirtzman, L., Hillier, L.W., Fisher, W.W., Vafeados, D., Kirkey, M., Hammonds, A.S., Gersch, J., Ammouri, H., *et al.* (2018). The ModERN Resource: Genome-Wide Binding Profiles for Hundreds of *Drosophila* and *Caenorhabditis elegans* Transcription Factors. *Genetics* 208, 937-949.

36. Lee, K.A., Kim, S.H., Kim, E.K., Ha, E.M., You, H., Kim, B., Kim, M.J., Kwon, Y., Ryu, J.H., and Lee, W.J. (2013). Bacterial-derived uracil as a modulator of mucosal immunity and gut-microbe homeostasis in *Drosophila*. *Cell* 153, 797-811.

37. Lemaitre, B., and Miguel-Aliaga, I. (2013). The digestive tract of *Drosophila melanogaster*. *Annu Rev Genet* 47, 377-404.

38. Li, H., Qi, Y., and Jasper, H. (2013). Dpp signalling determines regional stem cell identity in the regenerating adult *Drosophila* gastrointestinal tract. *Cell Rep* 4, 10-18.

39. Liehl, P., Blight, M., Vodovar, N., Bocard, F., and Lemaitre, B. (2006). Prevalence of local immune response against oral infection in a *Drosophila/Pseudomonas* infection model. *PLoS Pathog* 2, e56.

40. Love, M.I., Huber, W., and Anders, S. (2014). Moderated estimation of fold change and dispersion for RNA-seq data with DESeq2. *Genome Biol* 15, 550.

41. Micchelli, C.A., and Perrimon, N. (2006). Evidence that stem cells reside in the adult *Drosophila* midgut epithelium. *Nature* 439, 475-479.

42. Miguel-Aliaga, I., Jasper, H., and Lemaitre, B. (2018). Anatomy and Physiology of the Digestive Tract of *Drosophila melanogaster*. *Genetics* 210, 357-396.

43. Mundorf, J., Donohoe, C.D., McClure, C.D., Southall, T.D., and Uhlirova, M. (2019). Ets21c Governs Tissue Renewal, Stress Tolerance, and Aging in the *Drosophila* Intestine. *Cell Rep* 27, 3019-3033 e3015.

44. Neyen, C., Poidevin, M., Roussel, A., and Lemaitre, B. (2012). Tissue- and ligand-specific sensing of gram-negative infection in *Drosophila* by PGRP-LC isoforms and PGRP-LE. *J Immunol* 189, 1886-1897.
45. Ohlstein, B., and Spradling, A. (2007). Multipotent *Drosophila* intestinal stem cells specify daughter cell fates by differential notch signalling. *Science* 315, 988-992.
46. Paddibhatla, I., Lee, M.J., Kalamarz, M.E., Ferrarese, R., and Govind, S. (2010). Role for sumoylation in systemic inflammation and immune homeostasis in *Drosophila* larvae. *PLoS Pathog* 6, e1001234.
47. Paredes, J.C., Welchman, D.P., Poidevin, M., and Lemaitre, B. (2011). Negative regulation by amidase PGRPs shapes the *Drosophila* antibacterial response and protects the fly from innocuous infection. *Immunity* 35, 770-779.
48. Pfeiffer, B.D., Jenett, A., Hammonds, A.S., Ngo, T.T., Misra, S., Murphy, C., Scully, A., Carlson, J.W., Wan, K.H., Lavery, T.R., *et al.* (2008). Tools for neuroanatomy and neurogenetics in *Drosophila*. *Proc Natl Acad Sci U S A* 105, 9715-9720.
49. Reimand, J., Arak, T., and Vilo, J. (2011). g:Profiler--a web server for functional interpretation of gene lists (2011 update). *Nucleic Acids Res* 39, W307-315.
50. Ren, F., Shi, Q., Chen, Y., Jiang, A., Ip, Y.T., Jiang, H., and Jiang, J. (2013). *Drosophila* Myc integrates multiple signalling pathways to regulate intestinal stem cell proliferation during midgut regeneration. *Cell Res* 23, 1133-1146.
51. Ren, F., Wang, B., Yue, T., Yun, E.Y., Ip, Y.T., and Jiang, J. (2010). Hippo signalling regulates *Drosophila* intestine stem cell proliferation through multiple pathways. *Proc Natl Acad Sci U S A* 107, 21064-21069.
52. Ryu, J.H., Kim, S.H., Lee, H.Y., Bai, J.Y., Nam, Y.D., Bae, J.W., Lee, D.G., Shin, S.C., Ha, E.M., and Lee, W.J. (2008). Innate immune homeostasis by the homeobox gene caudal and commensal-gut mutualism in *Drosophila*. *Science* 319, 777-782.
53. Silverman, N., Zhou, R., Erlich, R.L., Hunter, M., Bernstein, E., Schneider, D., and Maniatis, T. (2003). Immune activation of NF-kappaB and JNK requires *Drosophila* TAK1. *J Biol Chem* 278, 48928-48934.
54. Srikanth, C.V., and Verma, S. (2017). Sumoylation as an Integral Mechanism in Bacterial Infection and Disease Progression. *Adv Exp Med Biol* 963, 389-408.

55. Takashima, S., Gold, D., and Hartenstein, V. (2013). Stem cells and lineages of the intestine: a developmental and evolutionary perspective. *Dev Genes Evol* 223, 85-102.
56. Troha, K., and Buchon, N. (2019). Methods for the study of innate immunity in *Drosophila melanogaster*. *Wiley Interdiscip Rev Dev Biol* 8, e344.
57. Varma, D., Bulow, M.H., Pesch, Y.Y., Loch, G., and Hoch, M. (2014). Forkhead, a new cross regulator of metabolism and innate immunity downstream of TOR in *Drosophila*. *J Insect Physiol* 69, 80-88.
58. Verma, V., Croley, F., and Sadanandom, A. (2018). Fifty shades of SUMO: its role in immunity and at the fulcrum of the growth-defence balance. *Mol Plant Pathol* 19, 1537-1544.
59. Vodovar, N., Vallenet, D., Cruveiller, S., Rouy, Z., Barbe, V., Acosta, C., Cattolico, L., Jubin, C., Lajus, A., Segurens, B., *et al.* (2006). Complete genome sequence of the entomopathogenic and metabolically versatile soil bacterium *Pseudomonas entomophila*. *Nat Biotechnol* 24, 673-679.
60. Vodovar, N., Vinals, M., Liehl, P., Basset, A., Degrouard, J., Spellman, P., Boccard, F., and Lemaitre, B. (2005). *Drosophila* host defence after oral infection by an entomopathogenic *Pseudomonas* species. *Proc Natl Acad Sci U S A* 102, 11414-11419.
61. Wilson, V.G. (2017). Viral Interplay with the Host Sumoylation System. *Adv Exp Med Biol* 963, 359-388.
62. Wimmer, P., Schreiner, S., and Dobner, T. (2012). Human pathogens and the host cell SUMOylation system. *J Virol* 86, 642-654.
63. Zaidman-Remy, A., Herve, M., Poidevin, M., Pili-Floury, S., Kim, M.S., Blanot, D., Oh, B.H., Ueda, R., Mengin-Lecreulx, D., and Lemaitre, B. (2006). The *Drosophila* amidase PGRP-LB modulates the immune response to bacterial infection. *Immunity* 24, 463-473.
64. Zhai, Z., Boquete, J.P., and Lemaitre, B. (2018). Cell-Specific Imd-NF-kappaB Responses Enable Simultaneous Antibacterial Immunity and Intestinal Epithelial Cell Shedding upon Bacterial Infection. *Immunity* 48, 897-910 e897.

## Appendix I : 3'mRNA seq and CHIP seq analysis

### I.a 3'mRNA seq analysis

3'mRNA specific cDNA library prep was made using Quantseq 3'mRNA-Seq library prep kit FWD for Illumina from Lexogen. The sequencing was performed on an Illumina NextSeq 550 platform. The data obtained was demultiplexed using the bcl2fastq package. The fastq files of each sample from different lanes were concatenated using a linux command line. The concatenated files were uploaded on the bluebee server (<https://lexogen.bluebee.com/quantseq/>) and used for further analysis. The following tools were a part of the bluebee pipeline and were used to analyse the data: BBDuk v35.92 (<https://jgi.doe.gov/data-and-tools/bbtools/bb-tools-user-guide/bbdduk-guide/>) for adapter trimming; FastQC v0.11.5 (<https://www.bioinformatics.babraham.ac.uk/projects/fastqc/>) for the quality check; STAR v2.5.2a (<https://github.com/alexdobin/STAR/blob/master/doc/STARmanual.pdf>) for aligning sequenced files to the genome of *Drosophila* (dmel\_r6); HTseq-count v0.6.0 (<https://htseq.readthedocs.io/en/master/>) for generating counts from data aligned to the genome; DESeq2 v4.1 (<https://bioconductor.org/packages/release/bioc/html/DESeq2.html>) for differential expression analysis. The raw counts obtained from HTseq were used to generate normalised counts or counts per million (CPM) using edgeR (<https://bioconductor.org/packages/release/bioc/html/edgeR.html>), Cluster3

(<http://bonsai.hgc.jp/~mdehoon/software/cluster/>) was used to generate dendrograms of expression patterns of genes based on CPM values.

### **I.b Codes used for 3'mRNA seq analysis**

```

# Demultiplexing pooled data post sequencing

bcl2fastq -R /path to run folder -o /path to output folder --
sample-sheet /path to sample sheet.csv

# Concatenation of demultiplexed files

cat [filename-whose-contents-is-to-be-copied] > [destination-
filename]

# Normalising counts using edgeR

a=read.table("rawcounts.csv", header=T, row.names = 1)

a1=cpm(a)

# PCA analysis

abc=read.table("rawcounts.txt", header=T, row.names = 1)

abc1=cpm(abc, log = T)

#logCPM is a preferred input for PCA analysis

pca1=prcomp(t(abc1))

#Plot PCA::install ggpl2

autoplot(pca1, data=pca1, label=TRUE, repel=TRUE, label.size=3)

```

### **I.c ChIP-seq analysis**

The model organism Encyclopedia of Regulatory Networks (modERN) consortium (<https://epic.gs.washington.edu/modERN/>) is a repository of several ChIP-seq datasets of

*Drosophila* proteins. Jra specific (ENCSR471GSA) ChIP-seq was performed from the whole wandering 3<sup>rd</sup> instar larvae. Input normalised files were directly available and downloaded from the website. The input normalised bigwig files were used to map the occupancy of Jra on the gene body of genes. The gene list used for this analysis consisted of all significantly differentially expressed genes in both 3'mRNA seq datasets from this study. The gene annotation file (gtf) of *Drosophila* was obtained from the Ensemble database ([https://asia.ensembl.org/Drosophila\\_melanogaster/Info/Index](https://asia.ensembl.org/Drosophila_melanogaster/Info/Index)). The peak calling and heatmap plotting was done using Deeptools v2.0 (<https://deeptools.readthedocs.io/en/develop/>).

#### **I.d Codes used for plotting Jra occupancy on ChIP-seq files**

# Deeptools compute matrix used to fetch defined regions from a bw file

```
computeMatrix          scale-regions          -S          Jra-
GFP_WA_W3L_IP_Rep0.tagAlign_VS_Jra-
GFP_WA_W3L_Input_Rep0.tagAlign.bw -R  all.gtf  -o  all1  --
outFileNameMatrix all1-matrix --outFileSortedRegions all1-bed -
b 2000 -a 2000 --transcriptID gene --transcript_id_designator
gene_symbol --binSize 50
```

#heatmap with bin50

```
plotHeatmap -m all1 --hclust 2 --kmeans 2 -o all-bin50.svg --
dpi 600 --outFileSortedRegions all_bin50-sortedregions4
```

**Table I.1: List of genes with enriched Jra peak on their promoters**

List includes significantly (FDR<0.1) differentially expressed genes from both 3'mRNA sequencing datasets. Log2 foldchange values are represented at 4hpi and 12 hpi post normalisation to UC. Empty cells indicate log2 FC values with FDR>0.1

| Gene symbol   | UC vs 4hpi        |                    |                   |                     | UC vs 12hpi       |                    |                   |                     |
|---------------|-------------------|--------------------|-------------------|---------------------|-------------------|--------------------|-------------------|---------------------|
|               | Jra <sup>WT</sup> | Jra <sup>SCR</sup> | w <sup>1118</sup> | Jra <sup>RNAi</sup> | Jra <sup>WT</sup> | Jra <sup>SCR</sup> | w <sup>1118</sup> | Jra <sup>RNAi</sup> |
| 14-3-3zeta    |                   |                    |                   |                     |                   | 0.46               |                   |                     |
| 26-29-p       |                   |                    | -0.76             |                     |                   |                    | -1.03             |                     |
| aay           | 1.16              |                    | 1.33              | 1.85                | 0.59              |                    |                   |                     |
| Acbp1         |                   |                    |                   |                     |                   |                    | -0.90             |                     |
| Acn           |                   |                    |                   |                     | 0.87              | 0.55               |                   |                     |
| ACOX1         |                   |                    |                   |                     |                   |                    | -1.52             |                     |
| Acsl          |                   |                    |                   |                     |                   |                    | -0.63             |                     |
| Act42A        |                   |                    | -0.71             | -0.71               |                   |                    | -0.63             |                     |
| Act5C         |                   |                    |                   |                     |                   |                    | -0.59             |                     |
| Adf1          |                   |                    |                   |                     | 0.89              |                    |                   |                     |
| Aef1          | 0.71              |                    |                   |                     | 0.73              | 0.46               |                   |                     |
| Akt           |                   |                    |                   |                     |                   | 0.56               | 1.13              |                     |
| alc           |                   |                    | -0.94             | -1.01               | -0.74             | -0.46              | -1.58             | -2.16               |
| Alh           |                   |                    |                   |                     | 1.02              | 0.67               |                   |                     |
| Alp12         |                   |                    |                   |                     |                   |                    | -1.13             |                     |
| alpha-Est9    |                   |                    | 0.62              |                     | 0.86              | 1.00               |                   |                     |
| alphaSnap     |                   |                    |                   |                     |                   |                    | -0.76             |                     |
| alphaTub84B   |                   |                    |                   |                     |                   | 0.35               | 0.53              |                     |
| Ance          |                   |                    | -0.70             | -1.07               | -1.07             | -0.60              | -1.95             | -1.08               |
| AnxB11        |                   |                    |                   |                     | 0.90              | 0.56               |                   |                     |
| AnxB9         |                   |                    |                   | -0.69               |                   |                    |                   |                     |
| aop           | 1.01              | 0.75               | 0.57              | 0.96                | 1.60              | 1.26               |                   | 1.96                |
| Apc           |                   |                    | -0.85             | -0.96               |                   |                    |                   |                     |
| aPKC          | 0.84              | 0.51               |                   |                     | 1.10              | 0.79               | 0.72              |                     |
| APP-BP1       |                   |                    |                   |                     |                   |                    | 1.66              |                     |
| Aps           |                   |                    |                   |                     |                   |                    | 0.80              |                     |
| Arl4          |                   |                    |                   |                     |                   | 0.49               |                   |                     |
| Arl5          |                   |                    |                   | 1.18                |                   |                    | 1.40              |                     |
| Arp2          |                   | 0.56               |                   |                     | 1.14              | 1.02               |                   |                     |
| Arp3          |                   |                    |                   |                     | 1.01              | 0.85               |                   |                     |
| Arpc2         |                   |                    |                   |                     | 0.92              | 0.87               |                   |                     |
| Art3          | 0.96              |                    |                   |                     |                   |                    |                   |                     |
| AsnS          | 1.01              | 0.70               |                   |                     | 1.07              | 0.77               |                   |                     |
| AspRS         |                   |                    |                   |                     |                   |                    | -0.53             |                     |
| asRNA:CR44069 |                   |                    |                   |                     | 1.99              |                    | 3.36              | 3.03                |
| asRNA:CR44095 |                   |                    |                   |                     | 1.65              | 1.09               |                   |                     |
| asRNA:CR44192 |                   |                    |                   | -1.70               |                   |                    |                   |                     |
| asRNA:CR44340 |                   |                    |                   |                     | 2.01              |                    |                   |                     |
| asRNA:CR44512 |                   |                    |                   |                     |                   |                    | 1.88              |                     |
| asRNA:CR45028 |                   |                    |                   |                     |                   |                    | 4.18              |                     |



|               |       |       |       |       |      |       |       |       |
|---------------|-------|-------|-------|-------|------|-------|-------|-------|
| asRNA:CR45108 |       |       |       |       |      |       | 2.90  |       |
| asRNA:CR45136 |       |       |       |       |      | 1.14  | 2.54  |       |
| asRNA:CR45281 |       |       |       |       |      |       |       | 2.88  |
| asRNA:CR45874 |       |       |       |       | 1.27 |       |       | 4.90  |
| asRNA:CR45928 |       |       |       |       |      |       | 2.59  |       |
| asRNA:CR45943 |       |       | -1.21 |       |      |       |       |       |
| asRNA:CR45999 |       |       |       |       | 1.41 | 0.82  |       |       |
| Atf3          |       |       | 0.65  |       | 0.76 | 0.61  | 1.00  |       |
| Atg17         |       |       |       |       | 0.61 |       |       |       |
| Atg18b        |       |       | -1.05 |       | 1.14 | 0.67  |       |       |
| Atg8a         |       |       | -1.50 | -1.45 |      |       | -1.28 | -1.72 |
| ATPsynbeta    |       |       |       |       |      |       | -0.78 |       |
| ATPsyndelta   |       |       |       |       |      |       | -0.48 |       |
| ATPsynE       |       |       |       | -0.57 |      |       | -0.80 |       |
| Atu           |       |       | 0.85  |       | 1.11 | 0.80  |       |       |
| Axud1         |       |       |       |       | 1.04 | 0.56  |       | 1.75  |
| B52           |       |       |       | 0.62  | 0.74 | 0.75  | 0.81  |       |
| Bacc          |       |       | -0.55 | -0.75 |      |       |       |       |
| baf           |       |       |       |       | 0.63 |       | 0.67  | 1.62  |
| Baldspot      | 0.60  |       |       |       | 1.02 | 0.71  |       |       |
| bark          |       |       | -1.10 |       | 0.94 | 0.60  |       |       |
| bchs          |       |       |       |       | 0.90 |       |       |       |
| BCL7-like     |       |       |       |       | 1.32 |       |       |       |
| be            | 0.76  |       |       |       | 1.47 | 0.94  |       |       |
| ben           |       |       |       |       |      |       | -0.49 |       |
| Best1         |       |       |       |       | 0.88 |       |       |       |
| betaTub56D    |       |       | 0.48  |       | 0.78 | 0.60  | 0.57  |       |
| bgm           |       |       | 0.91  | 1.00  |      | 0.63  | 0.68  |       |
| bic           |       |       | -0.39 |       |      |       | -0.92 |       |
| bif           |       |       |       |       | 0.86 | 0.52  |       |       |
| Blimp-1       |       |       |       |       | 0.94 | 0.42  |       |       |
| blw           |       |       |       | -0.60 |      |       | -0.89 |       |
| bmm           | 1.16  | 1.06  |       |       |      | 0.87  |       |       |
| BNIP3         | -0.72 | -0.57 | -1.46 | -1.37 |      | -0.51 | -0.86 |       |
| bocks         |       |       |       |       |      |       | 1.09  |       |
| bowl          |       |       |       |       | 1.06 | 0.82  | 1.03  |       |
| brat          |       |       |       |       | 0.71 | 0.48  |       |       |
| brk           |       |       |       |       | 1.05 | 1.08  | 1.32  |       |
| brm           |       |       |       |       | 0.63 | 0.46  |       | 1.41  |
| brwl          |       |       |       |       | 0.76 |       |       |       |
| Bsg           |       |       |       |       |      |       | -0.41 |       |
| BtbVII        |       |       |       |       | 0.62 |       |       | 1.29  |
| bys           |       | 0.63  |       |       |      |       |       |       |
| c(3)G         |       |       |       |       | 2.00 | 1.05  |       | 3.11  |
| C1GalTA       |       |       | -0.76 |       |      |       | -0.81 |       |
| cact          | 0.62  |       | 1.36  | 1.07  |      |       | 0.82  |       |

|         |      |       |       |       |       |       |       |       |
|---------|------|-------|-------|-------|-------|-------|-------|-------|
| cactin  |      |       |       |       | 1.63  | 0.85  | 1.34  | 1.66  |
| Cbs     |      |       |       |       |       |       | -1.11 |       |
| cbt     | 1.22 |       | 2.06  | 2.27  | 1.84  | 1.00  | 2.20  | 2.94  |
| CCT1    | 0.76 |       | 0.75  |       | 1.10  | 0.66  | 1.03  | 1.61  |
| CCT3    | 0.77 |       | 0.79  | 0.81  | 0.98  | 0.48  | 0.84  | 1.34  |
| CCT5    |      |       | 0.65  | 0.70  | 0.70  | 0.40  | 0.74  |       |
| CCT7    |      |       |       |       | 0.77  |       |       |       |
| Cdc42   |      |       |       |       | 0.87  | 0.62  |       |       |
| CDC50   |      |       | -0.52 |       | 0.96  |       |       |       |
| CenB1A  |      |       |       |       | 0.99  | 0.69  |       |       |
| CenG1A  |      | -0.59 |       | 1.07  | 1.27  | 0.46  |       | 1.53  |
| cer     |      |       |       | -1.01 |       |       | -1.89 |       |
| cert    |      |       |       |       | 1.30  | 0.58  |       |       |
| cg      |      |       |       |       | 0.65  | 0.53  |       |       |
| CG10082 | 0.83 |       | 0.64  |       | 1.18  | 0.58  | 0.99  |       |
| CG10098 |      |       |       |       | 1.27  | 0.85  | 1.24  |       |
| CG10214 |      |       |       |       |       | 0.66  |       |       |
| CG10324 |      |       |       |       | 0.93  | 0.67  |       |       |
| CG10337 | 1.40 |       | 0.79  |       | 2.07  | 1.44  |       |       |
| CG10365 |      |       |       | 1.78  |       |       |       | 1.60  |
| CG10383 |      |       |       | -0.86 | 1.00  |       |       |       |
| CG10413 |      |       | -0.76 |       |       |       | -1.04 |       |
| CG10428 |      |       |       |       | 0.65  |       |       |       |
| CG10467 |      | -0.71 | -1.06 |       | -0.96 | -1.02 | -1.67 |       |
| CG10555 |      |       |       |       | 0.75  | 0.47  |       |       |
| CG10623 |      |       | -1.18 | -1.40 |       | -0.56 | -1.79 | -2.15 |
| CG10660 |      |       |       |       | 0.83  | 0.72  | 0.67  |       |
| CG10809 |      |       |       |       | 1.46  | 0.98  | 1.66  |       |
| CG10914 |      |       |       |       |       | 0.73  |       |       |
| CG10939 |      |       |       |       |       | 0.51  |       |       |
| CG10948 |      |       |       |       | 0.95  | 0.57  | 2.13  | 1.96  |
| CG10962 |      |       |       |       | 2.15  |       |       |       |
| CG10984 |      |       |       |       |       |       | 1.62  |       |
| CG11050 |      |       | 0.64  |       |       | 0.55  |       |       |
| CG11089 | 0.94 |       |       |       |       |       |       |       |
| CG11109 |      |       |       |       | 0.87  | 0.60  |       |       |
| CG11151 |      |       |       |       |       |       | -1.00 |       |
| CG11267 |      |       | 0.72  | 0.67  |       |       | 0.57  |       |
| CG11275 |      |       |       |       | 0.76  |       | 1.96  | 2.17  |
| CG1129  |      |       |       |       | 1.13  | 0.51  |       |       |
| CG11309 |      |       |       |       |       |       | -1.16 |       |
| CG11417 |      |       |       |       | 0.72  | 0.58  |       | 1.80  |
| CG1146  |      |       |       | 0.76  | 0.54  | 0.40  | 1.28  |       |
| CG11791 |      |       |       |       | 0.76  | 0.51  |       |       |
| CG11899 |      |       | 0.91  |       | 1.39  | 1.11  | 0.97  |       |
| CG11975 |      |       | -0.79 |       |       |       |       |       |

|         |       |      |       |       |       |       |       |       |
|---------|-------|------|-------|-------|-------|-------|-------|-------|
| CG12004 |       |      |       |       | 0.63  |       |       |       |
| CG12054 |       |      |       | 0.56  | 1.02  | 0.73  | 1.08  | 1.32  |
| CG12112 | 1.30  | 0.76 | 0.79  |       | 2.25  | 1.66  | 1.19  |       |
| CG12116 |       |      |       |       |       | -0.37 |       |       |
| CG12129 |       |      |       | 1.52  | 0.65  |       |       |       |
| CG12194 |       |      | -1.05 | -1.27 | -1.46 | -0.55 | -2.74 | -1.78 |
| CG12560 |       |      |       |       |       |       | -1.37 |       |
| CG12581 |       |      |       |       |       | -0.54 |       |       |
| CG12643 |       |      |       |       | -2.08 |       |       | -2.80 |
| CG12814 |       |      |       | -1.43 |       |       |       |       |
| CG12868 | 1.91  |      | 2.28  | 1.75  | 2.89  | 1.69  | 2.49  |       |
| CG12896 | 3.81  |      | 4.46  | 3.78  | 2.84  |       | 3.04  |       |
| CG12926 |       |      | 0.71  |       | 1.12  | 0.84  | 0.79  |       |
| CG12991 | 0.70  |      |       | 0.81  | 1.55  | 1.03  | 1.25  | 2.30  |
| CG13014 |       |      |       |       | 1.03  | 0.79  |       |       |
| CG13085 |       |      |       |       |       |       | -1.34 |       |
| CG13097 |       | 0.54 |       |       |       | 0.38  |       | 1.96  |
| CG13255 |       |      | -1.03 | -1.50 | -1.00 | -0.79 | -1.59 | -1.32 |
| CG13315 |       |      | -0.80 | -0.69 |       |       | -1.71 | -2.01 |
| CG13321 | 0.98  |      |       |       | 1.56  | 0.84  |       |       |
| CG13392 |       |      |       |       | 0.99  | 0.76  |       |       |
| CG13398 |       |      |       |       |       |       | 0.87  |       |
| CG13482 | 1.12  |      |       |       | 1.03  | 0.48  | -0.54 |       |
| CG13631 |       |      |       |       |       |       | 0.84  | 1.65  |
| CG13850 |       |      |       |       |       | 0.72  | 1.12  |       |
| CG13896 |       |      |       |       | 1.65  |       |       |       |
| CG13933 |       |      |       |       |       |       |       | -2.17 |
| CG14434 |       |      |       |       | 0.90  | 0.80  |       |       |
| CG14440 |       |      | 0.99  |       |       |       |       | 1.60  |
| CG14478 |       |      |       |       | 0.96  | 0.65  | 0.69  | 1.58  |
| CG14567 |       |      |       |       | -0.96 |       |       |       |
| CG14767 |       |      | -1.35 | -1.37 |       |       | -0.99 |       |
| CG14818 |       |      | -0.53 |       |       |       | -1.29 | -1.36 |
| CG15083 |       |      |       | -0.89 |       |       |       |       |
| CG15210 |       |      | -0.50 | -0.96 |       |       | -1.12 |       |
| CG15211 |       |      |       |       | 1.35  | 1.35  |       |       |
| CG15653 |       |      |       |       |       |       | 1.17  |       |
| CG15717 |       |      |       |       | 0.77  | 0.64  |       |       |
| CG15747 |       |      |       |       | 1.00  | 0.65  |       |       |
| CG16717 |       |      |       |       | 0.82  | 0.77  |       |       |
| CG16721 | -0.79 |      | -1.83 | -1.52 |       | -0.59 | -0.96 |       |
| CG16791 |       |      |       |       | 0.76  | 0.41  |       | 1.50  |
| CG17002 |       |      |       |       |       |       | 1.33  |       |
| CG17260 |       |      | 1.60  |       | 0.91  | 0.38  | 2.00  |       |
| CG17266 |       |      |       | 1.08  | 0.95  | 0.74  |       | 1.61  |
| CG17271 |       |      | -0.54 | -1.06 | -0.55 | -0.57 | -2.32 | -1.41 |

|         |       |       |       |       |       |       |       |       |
|---------|-------|-------|-------|-------|-------|-------|-------|-------|
| CG17272 |       |       | -0.49 |       |       |       | -1.15 |       |
| CG17544 |       |       |       |       |       |       | -0.92 |       |
| CG17570 | 2.11  | 0.76  | 2.88  | 2.27  | 2.22  | 1.67  | 2.25  | 1.72  |
| CG17574 | 0.72  |       |       |       | 0.95  |       |       |       |
| CG17636 | -1.23 | -0.67 |       |       | -1.06 | -0.57 | -1.49 |       |
| CG1764  |       |       |       |       |       |       | 1.90  | 2.60  |
| CG17681 |       |       | 1.51  | 3.31  | 2.07  |       |       | 2.87  |
| CG17746 |       |       |       |       | 0.83  |       |       |       |
| CG17816 |       |       |       |       |       |       | 1.69  | 2.88  |
| CG1785  |       |       |       | 1.16  |       | 0.55  |       |       |
| CG17896 |       |       | 0.86  |       |       |       |       |       |
| CG1792  |       |       |       |       | 0.86  | 0.77  |       |       |
| CG17982 |       |       |       |       | 1.51  | 0.78  |       |       |
| CG18473 |       |       |       |       | 0.91  |       |       |       |
| CG18659 |       |       |       | 1.08  | 1.07  | 0.56  | 0.88  |       |
| CG1890  | 1.10  |       |       |       | 2.16  | 1.65  |       |       |
| CG1943  |       |       | -1.06 | -1.25 |       |       |       | -1.82 |
| CG1965  |       |       |       |       | 1.09  | 0.87  |       |       |
| CG2003  |       |       | 1.32  |       | 2.08  | 1.68  | 2.64  | 1.36  |
| CG2182  |       |       |       |       | 0.59  | 0.45  |       |       |
| CG2201  |       |       |       |       |       | 0.49  |       |       |
| CG2608  |       |       |       |       |       | 0.70  |       |       |
| CG2811  |       |       |       |       | -0.76 |       | -1.45 |       |
| CG2818  |       |       |       |       | 1.11  | 0.51  |       | 1.48  |
| CG2852  |       |       |       |       |       |       | -0.65 |       |
| CG2865  | 1.46  | 0.80  | 1.59  | 1.96  | 1.66  | 1.17  | 1.33  | 1.45  |
| CG2906  |       |       |       | 1.54  | 2.02  |       |       |       |
| CG2909  | 2.36  | 0.89  | 3.28  | 2.92  | 4.39  | 2.89  | 3.92  |       |
| CG2991  | 0.96  |       | 0.45  | 1.15  | 2.42  | 1.61  | 1.56  | 2.28  |
| CG30122 |       |       |       |       |       | 0.48  |       |       |
| CG30159 |       |       |       |       | 1.08  | 0.65  |       | 1.80  |
| CG30411 |       |       | -0.91 | -1.34 |       |       | -1.05 |       |
| CG31038 |       |       | 0.95  |       | 0.76  | 0.45  | 1.48  |       |
| CG31141 |       |       |       |       |       | -0.66 |       |       |
| CG31230 |       |       |       |       |       |       | 2.38  |       |
| CG31287 |       |       |       |       |       | -0.45 |       |       |
| CG31381 |       |       |       |       |       |       |       | 2.15  |
| CG31523 |       |       |       |       | 0.62  | 0.42  | 0.47  |       |
| CG3165  |       |       |       |       | 1.53  | 1.45  |       |       |
| CG31800 |       |       |       |       |       |       | -1.57 |       |
| CG31955 |       |       | 0.80  | 1.15  | 1.18  | 1.32  | 1.52  |       |
| CG32115 | 0.90  |       | 0.86  | 0.86  | 1.80  | 1.47  | 1.34  |       |
| CG32137 |       |       |       |       | 1.05  | 0.59  | 0.59  |       |
| CG32176 |       |       | 1.34  |       |       |       |       |       |
| CG32276 |       |       |       |       |       |       | -0.79 |       |
| CG32369 | 1.11  | 0.84  | 1.10  | 1.44  | 2.21  | 1.93  | 1.92  |       |

|         |       |       |       |       |       |       |       |       |
|---------|-------|-------|-------|-------|-------|-------|-------|-------|
| CG32428 |       |       | -0.82 | -0.91 |       |       | -0.98 |       |
| CG32452 |       |       |       | 1.89  |       | 0.83  |       |       |
| CG32486 | -0.76 | -0.59 | -1.41 |       |       | -0.68 |       |       |
| CG32576 |       |       |       |       |       |       | -1.67 |       |
| CG32767 |       |       | -0.77 |       |       |       |       |       |
| CG3277  |       |       |       |       |       | 0.62  |       |       |
| CG32772 |       |       |       |       | 0.79  | 0.52  |       |       |
| CG33116 | 1.07  |       |       |       | 2.13  | 1.77  | 0.68  |       |
| CG33120 |       |       |       |       | 0.70  |       |       |       |
| CG33170 |       |       |       |       |       |       | -0.68 |       |
| CG3348  | 1.39  | 1.04  | 2.52  | 2.62  | 2.35  | 2.06  | 2.58  | 1.74  |
| CG33514 |       |       | -0.87 | -0.84 | -0.71 |       | -1.54 | -1.25 |
| CG33695 |       |       | 1.32  |       |       |       | 1.52  |       |
| CG33926 |       |       |       |       |       |       | -1.03 |       |
| CG34112 |       |       |       |       |       |       | -1.28 |       |
| CG34126 |       |       |       |       | 0.68  |       |       |       |
| CG34133 |       |       |       | 0.98  | 1.01  | 0.70  |       | 1.28  |
| CG3420  |       |       |       |       |       |       |       | 1.53  |
| CG34228 |       |       |       |       |       |       | -1.16 |       |
| CG34232 |       |       | -1.63 | -1.01 | -1.02 | -0.93 | -2.20 |       |
| CG34279 |       |       |       |       | -1.20 |       |       |       |
| CG3437  |       |       |       |       |       |       | -2.08 |       |
| CG34376 |       |       |       |       |       |       | -2.18 |       |
| CG34417 |       |       |       |       |       |       | -0.76 |       |
| CG3448  | 1.14  |       | 2.03  |       | 2.38  | 1.91  | 2.29  |       |
| CG3529  |       |       |       |       | 1.04  | 0.49  |       |       |
| CG3566  |       |       |       | -0.69 |       |       |       |       |
| CG3609  |       |       | 0.89  |       |       |       |       |       |
| CG3792  |       |       | 1.48  |       | 1.20  | 1.62  | 2.25  |       |
| CG3862  |       |       |       |       | 0.98  |       |       |       |
| CG3961  |       |       | -0.94 |       |       | -0.38 | -2.50 |       |
| CG3987  |       |       |       |       | 0.97  |       | 0.56  |       |
| CG4004  |       |       |       |       | 1.20  | 0.73  |       | 1.83  |
| CG4080  |       |       |       |       | 0.92  |       |       |       |
| CG42240 | 1.55  | 0.64  | 3.01  | 2.57  | 3.60  | 2.18  | 4.34  | 4.76  |
| CG42258 |       |       | -0.70 | -0.77 |       |       |       |       |
| CG42327 |       |       | 0.82  |       | 0.81  | 0.56  | 1.18  |       |
| CG42359 | 0.89  |       |       |       | 1.09  | 0.63  |       |       |
| CG42364 |       |       |       |       | 1.04  | 0.94  |       | 4.16  |
| CG42365 | 3.37  | 0.84  | 3.89  | 3.72  | 4.86  | 3.94  | 4.11  | 3.46  |
| CG42668 |       |       |       |       | 0.97  | 0.61  | 1.05  |       |
| CG42674 |       |       |       |       | 1.33  | 1.16  | 0.75  | 1.62  |
| CG42699 |       |       |       |       | 0.77  |       |       |       |
| CG42709 |       |       | 0.77  |       | 1.87  | 1.49  | 2.14  |       |
| CG42806 |       |       | 0.96  |       |       |       |       |       |
| CG42855 |       |       |       |       |       | -0.47 |       |       |

|         |       |       |       |       |       |       |       |       |
|---------|-------|-------|-------|-------|-------|-------|-------|-------|
| CG4297  |       |       |       |       |       |       |       | 2.01  |
| CG43051 |       |       | -0.75 | -1.05 | -0.75 |       | -1.84 |       |
| CG43121 |       |       |       |       |       |       |       | 3.32  |
| CG4362  |       |       |       |       | 4.04  |       |       |       |
| CG43736 |       |       | 0.70  |       | 1.80  | 1.21  | 1.05  | 1.56  |
| CG44251 | 1.34  |       | 0.57  |       | 1.62  | 1.11  | 0.71  |       |
| CG45218 |       |       |       |       | 3.05  | 2.21  |       |       |
| CG4572  |       |       | -0.97 |       | -0.95 | -0.40 |       | -1.21 |
| CG4607  | 2.11  | 1.10  | 1.70  | 0.93  | 1.53  | 1.23  | 0.65  |       |
| CG4619  |       |       |       |       |       | 0.72  |       |       |
| CG46280 |       |       |       |       |       |       | -1.10 |       |
| CG46304 |       |       |       |       |       | -0.52 |       |       |
| CG4797  | 1.36  | 1.18  | 1.65  | 2.18  | 2.27  | 2.31  | 1.96  |       |
| CG4887  |       |       |       |       | 1.00  | 0.76  |       |       |
| CG5004  |       |       |       |       | 1.39  | 1.07  | 0.77  |       |
| CG5027  |       |       |       |       |       | 0.57  |       |       |
| CG5028  |       |       | -0.63 |       |       |       | -1.05 |       |
| CG5096  |       |       | -0.46 | -0.77 |       |       | -0.73 |       |
| CG5131  |       |       |       |       | 0.75  | 0.86  |       |       |
| CG5151  |       |       |       |       |       |       |       | 1.68  |
| CG5335  |       |       |       |       | 1.30  | 0.39  |       |       |
| CG5346  | 1.03  | 0.52  | 0.60  | 1.23  | 1.76  | 1.56  | 1.42  |       |
| CG5391  |       |       |       |       | -1.53 |       |       |       |
| CG5541  |       |       |       |       | 0.90  | 0.66  |       |       |
| CG5757  |       |       |       |       |       |       |       | 1.79  |
| CG5808  |       |       |       |       | 1.01  | 0.85  | 2.10  | 2.08  |
| CG5823  |       |       |       |       | 0.69  |       |       |       |
| CG5835  |       |       | 0.67  |       |       |       |       |       |
| CG5853  |       |       |       |       |       | 0.54  |       |       |
| CG5885  |       |       |       |       |       | -0.36 |       |       |
| CG5916  |       | 0.72  |       |       | 0.91  | 1.26  |       |       |
| CG5953  |       |       |       |       | 1.85  | 1.21  | 0.76  | 1.74  |
| CG5958  |       |       | 0.52  |       |       | 0.43  | -1.56 |       |
| CG5969  |       |       |       |       |       |       |       | 1.50  |
| CG6115  |       |       |       |       |       |       | 0.81  |       |
| CG6178  |       |       |       |       |       |       | -0.73 |       |
| CG6204  |       |       |       |       | 1.27  |       | 1.22  |       |
| CG6218  |       |       |       |       |       |       | -1.02 |       |
| CG6398  |       |       | -1.90 |       |       |       |       |       |
| CG6707  |       |       |       |       | 0.66  |       |       |       |
| CG6762  |       |       |       |       | 1.02  | 0.88  | 1.12  |       |
| CG6770  | -0.80 | -0.82 | -1.35 | -1.36 |       | -0.87 | -1.04 |       |
| CG6785  |       |       |       |       | 1.97  |       |       |       |
| CG6805  |       |       |       |       | 0.91  | 0.77  |       |       |
| CG6891  |       |       |       |       |       | 0.94  |       |       |
| CG7029  |       |       |       |       | 0.57  |       |       |       |

|        |       |      |       |       |       |       |       |       |
|--------|-------|------|-------|-------|-------|-------|-------|-------|
| CG7083 |       |      | -1.28 | -1.63 |       |       | -1.41 |       |
| CG7099 |       |      |       |       | 0.87  |       |       |       |
| CG7182 |       |      |       | 0.83  |       |       |       |       |
| CG7457 |       |      |       |       | 1.28  | 0.60  |       |       |
| CG7556 |       |      | -0.59 |       |       |       |       |       |
| CG7564 |       |      | 1.14  |       |       |       | 1.94  | 1.70  |
| CG7611 |       |      | -0.67 | -0.77 |       |       |       |       |
| CG7630 |       |      |       | -0.63 |       |       | -0.73 |       |
| CG7668 |       |      |       |       | 0.67  |       |       |       |
| CG7728 |       |      |       |       |       | 0.52  |       |       |
| CG7737 |       |      | 1.46  |       |       |       |       |       |
| CG7806 |       |      |       |       | 0.83  | 0.68  |       |       |
| CG7849 |       |      |       | 1.59  |       |       |       |       |
| CG7900 |       |      |       |       | 0.95  | 0.63  |       |       |
| CG7943 |       |      | 0.82  | 0.92  | 0.78  | 0.49  |       | 1.34  |
| CG7966 | 0.94  |      | 1.46  |       |       |       |       |       |
| CG8003 |       |      |       |       |       |       |       | 1.61  |
| CG8009 |       |      |       |       |       |       | -0.99 |       |
| CG8051 |       |      |       |       |       | 0.67  |       |       |
| CG8066 |       |      |       |       | 1.72  | 1.18  | 0.70  |       |
| CG8067 |       |      |       | 1.37  |       |       |       |       |
| CG8079 |       |      |       |       | 0.76  |       |       |       |
| CG8112 |       |      | -1.63 | -1.06 | -1.01 |       |       | -2.01 |
| CG8152 |       |      |       |       | 1.27  |       |       |       |
| CG8209 |       |      |       |       | 0.73  |       |       |       |
| CG8223 |       |      |       |       | 1.06  | 0.68  | 0.86  |       |
| CG8229 |       |      |       | 1.68  | 0.98  | 0.46  | 1.19  | 1.76  |
| CG8312 | 0.86  |      |       |       | 1.89  | 1.36  | 1.67  | 1.74  |
| CG8320 |       |      |       |       |       |       | -1.09 |       |
| CG8353 | 1.04  |      | 0.71  |       | 1.31  |       |       | -1.52 |
| CG8360 |       |      |       | -1.18 |       |       |       |       |
| CG8372 |       |      |       | -0.86 |       |       |       |       |
| CG8414 | 0.83  |      |       |       | 1.74  | 1.24  |       | 2.17  |
| CG8420 |       |      |       |       | -0.74 |       |       |       |
| CG8490 |       |      |       | 1.92  |       |       |       | 2.21  |
| CG8578 | 0.84  | 0.70 |       |       | 1.73  | 1.43  |       |       |
| CG8665 | -0.85 |      | -0.85 |       | -0.88 | -0.55 |       |       |
| CG8679 |       |      |       |       | 1.21  | 0.90  |       |       |
| CG8892 |       |      |       |       |       | 0.69  | 1.27  |       |
| CG8944 |       |      |       |       | 0.97  |       |       | 1.76  |
| CG8997 |       |      |       | -1.20 | -0.98 | -0.53 | -2.62 | -2.48 |
| CG9003 |       |      | -0.87 | -1.12 |       |       |       |       |
| CG9004 |       | 0.63 |       |       |       |       |       |       |
| CG9005 |       |      | -1.30 |       |       |       | -1.23 |       |
| CG9008 |       |      | -1.25 |       |       | -0.74 | -1.97 |       |
| CG9328 |       |      |       |       | -0.59 |       |       |       |

|              |       |  |       |       |       |       |       |       |
|--------------|-------|--|-------|-------|-------|-------|-------|-------|
| CG9338       |       |  |       |       |       | -0.41 |       |       |
| CG9399       |       |  | 0.68  |       |       |       |       |       |
| CG9471       |       |  |       |       |       | -0.60 | -1.23 |       |
| CG9596       |       |  |       |       | 0.97  | 0.78  |       | 1.70  |
| CG9663       | 0.90  |  | 0.67  |       | 2.08  | 1.14  | 1.39  |       |
| CG9667       |       |  |       |       | 0.77  |       |       |       |
| Charon       |       |  | 0.74  | 0.98  | 1.07  |       |       |       |
| Chchd2       |       |  |       |       | 0.66  |       |       |       |
| Chd64        |       |  | -0.93 | -1.02 |       |       | -1.16 | -1.54 |
| CHES-1-like  |       |  |       |       |       | 0.43  |       |       |
| chic         |       |  |       |       |       | 0.49  |       |       |
| chinmo       |       |  | 1.83  | 2.25  | 1.80  | 1.03  | 3.26  | 4.30  |
| CHMP2B       | 0.98  |  |       |       | 1.90  | 1.07  | 0.89  |       |
| Chro         |       |  | 1.35  |       | 0.90  | 0.57  | 1.54  | 1.89  |
| Chsy         |       |  |       |       |       | -0.63 |       |       |
| CIAPIN1      |       |  | 0.81  | 0.88  | 1.02  | 0.66  | 1.29  |       |
| cib          |       |  | -0.67 |       |       |       | -0.76 |       |
| Ciz1         |       |  | 0.78  | 0.79  | 1.06  | 0.57  | 1.19  |       |
| Ckl1alpha-i1 |       |  |       |       | 1.51  | 1.17  |       |       |
| ckn          |       |  |       |       |       | 0.76  |       |       |
| clu          |       |  |       |       | 0.58  |       |       |       |
| Cnot4        |       |  |       |       | 0.59  |       |       |       |
| Cnx99A       |       |  |       |       |       |       | -1.10 |       |
| cora         |       |  |       |       | 0.65  |       |       |       |
| Cortactin    |       |  |       |       | 1.23  | 1.00  |       |       |
| COX5A        |       |  |       | -0.62 |       | -0.31 | -0.79 |       |
| COX7C        |       |  |       | -0.60 |       |       | -0.78 |       |
| COX8         |       |  |       | -0.83 |       | -0.35 | -1.12 |       |
| cpa          |       |  |       |       | 1.24  | 0.69  | 0.57  |       |
| Cpsf5        |       |  | 0.80  | 0.92  | 0.69  | 0.67  |       |       |
| CR43727      |       |  |       |       |       |       |       | 2.87  |
| CR43972      |       |  |       |       |       |       | 3.33  |       |
| crc          |       |  |       |       | 1.17  | 0.61  | 1.45  |       |
| CrebA        | 0.64  |  | 0.81  | 0.84  | 0.79  | 0.52  | 0.93  |       |
| CrebB        | 0.73  |  |       |       | 1.50  | 0.97  | 0.98  |       |
| CREG         |       |  | -1.12 | -1.15 |       |       | -1.31 | -1.71 |
| Crtc         |       |  |       |       | 0.68  | 0.49  |       | 1.44  |
| Csl4         |       |  |       |       |       | 0.60  |       |       |
| CstF64       |       |  |       |       | 1.10  |       |       |       |
| Ctl2         |       |  |       | -1.21 |       |       |       |       |
| Ctr1B        |       |  |       | -1.21 | -1.06 | -0.79 | -1.97 | -2.71 |
| CtsB         |       |  | -0.79 | -0.81 | -0.53 | -0.48 | -1.54 | -1.30 |
| CtsF         | -0.75 |  | -1.72 | -1.90 | -0.89 | -0.58 | -1.95 | -2.01 |
| cu           | 0.73  |  | 1.64  | 1.88  |       | 0.53  |       |       |
| Cyp1         |       |  |       |       |       |       | -0.45 |       |
| Cyp6u1       |       |  |       |       |       | 0.50  |       |       |



|            |      |      |       |       |       |       |       |       |
|------------|------|------|-------|-------|-------|-------|-------|-------|
| Cyp6v1     |      | 0.55 |       |       |       | 0.70  |       |       |
| Cyp9f2     |      |      | -0.95 | -1.14 |       |       | -1.21 | -1.84 |
| cype       |      |      |       | -0.83 |       | -0.33 | -0.98 |       |
| Cyt-b5     |      |      |       |       | -0.57 |       | -0.95 |       |
| D2hgdh     |      |      |       |       |       |       | -1.50 |       |
| da         | 0.64 |      | 0.74  |       | 1.23  | 0.67  | 0.81  | 1.66  |
| Dad        | 0.89 |      | 1.11  | 0.82  | 1.36  | 1.05  | 1.91  | 2.01  |
| Dap160     |      |      |       |       | 0.60  | 0.48  |       |       |
| Dark       |      |      |       |       | 1.12  |       |       |       |
| daw        |      |      | 1.04  | 1.62  | 0.97  |       | 1.88  | 3.77  |
| Daxx       |      |      |       |       | 0.74  |       |       | 1.52  |
| dbe        |      |      |       |       |       | 0.47  |       |       |
| dco        |      |      |       |       | 0.83  | 0.40  |       |       |
| Den1       |      |      |       | 1.06  |       | 0.37  |       | 2.55  |
| Desat1     |      |      | -0.85 | -0.74 |       |       | -0.73 |       |
| Df31       |      |      |       |       | 0.64  | 0.37  | 0.91  |       |
| Dgp-1      | 0.95 |      | 2.42  | 1.58  | 3.24  | 1.13  | 3.92  | 3.62  |
| Dhdds      |      |      |       |       | 0.74  | 0.52  | 1.11  |       |
| Diap1      |      |      |       |       | 1.45  | 1.16  | 1.00  |       |
| Dic1       |      |      |       |       |       |       | -0.75 |       |
| didum      |      |      |       |       | 0.82  | 0.47  |       |       |
| Diedel     |      |      |       |       |       |       |       | 2.78  |
| DI         |      |      |       |       | 0.85  | 0.67  |       |       |
| dl         | 0.83 |      |       |       | 2.39  | 1.77  | 0.99  | 1.20  |
| Dlc90F     |      |      |       |       |       |       | 0.64  |       |
| Dlic       |      |      |       |       | 0.83  | 0.54  | 0.57  |       |
| Dmtn       |      |      |       |       | 0.76  |       |       | 1.72  |
| dnr1       |      |      |       |       | 1.26  | 0.84  |       | 2.56  |
| DOR        |      |      |       |       |       |       | 0.58  |       |
| Dp1        |      |      |       |       |       |       | -0.95 |       |
| Dph4       |      |      |       |       | 0.91  | 0.62  |       |       |
| Drat       | 1.55 | 0.60 | 0.75  | 1.34  | 2.32  | 1.11  | 1.00  | 1.89  |
| Dredd      |      |      |       |       | 0.76  | 0.65  |       |       |
| dsd        |      |      |       |       | 1.34  | 0.79  |       |       |
| dtn        |      |      |       |       | 0.54  |       |       | 1.82  |
| dUTPase    |      |      |       |       |       |       | 1.39  |       |
| Dyro       |      |      |       |       | 0.81  | 0.73  |       |       |
| E(var)3-9  |      |      |       | 1.48  | 1.25  | 0.69  |       |       |
| Edem2      |      |      | -0.92 |       |       |       | -1.81 |       |
| edl        |      |      |       |       | 0.83  |       |       |       |
| EDTP       |      |      | -1.58 |       |       | -0.51 | -1.38 |       |
| eEF1alpha1 |      |      |       |       |       |       | -0.61 |       |
| eEF2       |      |      |       |       |       |       | -1.03 | -1.39 |
| Efa6       |      |      |       |       | 0.94  | 0.72  |       | 1.81  |
| eIF1       |      |      |       |       |       |       | -0.48 |       |
| eIF2Bbeta  |      |      |       |       | 0.61  |       |       |       |

|            |      |      |       |       |      |       |       |       |
|------------|------|------|-------|-------|------|-------|-------|-------|
| eIF2beta   |      |      | 0.47  |       | 0.72 | 0.54  |       | 1.63  |
| eIF3b      |      |      |       | -0.59 |      |       | -0.56 |       |
| eIF3c      |      |      |       |       |      |       | -1.11 |       |
| eIF3I      |      |      | -0.85 | -0.70 |      |       | -0.91 | -1.55 |
| eIF4A      |      |      |       |       |      |       | -1.01 | -1.65 |
| eIF4EHP    |      |      |       |       |      | 0.59  | 0.63  |       |
| eIF4G2     |      |      | -0.64 |       |      |       |       |       |
| eIF6       | 1.45 | 0.62 | 2.17  | 2.36  | 2.86 | 1.48  | 2.83  | 2.41  |
| Eip63E     |      |      |       |       | 0.66 | 0.40  |       |       |
| Eip75B     | 1.09 |      | 2.23  | 2.14  | 1.60 | 1.49  | 2.63  | 2.01  |
| elav       |      |      |       |       |      |       |       | 2.02  |
| eIB        |      |      |       |       | 0.80 | 0.40  |       | 3.10  |
| EloC       |      |      |       |       |      |       | -0.70 |       |
| emb        |      |      |       |       |      |       |       | 1.43  |
| emc        |      |      |       |       |      |       | -0.98 |       |
| EndoGl     |      |      |       |       | 1.19 | 0.96  | 1.11  |       |
| Epp        |      |      |       |       |      |       |       | 1.75  |
| Ercc1      |      |      |       | 2.97  | 1.38 |       | 2.35  |       |
| Es2        |      |      | 1.09  |       | 0.99 | 0.79  | 2.14  |       |
| Ets21C     | 2.95 | 1.80 | 1.74  | 2.14  | 5.33 | 4.28  | 3.20  | 3.58  |
| ex         |      |      |       |       | 1.57 | 1.36  |       |       |
| exd        |      |      | -0.80 |       |      |       |       |       |
| Exo84      |      |      |       |       | 1.23 | 0.74  |       |       |
| FASN1      |      |      | 1.08  | 1.34  |      |       |       |       |
| fax        |      |      |       |       |      | -0.37 |       |       |
| fbl        |      |      |       |       | 0.56 |       |       |       |
| Fbp1       |      |      |       |       |      |       |       | -2.72 |
| Fer1HCH    |      |      |       |       |      |       | -1.02 | -1.21 |
| Fer2LCH    |      |      |       | -0.54 |      |       | -1.31 | -1.33 |
| Fib        |      | 0.53 |       |       |      |       |       |       |
| Fibp       |      |      |       |       |      | 0.59  |       |       |
| Fim        |      |      |       |       | 1.06 | 0.85  |       |       |
| fkx        |      |      |       | 0.80  | 1.45 | 0.93  | 0.83  | 1.85  |
| flil       |      |      |       |       | 0.83 | 0.72  |       |       |
| Flo2       |      |      |       |       | 1.15 | 0.75  | 1.33  |       |
| fok        |      |      | -1.05 | -0.92 |      | -0.67 | -1.53 |       |
| for        |      |      |       |       |      |       | 0.79  |       |
| fs(1)h     |      |      |       |       | 0.78 | 0.47  | 0.47  | 1.48  |
| Fur1       |      |      |       |       | 0.67 |       |       |       |
| Gadd45     | 4.21 | 2.59 | 4.28  | 4.39  | 4.62 | 4.18  | 4.55  | 3.55  |
| Galphaf    |      |      |       | 1.22  | 1.13 | 1.09  |       | 1.34  |
| Galphai    | 0.76 |      |       |       | 1.92 | 1.21  | 1.01  | 2.10  |
| Galphaq    |      |      |       | -1.28 |      |       |       |       |
| gammaSnap1 |      |      |       |       |      |       | -0.94 | -1.36 |
| Gapdh2     |      |      |       |       |      |       | -0.58 | -1.30 |
| Gas41      |      |      | 1.26  |       |      |       |       |       |

|         |      |       |       |       |       |       |       |       |
|---------|------|-------|-------|-------|-------|-------|-------|-------|
| GATAd   | 0.79 |       |       |       | 1.61  | 1.19  |       | 1.47  |
| Gclm    |      |       |       |       | -0.57 |       | -0.84 |       |
| Gcn5    | 1.33 |       | 1.62  |       | 2.61  | 1.63  | 2.96  | 2.60  |
| Gga     |      |       |       |       |       | 0.50  |       |       |
| ghi     |      |       |       |       | 1.54  | 1.01  | 1.22  |       |
| Gk2     |      |       | 1.46  | 1.14  | 1.06  | 0.62  | 1.51  | 2.01  |
| GlcT    | 0.97 |       |       | 0.99  | 1.87  | 1.12  | 1.25  |       |
| glec    |      |       |       |       | 0.83  | 0.75  | 1.70  | 1.57  |
| Gli     | 0.88 |       |       |       | 1.26  | 0.83  |       |       |
| glo     |      |       |       |       |       | 0.54  |       |       |
| GlyRS   |      |       | 0.62  |       |       |       |       |       |
| Gmd     | 1.01 |       | 0.75  | 0.94  | 1.72  | 1.14  | 0.96  | 1.50  |
| GMF     |      |       | -0.70 |       |       |       |       |       |
| Gnpat   | 1.14 |       | 0.91  |       | 1.64  | 1.34  | 1.15  | 1.55  |
| Got2    |      |       | 0.82  | 0.82  | 1.02  | 0.36  | 1.72  |       |
| Gp150   |      |       | -0.75 | -0.63 |       |       | -0.73 |       |
| Gpat4   |      |       |       |       | -0.65 |       | -1.78 | -1.64 |
| gpp     |      |       |       | 0.83  |       |       |       | 1.79  |
| Gprk2   |      |       |       |       | 1.36  | 0.71  | 1.06  | 1.71  |
| Graf    |      |       |       |       | 0.79  | 0.43  |       |       |
| gro     |      |       |       |       |       |       | 0.83  |       |
| GstD1   |      |       | 1.04  | 0.56  | 0.69  |       | 0.66  |       |
| GstE12  |      |       |       |       |       |       | -0.63 |       |
| GstO3   |      | -0.80 | -0.60 |       | -1.10 | -1.15 | -0.61 |       |
| GstS1   |      |       | 1.15  | 1.03  |       |       | 1.16  |       |
| GstT4   |      | -0.68 | -1.96 | -1.29 | -0.92 | -0.65 | -2.78 | -2.38 |
| h       | 2.19 | 1.18  | 2.40  | 2.50  | 2.29  | 1.69  | 1.84  | 2.76  |
| Hacl    |      |       |       |       |       |       | -0.63 |       |
| HDAC4   |      |       |       |       |       |       | 0.84  | 1.71  |
| hdc     |      |       |       |       | 1.08  | 0.53  |       |       |
| hdly    |      |       |       |       | 1.15  | 0.83  | 2.99  |       |
| Herp    |      |       |       |       |       | -0.62 |       |       |
| Hex-A   |      |       | 0.65  |       | 0.84  | 0.43  | 1.01  |       |
| hh      | 1.90 |       | 1.83  | 0.91  | 2.12  | 1.18  | 1.78  |       |
| hid     |      |       |       |       |       | 0.73  |       | 2.09  |
| Hip1    |      |       | -0.66 |       | 0.91  | 0.67  |       |       |
| His4r   |      |       | -0.79 | -0.94 | -0.75 | -0.57 | -1.43 | -1.79 |
| HmgD    |      |       |       |       |       | 0.50  |       |       |
| HmgZ    |      |       |       |       |       |       | -0.87 | -1.62 |
| Hph     |      |       | -0.84 |       |       | -0.54 |       |       |
| Hr39    |      |       |       |       | 0.64  |       |       |       |
| Hr96    | 0.76 |       |       | 1.07  | 1.34  | 1.27  | 1.10  | 1.56  |
| Hrb87F  |      |       |       |       | 0.71  |       |       | 1.72  |
| Hsc70-3 | 0.79 |       | 0.59  |       |       |       |       |       |
| Hsc70-4 |      |       |       |       |       |       | -0.55 |       |
| Hsc70-5 |      |       | 0.64  |       |       |       |       |       |

|            |      |      |       |       |       |       |       |       |
|------------|------|------|-------|-------|-------|-------|-------|-------|
| Hsp23      |      |      | -2.04 | -2.13 |       |       | -3.22 | -3.32 |
| Hsp26      |      |      | -1.98 | -2.27 |       |       | -3.57 | -2.99 |
| Hsp27      |      |      | -2.29 | -1.73 |       |       | -3.09 | -2.08 |
| Hsp68      |      |      | -1.81 | -1.50 |       |       | -2.58 |       |
| hts        |      |      |       |       |       | 0.34  |       |       |
| Hus1-like  |      |      |       |       |       |       |       | 3.21  |
| ifc        |      |      |       |       | 1.38  | 0.84  | 0.52  |       |
| lfrd1      | 1.98 |      | 2.58  | 2.79  | 3.20  | 2.56  | 2.96  | 2.66  |
| imd        |      |      |       |       | 0.91  | 0.60  |       |       |
| Ino80      |      |      |       |       | 0.71  | 0.62  |       | 1.81  |
| InR        |      |      |       |       | 0.91  | 0.47  |       | 1.66  |
| IntS4      |      |      |       |       |       | 0.55  |       |       |
| IntS6      |      |      |       |       | 0.86  | 0.62  |       | 1.39  |
| Ip259      |      |      | -0.89 | -0.90 | -0.67 | -0.40 | -1.75 | -1.69 |
| IP3K2      |      |      |       |       | 0.76  |       | 1.09  |       |
| Ipk2       | 1.18 |      |       |       | 3.42  | 2.58  | 1.84  |       |
| Irbp18     |      |      |       |       | 0.99  | 0.50  |       | 1.91  |
| Ire1       |      |      | -0.73 |       |       |       |       |       |
| isoQC      |      |      |       |       |       |       | -1.37 |       |
| Jafrac1    |      |      | 0.51  |       |       |       | -0.96 |       |
| Jheh1      |      |      |       |       | -0.76 | -0.52 | -1.38 |       |
| JIL-1      |      |      |       |       | 0.55  | 0.50  |       | 1.30  |
| Jra        |      |      |       |       | 2.02  | 1.63  | 0.96  |       |
| jvl        |      |      |       |       | 0.62  |       |       |       |
| Jwa        |      |      | -0.49 | -0.81 |       |       | -1.36 |       |
| Kap-alpha3 |      |      |       |       |       |       | -0.74 |       |
| Kat60      |      |      |       |       | 0.78  |       |       |       |
| kay        | 0.73 |      | 0.64  | 0.87  | 1.88  | 1.16  | 1.53  |       |
| Kdm2       |      | 0.60 |       |       | 1.20  | 0.94  |       |       |
| kibra      | 0.67 |      |       |       | 1.59  | 0.94  |       | 1.55  |
| Klp10A     |      |      |       |       | 1.05  | 0.52  | 1.47  |       |
| Klp31E     |      |      | -1.20 |       |       |       |       |       |
| Klp64D     |      |      |       |       |       | 0.66  |       |       |
| kra        |      |      | 0.55  |       | 0.79  | 0.53  | 0.85  |       |
| Kr-h1      | 0.87 | 0.66 | 2.34  | 1.17  | 1.81  | 1.61  | 2.93  |       |
| Krn        | 0.94 |      |       |       | 1.82  | 0.83  |       |       |
| l(1)G0320  |      |      |       |       | -0.55 |       | -1.29 | -1.24 |
| l(2)gd1    |      |      |       |       | 1.26  | 0.56  |       |       |
| l(2)k01209 |      |      | 0.75  | 1.19  | 1.34  | 1.34  | 1.72  | 2.25  |
| l(2)k09848 |      |      |       |       |       | 0.54  |       |       |
| l(3)02640  |      |      | 1.23  | 1.23  | 0.70  |       | 1.21  | 1.64  |
| l(3)05822  |      |      |       |       | 1.14  | 0.51  |       |       |
| l(3)07882  |      | 0.72 |       |       |       | 0.64  |       |       |
| l(3)73Ah   |      |      |       |       |       |       | 1.30  |       |
| L2HGDH     |      |      | -0.69 |       |       |       |       |       |
| La         | 1.11 | 0.64 | 1.08  | 1.30  | 2.01  | 1.58  | 1.77  | 1.18  |

|                |      |  |       |       |       |       |       |       |
|----------------|------|--|-------|-------|-------|-------|-------|-------|
| lawc           |      |  |       |       | 0.83  |       |       |       |
| Ldh            |      |  |       |       | 1.62  | 1.47  |       |       |
| levy           |      |  |       | -0.88 | -0.46 | -0.33 | -0.92 |       |
| LIMK1          |      |  | -0.99 |       |       |       |       |       |
| Lis-1          |      |  |       |       | 0.99  | 0.52  | 0.90  |       |
| Lk6            |      |  | -1.04 | -1.01 |       | -0.36 | -1.24 |       |
| lncRNA:CR30055 | 0.99 |  | 1.46  | 2.31  | 1.89  | 1.14  | 1.92  | 3.53  |
| lncRNA:CR31044 |      |  |       | -1.05 |       |       | -1.42 |       |
| lncRNA:CR32582 |      |  |       |       |       |       |       | -3.09 |
| lncRNA:CR32636 | 1.76 |  | 2.64  | 2.24  | 1.66  | 0.93  | 2.08  | 3.45  |
| lncRNA:CR33963 |      |  |       |       |       |       | -1.87 |       |
| lncRNA:CR42549 |      |  | -0.87 |       |       |       |       |       |
| lncRNA:CR42862 |      |  | -1.01 | -0.80 |       |       | -0.74 |       |
| lncRNA:CR42874 |      |  |       |       |       | 0.83  |       |       |
| lncRNA:CR43126 |      |  |       |       | 2.95  | 1.89  |       |       |
| lncRNA:CR43287 |      |  |       |       |       |       | 2.25  |       |
| lncRNA:CR43301 |      |  |       |       | 1.12  |       |       |       |
| lncRNA:CR43314 |      |  | -0.70 |       |       |       |       |       |
| lncRNA:CR43399 |      |  |       |       |       |       | 2.96  | 2.75  |
| lncRNA:CR43493 |      |  | -1.14 |       |       |       |       |       |
| lncRNA:CR43496 |      |  |       | 1.37  | 1.56  | 1.24  |       | 1.77  |
| lncRNA:CR43704 |      |  |       |       |       |       | 2.46  |       |
| lncRNA:CR43900 |      |  |       |       |       |       | 2.03  |       |
| lncRNA:CR43907 |      |  |       |       | 1.77  | 1.60  | 2.45  |       |
| lncRNA:CR43918 |      |  |       |       |       |       | 3.28  |       |
| lncRNA:CR43928 |      |  |       |       | 2.80  |       |       | 4.75  |
| lncRNA:CR43995 |      |  |       |       | 1.73  |       |       |       |
| lncRNA:CR44209 |      |  |       |       | -1.58 |       |       |       |
| lncRNA:CR44218 |      |  |       |       | 1.25  |       |       |       |
| lncRNA:CR44331 |      |  |       |       | 1.41  | 1.08  |       |       |
| lncRNA:CR44478 |      |  |       | 1.66  | 5.80  | 3.98  | 6.24  | 3.46  |
| lncRNA:CR44526 |      |  | 1.28  |       | 1.61  |       | 1.72  |       |
| lncRNA:CR44758 |      |  |       |       | 1.13  |       | 1.56  |       |
| lncRNA:CR44773 | 0.95 |  |       |       | 3.30  | 2.57  | 3.15  | 3.26  |
| lncRNA:CR44809 |      |  | 1.65  |       | 3.23  | 2.42  | 4.11  |       |
| lncRNA:CR44867 |      |  |       |       | 3.23  |       |       |       |
| lncRNA:CR44868 |      |  |       |       | 2.81  |       | 2.64  |       |
| lncRNA:CR45187 |      |  |       |       | 1.52  |       |       |       |
| lncRNA:CR45393 |      |  |       |       | 3.17  |       |       |       |
| lncRNA:CR45531 |      |  |       |       | 1.02  | 1.29  |       | 4.37  |
| lncRNA:CR45650 |      |  |       |       | 2.43  |       |       | 4.17  |
| lncRNA:CR45668 |      |  |       |       | 1.47  |       |       |       |
| lncRNA:CR45677 |      |  |       |       | 1.86  |       |       |       |
| lncRNA:CR45805 |      |  |       |       | 2.01  |       |       |       |
| lncRNA:CR45949 |      |  |       |       | 1.77  |       | 1.96  |       |
| lncRNA:CR46015 |      |  |       |       |       |       | 2.93  |       |

|                 |      |       |       |      |       |       |       |       |
|-----------------|------|-------|-------|------|-------|-------|-------|-------|
| lncRNA:CR46204  |      |       |       |      | 6.60  | 4.62  | 5.60  | 6.04  |
| lncRNA:Hsromege |      |       | 0.56  |      |       |       | 1.09  |       |
| lost            |      |       |       |      |       | 0.39  |       |       |
| LPCAT           |      |       |       |      | 0.65  | 0.48  |       |       |
| lqf             |      |       |       |      | 1.08  | 0.61  | 0.75  |       |
| Lrch            |      |       |       |      | 0.86  | 0.56  |       |       |
| Lsd-1           |      |       | -0.83 |      |       |       | -2.39 |       |
| Lsd-2           |      |       |       |      |       |       | -1.36 |       |
| Lsp1gamma       |      |       |       |      |       |       | -1.94 | -2.75 |
| Map205          |      |       | -0.76 |      |       |       | -0.71 |       |
| MAPk-Ak2        |      |       |       |      | 0.83  |       |       |       |
| mask            |      |       |       |      | 0.62  | 0.37  |       |       |
| Mcad            |      | -0.47 | -0.49 |      | -0.85 | -0.62 | -1.87 | -1.54 |
| MCU             | 0.64 |       |       | 1.79 | 2.10  | 1.55  | 2.68  | 3.22  |
| Mdh1            |      |       |       |      |       |       | -0.50 |       |
| Mdr49           | 1.56 | 0.70  | 1.52  | 0.93 | 1.87  | 0.96  | 1.17  |       |
| Mec2            |      |       |       |      | 1.37  | 1.07  | 0.64  |       |
| MED15           |      |       |       |      |       |       | 1.84  |       |
| MED16           |      |       |       |      | 0.90  |       |       |       |
| MED27           |      |       |       |      |       |       | 1.84  |       |
| Mef2            |      |       |       |      | 0.96  | 0.79  | 1.00  |       |
| Mekk1           |      |       |       |      | 1.89  | 1.36  |       | 1.82  |
| melt            | 1.11 |       |       |      | 1.66  | 1.19  |       |       |
| Meltrin         |      |       |       |      | 0.73  |       |       |       |
| mesh            |      |       |       |      | 1.17  | 0.70  |       |       |
| Mettl3          |      |       |       |      | 0.60  | 0.57  |       | 1.60  |
| Mhcl            |      |       |       |      |       |       |       | 1.75  |
| Mic26-27        |      |       |       |      |       |       | 0.55  |       |
| MICAL-like      |      |       |       |      | 1.01  | 1.00  |       |       |
| Mkk4            |      |       |       |      | 0.86  |       |       |       |
| Mkp3            | 0.65 |       |       |      | 1.48  | 1.02  | 1.23  | 1.50  |
| mlt             |      |       |       |      |       | -0.47 |       | -1.11 |
| MME1            |      |       |       |      | 1.41  | 0.94  | 0.94  |       |
| Mmp2            |      |       |       |      | 1.57  | 0.68  | 1.11  | 1.66  |
| Mms19           |      |       |       | 1.17 |       |       |       |       |
| mnb             |      |       |       |      | 0.90  | 0.50  | 0.77  | 1.76  |
| Mocs1           | 2.20 |       | 2.47  | 2.55 | 3.22  | 2.15  | 3.12  | 2.77  |
| Moe             |      |       |       |      |       | 0.52  |       |       |
| moody           |      |       |       |      | 1.17  | 0.70  |       |       |
| mor             |      |       |       |      | 0.89  | 0.69  |       |       |
| MP1             |      |       | -1.48 |      |       |       |       |       |
| MRG15           |      |       |       |      | 0.93  | 0.65  |       |       |
| mRpL20          |      |       |       |      |       | 0.44  |       |       |
| mRpL33          |      |       |       |      |       |       | -0.71 |       |
| mRpL34          |      |       |       |      |       | 0.43  |       |       |
| mRpS10          |      |       |       |      | 0.67  |       |       |       |

|           |      |  |       |       |       |       |       |      |
|-----------|------|--|-------|-------|-------|-------|-------|------|
| mRpS23    |      |  |       |       |       | 0.65  |       |      |
| Mrtf      |      |  |       |       | 1.54  | 1.02  | 1.04  | 1.71 |
| MSBP      |      |  | -0.49 |       |       |       | -0.93 |      |
| msn       |      |  | -0.60 |       | 1.54  | 1.01  |       |      |
| Msr-110   |      |  |       |       |       |       | -1.07 |      |
| MTA1-like |      |  |       |       | 1.21  | 0.76  |       | 1.39 |
| mthl14    |      |  |       |       | 1.54  | 1.30  | 0.71  |      |
| mthl3     |      |  |       |       | 1.01  |       |       |      |
| Mtp       |      |  |       | 1.37  |       |       |       |      |
| Mtpbeta   |      |  |       |       |       |       | -1.06 |      |
| mts       |      |  |       |       |       | 0.40  |       |      |
| mtSSB     |      |  | 0.79  | 0.87  | 0.80  | 0.93  |       | 1.77 |
| mura      |      |  | -0.93 | -1.03 |       | -0.50 | -1.44 |      |
| Mvb12     |      |  |       |       | 1.14  |       | 1.56  |      |
| Mvl       |      |  |       |       |       |       | -1.02 |      |
| Mybbp1A   | 0.86 |  |       |       | 0.82  | 0.67  |       |      |
| mys       |      |  |       |       | 1.44  | 1.01  |       |      |
| nclb      |      |  |       | 0.79  |       |       |       |      |
| ND-42     |      |  |       | -0.56 |       |       | -0.67 |      |
| ND-ASHI   |      |  |       | -0.74 | -0.47 |       | -0.91 |      |
| Ndf       |      |  |       |       | 0.69  | 0.41  |       |      |
| Ndfip     |      |  |       |       | 0.76  | 0.59  | 0.93  |      |
| ND-SGDH   |      |  |       | -0.58 |       |       | -0.67 |      |
| Neb-cGP   |      |  |       | -0.66 |       |       | -0.81 |      |
| nej       |      |  |       |       | 0.82  | 0.52  |       | 1.73 |
| nero      |      |  |       |       |       | 0.43  |       |      |
| Nhe3      | 0.58 |  |       |       | 2.02  | 0.55  | 1.56  | 1.56 |
| NijA      |      |  |       |       | 1.85  | 0.73  | 1.74  |      |
| NiPp1     |      |  | 1.28  |       |       |       |       |      |
| NK7.1     |      |  |       | 0.91  | 1.15  | 1.05  | 1.48  | 1.62 |
| nkd       |      |  |       |       | 0.82  | 0.77  |       | 2.82 |
| Nmda1     |      |  |       |       | 1.40  | 0.68  |       |      |
| noc       |      |  | 0.76  | 1.04  | 0.91  | 0.74  | 1.53  | 2.19 |
| nonA      |      |  |       |       |       | 0.45  |       |      |
| norpA     |      |  |       |       |       |       |       | 1.84 |
| Not1      |      |  | -0.82 | -0.66 |       |       | -0.89 |      |
| Nrt       |      |  |       |       |       |       | -2.19 |      |
| nsl1      |      |  |       |       |       |       |       | 1.26 |
| Nsun5     |      |  |       |       | 1.13  | 0.70  |       |      |
| Ntf-2     |      |  | 0.64  |       | 0.61  |       |       |      |
| Nuak      |      |  |       |       |       |       | 1.19  |      |
| Nup153    |      |  |       |       | 0.68  |       |       |      |
| Nup35     |      |  | 1.05  |       |       |       | 1.53  |      |
| Nup98-96  |      |  | 0.79  |       | 1.19  | 0.75  | 1.41  |      |
| Oatp30B   |      |  |       |       |       |       |       | 1.99 |
| Oatp74D   |      |  |       |       | 2.11  | 1.48  | 1.71  | 2.13 |

|         |      |       |       |       |       |       |       |       |
|---------|------|-------|-------|-------|-------|-------|-------|-------|
| Obp99b  |      |       |       | -1.37 |       |       |       | -2.96 |
| Oda     |      |       | -0.79 | -0.74 | -0.51 | -0.40 | -1.30 | -1.39 |
| Orct2   |      |       | 1.38  |       | 0.94  | 0.81  |       |       |
| oys     |      |       | -1.29 |       |       |       | -0.95 |       |
| P32     |      |       |       | 0.78  |       | 1.01  |       |       |
| p38a    |      |       |       |       |       | 0.69  | -1.04 |       |
| pAbp    |      |       |       |       |       |       | -0.47 |       |
| Paip2   |      | -0.51 | -1.38 | -1.46 |       | -0.58 | -0.74 |       |
| PAN3    |      |       | -0.65 |       |       |       | -0.75 |       |
| PAPLA1  |      |       | -0.76 |       |       |       | -1.05 |       |
| pasi2   |      |       |       |       |       | -0.77 |       |       |
| Pc      |      |       |       |       | 0.91  |       |       |       |
| PCB     |      |       | 0.76  |       |       |       |       |       |
| pcs     |      |       |       |       | 1.00  | 0.53  |       |       |
| pdgy    | 0.96 |       | 0.82  | 0.78  | 1.07  | 1.16  | 0.87  |       |
| Pdk1    | 0.76 | 0.48  | 0.98  |       | 0.99  | 0.89  |       |       |
| Pdss2   |      |       | 1.21  |       | 0.77  | 0.82  | 1.85  |       |
| peb     | 0.85 | 0.54  | 0.81  | 0.83  | 1.27  | 1.02  | 1.02  |       |
| Pect    |      |       |       |       | 1.06  | 0.86  | 0.84  |       |
| peng    |      |       |       |       |       | 0.72  |       |       |
| Pep     |      |       | 0.75  |       | 1.06  | 0.77  | 1.14  |       |
| pes     |      |       |       |       | 0.85  | 0.68  |       |       |
| Pex11ab |      |       |       |       |       |       | -1.39 |       |
| Pez     |      |       |       |       | 1.40  | 0.71  |       |       |
| Pfdn5   |      |       |       |       |       | 0.35  |       |       |
| Pgk     |      |       |       | -0.78 |       |       | -1.20 |       |
| Pgm1    |      |       |       |       |       |       | -0.63 |       |
| ph-d    |      |       |       |       | 0.92  |       |       |       |
| phol    | 0.62 |       | 0.96  | 1.09  | 1.22  | 0.55  | 1.26  | 1.93  |
| ph-p    |      |       |       |       | 0.98  | 0.65  |       |       |
| Phs     |      |       |       |       | 0.78  |       |       |       |
| Pi3K21B |      |       | 0.80  |       | 0.72  | 0.62  | 1.02  |       |
| Pi3K92E |      |       |       |       | 1.21  | 0.78  |       |       |
| pic     |      |       |       |       | 1.33  | 1.10  | 1.03  | 1.55  |
| PIG-A   |      |       |       |       | 1.92  | 1.72  | 1.93  |       |
| pins    |      |       |       |       | 1.02  |       |       |       |
| pirk    | 2.69 | 2.73  |       |       |       | 0.74  | -2.28 | -2.60 |
| pita    |      |       |       | 0.94  |       | 0.52  |       |       |
| Pits    |      |       | 0.85  | 1.09  | 1.08  | 0.73  | 1.39  | 3.09  |
| Pitslre |      |       |       |       | 0.67  | 0.39  | 0.95  |       |
| Plzf    |      | -0.85 |       |       | 2.29  | 0.75  | 1.85  |       |
| PMCA    |      |       | -0.83 | -0.75 |       |       | -1.05 |       |
| pnut    |      |       |       |       | 1.33  | 0.67  |       |       |
| PNUTS   |      |       |       | 0.74  | 1.14  | 0.69  | 1.09  | 1.15  |
| pod1    |      |       |       |       | 1.01  | 0.71  |       |       |
| Poll    |      |       |       |       | 0.92  | 0.74  |       |       |



|           |       |       |       |       |       |       |       |       |
|-----------|-------|-------|-------|-------|-------|-------|-------|-------|
| Pomp      |       |       | -0.52 |       |       |       |       |       |
| Pop1      |       |       |       |       | 1.30  | 1.06  |       |       |
| Pp2A-29B  |       |       | -0.50 |       |       |       |       | -1.30 |
| Pp2B-14D  |       |       |       |       | 0.64  |       |       |       |
| Pp2C1     |       |       |       |       | 0.79  |       | 1.49  |       |
| Ppa       | 0.70  |       |       |       | 0.96  | 0.40  |       |       |
| prage     |       |       |       |       | 1.01  | 0.41  | 0.87  |       |
| PRAS40    |       |       |       |       | 0.77  |       |       |       |
| PRL-1     |       |       |       |       |       | 0.60  |       |       |
| Prp3      |       |       |       |       | 0.96  | 0.59  | 1.29  |       |
| Prp38     |       |       |       |       | 0.90  | 0.60  |       |       |
| prtp      |       |       |       |       |       |       | -1.44 |       |
| Psc       |       |       | 0.93  | 1.06  | 1.57  | 1.36  | 1.91  |       |
| puc       |       | 0.50  |       |       | 1.10  | 1.09  | 0.95  | 1.38  |
| puml      |       |       | 0.47  | 0.57  |       | 0.46  |       |       |
| Pvr       |       |       |       |       | 1.54  | 0.96  | 0.96  |       |
| PyK       |       |       |       |       |       |       | 0.54  |       |
| qkr58E-3  |       |       |       |       |       |       | -1.08 |       |
| Rab18     |       |       | -0.72 | -0.84 |       |       | -0.99 |       |
| Rab23     |       |       |       |       |       |       | -2.65 |       |
| Rab32     |       |       | 0.89  |       | 0.67  | 0.43  | 1.22  |       |
| Rab35     |       |       |       |       | 1.10  | 0.71  | 1.15  | 1.69  |
| Rab7      |       |       | -0.81 | -0.80 |       |       | -0.80 | -1.59 |
| RabGGTa   |       |       |       |       | 1.36  | 0.77  | 0.67  |       |
| Rac2      | 0.77  |       |       |       | 1.28  | 0.85  |       |       |
| Rack1     |       |       |       | -0.58 |       |       | -1.06 |       |
| Rad23     |       |       |       |       | 0.89  | 0.51  |       |       |
| Rala      |       |       |       |       | 1.13  | 0.71  |       |       |
| RanBPM    |       |       | -0.80 |       |       |       |       |       |
| Ras85D    |       |       |       |       |       | 0.61  |       |       |
| RasGAP1   | 0.99  |       |       |       | 1.74  | 1.04  | 1.39  |       |
| RASSF8    |       |       |       |       | 0.86  | 0.71  |       |       |
| Rb97D     |       |       |       |       |       |       | 1.79  |       |
| Rbsn-5    |       |       |       |       | 0.69  | 0.60  |       |       |
| Rcd2      |       |       |       |       |       | 0.93  |       |       |
| Rcd4      |       |       | 2.40  | 1.89  |       |       | 2.55  |       |
| rdgBbeta  |       |       |       | 1.24  |       |       | 1.47  |       |
| rdog      | 1.16  |       | 1.23  | 1.82  | 2.23  | 1.19  | 1.85  | 2.47  |
| RecQ5     |       |       |       |       | -0.64 | -0.54 |       |       |
| Rel       | 2.05  | 0.71  | 1.18  | 1.08  | 2.21  | 1.21  | 1.06  |       |
| Rep       |       |       |       |       | 1.47  | 0.74  |       |       |
| rho       |       |       |       |       |       | 0.67  | 2.95  | 3.07  |
| Rho1      |       |       |       |       | 0.62  | 0.40  |       |       |
| RhoGAP16F |       |       |       | 0.66  | 0.80  | 0.60  |       |       |
| RhoGAP18B |       |       |       |       | 1.36  | 0.74  | 0.99  |       |
| RhoGAP68F | -0.66 | -0.53 | -1.09 | -1.09 |       | -0.55 | -1.46 | -1.37 |

|           |       |       |       |       |       |       |       |       |
|-----------|-------|-------|-------|-------|-------|-------|-------|-------|
| RhoGAP92B |       |       |       |       | 1.15  | 0.67  |       |       |
| RhoGDI    |       |       |       |       | 0.80  | 0.44  |       |       |
| RhoGEF2   |       |       |       |       | 0.66  | 0.42  |       |       |
| RhoL      |       |       |       |       | 0.87  | 0.65  |       |       |
| rin       |       |       |       |       |       | 0.55  |       |       |
| ringer    | -0.93 | -0.96 | -0.96 | -0.98 | -0.93 | -0.68 | -1.33 |       |
| Rip11     |       |       |       |       | 0.90  | 0.47  | 0.59  |       |
| Rlb1      |       |       |       |       |       |       |       | 2.12  |
| RluA-1    |       |       |       |       | -1.20 | -0.93 | -3.93 |       |
| Rok       |       |       |       |       | 0.83  | 0.65  |       |       |
| row       |       |       |       |       |       | 0.47  |       |       |
| RpA-70    | 0.86  |       | 1.66  | 1.05  | 2.05  | 1.20  | 2.20  |       |
| RpL10Ab   |       |       | -0.52 | -0.88 | -0.73 | -0.49 | -1.47 | -1.48 |
| RpL12     |       |       | -0.75 | -0.98 | -0.79 | -0.52 | -1.66 | -1.40 |
| RpL13     |       |       | -0.54 | -0.89 | -0.71 | -0.51 | -1.56 |       |
| RpL13A    |       |       | -0.41 |       | -0.60 |       | -1.17 |       |
| RpL14     |       |       | -0.55 | -0.93 | -0.66 | -0.48 | -1.44 | -1.42 |
| RpL17     |       |       |       | -0.70 |       |       | -1.39 |       |
| RpL18     |       |       |       |       |       |       | -1.13 |       |
| RpL18A    |       |       | -0.58 | -0.95 | -0.67 | -0.53 | -1.55 | -1.22 |
| RpL22     |       |       | -0.61 | -0.69 |       |       | -1.60 |       |
| RpL23     |       |       |       |       |       |       | -1.08 |       |
| RpL26     |       |       | -0.49 | -0.60 |       |       | -1.47 | -1.16 |
| RpL27     |       |       | -0.63 | -0.70 | -0.73 | -0.46 | -1.63 | -1.16 |
| RpL28     |       |       | -0.59 | -0.86 | -0.70 |       | -1.56 | -1.67 |
| RpL3      |       |       |       |       |       |       | -1.14 |       |
| RpL32     |       |       | -0.59 | -0.87 | -0.76 | -0.53 | -1.55 |       |
| RpL34b    |       |       | -0.49 | -0.66 |       |       | -1.39 | -0.96 |
| RpL35A    |       |       | -0.53 | -0.71 | -0.86 | -0.53 | -1.48 |       |
| RpL36     |       |       | -0.47 | -0.75 |       |       | -1.41 | -1.09 |
| RpL37A    |       |       | -0.50 | -0.76 | -0.61 | -0.48 | -1.46 | -1.09 |
| RpL37a    |       |       | -0.47 |       |       |       | -1.23 |       |
| RpL41     |       |       | -0.47 | -0.80 | -0.61 | -0.44 | -1.04 | -1.44 |
| RpL6      |       |       | -0.37 | -0.60 |       |       | -1.20 |       |
| RpL7      |       |       | -0.41 | -0.81 |       | -0.35 | -1.23 | -1.30 |
| RpL8      |       |       |       | -0.63 |       |       | -1.08 |       |
| RpLP1     |       |       | -0.38 |       |       |       | -1.20 |       |
| RpS13     |       |       | -0.54 | -0.83 | -0.63 | -0.45 | -1.40 | -1.48 |
| RpS14a    |       |       | -0.45 | -0.73 |       |       | -1.20 |       |
| RpS14b    |       |       | -0.43 | -0.74 |       |       | -1.31 |       |
| RpS15Aa   |       |       |       | -0.61 |       |       | -1.17 | -1.08 |
| RpS17     |       |       | -0.42 | -0.87 |       |       | -1.37 |       |
| RpS19a    |       |       | -0.52 | -0.76 | -0.66 | -0.43 | -1.36 | -1.42 |
| RpS2      |       |       |       |       |       |       | -1.16 | -1.28 |
| RpS20     |       |       | -0.59 | -0.74 |       |       | -1.21 | -1.28 |
| RpS21     |       |       |       | -0.80 |       |       | -1.16 |       |

|            |      |       |       |       |       |       |       |       |
|------------|------|-------|-------|-------|-------|-------|-------|-------|
| RpS23      |      |       | -0.45 | -0.77 |       |       | -1.43 | -1.55 |
| RpS27      |      |       | -0.41 | -0.75 |       |       | -1.07 |       |
| RpS27A     |      |       | -0.52 | -0.74 | -0.58 | -0.42 | -1.31 | -1.46 |
| RpS28b     |      |       | -0.55 | -0.82 | -0.55 | -0.40 | -1.39 | -1.22 |
| RpS3A      |      |       | -0.41 |       |       |       | -1.15 |       |
| RpS4       |      |       | -0.43 | -0.73 |       |       | -1.30 |       |
| RpS5a      |      |       | -0.53 | -0.59 | -0.80 | -0.37 | -1.32 |       |
| RpS6       |      |       | -0.58 | -0.70 | -0.68 | -0.43 | -1.52 | -1.60 |
| RpS9       |      |       |       |       |       |       | -0.93 | -1.25 |
| Rtca       |      |       | 1.19  |       | 0.72  | 0.66  |       |       |
| rut        |      |       |       |       |       |       |       | 1.66  |
| Samuel     |      |       |       |       | 0.89  | 0.56  |       |       |
| sau        |      |       |       |       | 0.83  | 0.53  | 1.11  |       |
| SC35       |      |       |       |       | 0.81  | 0.42  |       |       |
| SCAP       |      |       |       |       | 0.94  | 0.63  |       |       |
| schlank    |      |       |       |       |       | 0.45  |       |       |
| scrib      |      |       |       |       | 0.75  | 0.56  |       |       |
| scyl       | 1.11 | 0.52  | 1.15  | 1.54  | 0.96  | 0.58  | 0.98  | 2.12  |
| sd         |      |       |       |       | 0.60  |       |       |       |
| SdhA       |      |       |       |       |       |       | -0.62 |       |
| SdhC       |      |       |       | -0.62 |       | -0.33 | -0.92 |       |
| sds22      |      |       |       |       | 0.96  | 0.59  |       |       |
| Sec61alpha |      |       |       | -0.66 |       |       | -1.16 | -1.50 |
| SecS       |      |       |       |       |       | 0.60  |       |       |
| SelG       |      |       |       |       |       |       | -1.08 |       |
| Septin2    |      |       |       |       | 0.76  |       |       |       |
| Serinc     |      |       | -1.17 |       |       |       | -0.96 |       |
| Sesn       |      |       |       |       |       | -0.40 |       |       |
| Setx       |      |       |       | -2.15 |       |       |       |       |
| SF2        |      |       |       |       |       | 0.37  |       |       |
| Sf3a1      |      |       | 1.25  |       | 0.75  | 0.71  | 1.52  |       |
| Sfxn1-3    |      |       |       |       |       |       | 1.27  |       |
| sgll       |      |       |       |       | 1.28  | 0.62  | 0.84  |       |
| SH3PX1     |      |       |       | 0.72  | 1.39  | 1.29  | 0.85  |       |
| Shc        |      |       |       |       |       | 0.63  |       |       |
| shep       | 0.57 |       |       |       | 0.77  | 0.54  |       |       |
| shg        |      |       |       |       | 0.60  | 0.51  |       |       |
| shrb       |      |       |       |       | 1.30  | 0.75  |       |       |
| Shrm       |      |       |       |       | 1.44  | 0.81  | 0.62  |       |
| simj       |      |       | 0.90  | 1.73  | 1.07  | 0.50  | 1.65  | 2.74  |
| Sirt1      | 0.62 |       | 0.70  | 0.75  | 1.54  | 0.71  | 1.37  | 1.21  |
| Sk1        | 1.38 |       |       |       | 3.28  | 2.77  | 1.66  | 1.30  |
| skd        |      |       |       |       | 1.21  | 0.61  | 1.02  | 2.33  |
| SkpA       |      |       |       |       |       |       | -0.46 |       |
| SLC5A11    |      | -0.57 |       |       |       | -0.50 |       |       |
| slmb       |      |       |       |       |       |       |       | 1.40  |

|                    |      |      |       |       |      |      |       |       |
|--------------------|------|------|-------|-------|------|------|-------|-------|
| Slu7               |      |      | 1.10  |       |      |      | 1.41  |       |
| SmB                |      | 0.64 | 1.09  |       | 1.12 | 1.17 | 1.30  |       |
| SmD3               |      |      | 0.67  |       | 1.00 | 0.66 | 0.85  | 1.41  |
| Smg5               |      |      |       |       | 1.60 | 0.62 | 0.95  |       |
| Smr                |      |      |       |       | 0.59 | 0.47 |       |       |
| Snap24             |      |      |       |       | 1.23 | 0.71 |       |       |
| snoRNA:Me18S-A1576 |      |      |       |       | 1.04 |      |       |       |
| Snx27              |      |      |       |       | 1.74 | 1.34 | 1.56  | 2.41  |
| Snx3               |      |      |       |       |      |      | 0.87  |       |
| Socs36E            | 2.05 | 1.11 | 1.27  | 1.89  | 4.11 | 3.38 | 2.83  | 2.87  |
| Sodh-2             |      |      |       |       |      |      |       | 3.93  |
| Son                |      |      | 1.39  | 1.34  | 0.59 |      | 1.51  | 2.00  |
| Sox14              |      |      |       |       | 0.80 |      |       |       |
| SpdS               |      |      | 1.47  |       |      |      |       |       |
| spict              | 0.72 |      |       |       | 1.46 | 1.00 | 0.72  |       |
| spin               |      |      |       |       | 0.98 | 0.68 | 0.96  |       |
| Spn                |      |      |       |       |      | 0.41 |       |       |
| Spn55B             | 0.91 |      |       |       | 1.81 | 1.14 |       |       |
| spt4               |      |      | 0.99  | 1.14  |      |      |       |       |
| Sptr               |      |      |       |       |      |      | -1.05 |       |
| sqh                |      |      |       |       | 1.18 | 0.73 | 0.58  |       |
| sqz                |      |      |       |       |      |      |       | 3.61  |
| SREBP              |      |      | -0.79 | -0.77 |      |      | -1.17 | -1.39 |
| Srp72              |      |      |       |       | 0.65 |      |       |       |
| Sry-delta          |      |      |       |       | 0.99 | 0.62 |       |       |
| Ssk                |      |      |       |       | 0.85 | 0.56 |       |       |
| Ssl1               |      |      |       |       | 1.05 |      |       | 2.49  |
| SsRbeta            |      |      |       |       |      |      | -0.68 |       |
| step               |      |      |       |       | 1.78 | 1.31 |       | 1.93  |
| Strica             | 1.05 |      |       |       | 2.43 | 2.08 | 1.49  |       |
| stv                | 0.71 |      |       |       | 1.29 | 0.76 |       |       |
| stwl               |      |      |       |       | 0.90 | 0.77 |       |       |
| stx                |      |      | 0.57  |       | 1.45 | 1.06 | 0.72  | 1.66  |
| Su(P)              |      |      |       |       |      | 0.53 |       |       |
| Su(z)2             |      |      |       | 1.41  | 1.22 | 0.98 | 1.98  | 2.32  |
| Sur-8              |      |      | -0.58 |       | 0.74 |      |       |       |
| Surf6              | 0.73 | 0.67 |       |       | 0.71 | 0.74 |       |       |
| sut1               |      |      |       |       |      | 0.43 |       |       |
| Swip-1             |      |      |       |       | 1.31 |      | 0.74  |       |
| Syx1A              |      |      |       |       | 1.03 | 0.76 | 0.80  | 1.73  |
| Syx4               | 0.75 | 0.53 | 0.61  |       | 1.16 | 1.21 | 0.86  |       |
| Taf8               |      |      |       | 1.40  |      |      | 1.77  |       |
| tai                |      |      |       |       | 1.19 | 0.70 | 0.83  |       |
| Tailor             |      |      |       | 0.99  | 0.61 |      | 1.05  | 2.25  |
| tara               |      |      | 1.53  |       |      |      | 1.71  |       |
| Tcs5               |      |      |       |       | 0.99 | 0.64 |       |       |

|                  |      |      |       |       |      |       |       |       |
|------------------|------|------|-------|-------|------|-------|-------|-------|
| Tctp             |      |      | -0.51 | -0.72 |      |       | -1.00 | -1.46 |
| Tep4             | 0.54 |      |       |       | 1.10 | 0.59  |       |       |
| TfIIA-S          |      |      | -0.89 |       |      |       | -1.46 |       |
| THADA            |      |      |       |       | 1.40 |       |       |       |
| Thor             | 0.95 |      | -1.20 | -1.23 | 1.53 |       | -1.34 | -1.81 |
| Tis11            |      |      |       |       |      | 0.43  |       |       |
| Tlk              |      |      |       |       | 0.88 | 0.57  |       | 1.20  |
| Tmem63           |      |      | -0.80 |       |      |       |       |       |
| Tnpo             |      |      |       |       | 0.71 |       |       |       |
| Tom7             |      |      |       |       |      |       | -0.87 |       |
| Tomosyn          |      |      |       |       | 0.67 |       |       |       |
| Top1             |      |      | 0.71  |       | 0.61 |       |       |       |
| Tpst             |      |      |       | -1.37 |      |       |       |       |
| trbl             |      |      |       |       | 2.02 | 0.58  |       |       |
| Treh             |      |      |       |       |      |       | -1.15 | -1.75 |
| tRNA:Trp-CCA-2-2 |      |      |       |       | 1.60 |       |       |       |
| Trp1             |      |      |       | -0.66 |      |       | -0.67 |       |
| Tsp29Fa          |      |      | -0.47 |       |      |       |       |       |
| Tsp29Fb          |      |      | -0.41 |       |      |       | -0.39 |       |
| Tsp3A            |      |      |       |       | 1.06 |       |       |       |
| Tsp42Ed          |      |      |       |       | 1.32 | 0.72  | 0.54  |       |
| Tsp42Ef          |      |      |       |       | 0.85 | 0.89  |       |       |
| Tsp42Eq          |      |      | -0.45 |       |      |       | -1.05 |       |
| Tsp42Er          |      |      | -0.54 |       |      | 0.94  |       |       |
| tsr              |      |      |       |       | 0.96 | 0.52  |       |       |
| Tudor-SN         |      |      |       | -0.67 |      |       | -0.86 |       |
| twf              | 0.70 |      |       |       | 1.20 | 0.76  |       |       |
| U2af50           |      |      |       |       | 0.56 |       | 0.95  |       |
| Uba1             |      |      |       |       | 0.59 |       |       |       |
| Uba2             |      |      |       |       | 0.70 |       |       |       |
| UbcE2H           |      |      | -1.10 | -1.13 |      | -0.48 | -0.83 |       |
| Ubi-p5E          |      |      |       |       |      |       | -0.47 |       |
| Ubi-p63E         | 0.65 |      | 1.00  | 0.66  | 0.55 |       | 0.96  |       |
| Ubr1             |      |      | -0.74 | -1.01 |      |       |       |       |
| Ufc1             |      |      |       |       |      |       | -1.45 |       |
| Ufd4             |      |      | -0.76 |       |      |       | -1.27 |       |
| Ugt301D1         |      |      |       |       |      |       |       | -1.38 |
| Uhg1             | 0.94 | 0.86 |       | 1.20  |      | 0.80  |       |       |
| Uhg2             |      |      |       | 1.34  |      |       |       |       |
| Uhg4             |      |      |       | 1.10  |      |       |       |       |
| Uhg8             |      |      |       | 2.25  |      |       |       |       |
| Unc-115a         |      |      |       |       | 0.96 | 0.61  |       |       |
| uno              |      |      |       |       |      |       |       | 3.20  |
| UQCR-14          |      |      | -0.42 | -0.73 |      | -0.31 | -1.33 | -1.05 |
| UQCR-6.4         |      |      |       | -0.63 |      |       | -0.89 |       |
| ValRS            |      |      | -0.95 |       |      |       | -1.40 |       |

|         |      |       |       |       |       |       |       |       |
|---------|------|-------|-------|-------|-------|-------|-------|-------|
| Vamp7   |      |       |       | -0.68 |       |       |       |       |
| vari    |      |       |       |       | 1.11  |       |       |       |
| veil    |      |       |       |       |       |       | -0.54 |       |
| ver     | 1.28 |       | 1.18  | 2.36  | 2.67  | 1.68  | 2.18  | 2.57  |
| Vha13   |      |       |       | -0.56 |       |       | -1.00 |       |
| Vha16-1 |      |       | -0.82 | -0.89 | -0.73 |       | -1.48 | -1.22 |
| Vha36-1 |      |       | -0.55 | -0.69 | -0.64 | -0.43 | -1.25 |       |
| Vha55   |      |       | -0.77 | -0.72 | -0.68 | -0.45 | -1.47 | -1.27 |
| viaf    | 1.00 | 0.65  |       |       | 1.58  | 1.73  | 1.16  |       |
| Vps2    |      |       |       |       | 1.30  | 0.85  |       |       |
| Vps24   |      |       |       |       | 1.69  | 1.08  | 1.19  |       |
| Vps28   |      |       |       |       | 1.01  | 0.46  |       |       |
| Vps36   |      |       |       |       | 0.81  | 0.54  |       |       |
| Vps60   |      |       |       |       | 0.92  | 0.47  |       |       |
| vri     |      |       | 1.15  | 1.20  | 1.46  | 1.28  | 2.13  | 1.79  |
| vsg     |      |       |       |       |       | 0.35  | -0.49 |       |
| Vti1b   |      |       |       |       |       |       | -1.45 |       |
| wde     |      |       | 0.81  |       | 0.94  | 0.77  |       | 1.50  |
| wdp     | 0.92 |       |       |       | 1.16  | 0.63  |       | 1.62  |
| whd     |      | -0.84 | -1.31 | -1.28 | -0.72 | -1.06 | -1.95 | -1.57 |
| wit     |      |       |       |       |       |       | -1.21 |       |
| wnd     |      |       |       |       | 1.56  | 1.02  | 1.15  | 2.43  |
| x16     |      |       |       |       | 0.96  |       |       |       |
| Xbp1    |      |       | -0.49 |       |       |       | -0.96 | -1.29 |
| Xe7     |      |       |       |       | 0.54  |       |       |       |
| Xrp1    | 1.54 | 0.55  | 1.48  | 1.62  | 2.62  | 1.87  | 1.90  | 1.96  |
| yip2    |      |       | 0.83  |       | 0.76  | 0.87  | 0.79  |       |
| Zasp52  |      |       | -0.78 |       |       |       |       |       |
| Zdhhc8  |      |       |       |       | 1.40  | 0.90  | 0.77  |       |
| Zfrp8   |      |       | 0.92  |       | 1.12  | 0.65  |       |       |
| zip     |      |       |       |       | 1.34  | 0.74  |       |       |
| Zip71B  |      |       | -1.06 |       |       |       |       | -1.66 |
| Zip99C  | 0.80 | 0.64  | 0.91  | 0.83  |       |       | -0.72 |       |
| Zn72D   |      |       | 0.97  | 1.02  |       |       | 1.64  |       |
| ZnT63C  |      |       |       |       |       |       | -0.93 |       |
| ZnT86D  |      |       |       |       |       |       | -1.56 |       |

## Appendix II : Generation of Jra antibody

Full-length Jra was cloned into pET-45b(+) vector with an N-terminal His tag, expressed in BL21(DE3) strain of *E.coli* and purified using Ni-NTA agarose beads. Post purifications, the eluate was subjected to size exclusion chromatography and the dialysed fraction was used to raise antibodies in a rabbit.

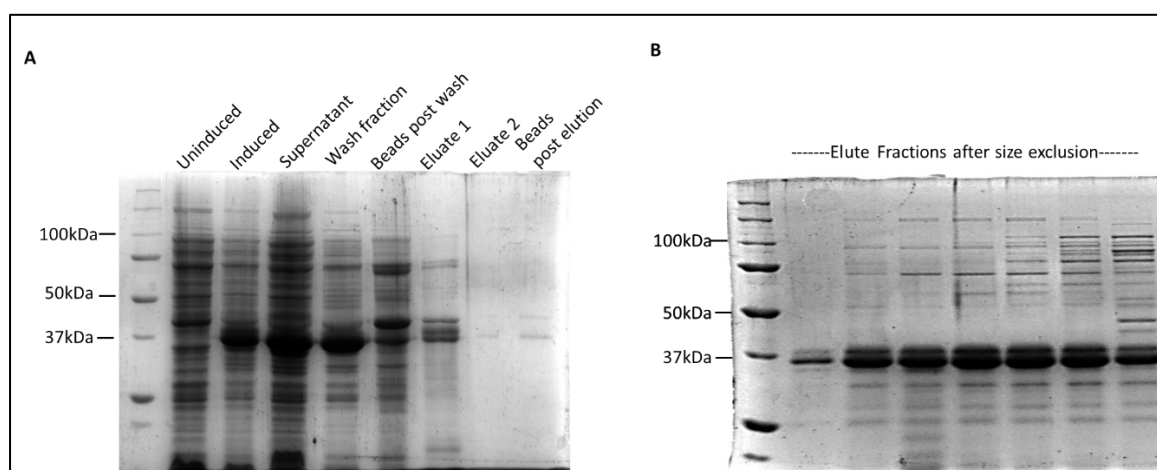


**Figure II.1: Purification of Jra**

**A.** Coomassie gel image depicting different purification steps of Jra from BL21(DE3) strain of *E. coli*. Jra was expressed in ample quantity and seen as a thick band in the induced fraction at 37kDa. The expressed protein was soluble and can be seen on the supernatant after the cell lysis. Surprisingly, only a small quantity of soluble Jra was bound to the Ni-NTA beads and most of Jra was seen in the wash fraction of the beads. The less amount which was bound to the beads was completely eluted using 500mM of imidazole (eluate 1).

**B.** Coomassie gel image depicting different purification steps of Jra using an S200 preparative column. The wash fraction that was collected in the previous step, was dialysed, concentrated and subjected to size exclusion chromatography. Jra was observed as a large oligomeric form with an estimated size of 1MDa (data not shown). Post chromatography, the purified protein was collected as 1 ml eluates and loaded on an agarose gel that is depicted. All the eluates were pooled, further dialysed and concentrated into 1ml final concentrate.

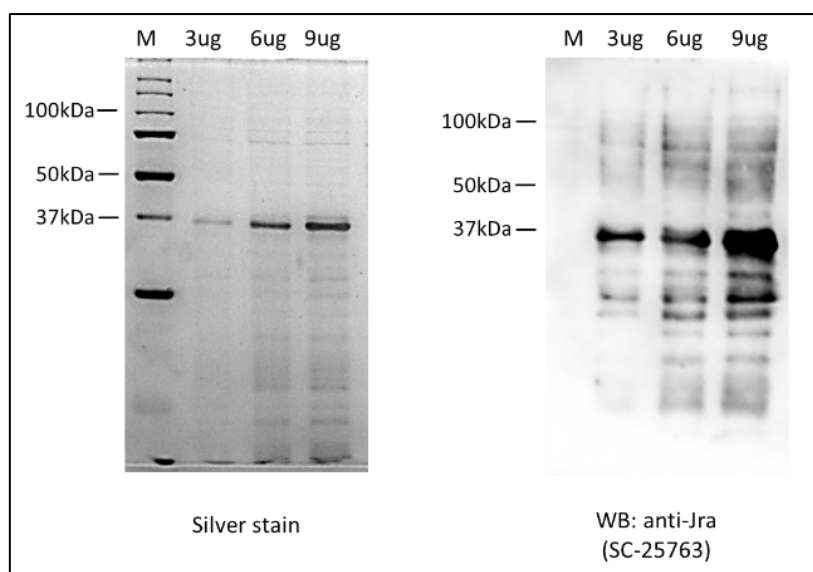


**Figure II.2: Purified Jra after size exclusion chromatography**

- A.** Silver stain gel image of purified Jra post size exclusion chromatography. Purified Jra is seen as a single band at 37kDa with minimum contaminants.
- B.** Western blotting image of purified Jra using a commercially available antibody recognises a prominent band at 37kDa. Bands seen below 37kDa could be semi translated forms of Jra and bands seen above 37kDa could be oligomeric forms of Jra.

### Binding of Rabbit anti-Jra serum (Pre-bleed, 1st, 2nd, 3rd, 4th and 5th bleeds) to Jra in Indirect ELISA

**Indirect ELISA (Assay Conditions):**

| Conditions         | Samples used   | Diluent | Incubation Details      |
|--------------------|--|---------|-------------------------|
| Antigen coating    | Jra (3µg/ ml)  | PBS     | O/N at 4 <sup>o</sup> C |
| Blocking           | 5% Skimmed Milk  | PBS     | 45 min at RT            |
| Primary Antibody   | Rabbit anti-Jra serum (Pre, 1 <sup>st</sup> , 2 <sup>nd</sup> , 3 <sup>rd</sup> , 4 <sup>th</sup> and 5 <sup>th</sup> Bleed) | PBS     | O/N at 4 <sup>o</sup> C |
| Secondary antibody | Goat anti- rabbit IgG-HRP  | PBST    | 1:2000; 45 min at RT    |
| Substrate          | TMB  | -       | 20 min                  |
| O.D                | 450 nm   |         |                         |
| Assay volume       | 50 µl (Nunc Plate)   |         |                         |

| Binding of Rabbit anti-Jra serum (Pre-bleed, 1st bleed, 2nd bleed, 3rd bleed, 4th bleed and 5th bleed) to Jra in Indirect ELISA |              |           |           |           |           |           |
|---|--------------|-----------|-----------|-----------|-----------|-----------|
| Reciprocal of antibody dilution   | OD at 450 nm |           |           |           |           |           |
|   | Pre-Bleed    | 1st bleed | 2nd bleed | 3rd bleed | 4th bleed | 5th bleed |
| 1000  | 0.38         | 2.40      | 2.74      | 2.64      | 2.75      | 2.85      |
| 4000  | 0.09         | 2.44      | 2.74      | 2.57      | 2.71      | 2.71      |
| 16000   | 0.02         | 2.08      | 2.51      | 2.42      | 2.48      | 1.61      |
| 64000   |              | 0.84      | 1.49      | 1.63      | 1.47      | 0.64      |
| 256000  |              | 0.21      | 0.50      | 0.57      | 0.44      | 0.16      |
| 1024000   |              |           |           |           |           | 0.07      |



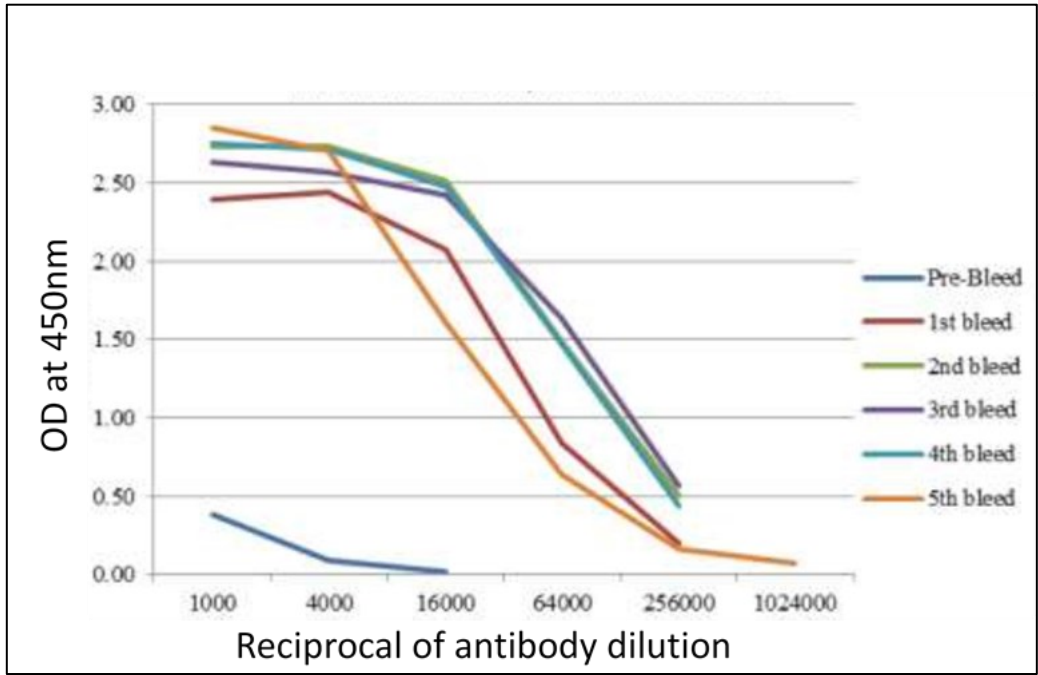


Figure II.3: Binding of anti-Jra sera to Jra in an indirect ELISA experiment

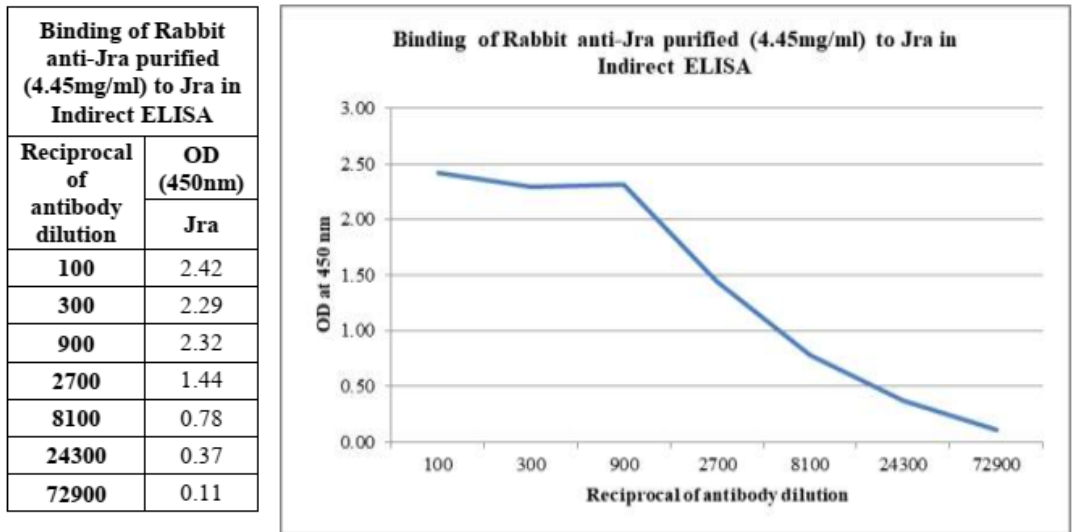


Figure II.4: Binding of purified anti-Jra antibody to Jra in an indirect ELISA experiment